Exploring the biology of the fungus
Candida albicans in the gut of gnotobiotic mice

Untersuchung der Biologie des Hefepilzes
Candida albicans im Verdauungstrakt
gnotobiotischer Mäuse

Doctoral thesis for a doctoral degree
at the Graduate School of Life Sciences,
Julius-Maximilians-University, Würzburg,
Section Infection and Immunity

Submitted by

Marie-Therese Eckstein

From

Mosbach

Würzburg 2020

Submitted on:

Members of the Doctoral Thesis Committee

Chairperson: Prof. Dr. Thomas Rudel

Primary Supervisor: Dr. J. Christian Pérez

Supervisor (Second): Dr. Martin Fraunholz

Supervisor (Third): Prof. Dr. Joachim Morschhäuser

Date of Public Defence:

Date of Receipt of Certificates:

Acknowledgements

Summary

The human body is colonized by trillions of microbes from all three domains of life – eukaryotes, bacteria and archaea. The lower gastrointestinal tract is the most densely colonized part of the body, harbouring a diverse and dynamic community of microbes. While the importance of bacteria in this so-called microbiota is well acknowledged, the role of commensal fungi remains underexplored. The most prominent fungus of the human gastrointestinal microbiota is *Candida albicans*. This fungus occasionally causes life-threatening disseminated infections in individuals with debilitated immune defences. It is this "pathogenic" facet that has received the most attention from researchers in the past, leaving many aspects of its "commensal" lifestyle understudied. Using gnotobiotic mice as a model system to explore the biology of *C. albicans* in the mammalian gut, in this dissertation I establish the global response of the host to *C. albicans* monocolonization as well as the spatial distribution of the fungus in the intestine in the context of co-colonization with single gut bacterial species. The fungus elicited transcriptome changes in murine intestinal tissue, which included the activation of a reactive oxygen species-related defence mechanism and the induction of regulators of the circadian clock circuitry. Both responses have previously been described in the context of a complete bacterial microbiota. Imaging the intestine of animals monocolonized with the fungus or co-colonized with *C. albicans* and the gut bacteria *Bacteroides thetaiotaomicron* or *Lactobacillus reuteri* revealed that the fungus was embedded in a *B. thetaiotaomicron*-promoted outer mucus layer in the murine colon. The gel-like outer mucus constitutes a unique microhabitat, distinct in microbial composition from the adjacent intestinal lumen. This finding indicates that bacteria can shape the specific microhabitat occupied by the fungus in the intestine. Overall, the results described in this dissertation suggest that gnotobiotic mice constitute a valuable tool to dissect multiple aspects of the interactions among host, commensal fungi and cohabiting bacteria.

Zusammenfassung

Der menschliche Körper beheimatet Billionen von Mikroorganismen aus allen drei Domänen des Lebens – Eukaryoten, Bakterien und Archaeen. Der menschliche Dickdarm ist dabei das am dichtesten besiedelte Organ des Körpers. Er beherbergt eine sehr diverse und dynamische Gemeinschaft von Mikroorganismen. Während die Relevanz der so genannten Mikrobiota weitreichend anerkannt ist, wurde die Bedeutung der kommensalen Pilze bisher noch vernachlässigt. Der am häufigsten vorkommende Pilz im menschlichen Gastrointestinaltrakt ist *Candida albicans*. Der Hefepilz kann vor allem in Patienten mit geschwächtem Immunsystem zum Ursprung lebensbedrohlicher Krankheiten werden. Diese Pathogenität des Pilzes wurde in den letzten Jahren ausführlich beleuchtet, wohingegen die kommensalen Aspekte des Pilzes vernachlässigt wurden. In dieser Dissertation habe ich, mit Hilfe von gnotobiotischen Mausmodellen, (i) das Leben von *C. albicans* im Säugetierdarm untersucht, (ii) die Reaktion des Wirts auf diese Kolonisierung ermittelt, (iii) sowie das Kolonisierungsverhalten und die Interaktionen von verschiedenen Darmbakterienspezies und *C. albicans* erforscht. Durch die alleinige Kolonisierung des Darms mit *Candida albicans* konnte ich Veränderungen im Transkriptom der Darmepithelzellen nachweisen, wie etwa die Aktivierung einer reaktiven Sauerstoffspezies-vermittelten Wirtsantwort und die Induktion von mehreren Regulatoren des zirkadianen Rhythmus. Beide dieser Wirtsreaktionen wurden zuvor nur in der Anwesenheit einer bakteriellen Mikrobiota nachgewiesen. Durch die Visualisierung der Pilzzellen im Darm während der Monokolonisierung, sowie während der Kolonisierung des Darms mit dem Pilz und den Darmbakterien, *Bacteroides thetaiotaomicron* oder *Lactobacillus reuteri,* konnten wir zeigen, dass der Pilz den von *B. thetaiotaomicron* neu geschaffenen Lebensraum, die äußere Mukusschicht, besiedeln kann. Diese äußere gelartige Mukusschicht ist ein einzigartiger Lebensraum, welcher sich stark von der inneren, sterilen Mukusschicht unterscheidet. Diese Erkenntnisse deuten darauf hin, dass einzelne Bakterienspezies den Lebensraum des Pilzes verändern können.

Zusammenfassend konnte ich feststellen, dass die gnotobiotischen Mausmodelle sich sehr gut eignen, um die unterschiedlichen Aspekte der kommensalen Kolonisierung des Darms durch *C. albicans,* sowie dessen Interaktionen mit dem Wirt und den anwesenden Bakterien zu untersuchen.

Abbreviation Index

% (v/v)	% (volume/volume)
% (w/v)	% (weight/volume)
°C	degree Celsius
Δ	delta; Deletion
μg	micro-Gram
μM	micro-Molar
μmol	micro-Mol
BAM	Binary Alignment Map
BSA	Bovine Serum Albumin
cDNA	complementary DNA
cfu	Colony-forming units
CO_2	Carbon dioxide
CY5	Cyanine 5
CY3	Cyanine 3
d	day
DAPI	4′,6-Diamidino-2-Phenylindole
ddH_2O	distilled Water
DMSO	Dimethyl sulfoxide
DNA	Deoxyribonucleic acid
dNTP	Deoxyribonucloside triphosphate
dsDNA	double stranded DNA
DTT	Dithiothreitol
e.g.	exempli gratia
EDTA	Ethylenediaminetetra acetic acid
EtOH	Ethanol
FISH	Fluorescence *in situ* hybridization
g	gram
G-CSF	Granulocyte-Colony Stimulating Factor
GUT	Gastrointestinally induced Transition
h	hour
H_2	Hydrogen
HCl	Hydrochloric acid
IBD	Inflammatory bowel disease
IF	Immunofluorescent staining
K_2HPO_4	Dipotassium phosphate
KH_2PO_4	Monopotassium phosphate
M	molar
mg	milli-Gram
$MgCl_2$	Magnesium chloride

min	minute
ml	milli-Liter
mRNA	messenger RNA
N_2	Nitrogen
Na_2HPO_4	Disodium phosphate
NaCl	Sodium chloride
NaH_2PO_4	Monosodium phosphate
NaOH	Sodium hydroxide
NAT	Nourseothricin
ng	nano-Gram
NS	not significant
OD_{600nm}	Optical density at 600 nm
Oligo	Oligonucleotide
OMM^{12}	Oligo Mouse Microbiota
ON	Over Night
ORF	Open Reading Frame
P	p-value
PAGE	Polyacrylamide Gel Electrophoresis
PBS	Phosphate Buffered Saline
PCA	principal component analysis
PCR	Polymerase Chain Reaction
PVDF	Polyvinylidene fluoride
qPCR	quantitative PCR
RNA	Ribonucleic Acid
RNAseq	RNA-sequencing
ROS	Reactive Oxygen Species
rpm	Revolutions per minute
rRNA	ribosomal RNA
RT	Room Temperature
SD	Standard Deviation
SDS	Sodium Dodecyl Sufate
sec	Second(s)
SPF	Specific pathogen free
Tris	Tris(hydroxymethyl)aminomethan
TBS	Tris-buffered Saline
TBS-T	Tris-buffered Saline with Tween-20
V	Volt
W	Watt
WB	Western blot
WIG	Wiggle
WT/wt	Wild type
YPD	Yeast Extract–Peptone–Dextrose

List of Figures

List of Tables

Table of Contents

XIII

1.Introduction

1.1 The human microbiota

The human body is host to trillions of microbes from all three domains of life – bacteria, archaea and eukaryotes. The human skin and all mucosal surfaces are laden with microbial communities (Egert & Simmering, 2016). The entire set of microbes and all detectable genetic material of non-human origin is termed the microbiome (Huttenhower *et al.*, 2012a; Methé *et al.*, 2012). While the role of bacteria associated with the human body has become clearer due to extensive research in the past few decades, the role of fungi in the human microbiome has largely been neglected (J. Li *et al.*, 2018). Similar to bacterial communities, the composition of the fungal microbiota, which is termed mycobiota, varies greatly among different sites within the host (Figure 1 adapted from (Underhill & Iliev, 2014; Limon *et al.*, 2017). Like the bacteria of the microbiota (A. J. Wolf & Underhill, 2018), some fungi of the human mycobiota are opportunistic pathogens, meaning that in healthy individuals these microbes are found as part of the commensal community colonizing the human body. But then upon certain changes of the environment of this microbe, however, a variety of diseases can be caused, some of which can be life-threatening (Polvi *et al.*, 2015). The changes that lead to this shift of lifestyle can be as small as a change of pH in the niche, the availability of nutrients or a shift in the microbial community (Koch *et al.*, 2018; Lu *et al.*, 2014). Additionally, major interventions like an injury or surgery as well as drug/antibiotic treatment can affect the host environment. All the diverse niches of the human body are colonized with microbes forming a diverse and fluctuating microbiota.

1.2 The human mycobiome

When colonizing the human body, the skin is the first point of contact of the fungus and the host. Depending on the nature of the skin (dry or moist) the fungal community can vary: most of the dry skin harbour strains of the fungus *Malassezia* spp. (Costello *et al.*, 2009; Grice *et al.*, 2009; Velegraki *et al.*, 2015). Whereas moist skin, like feet, have been associated with a greater fungal diversity where up to 80 different genera have been described (Findley *et al.*, 2013). The characteristics of the body site shape the microbial community that colonizes the specific body niche.

The orifices of the human body that are accessible to the environment, namely the lung, the urogenital tract, the oral pharyngeal tract and the gastrointestinal tract are easily colonized, as they are exposed to microbes from the surroundings (Huttenhower *et al.*, 2012b). Environmental fungi or their spores, that are constantly inhaled by a healthy individual, are regularly cleared from the lungs and usually only represent a problem in patients with compromised lung function (Delhaes *et al.*, 2012; Pihet *et al.*, 2009). The oral mucosa harbours a great diversity of bacteria as well as fungi (>75 genera), one of the most prominent fungal genera is *Candida*. The role of these commensal fungi in the oral cavity has not been explored in detail. However, overgrowth can cause oral thrush, which is common in newborns and in immunosuppressed individuals like people with AIDS and cancer patients receiving chemotherapy. Oral thrush appears when the fungus overgrows and switches from a commensal lifestyle to its pathogenic state (Millsop & Fazel, 2016; Vila *et al.*, 2020). The urogenital tract of women is mostly colonized by the dominating bacterial *Lactobacillus* species. By the production of lactic acid these bacteria maintain the low pH of this environment that suppresses fungal growth. A decrease in these lactic acid producing bacteria can enforce the overgrowth of commensal fungi that are found associated with the vaginal mucosa. The composition and the diversity of the fungal mycobiota is formed by the biology of the niche, all niches of the human body that are colonized by

fungi are usually as well colonized by bacteria, together they maintain a balanced environment.
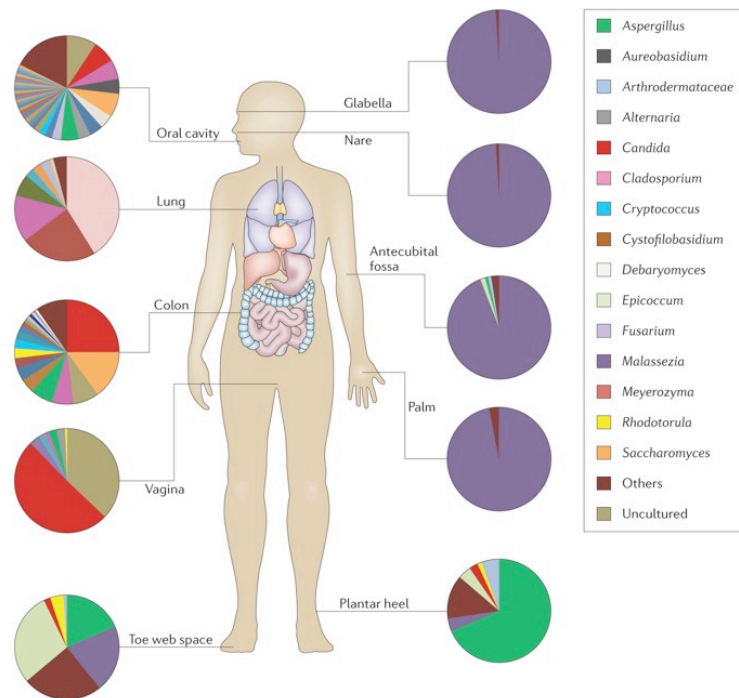
Figure 1: Diversity of commensal fungi colonizing the human body

The fungal part of the microbiota – the mycobiota, is less well studied than the bacteria that colonize the mammalian body. All mucosal surfaces and the skin are colonized not only by bacteria but also by different fungi. The scheme depicts the fungal diversity on the different body sites, each colour in the pie charts represent a fungal phylum. The commensal fungus *Candida albicans* is indicated in red and is associated mostly with the oral and vaginal cavity as well as the gastrointestinal tract of humans (adapted from Underhill & Iliev, 2014).

1.3 The gastrointestinal microbiota

The part of the human body harbouring the highest density of microbes is the gastrointestinal tract. The gastrointestinal microbiota has been studied intensively in the last decades. The microbiota of the human intestine is composed of approximately 400-1000 different species of bacteria, and between 63 and 220 different genera of fungi (Gouba & Drancourt, 2015; X. V. Li *et al*., 2019). The quantity of the mycobiome of the gastrointestinal tract

varies in many studies but despite the different sequencing methods used in the studies, it has been suggested that we can find a "core mycobiome" which is shared among big parts of the population, with an additional more diverse fungal community consisting of some less represented fungal species (X. V. Li *et al.*, 2019). Amongst the most abundant fungi in the gut are species of the genus *Saccharomyces*, *Candida*, *Cladosporium and Penicillium* (Hoffmann *et al.*, 2013; Mar Rodríguez *et al.*, 2015).

The predominant bacterial colonizers of the gastrointestinal tract belong to the phyla of *Firmicutes* and *Bacteroidetes* (Barko *et al.*, 2018). The diversity and numbers of bacteria increase from the oesophagus (10^2 cfu/ml content) down towards the rectum (10^{12} cfu/ml content) (Power *et al.*, 2014). While the pH increases from stomach to colon (Nugent *et al.*, 2001), oxygen levels are decreasing in the intestine (Canny & McCormick, 2008). The gut microbiota derives most of its nutrients from the dietary carbohydrates consumed by the host (Makki *et al.*, 2018; Yadav *et al.*, 2018). Many colonic organisms like *Bacteroides, Bifidobacterium* and *Fecalibacterium* species can utilize carbohydrates or dietary compounds like oligosaccharides that are indigestible to the host (Wrzosek *et al.*, 2013). These bacteria can ferment these complex compounds for their own use and as by-products they generate for example short chain fatty acids (SCFA) (Kasubuchi *et al.*, 2015). These SCFA which are produced by the bacteria during the fermentation can then be absorbed by the host and their nutritional value would have been inaccessible for the host without the pretreatment by the bacteria (Macfarlane & Macfarlane, 2003; Sonnenburg *et al.*, 2005a). Up to 10 % of the nutrients that humans absorb are only available for our digestion because of the presence of gut bacteria (Bäckhed *et al.*, 2004). Some bacterial species encode many more enzymes for carbohydrate metabolism than the human host, like the common gut bacterium *Bacteroides thetaiotaomicron* (Martens *et al.*, 2008). Therefore, the highly diverse gastrointestinal microbiota, consisting of microbes from all three domains of live, plays a beneficial role in the nutrient uptake of the host.

1.4 The polymorphic fungus *Candida albicans*

A fungus that is found on many different human body sites is *Candida albicans*. The fungus is a common resident of the vaginal, oral, and gastrointestinal tract of healthy humans (Figure 1, Underhill & Iliev, 2014). *C. albicans* resides on and in the human body as a commensal. However, under certain circumstances, the fungus can cause candidiasis, an oral or vaginal thrush, and in severe cases disseminate from its commensal niche into the bloodstream of the host and cause life threatening systemic infections (Hube, 2004; Kumamoto *et al.*, 2020). During colonization of the host, *C. albicans* is kept in place by an intact physical barrier maintained by the host, the immune system of the host, and the presence of competing commensal microbes (Bougnoux *et al.*, 2006; Brown & Netea, 2012). *C. albicans* and its biology has most commonly been studied in the context of the infectiousness of the fungus (Kumamoto & Vinces, 2005). *C. albicans* is polymorphic, meaning the fungus can adopt different morphologies (Figure 2). The round yeast morphology of the fungus, also stated as white phenotype, has been connected to the commensal state of the fungus (Figure 2 A) (Pérez, 2019). Changes in the environment like temperature, CO_2 levels, pH changes or the availability of nutrients can trigger the fungus to grow in its filamentous form, in this state the cells adopt the elongated hyphal form (Figure 2 C) (Du & Huang, 2016; Huang, 2012; J. Kim & Sudbery, 2011; Saville *et al.*, 2003). This morphology is commonly recovered from infection sites. The yeast-to-hyphae transition of *C. albicans* was discovered as one of its major virulence traits (Jacobsen *et al.*, 2014; Saville *et al.*, 2003). The morphology where the elongated fungal cells are connected to each other but the single cells are still separated by a septum is named pseudohyphae (Figure 2 B) (Crampin *et al.*, 2005; Diamond & Krzesicki, 1978), in contrast to the true hyphae these cells can still bud, they are found in infectious sites or in states where a rapid growth of the fungus is favoured (Noble *et al.*, 2017). The fungus *C. albicans* is a diploid organism. In order to mate with other cells, the fungus adopts the oval shaped opaque cell type (Figure 2 E) (Bennett, 2015). In these rough and

grey appearing cells the mating efficiency is the highest. The GUT phenotype (Gastrointestinally-indUced Transition) was described by the group of Suzanne Nobel (Pande *et al*., 2013) who found an oval shaped form of *C. albicans* cells in the intestine of mice (Figure 2 D). They described the GUT cells to have a fitness advantage over the commensal white morphology in the mammalian intestine. The commensal *C. albicans* cells that colonize the oral and vaginal tract of humans are mostly present in the round yeast morphology (Figure 2 A). If the fungus plays any beneficial role for the host during this colonization is unknown. In immunocompromised individuals, however, the fungus can overgrow in these natural habitats and use its hyphae to penetrate into the host epithelium causing candidiasis (Netea *et al*., 2015). The identification of the *C. albicans* morphology allows drawing conclusions about the lifestyle of the fungus under the different growth conditions or in different niches.
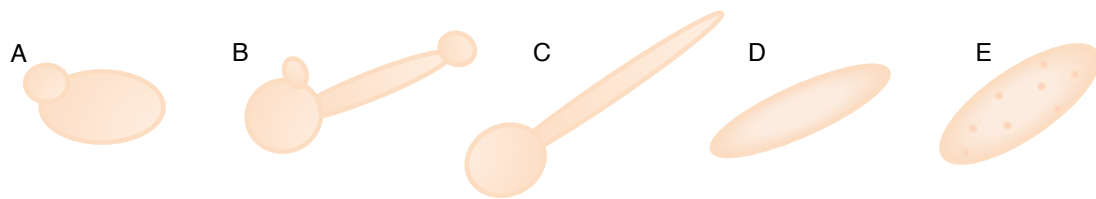
Figure 2: The morphologies of the fungus *Candida albicans*

The different phenotypes of *C. albicans* can provide information on the lifestyle of the fungus. Under standard laboratory conditions as well as in a commensal state the cells can be found in its round yeast shape, the white morphology (A). Pseudohyphae (B) are an intermediate between this white phenotype and the true hyphae, the elongated cells can still bud and are separated by a septum. The true hyphal form (C) of *C. albicans* is distinctly different from the pseudohyphae, each hypha is one elongated cell. This state is not reversible into the white phenotype. The GUT cells (D) are described as the phenotype that is found in the intestine of mammals and the opaque cell type (E) is formed to increase positive mating events.

1.5 The microbiota in health and disease

The microbial communities that thrive in and on the human body are closely connected to the fitness of the human host. The role of the microbiota in health and disease of the host has mostly been recognized by studying the bacterial part of the microbiota (Biedermann & Rogler, 2015; Limon *et al.*, 2017). It has been established that these microbial communities can influence a diverse set of biological functions in the host, ranging from the availability of nutrients and their digestion, the control of inflammatory gastrointestinal diseases up to affecting the behaviour of the host via the gut-brain-axis (Biedermann & Rogler, 2015; Burokas *et al.*, 2015; Cryan *et al.*, 2019; Garrett, 2015). As described for gut bacterial communities, maintaining an appropriate mycobiota appears to also be essential for human health (Jiang *et al.*, 2017). Similar to the bacterial microbiota, the fungal component of the gut community can also be disturbed in multiple ways. Treatment with antifungal drugs, for example, can severely alter the composition of the fungal community (some species are reduced but others can expand) causing a severe dysbiosis of the mycobiota (Iliev & Leonardi, 2017; Lamont & Hajishengallis, 2015). Studies have revealed that an imbalanced bacterial microbiota has an impact on numerous diseases (Limon *et al.*, 2017) and the same seems to be true for an imbalanced fungal community (Wheeler *et al.*, 2016).

While about 70 % of the human population carry the fungus *C. albicans* in their intestines (Castillo *et al.*, 2011; Koh, 2017; Schulze & Sonnenborn, 2009), disseminated infections in healthy individuals initiating in the gut are particularly rare (Koh, 2017). In disease related studies, the microbiota, including *C. albicans,* have been associated with conditions causing colitis, like inflammatory bowl disease (IBD) (Richard *et al.*, 2018; Sokol *et al.*, 2017a). IBD is a severe pathological chronic inflammation of the gastrointestinal tract, this condition includes diseases like Crohn's disease (CD) and ulcerative colitis (UC) (Khan *et al.*, 2019). IBD is thought to arise from several factors, involving the host immune system and genetics, environmental components and the intestinal microbiota. Currently there are

no efficient treatments for IBD. But without doubt the micobiota of IBD patients and its dysbiosis plays a role in the severity of the disease. If this microbial imbalance is a cause or an effect of the colitis remains unclear. Several microbiota-modulating risk factors like the use of antibiotics, smoking, and diet have been linked to the pathogenesis of IBD. In animal studies using germfree mice it has been shown that the absence of a microbiota prevents the development of colitis even in mice that are genetically susceptible for IBD (Veltkamp *et al.*, 2001). And the transfer of the microbiota out of an inflamed colon of a diseased animal is able to cause colitis in the before healthy animal receiving the transplant (Ohkusa *et al.*, 2003; Schaubeck *et al.*, 2016). The composition, as well as the diversity of the microbiota plays a role in the disease outbreak and several single species were found to be involved in the severity of the condition. *Fusobacterium*, *Helicobacter*, *Campylobacter*, as well as adherent and invasive *Escherichia coli* species have been reported with a higher prevalence in IBD patients. In several studies a high abundance of the fungus *C. albicans* was reported in IBD patients (Chehoud *et al.*, 2015; Hold *et al.*, 2014; Sokol *et al.*, 2017a). Studies revealed that during acute colitis the diversity of the microbiota is decreased in favour of the fungal part of the community (Lam *et al.*, 2019; Mukherjee *et al.*, 2015; Sokol *et al.*, 2017b). The condition of inflammatory bowel disease is intensively studied and although it is clear that the microbiota is participating in the pathogenesis of the condition, a direct link between the disease and the microbiota is still missing.

Despite the many reports of fungi being a detrimental part of the microbiota, recent studies found evidence that commensal fungi can benefit the host. Jiang *et al*. discovered by using an animal model that the presence of the fungus *C. albicans* in the intestine leads to a decrease of severity in induced colitis. The animals in the study were pre-treated with antibiotics and their reduced microbiota was not able to prevent severe colitis, the addition of *C. albicans* cells, and even parts of the fungal cell wall component, restored the benefits of the healthy microbiota and was functionally able to replace intestinal bacteria. In general, a dysbiosis of the mycobiota has a destabilizing

effect on the whole microbiota and a gut community disrupted by antifungal or antimicrobial drugs is more susceptible to disease.

2. Gastrointestinal colonization by the fungus

2.1 Introduction

Colonization of the human gut by the fungus *C. albicans*

2.1.1 Biology of *C. albicans* in gut colonization

The gastrointestinal tract is a reservoir of *C. albicans* in humans. Most individuals are colonized by the fungus in early childhood and despite the fact that this fungal pathogen is causing hundreds of millions of symptomatic infections every year, in most individuals the fungus persists quietly over the whole lifespan of the colonized individual (Bongomin *et al.*, 2017; Iliev *et al.*, 2012). As mentioned above, controlling the morphology of the fungus, namely the yeast-to-hyphae switch, is of great importance for the pathogenesis of *C. albicans*. This switch, transforming commensal yeast-shaped cells into invasive hyphal-shaped cells, is activated by a long list of settings. The environment of the gut includes several of these conditions that are able to activate the yeast-to-hyphae switch. The temperature of the human body (37 °C), the hypoxic and hypercarbic conditions are reported to induce hyphae formation (Netea *et al.*, 2015). Observing the morphology of *C. albicans* during gastrointestinal colonization has been inconsistent. While *C. albicans* cells recovered from a conventional animal model have been reported to be either 90 % yeast shape (Vautier *et al.*, 2015; White *et al.*, 2007) or 70 % hyphae (Witchley *et al.*, 2019a). Other groups established the term of a GUT phenotype in response to their observation of oval-shaped *C. albicans* cell which were distinctively different from the opaque and yeast form of the fungus (Pande *et al.*, 2013). In studies conducted by our research group using a gnotobiotic mouse model, we predominantly recovered yeast shaped cells from the intestine of the animals (Böhm *et al.*, 2017). The spatial distribution

of *C. albicans* in the different parts of the intestine and the interactions with the host and other gut microbes remain only poorly studied.

2.1.2 Animal models of *C. albicans* gut colonization

Rodents, like rats and mice are the most common mammals used for gut colonization studies. However, the fungus *Candida albicans* is not part of the commensal microbiota of conventional rodents and common laboratory mice are resistant to colonization by *C. albicans*. To allow colonization of these animals by the fungus, the mice have to be treated with a mix of antibiotics prior and during the period of colonization. The antibiotics, which are usually administered in the drinking water of the animals, reduce the microbial load in the gastrointestinal tract and allow *C. albicans* to settle in. Gut colonization is achieved by oral gavage. During this procedure small amounts of liquids are injected directly into the stomach of animals using a gavage needle. Conventional mice have to be supplied with antibiotics during the time course of infection. This experiment is easy to conduct in all animal facilities. One disadvantage is that the treatment with the antibiotic cocktail reduces but does not remove all bacteria. Therefore, the composition of the microbiota remains unknown during the experiment and the same is true for the fungal part of the commensal microbiota. A much more controlled model are gnotobiotic animals, these animals are born and raised in germfree isolators and therefore harbour only the microbe they were infected with. As a consequence all the reactions of the animals during an experiment result from the introduction of the microbe to the gnotobiotic animal. The gnotobiotic mouse model has been established in previous studies involving gut colonization with *C. albicans* (Böhm *et al.*, 2017). The maintenance of a gnotobiotic rodent facility is technically complex and needs specially trained staff, therefore experiments with gnotobiotic animals can only be conducted in sufficiently equipped facilities. Despite the fact that working with gnotobiotic animals is more time and equipment consuming than experimenting with conventional animals, the results might not always recapitulate the whole picture due to the

absence of the commensal microbiota. Both gut colonization models, conventional and gnotobiotic, are commonly used and need to be selected depending on the research question.

Gut microbiota and intestinal immune responses

2.1.3 Overview of intestinal immune response elicited by gut bacteria

In order to protect the organism from invasion of bacteria, which might lead to severe disease, the host has to constantly keep all members of the microbiota in check. The requirement for a healthy host is the balance between tolerating the commensal bacteria and preventing the overgrowth of pathogenic bacteria present in the intestine (Belkaid & Harrison, 2017). To prevent translocation of the microorganisms from the lumen of the gut into the epithelium or even into the blood stream, the host developed effective mechanisms to maintain the required distance. One way the host keeps the distance to the bacteria in the colon is the mucus layer. This physical barrier is produced by specific cells, namely the goblet cells, of the epithelium and the inner mucus layer covering the colon epithelia is devoid of bacteria in a healthy host (Linden *et al.*, 2008). This mucus layer is a physical barrier for invading microbes and the thickness of the layer depends on the presence of the microbiota (Schroeder, 2019b). In other parts of the intestine, like the ileum where the mucus layers are not as prominent as in the colon, antimicrobial peptides, such as lectins and defensins, play a more important role (Antachopoulos & Roilides, 2005). Cytokines and other host-produced molecules are necessary for the recruitment of immune cells like T lymphocytes or neutrophils (Round & Mazmanian, 2009). Recently it has been described that different species of gut bacteria control diverse immunological functions in the host (Kamada *et al.*, 2013; Pickard *et al.*, 2017). The gut commensal *Bacteroides fragilis*, for example, is producing an immunomodulatory polysaccharide (PSA) that enables the host to induce an immune response during inflammation of the

intestine induced by *Helicobacter hepaticus* (Round & Mazmanian, 2009). Inflammation of the gut with *H. hepaticus* leads to increased IL-17, IL-23, and tumor-necrosis factor (TNF) levels. When the host senses the *B. fragilis* produced PSA the T helper cells (T$_H$) express IL-10 and suppresses the production of IL-17, IL-23 and TNF, and by this regulation the host regains control of the intestinal inflammation (Round & Mazmanian, 2009). Also other evidence gained from germfree mouse experiments suggests that bacterial species and the molecules they produce have immunomodulatory effects. Germfree mice with an impaired immune system were only able to benefit from the presence of the microbiota if bacteria from the phyla *Bacteroidetes* were present. Otherwise, the defective immune response of the mice persisted (Ivanov *et al.*, 2008). A more general reaction of the host due to microbial colonization is the production and release of reactive oxygen species (ROS), which kill or repel bacteria (Jones *et al.*, 2012). The gut microbes interact closely with the host, some effects like the production of a thick mucin barrier in the colon or the production of reactive oxygen species (ROS) are broad responses to the colonization of the gastrointestinal tract (Jones *et al.*, 2012). Other effects are induced by single microbes communicating with the host using messenger molecules for signalling.

2.1.4 Intestinal epithelial oxidative stress response during microbial colonization

One way in which the human body reacts to the colonization of microorganisms is the production of reactive oxygen species (ROS). The NADPH oxidase family (NOX) is part of the innate immune system and an important component of the host response. Members of the NOX family are transmembrane proteins that transport electrons across biological membranes, the acceptor of these electrons is usually oxygen and the function of these enzymes is therefore the generation of reactive oxygen species (ROS) (Bedard & Krause, 2007). These oxygen-derived radicals can

interact with numerous lipids, proteins, nucleic acids or inorganic molecules (Brandes *et al.*, 2014). The function of the targeted molecules is usually destroyed by the interaction with ROS, which makes ROS one of the major forces in biological damage (Bedard & Krause, 2007). The production of ROS is not only involved in cellular damage and pathogen killing but also in a lot of regulatory processes and can be found in all types of tissues.

Two well-studied enzymes that are involved in the production of ROS are DUOX1 and DUOX2. The two enzymes were discovered in the thyroid, together with their maturation factors, which are ER proteins called DUOXA1 and DUOXA2 (Grasberger & Refetoff, 2006). DUOX2 can be found in the salivary glands, (Geiszt & Leto, 2004), the airway epithelium (Forteza *et al.*, 2005), and the gastrointestinal tract, including duodenum, colon, and cecum (Ameziane *et al.*, 2005; Dupuy *et al.*, 2000). The DUOX proteins can, in a calcium dependent manner, produce superoxide molecules (O_2^-) which are quickly dismutated to hydrogen peroxide (H_2O_2) (Ameziane *et al.*, 2005; Geiszt *et al.*, 2003; Geiszt & Leto, 2004). This H_2O_2 is then the active agent against bacteria. In the gastrointestinal mucosal epithelium the ROS-dependent defence mechanism against bacteria is achieved by DUOX and the myeloperoxidase produces in neutrophil granulocytes (El Hassani 2005, Leto 2004, Leto 2003). Therefore DUOX2 has been suggested to have an important role in killing bacteria as part of this host defence. While ROS production is a valuable tool to keep the microbiota in check, an overproduction of ROS in the gastrointestinal tract can also have adverse effects on the host. The production of ROS is not only mediated by DUOX but also by other members of the NOX family (NOX1/NOX2), as part of the host response to the microbiota, and the high expression of ROS has been connected with the progression of inflammatory bowel disease and colorectal cancer by DNA-damage (Coussens & Werb, 2002; Itzkowitz & Yio, 2004). Therefore a fine-tuning of ROS-production needs to take place in these mucosal interfaces. While a lack of ROS production allows pathogens to enter the tissues of the host, an overproduction is potentially harmful to the host itself due to the high unspecific activity of the oxygen species.

Microbiota and the circadian clock circuitry

2.1.5 Overview of the circadian clock regulatory circuit

The circadian clock is the internal pacemaker that sustains a rhythmicity of about 24 hours in the body in the absence of any external factors (Fu & Lee, 2003). Organisms from all domains of life, from unicellular bacteria and fungi, over plants or insects up to mammals feature a diverse molecular clock machinery. The mammalian pacemaker is located in the suprachiasmatic nuclei (SCN) of the brain and controls the activity of circadian clocks that can be found in most other peripheral tissues (Mohawk *et al.*, 2012). The circadian clock regulates hundreds of functions in the human body by autoregulatory feedback loops of transcriptional activators and repressors as well as post-translational modifications like phosphorylation, ubiquitination, acetylation, and many more (Asher & Sassone-Corsi, 2015; Partch *et al.*, 2014). Many environmental stimuli have effects on the circadian clock. The most powerful is light. The diurnal rhythm of day and night is so important, it is not only sensed by the eyes of individuals but as well by a subset of melanopsin-expressing retinal ganglion cells reporting directly to the SCN. This way, even most blind individuals maintain a circadian 24 hour rhythm (Hastings *et al.*, 2018). Other environmental factors contributing to the pacemaker are for example the uptake of nutrition or physical activity (Thaiss *et al.*, 2015). Taken together, the circadian clock including all the peripheral clocks in all tissues and organs control all major functions in the body, most importantly the metabolism, the endocrine/renal/cardiovascular systems, cell differentiation and tumor control, the immune system (J. H. Kim *et al.*, 2020; Thaiss *et al.*, 2015). Most of the circadian clock related genes are regulated by negative feedback loops (Sahar & Sassone-Corsi, 2009). Positive regulators like CLOCK and BMAL1 induce the transcription of CLOCK-controlled genes, the corresponding proteins are then repressing their own expression in a negative feedback loop. Additionally, these positive regulators regulate the expression of negative regulators like the cryptochromes (CRY1 and CRY2) and period family (PER1, PER2, and PER3). CLOCK and BMAL1 are transcription

factors that work together by forming a complex to induce expression of the PER and CRY proteins. If the amount of PER and CRY proteins pass a certain threshold in the cell they migrate into the nucleus and block the CLOCK-BAML1 complex from transcription, thereby closing the negative feedback loop. A new loop can only start once the repressing PER and CRY proteins in the nucleus are degraded (Cox & Takahashi, 2019). The circadian rhythm is generated by the core clock genes CLOCK, BMAL1 and the PER and CRY proteins. Some genes controlled by these core clock genes are transcription factors themselves, such as albumin D-box binding protein (DBP), RAR-related orphanreceptor α (RORα) and REV-ERBα. These genes can then again regulate the cyclic expression of other genes (Fontaine *et al.*, 2003; Preitner *et al.*, 2002). The complex transcriptional regulatory circuits are highly diverse and it has been described that the oscillation of transcripts is greatly depending on the tissue type (Akhtar *et al.*, 2002; Panda *et al.*, 2002).

2.1.6 Gut microbiota affects circadian clock regulation

One of the major environmental stimuli shaping the circadian clock circuits besides light is the uptake of nutrients. In several studies containing human or animal subjects, is has been reported that the disruption of the feeding rhythmicity leads to chronic circadian misalignment (J. H. Kim *et al.*, 2020; Morris *et al.*, 2017). This distorted diurnal rhythm results in dysbiosis of the microbiota and metabolic conditions like obesity or diabetes. In humans this has been often reported for frequent international travellers or shift workers (Kervezee *et al.*, 2018; Morris *et al.*, 2017). Eran Elinav (Thaiss *et al.*, 2015) provided evidence that the diurnal variations in the microbial community composition are sufficient to disrupt the circadian oscillators and imbalance the diurnal metabolism of the host, resulting for example in obesity. Built on the knowledge that the intestinal microbiota affects body fat accumulation in mammals, the group of Lora Hooper (Wang *et al.*, 2017) gained insights on which genetic factors contribute to the microbiota-driven metabolic mechanisms of the host. The expression of the circadian transcription factor

Nfil3 is diurnally oscillating in intestinal epithelial cells. The amplitude of produced NFIL3 depends on the microbiota and the core circadian clock transcriptional repressor REV-ERBα. The microbiota acts through NFIL3 and regulates the lipid uptake and storage of the host by the signal transducer and activator of transcription 3 (STAT3). These results provide a clue on how the microbiota or the disruption of the internal circadian clock can lead to metabolic diseases like obesity, diabetes or cardiovascular disease (Weiss & Hennet, 2017).

2.2 Results

C. albicans colonization of the germfree gut

2.2.1 Colonization rate of *C. albicans* in the gastrointestinal tract

To study gut colonization by the commensal fungus *C. albicans*, a gnotobiotic mouse model was used in this study. The experimental model using gnotobiotic NMRI mice (outbred mouse model that was developed by Lynch *et al* 1937 in the Naval Medical Research Institute) for gut colonization was established in collaboration with the research group of Prof. Dr. André Bleich at the Medical University Hospital in Hannover. The 7-to-10 week-old animals of both sexes were orally gavaged with 1 x 10^7 *C. albicans* cells (Figure 3 A) and colony forming units (cfu) recovered from feces were evaluated to monitor the colonization levels in the gastrointestinal tract. Already after a minimum of one day past colonization, the levels of detectable *C. albicans* are around 5 x 10^7 cfu per gram of feces. These counts are consistent in multiple conducted experiments at all evaluated time points (Figure 3 B). To find if there is a preference of *C. albicans* for some particular compartment in the gastrointestinal tract, cfu were evaluated from different parts of the mouse intestine. Although the recovered numbers are slightly lower in the ileum (5 x 10^6 cfu/g feces) the overall fungal burden in the studied organs are comparable (5 x 10^6 cfu/g feces in the ileum to 1 x 10^8 cfu/g feces in the distal colon) (Figure 3 C) and similar to previously described experiments using gnotobiotic mice (Böhm *et al.*, 2017).

2.2.2 Distribution of *C. albicans* cells throughout the digestive tract

Since *C. albicans* can be found in similarly high amounts throughout the intestine of monocolonized animals, the distribution of fungal cells in cross-sections (from epithelium to the lumen) were inspected using microscopy.

Fluorescence *in situ* hybridization (FISH) was performed to distinguish fungal cells from the epithelium or cell debris in the lumen of the intestine. With a *C. albicans* specific fluorescent labelled (Cy3) oligo-nucleotide probe, fungal cells are visible in green, whereas the nuclei of the host tissue are stained with DAPI and therefore visible in blue (Figure 3 D). *Candida* cells can be observed in the lumen as well as in close proximity to the epithelium throughout the intestine. In the ileum few cells can be observed in close contact with the epithelial cells or even in between the ileal villi (Figure 3 D). In the cross-sections of colon samples, *C. albicans* is never found in contact with the host cells. The lumen of a healthy colon is always clearly separated from the epithelial cells by the host produced mucus layers (stained with anti-Muc2 antibody in red). Fungal cells are likely to be found associated with these mucus layers close to the epithelium or randomly distributed in the lumen of the colon (Figure 3 E and F). Colonization of the mouse intestine with *C. albicans* seems to be consistent in terms of numbers throughout the digestive tract, while the localization of the fungal cells varies among different intestine regions.
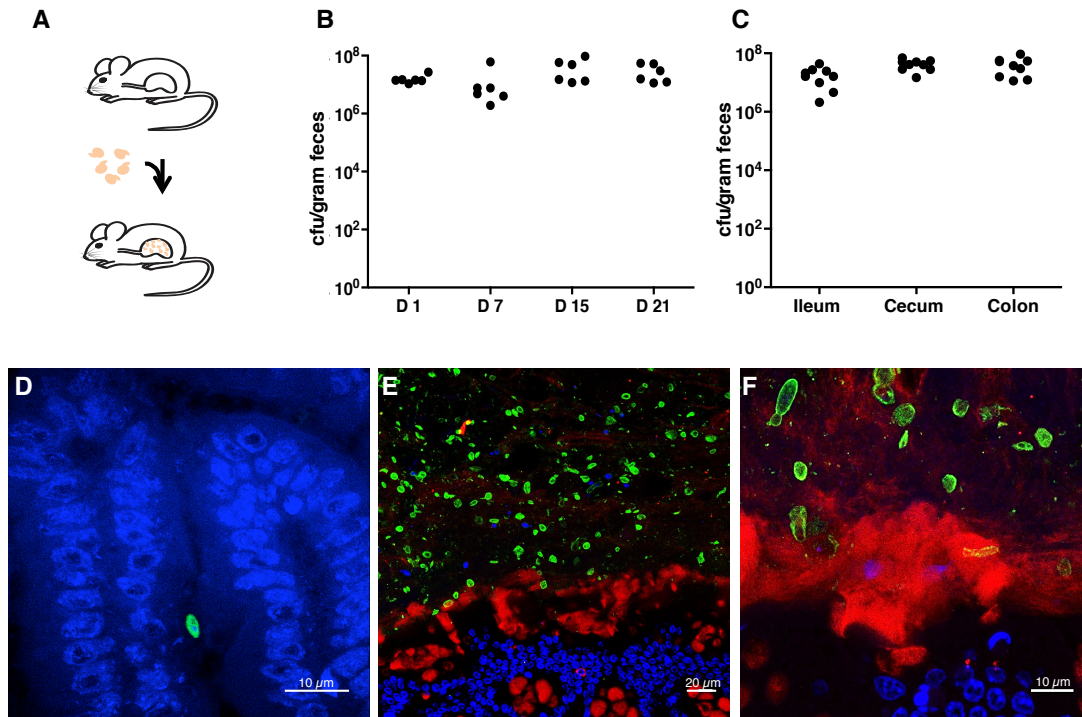
Figure 3: Gastrointestinal colonization of gnotobiotic mice by the fungus *C. albicans*.

To study gastrointestinal colonization, a gnotobiotic mouse model was used. Germfree mice were orally gavaged with a fungal suspension (1 x 10^7 cells/ml) (A) and feces of the infected animals were plated to monitor the fungal burden at different time points (B) and from different parts of the intestine (C). To investigate the distribution of the fungus in the intestine, tissue samples were stained. The fungus, stained green, is colonizing all parts of the intestine, shown here are the ileum (D) and the colon (E and F). In the colon the mucus layer (red) prevents contact of the epithelium by the fungus. In the ileum single fungal cells can be detected deep in between the ileal villi (D).

2.2.3 Morphology of *C. albicans* cells in the murine intestine

C. albicans is a polymorphic fungus and the different morphologies of the fungus have been studied extensively (Gow *et al.*, 2012; Jacobsen *et al.*, 2014). Many virulence traits have been associated with the filamentous form of the fungus (Saville *et al.*, 2003; D. R. Soll, 2014), while the yeast shaped round morphology is mostly found when *C. albicans* is associated with commensalism (Gow *et al.*, 2012; A. H. Soll & Fass, 2003). During

35

monocolonization of the intestine of gnotobiotic animals the round yeast morphology of *C. albicans* was observed almost exclusively; about 95 % of cells were in round shape. (The quantification was done by counting fungal cells in pictures of the colon and ileum from 5 different monocolonized mice, by analysing 5 pictures per sample). This finding is in agreement with previous studies using gnotobiotic mice in a *C. albicans* gut colonization model (Böhm *et al.*, 2017). The morphology was monitored in the ileum and the colon of monocolonized mice. The high prevalence of the yeast morphology present throughout the whole intestine supports the hypothesis of a commensal colonization without harmful effects for the host.

Murine host response to *C. albicans* colonization

2.2.4 Cytokine response

The antifungal host response during infection involves parts of the innate as well as the adaptive immune response (Antachopoulos & Roilides, 2005). We are confident that during the gut colonization of germfree mice with *C. albicans* no dissemination of the fungus into the blood stream did take place and the barrier function of the gastrointestinal tract, which is part of the innate immunity, was not disrupted during monocolonization with the fungus. Because the colonized animals were healthy and showed no sign of disease. Nevertheless, to detect if the host responded to the fungal colonization the levels of seven different cytokines were measured using the Luminex® assay (R&D Systems). The interleukins IL-1α, IL-1β, IL-6, IL-17α, as well as the IL-8 homologs found in mice, CXCL1 and CXCL2, and the granulocyte colony-stimulating-factor (G-CSF) were measured in colon tissue and serum from mice colonized with *C. albicans* and compared to uninfected control animals. In all samples, both for germfree mice and *C. albicans* monocolonized animals, the detected cytokine amounts were low to the limit of detection of the Luminex® assay (Table 1). In the case of the pro-inflammatory cytokine CXCL2, that is produced by epithelial cells (Dinarello, 1997), and IL-17α, which is the regulator of a chemokine recruiting cascade, the amounts of

cytokines were below the detectable threshold in all tested samples. For the other tested cytokines IL-1α, IL-1β, IL-6, and CXCL1 the detected levels were comparably low in mouse colon colonized with *C. albicans* and germfree control animals.

The G-CSF is a part of the innate immunity and is involved in the activation of mature phagocytic cells. In our comparison of germfree and monocolonized colon tissue samples the levels of G-CSF are not changed due to *C. albicans* presence. Although these seven cytokines were chosen because they have been described to be involved in the immune response of the host during fungal infections (Antachopoulos & Roilides, 2005; Richardson & Moyes, 2015; Zhang & An, 2007), none of the chosen seven cytokines show increased presence due to intestinal colonization with *C. albicans*. All cytokine levels were additionally measured in the serum of infected mice. Despite the fact that mice that were colonized with *C. albicans* didn't suffer from disseminated infections, the G-CSF levels of the blood serum of colonized animals were higher compared to the uninfected controls. All other cytokines measured in the serum were very low and close to the detection limit in both of the tested sample types. The colonization of the intestine with the commensal fungus *C. albicans* seems to not globally induce cytokine production in the host.

Table 1: Cytokines measured in colon tissue and serum (as indicated) of gnotobiotic and *C. albicans*-infected animals.

Cytokine	Uninfected pg/ml	*C. albicans*-infected pg/ml
CXCL1	33.15 (±3.18)	22.31 (±1.34)
IL-1α	53.89 (±7.47)	41.23 (±9.36)
IL-1β	134.28 (±15.05)	97.72 (±44.79)
IL-6	10.08 (±4.09)	8.66 (±0.55)
G-CSF	18.98 (±5.34)	13.69 (±2.33)
G-CSF Serum	5.22 (±3.48)	101.23 (±110.41)

Shown is the mean gained by analysing the colon tissue/serum of n=6 animals ± SD, all measurements were performed in technical duplicates.

2.2.5 Transcriptome profiling of colon tissue

To detect host response changes due to *C. albicans* gut colonization on the transcriptional level, RNAseq of colon tissue was performed. Colon tissue samples from gnotobiotic monocolonized mice were compared to colon tissue collected from germfree mice (n= 4). The RNA was extracted from 1 cm long part of the proximal colon. After extraction of the RNA, the library preparation and sequencing of the samples was performed by GATC Biotec AG, Konstanz, Germany. The single-end Illumina sequencing produced between five and 15 million reads per sample. The 50 bp long reads were clipped, quality checked, and around 90 % of the sequenced reads were able to be mapped to the mouse genome, the analysis was performed using the DESeq2 (Love *et al.*, 2014) package in R studio. Overall the reaction of the host was rather mild, given that the highest detected fold change in the dataset is ± 2. Table 2 shows a list of all genes regulated with a *p*-value of 0.01 or lower. The MA plot (Figure 4) shows the distribution of the 33 genes that showed different levels comparing germfree and *C. albicans*-colonized mice. Five of these genes that encode for immunoglobulins are up-regulated in the infected samples. This indicates that, although the host response is only moderate, still some genes of the defence mechanism of the host are activated. These

results are in agreement with the cytokine measurements we performed and described above. The reaction of the host to the gastrointestinal colonization with the fungus is very mild and is not inducing strong inflammatory responses as we can see only little cytokine production and relatively small changes in the transcriptome. Striking as well is the abundance of genes associated with the circadian clock circuitry in our list of differentially expressed genes. In total nine of the 33 significantly regulated genes are known to be involved with the circadian clock. Additionally, the two DUOX genes, which are known to be involved in the oxidative stress response of the host during bacterial colonization, were among the up-regulated genes in the presence of *C. albicans*. The transcriptomic profile of colon tissue samples from mice colonized with *C. albicans* are only marginally different from germfree control animals. This supports the hypothesis that the fungus colonizes as a commensal in healthy individuals and is not provoking strong immune responses.
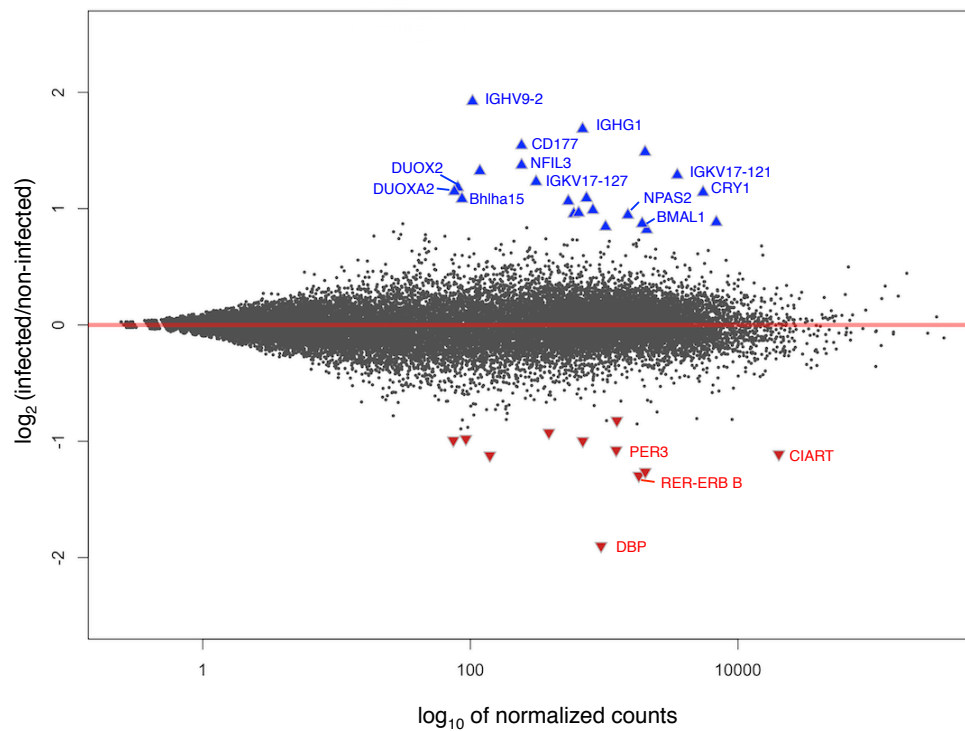
Figure 4: Overview of the transcriptomic data comparing germfree to *C. albicans*-colonized colon samples.

The MA plot shows the expression of all mouse genes in an infected/non-infected ratio. Every dot indicates a mouse gene; the coloured triangles indicate that the expression difference of the gene is significantly different (p-value ≤ 0.01) in the compared sample types. Red symbols indicate down-regulation of the gene in *C. albicans* presence, symbols displayed in blue show genes that are up-regulated in colon tissue of mice when they are colonized with the fungus.

Table 2: Transcripts with significantly different levels in colon tissue of germfree or *C. albicans*-colonized mice.

Genes significantly (*p*-value ≤ 0.01) regulated during fungal colonization of the intestine. Marked in blue are genes previously described in the circadian clock circuitry and highlighted in yellow genes potentially involved in the oxidative stress response to the host during microbial colonization.

log$_2$ fold change (inf./non-inf.)	Name	Function	OMIM	Mouse gene ID
1.92	IGHV2-9	immunoglobulin heavy variable 2-9	600949	ENSMUSG00000096638
1.69	IGHG1	immunoglobulin heavy constant gamma 1	147100	ENSMUSG00000076614
1.54	CLCA4B	chloride channel accessory 4B	616857	ENSMUSG00000074195
1.49	CD177	CD177 antigen	162860	ENSMUSG00000052212
1.37	NFIL3	nuclear factor, interleukin 3, regulated	605327	ENSMUSG00000056749
1.32	IGKV17-121	immunoglobulin kappa variable	146980	ENSMUSG00000076514
1.29	DUOX2	dual oxidase 2	606759	ENSMUSG00000068452
1.23	DUOXA2	dual oxidase maturation factor 2	612772	ENSMUSG00000027225
1.18	Pla2g2a	phospholipase A2, group IIA	172411	ENSMUSG00000058908
1.15	IGKV17-127	immunoglobulin kappa light chain variable	146980	ENSMUSG00000076508
1.14	FOS	FBJ osteosarcoma oncogene	164810	ENSMUSG00000021250
1.09	CRY1	cryptochrome 1	601933	ENSMUSG00000020038
1.08	Bhlha15/Mist1	basic helix-loop-helix family, member a15	608606	ENSMUSG00000052271
1.06	SLC30A10	solute carrier family 30, member 10	611146	ENSMUSG00000026614
0.99	STEAP4	metalloreductase STEAP4	611098	ENSMUSG00000012428
0.96	CECAM1	carcinoembryonic antigen-related cell adhesion molecule 10	109770	ENSMUSG00000054169
0.96	DHRS9	dehydrogenase/reductase	612131	ENSMUSG00000027068
0.95	NPAS2	Neuronal PAS domain protein 2	603347	ENSMUSG00000026077
0.88	TFRC	transferrin receptor	190010	ENSMUSG00000022797
0.87	ARNTL/BMAL1	aryl hydrocarbon receptor nuclear translocator-like	602550	ENSMUSG00000055116
0.84	TRIM40	tripartite motif containing protein 40	616976	ENSMUSG00000073399
0.82	DUSP1	dual specificity phosphatase 1	600714	ENSMUSG00000024190
-0.82	CLDN4	claudin 4	602909	ENSMUSG00000047501
-0.93	GJB5	gap junction protein, beta 5	604493	ENSMUSG00000042357
-0.98	ABCC2	TP-binding cassette, sub-family C	601107	ENSMUSG00000025194
-0.99	IQCH	IG- motive containing protein	612523	ENSMUSG00000037801
-1.01	MAL	myelin and lymphocyte protein	188860	ENSMUSG00000027375
-1.08	PER3	period circadian clock 3	603427	ENSMUSG00000028957
-1.11	CA1	carbonic anhydrase 1	114800	ENSMUSG00000027556
-1.12	CIART	circadian associated repressor of transcription	615782	ENSMUSG00000038550
-1.26	TEF	thyrotroph embryonic factor	188595	ENSMUSG00000022389
-1.31	NR1D2,REV-ERBβ	nuclear receptor subfamily 1	602304	ENSMUSG00000021775
-1.90	DBP	D site albumin promoter binding protein	124097	ENSMUSG00000059824

2.2.6 Regulators of the circadian clock program

In the analysis of the transcriptome data from colon tissue, several genes of the circadian clock circuitry were differentially regulated, due to the presence of *C. albicans* in the intestine of mice. Genes like *Per3* and *Cry1* are well-studied regulators that are involved in several oscillating mechanisms throughout the body. Additionally transcriptional regulators (*Dbp, Nfil3*) and transcriptional repressors (*Rev-erbα, Ciart*) of circadian clock genes were significantly regulated in *C. albicans* presence in the colon. In each peripheral organ or even in different tissues, the oscillatory cycles involve different genes. And so far there is not much known about the circadian rhythms of the lower digestive tract. Comparing the results of the RNAseq experiment to literature, we found that it was described before that in the liver of mice the circadian regulators *Nfil3* and *Rev-erbα* repress each other (Duez *et al.*, 2008; Mitsui *et al.*, 2001). In our data set the *Nfil3* expression is up-regulated in the *C. albicans*-infected animals whereas *Rev-erbα* expression is lower. This indicates that the high abundance of differently regulated circadian clock genes in our dataset is not random but rather follows the patterns that have been previously described. The group of Lora Hooper (Wang *et al.*, 2017) recently made the connection that the gut microbiota is regulating the lipid storage of the host in dependence of the circadian clock circuitry. They measured the *Nfil3* levels in germfree mice and compared them to samples from conventional mice. The expression of the *Nfil3* gene is significantly lower in sterile mice compared to mice harbouring a conventional microbiota. We found the same expression change in our dataset: Mice colonized only with the fungus *C. albicans* showed much higher expression of *Nfil3* compared to the germfree controls. This suggests that colonization of the intestine by a single fungal species can achieve similar transcriptional changes as previously observed for the whole microbiota.

For the transcriptomic analysis we used tissue of the whole colon. To detect in more detail which cell types expressed specific proteins in different locations, further methods were applied. To detect the NFIL3 and REV-ERBα

expression on the protein level and to observe the distribution of the proteins in the colon tissue, we stained colon sections with antibodies against NFIL3 or REV-ERBα. Using an antibody against NFIL3 protein on colon tissue samples from germfree and *C. albicans* monocolonized animals, a clear pattern of distribution was observed. The NFIL3 protein is mostly found on the bottom of the crypts in the colon of both colonized and un-colonized animals, but the number of crypts expressing NFIL3 is higher in animals colonized with *C. albicans* (Figure 5 A and B). The average number of crypts producing NFIL3 in colonized mice is around 30 %. In germfree mice only around 10 % of the crypts show an NFIL3 signal (Figure 5 C). The higher abundance of NFIL3 in colonized animals is in congruence with the results of our transcriptomic data, as well as the findings of the Hooper lab (Figure 5 D).
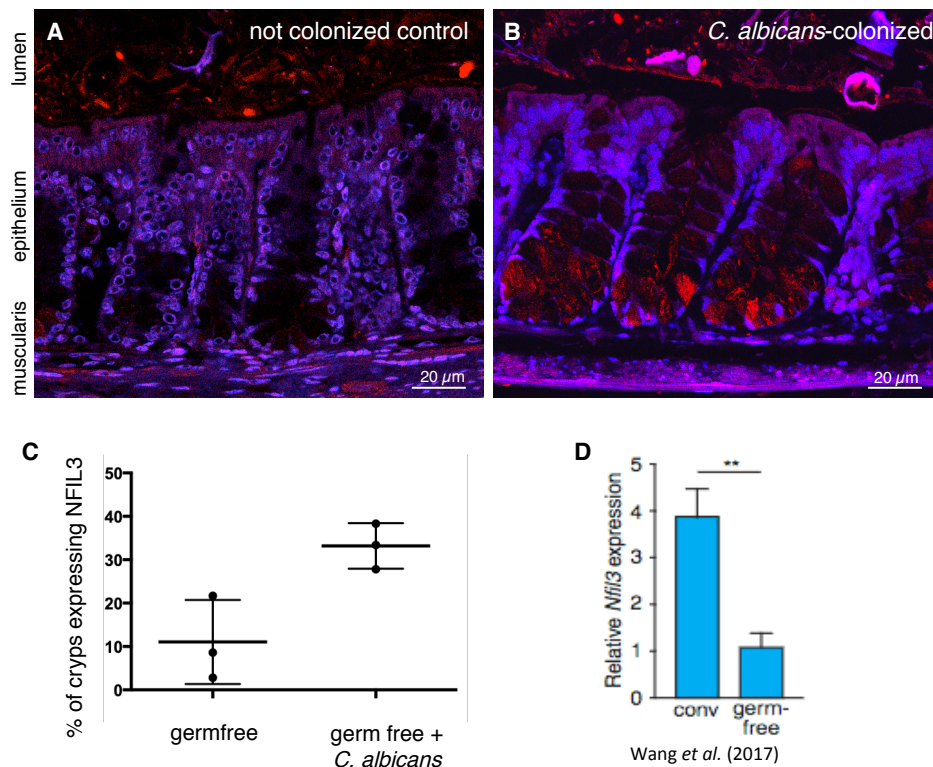
Figure 5: Expression and spatial distribution of the circadian clock regulator NFIL3 in gnotobiotic animals colonized by *C. albicans*.

The spatial distribution of the circadian clock regulator NFIL3 in colon tissue of germfree (A) and *C. albicans* colonized animals (B) was investigated by immunofluorescent staining. NFIL3 (red) is located at the basal side on the bottom of the colonic crypts (A and B). The amount of detected NFIL3 is higher in colonized animals when compared to sterile control colon sections (C). This correlates with previous published data (Wang *et al.*, 2017) (D) and with the transcriptomic data we obtained from mouse colon (Table 2).

The REV-ERBα protein is a repressor of the *Nfil3* gene. In our transcriptomic dataset the *Rev-erba* expression was lower in *C. albicans* presence, whereas the NFIL3 gene was expressed at higher levels. To detect changes in the REV-ERBα protein level and its location we used an antibody against REV-ERBα on colon tissue. The protein was distributed in the apical epithelium in close proximity to the gut lumen in both colonized and germfree mice samples (Figure 6 A and B). Additionally, in a higher magnification, it was observed that in germfree animals the REV-ERBα signal was co-localized with the nuclei of the epithelial cells (Figure 6 C), whereas in animals colonized with *C. albicans,* the REV-ERBα signal seemed to localize in the cytoplasm of the

epithelial cells (Fig 6 D). For other proteins of the circadian clock circuitry it has been described that the protein localization oscillates between cytoplasm and nucleus and thereby the functionality of the protein is oscillating (Griffin *et al.*, 1999; Kume *et al.*, 1999). The localization shift of the protein REV-ERBα might be important for its role in the circadian clock, as it might affect the activity of the protein as a repressor.
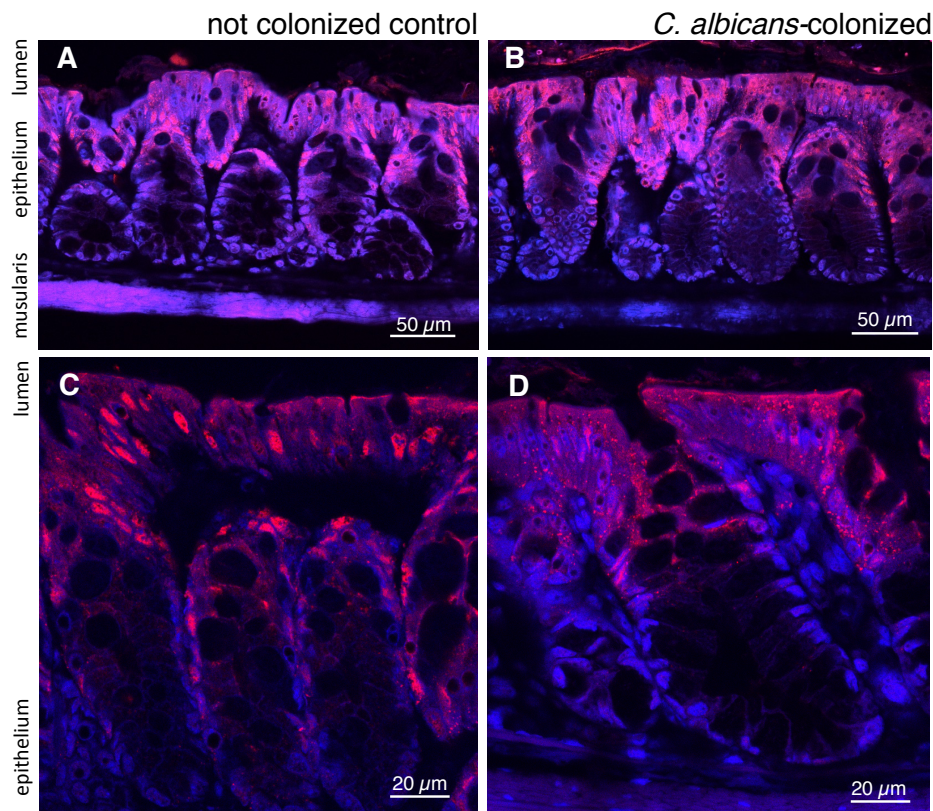
Figure 6: Spatial distribution of the circadian clock repressor REV-ERBα in colon tissue of gnotobiotic and *C. albicans*-colonized mice.

The localization of circadian clock repressor REV-ERBα (red) was visualized using immunohistochemistry staining on colon tissue of germfree (A and C) and *C. albicans*-colonized mice (B and D). Localization of the protein to the apical epithelial cells, close to the lumen was not altered due to the fungal colonization. In higher magnifications (C and D) REV-ERBα signal was detected mostly in the nuclei of the epithelial cells in the germfree sample (C), whereas it is located in the cytoplasm of the apical epithelial cells in colonized tissue (D).

2.2.7 Oxidative stress response

It has been reported that DUOX2/DUOXA2 are involved in the oxidative stress response of the host mucosae during bacterial colonization (Ameziane *et al.*, 2005; Carvalho & Dupuy, 2013). Comparing transcriptomic data from mouse colon colonized with *C. albicans* and germfree tissue, the two genes *Duox2* and its maturation factor *DuoxA2* were significantly more expressed in colonized animals (Table 2). To observe the exact location where the *Duox2/DuoxA2* genes were transcribed in the colon tissue, fluorescence *in situ* hybridization (FISH) with RNA probes was performed (RNA FISH). With this highly sensitive experimental setup, every RNA copy of a specific gene is amplified with a fluorophore and can be detected and visualized with a confocal microscope. The method was used on both germfree colon tissue and *C. albicans*-colonized colon tissue. The distribution of the maturation factor *DuoxA2* transcripts are similar in both sample types, the red dots of the single transcripts are located throughout the whole epithelium without any preference (Figure 7 A and B). The distribution of the *Duox2* transcripts, however, is significantly different comparing germfree tissue and *C. albicans*-colonized colon. The expression of the gene is taking place in the apical epithelium close to the lumen and is visually higher in tissue samples colonized with *C. albicans* (Figure 7 B). Predominantly the apical epithelial cells, that are the closest to the fungal cells in the lumen of the colon, express the *Duox2* gene in infected as well as in not-infected colon tissue. The higher abundance of detectable RNA copies point to the same conclusion as the transcriptional data and indicates that the colonization of the intestine with the fungus *C. albicans* can activate mechanisms that have before only been described to be activated by the commensal microbiota (Cheng *et al.*, 2012).
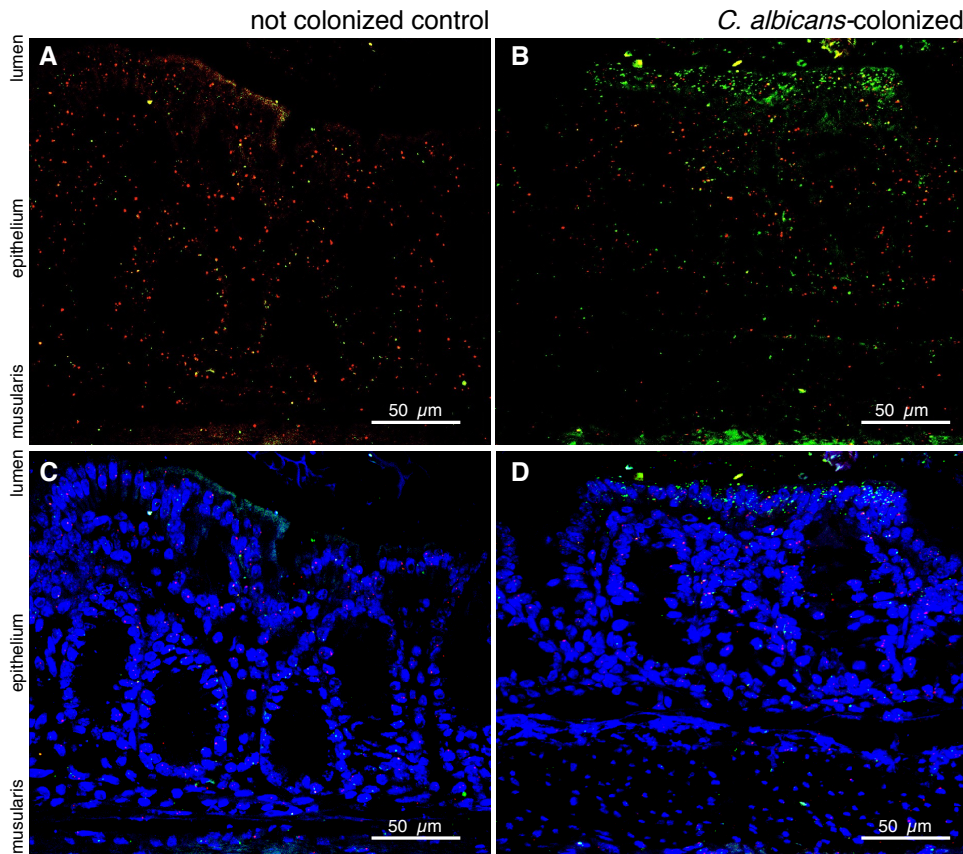
Figure 7: *Duox2/DuoxA2* expression changes in colon tissue colonized with the fungus *C. albicans*.

Single mRNA transcripts of the genes *Duox2* (green) and *DuoxA2* (red), were stained in colon tissue of germfree (A and C) and *C. albicans*-colonized mice (B and D) using RNA FISH. Distribution of *Duox2* in the colon epithelium is localized close to the lumen of the colon of infected animals (B and D). In germfree animals the detected signal appeared lower (A and C).

In liver and kidney cells the oxidative stress response has been described to be controlled by the D-Box-binding protein (DBP) that is part of the circadian clock circuitry (Cho *et al.*, 2013; Gachon *et al.*, 2006; MacFie *et al.*, 2014). In our transcriptomic dataset the expression of *Dbp* was significantly lower in mice colonized with *C. albicans* compared to the germfree control (Table 2). To visualize the distribution of the *Dbp* expression, RNA probes for the *Dbp* transcript were used in a RNA FISH experiment. The distribution of the *Dbp* expression was not altered in the colon tissue samples due to *C. albicans* colonization (Figure 8 A and B). The presence of the *Dbp* RNA is highly co-localized with the nuclei of the epithelium. This did not change due to the

47

fungal colonization. Maybe, unlike in liver or kidney cells, the oxidative stress response is not dependent on *Dbp* in the intestine.

The overlay of the three used probes in the RNA FISH experiment, *Duox2*, *DuoxA2*, and *Dbp* (Figure 8), summarize the above mentioned findings: The *Duox2* gene is expressed primarily in the apical epithelial cells close to the lumen, especially during the colonization of the intestine with *C. albicans*; the maturation factor *DuoxA2* is constitutively mild expressed throughout the whole colon tissue, and the *Dbp* expression as well is constitutively present in the whole colon tissue (Figure 8 C and D).
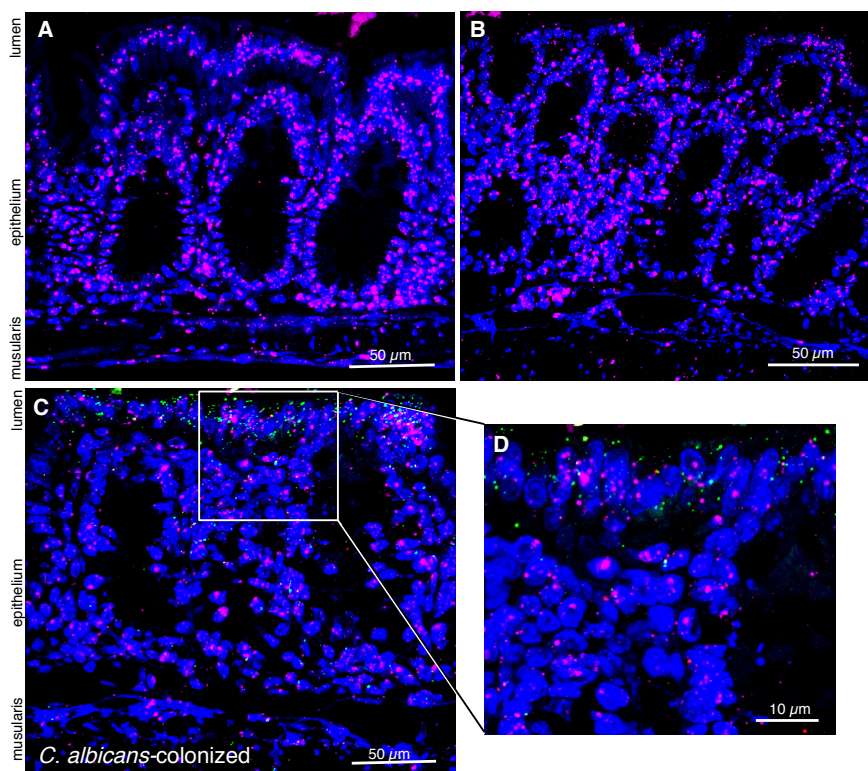
Figure 8: Expression of the circadian clock transcription factor DBP in colon tissue of germfree and *C. albicans*-colonized mice.

Dbp expression in colon tissue was investigated by staining single *Dbp* mRNA transcripts with the RNA FISH method. The signal of the expression of *Dbp* (purple) was not changed comparing germfree tissue (A) and *C. albicans*-colonized tissue (B). The localization of the transcripts was mostly in the nucleus of the epithelial cells (D). A merged picture shows the distribution of *Duox2* mRNA (green), its maturation factor *DuoxA2* mRNA (red) and the *Dbp* mRNA (purple) (C and D) that we hypothesized to be involved in the oxidative stress response of the *Duox2/DuoxA2* genes in mouse colon colonized with the fungus *C. albicans*.

To have a more flexible model for the *Duox2* expression, without the need of animals, we established a model with a human colorectal adenocarcinoma cell line. The C99 cell line has been reported previously to express DUOX2/DUOXA2 protein and release H_2O_2 (MacFie *et al.*, 2014). Using the cell line, several approaches were followed. To investigate if an up-regulation of the *Duox2/DuoxA2* genes is taking place in the C99 cells due to the presence of *C. albicans*, RNA of the cell line was collected for qPCR. Additionally, to validate the abundance of DUOX2 protein in the C99 cells, samples for western blots were collected. To find out what causes the up-regulation of *Duox2*, multiple experiments were performed, infecting the C99 cell layer with *C. albicans* cells, heat inactivated *C. albicans* cells, *C. albicans* cell wall protein mannan, sterilized feces and, as a positive control, the cells were treated with 5-aminosalicylic acid (ASA), which was used in the previous study of Andrew Silver (MacFie *et al.*, 2014). ASA is a chemical that is commonly used for the treatment of ulcerative colitis. This anti-inflammatory drug is scavenging reactive oxygen species (ROS). These ROS, particularly H_2O_2, causes single and double-strand breaks in DNA, causing cellular transformations that can lead to cancer (Sedelnikova *et al.*, 2010). The functional mechanism of the drug was found to be rather paradox. The treatment of C99 cells with ASA increased the expression of the *Duox2* gene in the study by Andrew Silver (MacFie *et al.*, 2014), which would be expected to lead to increased H_2O_2 production. In our experimental procedures, we used ASA as a positive control for induction of the DUOX2 protein production. Using a western blot-based method we detected decreased production of the DUOX2 protein in the presence of ASA (Figure 9). No differences in the amounts of DUOX2 were observed in the C99 cells threated with live *C. albicans* cells, fungal cell wall proteins or sterilized intestinal content. Also changes in incubation times and concentrations did not lead to different amounts of DUOX2 protein.

In a similar experimental setup, we performed qPCR on RNA that was extracted from the C99 cell line under different conditions to detect *Duox2* expression. The incubation of the C99 cell line with ASA led to a decrease of

Duox2 gene expression, this is in conclusion with our experimental output of the western blots, but diametrically opposite to the findings of Andrew Silver. The treatment of the cell line with *C. albicans* cells, fungal cell wall proteins or sterilized intestinal content did not result in up-regulated *Duox2* expression in the cells. Due to the different reaction of the C99 cells compared to the mouse colon, our intention to use this cell line as a model to gain insights into what part of the fungus (secreted molecules, cell wall structures) are triggering the changes in RNA expression, that we observed in the transcriptomic analysis, unfortunately remained unsatisfied.
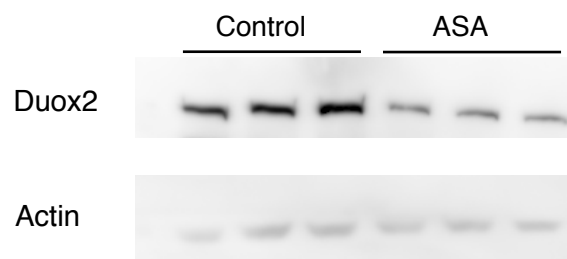
Figure 9: Western blot of DUOX2-release of C99 cell line cells.

The expression of *Duox2 in vitro* in a colon adenocarcinoma cell line (C99) was reduced by the treatment with 5-aminosalicylic acid (ASA). Three biological replicates were loaded per sample, the expression was detected by western blot using the antibodies listed in Table 6.

2.3 Discussion

C. albicans is one of the most prominent fungi found associated with the mammalian body and can colonize all body orifices. While previous studies mostly focused on the pathogenesis of *C. albicans*, I have investigated the commensal lifestyle of this fungus in the gastrointestinal track of gnotobiotic mice. Although the fungus is known to be able to disseminate from local infection sites into the blood stream of patients, which causes them to suffer life-threatening infections, the fungus persists commensally in healthy humans for the whole lifespan of the individuals without causing any complications.

Extensive research has been carried out to unravel how the fungus, under some conditions, becomes a lethal pathogen. However, there is limited knowledge about the lifestyle of *C. albicans* in the gastrointestinal tract. In this chapter of my dissertation, I have investigated how the host responds to colonization of the gut with the fungus. Additionally, I examined the spatial distribution and morphology that *C. albicans* adopts in the gastrointestinal tract.

In our study we used gnotobiotic animals to monitor *C. albicans* in the gut of mice. Conventional rodents are resistant to the colonization by the fungus due to their indigenous microbiota. Only the administration of an antibiotic drug cocktail, before and during the colonization of the fungus, depletes the microbiota to the extent that the fungus can permanently colonize the gut. We aimed to determine the specific response of the host to the colonization of *C. albicans*; therefore, antibiotic-treated conventional animals were not ideal for our study. Instead we used mice that were born and raised under sterile conditions. These gnotobiotic animals only carry microbes to which they were deliberately exposed to. As described before by Böhm *et al.* (2017), during the colonization of the gastrointestinal tract with *C. albicans* the mice showed no sign of disease and behaved completely normal. The fungal burden we observed in our animals is comparable to that of previously published data in gnotobiotic gut colonization models of *C. albicans* (Böhm *et al.*, 2017; Phillips & Balish, 1966). Within 24 hours after inoculation, *C. albicans* establishes

colonization of the gut, which remains stable over the course of at least three weeks. Although there are no competing microbes present, the fungal numbers do not increase any further than 5 x 10^7 cfu/g in any examined part of the gastrointestinal tract.

The gnotobiotic gut colonization model that we used in our studies show consistent colonization of the gut with the fungus *C. albicans*, that adopts the round yeast morphology, which is associated with commensalism. The morphology of the polymorphic fungus is an indicator of the lifestyle of *C. albicans*. The round yeast morphology is associated with commensalism whereas the hyphal forms of the fungus are typically associated with pathogenesis. The observation of the morphology can therefore provide valuable information regarding the lifestyle of the fungus. In our gnotobiotic animals monocolonized with *C. albicans* we predominantly observe the round yeast morphology of fungal cells (Figure 3 E). This is in agreement with previous work published by our research group (Böhm *et al.*, 2017; Pérez & Johnson, 2013). In other studies, however, the encountered morphologies of the fungus in the gut differ from each other, especially when using conventional, antibiotic treated animals. The morphology observations using the conventional mouse model have been reported to be 90 % yeast shape (Vautier *et al.*, 2015; S. J. White *et al.*, 2007), 70 % hyphae (Witchley *et al.*, 2019a) or mostly in the GUT phenotype (Pande *et al.*, 2013). These results indicate that different colonization models can lead to different observations of the *C. albicans* morphology.

In order to investigate the host reaction to commensal fungal colonization, we measured the levels of seven cytokines that have been described, to be released during fungal infections. While cytokine levels in the colon were either below the detection limit or unchanged upon *C. albicans* colonization, the serum of the colonized animals showed increased levels of G-CSF. G-CSF is a necessary molecule for the maturation of phagocytic cells, the enrichment of the molecule was only detected in the serum of the colonized animals but not locally in the colon tissue. Overall, the cytokine survey suggests that the colonization of the gut of gnotobiotic mice with the fungus *C.*

albicans did not induce massive cytokine production, at least of those molecules previously found to be activated in fungal infections. This would support the hypothesis that *C. albicans* is growing strictly as a commensal in our experimental setup, because there was no evidence of any strong immune response.

Because the levels of several cytokines were below the detection limit, we chose to also apply a more sensitive approach, namely RNA sequencing. This analysis revealed a very mild response of the host to the gastrointestinal colonization. The transcriptomic data shows five immunoglobulin gene transcripts and the antigen CD177 significantly up-regulated in the colon of *C. albicans*-colonized mice. This finding indicates that the presence of the fungus in the gastrointestinal tract is not unrecognized by the host and that some aspect of the adaptive immune system is activated. One of the more surprising findings, however, was that nine of 33 genes with differential expression (*p*-value of 0.01) in our dataset were directly connected to the circadian clock circuitry. Even core clock genes like *Bmal1*, *Per3* and *Cry1* belong to the list of genes that were regulated differently due to *C. albicans* presence in the gut. In the colon, genes of the circadian clock circuitry have been connected to the progression of colorectal cancer (Karantanos *et al.*, 2014) as well as the uptake and storage of lipids (Wang *et al.*, 2017). So far it has not been described that the colonization of the gut by *C. albicans* impacts the circadian clock circuitry. However, many of the circadian clock-related genes, that we found differently regulated in our dataset, have been described previously. In immune cells, for example, it was reported that NFIL3 and REV-ERBα proteins repress each other`s gene expression (Gachon *et al.*, 2006; Weger *et al.*, 2019) and a REV-ERBα increase leads to an increase of the DBP protein in liver cells (Narumi *et al.*, 2016). Although this has not been shown for colon tissue, we see *Rev-erba* and *Dbp* down-regulated while *Nfil3* is up-regulated in the colon tissue colonized with *C. albicans*. Additionally, increased *Nfil3* levels in the colon have been described before in the presence of the conventional microbiota, when compared to germfree animals (Wang *et al.*, 2017). The increase of *Nfil3* mRNA was shown to be due to the

microbiota. Our results, on the other hand, indicate that a single member of the microbiota, namely the fungus *C. albicans*, is sufficient to activate the expression of *Nfil3*. Previously, it has been described that an increase in *Nfil3* expression controls a lipid metabolic program. By that the gastrointestinal microbes control the lipid absorption in the gastrointestinal tract and the export of the lipids in intestinal epithelial cells via the induction of *Nil3* expression (Wang *et al.*, 2017).

For the transcriptomic analysis we used whole colon tissue. To find out more specifically where in the tissue *Nfil3* and *Rev-erba* are expressed, we used immunohistochemistry. We could clearly see that the NFIL3 protein is located on the basal site, at the bottom of the crypts (Figure 5 B) and that significantly more crypts in the colon contain NFIL3 protein in the presence of *C. albicans* (Figure 5 C). For the REV-ERBα protein no significant difference was observable in the colon tissue of gnotobiotic and *C. albicans* colonized animals, however, the location of the protein in the colon tissue was mostly close to the lumen of the colon in the outer epithelial cells. Additionally, we observed a shift of the localization of the REV-ERBα protein in the cell depending on the colonization status. In germfree animals, the protein was located in the nuclei of the cells, whereas the protein seemed to be more likely to be distributed in the cytoplasm of the outer epithelial cells when the animals were colonized with *C. albicans*. Many proteins migrate in between the cytoplasm and the nucleus of a cell, *e.g.* transcription factors/repressors, thereby regulating their activity. Taking into account that *Rev-erba*, a transcriptional repressor, is localized differently in colonized and germfree mice, the activity of the factor might be regulated in response to the presence of the fungus. Knowing that *Nfil3* is one of the target genes of REV-ERBα, we presume that in colon tissue of germfree animals REV-ERBα is located in the nucleus actively suppressing *Nfil3* expression, whereas in tissue colonized with *C. albicans* there would be up-regulation of *Nfil3* expression due, at least in part, to the switch in localization of the REV-ERBα protein towards the cytoplasm.

The dual oxidase DUOX2 and its maturation factor DUOX2A have been suggested to be involved in the production of ROS as part of the innate immunity. As described before, *Duox2* is expressed in mucosal surfaces, like the upper airways, in epithelial cells close to the lumen where the microbes are located (Cho *et al.*, 2013). The expression of *Duox2* in the colon has been reported to be induced by the microbiota (Sommer & Bäckhed, 2015). The evaluation of our transcriptomic dataset, however, demonstrates that the presence of a single fungal species, *C. albicans*, is as well sufficient to induce this expression. Additionally, we examined the location of the *Duox2* expression in the colon tissue of mice monocolonized with *C. albicans*. Through FISH we were able to show that the expression of the *Duox2* transcript was enriched during fungal colonization and distinctly localized in the cells of the outer epithelium, close to the lumen of the colon, while the location and amount of the maturation factor *Duox2A* transcripts did not alter during colonization by the fungus.

In order to identify the component of *C. albicans* that leads to *Duox2* induction, we performed cell-line based experiments. Therefore, we used the C99 colon carcinoma cell line that is able to produce H_2O_2. After the treatment of the C99 cell line with *C. albicans* cells, fungal cell wall proteins or sterilized intestinal content we evaluated the *Duox2* expression in the cells of the cell line by qPCR and western blot, however, could not observe any differentiated *Duox2* expression. If this was due to the marginal RNA/protein changes, insufficient binding of qPCR primers or antibody or the experimental set up needs to be evaluated further. Although we incorporated an already described positive control we were only able to obtain directly opposite effects of the DUOX2 production due to the control compared to the previously documented ones. Even though cell-line experiments have the advantage to be easier, cheaper, faster, less ethically challenging than mouse-experiments, this particular model was found not to be appropriate to address our question.

In conclusion, we established a stable monocolonization system of gnotobiotic animals with the fungus *C. albicans* and discovered that the colonization of the gut with one single fungal species can induce *Nfil3* and *Duox2* expression,

which before had only been shown to be induced by the collective commensal microbiota. Additionally, the transcriptomic dataset provided an interesting lead on the potential involvement of a commensal fungus in inducing the mammalian circadian clock circuitry.

3. Fungal - bacterial interactions in the mammalian gut

3.1 Introduction

Fungal – bacterial interactions in the mammalian host

3.1.1 Interplay between fungi and bacteria in the context of human health and disease

Interactions between fungi and bacterial species can be found wherever the two species grow in the same niche. On the host, this is mostly the case for the skin and mucosal surfaces like the mouth, the gastrointestinal tract or the lower female reproductive tract (Peleg *et al.*, 2010). These interkingdom interactions can occur in different ways: via direct physical cell-to-cell contact, or indirect either by secretion and recognition of chemical molecules or by changes of the environment, like a change of the pH (Power *et al.*, 2014). Looking at cross-kingdom interactions, especially the lifestyle of the mixed biofilm has been studied intensively. The microbial species growing in mixed biofilms mostly have synergistic effects on each other and the structure of the biofilm protects the microbes from different environmental stresses, like mechanical stress, drugs or antimicrobials produced by the host, drought, starvation and many more. In general, cross-kingdom interactions can be synergistic or have antagonistic effects on the growth of the bacteria or the fungus or both (Frey-Klett *et al.*, 2011).

Interactions between different microbes are usually observed whenever bacteria and fungi compete for the same source of nutrients or for the same space in a limited environment. In the oral cavity, *Streptococci* can cause common oral denture stomatitis. In a mixed biofilm with *Candida* species they co-aggregate strongly and form dental plaques that lead to further complications. The *Streptococci* physically interact with the *Candida* cells by cell surface receptors and the fungus produces adhesins to strengthen the cohesion between the growing biofilm and saliva-covered surfaces (Koo *et al.*,

2018). The pathogenic bacterium *Pseudomonas aeruginosa* and the fungus *C. albicans* both have been reported to thrive and cause infections at many different host sides, like in burn wounds on the skin or lung infections, especially during chronic diseases like cystic fibrosis (Delhaes *et al.*, 2012). *P. aeruginosa* has an antagonistic effect on *C. albicans* and represses the growth of the fungus *in vivo*. This detrimental effect has been observed to be even more severe when the fungus grows in its filamentous form (Lauer *et al.*, 2007).

Whenever two opportunistic pathogenic species grow as symbionts, the outcome for the host is usually worsened, especially if the microbes form biofilms. These mixed species biofilms are often found on medical devices like catheters or implants and can cause nosocomial infections in patients (Curvale-Fauchet *et al.*, 2004). Clinically relevant fungi and bacteria colonize these medical devices and the treatment of these mixed species biofilms is not only aggravated because the microbes that are causing the infection are from different phyla, but also their lifestyle as a biofilm makes the treatment even more difficult (Klotz *et al.*, 2007). Within the biofilm, the microbes can communicate easily by *quorum sensing*, due to their close proximity. This crosstalk via the exchange of chemical molecules enhances the access to nutrients or new niches. By communicating, the collectivity of microbes can enable a shared defence mechanism against the host or other competitive microbes (Hogan, 2006; Tropini *et al.*, 2017). Inter-kingdom interactions are a common threat in hospitalized individuals, where the severity of the infection and the already weakened constitution of the patient often have detrimental effects.

3.1.2 Overview of documented examples of interactions between *C. albicans* and gut bacteria

The human gastrointestinal tract is densely colonized with fungi and bacteria. The entire inter- and inner-kingdom interactions that are taking place in this

environment is highly complex and dynamic. Nevertheless, the scientific community weekly unravels interactions that occur in the gastrointestinal tract. Many studies so far focus on the pathogenesis of fungi when the protective function of the bacterial microbiota (or single species) is absent. These demonstrated, for example, that in antibiotic treated animals the colonization of the intestine by *C. albicans* can cause gastritis or severe inflammation (Mason *et al.*, 2012; Savage, 1969), or that probiotic protective bacteria like *Lactobacillus* spp. are decreased in numbers during the colonization by *C. albicans* (Mason *et al.*, 2012). In blood stream infection models the combination of the fungus *C. albicans* and bacterial *E. coli* species lead to an increased virulence and mortality for the host, compared to the single strain infection models (Cabral *et al.*, 2018).

Several interactions have been studied between the common gut bacteria *Bacteroides thetaiotaomicron* and the prominent fungus of the gastrointestinal tract, *C. albicans*. The lab of Andrew Koh (Fan *et al.*, 2015) showed that this anaerobic bacterium is necessary for maintaining the colonization resistance against *C. albicans* in conventional mice. They revealed a host mechanism protecting against *C. albicans* colonization: the secretion of the antimicrobial peptide LL-37, which is induced in the presence of *B. thetaiotaomicron* in the intestine of the host. Furthermore it has been described that the saccharolytic bacterium *B. thetaiotaomicron* is capable of degrading parts of the fungal cell wall (α-mannans) of *C. albicans* (Cuskin *et al.*, 2015). Despite the poor reputation that many fungi still hold, several studies have been describing the beneficial effect of fungi, especially *C. albicans,* on the health of the host during gastrointestinal colonization (Jiang *et al.*, 2017).

Defined gut microbial communities

3.1.3 The Oligo12-Mouse Minimal Microbiota

On the bacterial side, the gastrointestinal microbiota consists of approximately 400 different species (Barko *et al.*, 2018). The microbiota is very dynamic and varies between individuals. To have a more defined composition, mainly for scientific experiments, the model of a minimal microbiota was established. A minimal microbiota combines the advantages of a microbiota without the trouble of the uncountable amounts of different microbes, their byproducts or their interactions. The limited number of microbes present in a flora allows to investigate direct interactions between bacterial strains or the host while mimicking the complexity of a conventional microbiota to the host. The first minimal flora was put forward by Russel W. Schaedler in the mid-sixties, and consisted of eight bacterial species (Schaedler *et al.*, 1965). In 1978 the consortium was slightly changed by Roger Orcutt and named altered-Schaedler flora (ASF) (Dewhirst *et al.*, 1999). Among others this community is still used in experimental procedures. The composition of the bacterial community tried to reflect the variety of the bacterial strains commonly culturable in the gastrointestinal tract of laboratory mice. Recently the working group of Bärbel Stecher from the Ludwig-Maximilians-University in Munich (Germany) put forward another bacterial community using a genome-guided approach. This community, termed Oligo-Mouse Microbiota (Oligo-MM[12]), consists of twelve bacterial strains that represent members of all the major bacterial phyla in the murine gut of mice (Table 3). This Oligo-MM[12] was established in germfree mice and then transferred horizontally to their offspring or other germfree mouse breeds by co-housing.

Table 3: Composition of the Oligo-MM[12].

Designed by the group of Bärbel Stecher, LMU (adapted from Brugiroux *et al.*, 2016).

Taxonomic Classification	Strain ID	DSM nr.	Classification
phylum Actinobacteria			
class Actinobacteria			
order Bifidobacteriales			
family *Bifidobacteriaceae*	YL2	26074	*Bifidobacterium longum*
phylum Bacteroidetes			
class Bacteroidia			
order Bacteroidales			
family *Muribaculaceae*	YL27	28989	*Muribaculum intestinale*
family *Bacteriodaceae*	I48	26085	*Bacteroides caecimuris*
phylum Proteobacteria			
class Betaproteobacteria			
order Burkholderiales			
family *Sutterellaceae*	YL45	26109	*Turicimonas muris*
phylum Verrucomicrobia			
class Verrucomicrobiae			
order Verrucomicrobiales			
family *Verrucomicrobiaceae*	YL44	26127	*Akkermansia muciniphilia*
phylum Firmicutes			
class Bacilli			
order Lactobacillales			
family *Enterococcaceae*	KB1	32036	*Enterococcus faecalis*
family *Lactobacillaceae*	I49	32035	*Lactobacillus reuteri*
class Clostridia			
order Clostridiales			
family *Lachnospiraceae*	YL32	26114	*Clostridium clostridioforme*
	YL58	26115	*Blautia coccoides*
family *Ruminococcaceae*	YL31	26117	*Flavonifractor plautii*
	KB18	26090	*Acutalibacter muris*
class Erysipelotrichia			
order Erysipelotrichales			
family *Allobaculum*	I46	26113	*Clostrdium innocuum*

3.1.4 Microbiota-mediated colonization resistance

A healthy commensal gut microbiota provides a key defence mechanism against pathogenic bacteria or fungi. To some extent, the presence of a bacterial community can be enough to cause colonization resistance simpely by occupying the niche the pathogen was aiming for. In other cases, like the one described by the lab of Andrew Koh (Fan *et al.*, 2015), the presence of

the gut commensal *Bacteroides thetaiotaomicron* in laboratory mice is inducing a transcription factor, the hypoxia-inducible factor 1- α (HIF-1α), that activates cascades in the innate immune response and activates the production of the antimicrobial peptide LL- 37. The LL-37 peptide produced in the host repels the fungus *Candida albicans* and limits its capability for colonization. Other studies described the importance of a single bacterium from the phylum of Deferribacteres, called *Mucispirillum schaedleri*, providing a protection from colonization of non-typhoidal *Salmonella enterica* serovar Typhimurium strains causing colitis (Herp *et al.*, 2019). Previously, the same group described protection of the host from *Salmonella* infections by a collection of murine bacterial strains (Brugiroux *et al.*, 2016). These examples show that the protective effects against pathogenic members of the microbiota can be in a direct competitive bacterial-bacterial manner or be mediated by bacteria but executed by the host.

3.1.5 Dysbiosis – the microbiota in imbalance

The more insights we gain from research about the interactions of the microbes in the host, the clearer it gets that the probably most important feature of the microbiota is its balance (Power *et al.*, 2014). Many of the commensal gut bacteria or fungi can cause infections if the balance of the microbiota gets disrupted. In the commensal microbiota, the composition of different species is highly diverse and extremely competitive. Unless the environment shifts into one of the microbes favor, the continuous competition of all the abundant species maintain a healthy microbial diversity. A dysbiosis in this extremely complex environment, on the other hand, can lead to severe health issues for the host. Dysbiosis of the intestinal microbiota as well as the mycobiota has been reported in many metabolic diseases like obesity, diabetes or cardiovascular disease. In many cases, like for inflammatory bowel disease, it is not clear if the dysbiosis of the microbiota is the result of the condition or the cause for the disease (J. Li *et al.*, 2018; Weiss & Hennet, 2017; Wheeler *et al.*, 2016). It has been described previously that the

dysbiosis of the gastrointestinal microbiota can be induced by anti-fungal drug treatment. The administration of an anti-fungal drug cocktail altered the fungal community of the animals, resistant fungal species overgrew, whereas other fungi were depleted by the anti-fungal drugs. At the same time, the bacterial microbiota changed as well and when the researchers challenged these mice by inducing colitis or asthma, the outcome was much more severe in animals with an imbalanced microbiota compared to untreated controls. The addition of a mix of fungal commensals restored the protective effect of the microbiota and led to only mild symptoms. A balanced microbiota can protect the host from colonization of unwanted harmful pathogens, help regulate the immune response or even protect against infections and this effect is not only limited to local effects in the gut but also true for peripheral organs (Harbour *et al.*, 2014; Mohawk *et al.*, 2012).

The bacterial gut commensals *Bacteroides thetaiotaomicron* and *Lactobacillus reuteri*

3.1.6 The saccharolytic bacterium *B. thetaiotaomicron*

The human colon contains trillions of microbes, around 90 % of this community are bacterial species belonging to the phyla of Bacteroidetes and Firmicutes (Eckburg *et al.*, 2005; Ley *et al.*, 2008). The obligate anaerobe gram-negative *Bacteroides thetaiotaomicron* is one of the most abundant species in the gastrointestinal tract that colonizes humans already during birth or shortly after (Reid, 2004; Simon & Gorbach, 1986). The commensal Bacteroides species, including *B. thetaiotaomicron* can cause infections on the skin, soft tissue and other organs in immunocompromised patients. Additionally, the life threatening bacteremia that can be caused by bacteria in the bloodstream after a perforation of the gastrointestinal tract is mostly caused by *B. thetaiotaomicron* (Wexler, 2007). The colon is a very rich environment providing high amounts of nutrients, including complex dietary polysaccharides as well as host-derived glycans. The microbiota encodes for a wide range of carbohydrate degrading enzymes which allow the processing

of otherwise indigestible polysaccharides for the host (Flint *et al.*, 2012; Rogers *et al.*, 2013). *B. thetaiotaomicron* has an extensive gene repertoire to digest carbohydrates. It contains 88 polysaccharide utilization loci (PULs) that encode homologs of the starch utilization system (Sus genes) which are responsible for utilization and binding of starch (Martens *et al.*, 2008) and 172 glycosylhydrolases which enable it to use a wide spectrum of dietary carbohydrates available in the human intestine (Xu *et al.*, 2003, 2004). *B. thetaiotaomicron* has been reported to encode more glycosylhydrolases than any other sequenced bacterium and equipped with these genetic tools, it appears to be able to cleave most of the natural occurring glycosidic bonds (Xu *et al.*, 2003, 2004). Apart from the high amounts of dietary polysaccharides that are present in the colon, the host is constantly shedding heavily O-glycosylated proteins (mucins) into the lumen of the intestine, as a part of the defence mechanism against the microbiota. Many gut species, including *B. thetaiotaomicron*, are able to digest and consume these mucins that are produced by special epithelial cells of the host, the goblet cells (Martens *et al.*, 2008; Sonnenburg *et al.*, 2005b). In numbers, the human host derives 10-15 % of its caloric intake from oligosaccharides that have been fermented by the microbiota (Xu *et al.*, 2004). The saccharolytic bacterium *B. thetaiotaomicron* encodes a broad spectrum of genes that enables this gut bacterium to thrive in the gastrointestinal tract of mammals.

3.1.7 The probiotic bacterium *Lactobacillus reuteri*

The gram-positive lactic acid producing *Lactobacillus reuteri* is one of the most universal members of the microbiota of all mammals. *L. reuteri* can be found at many different body sites, including the gastrointestinal tract, the oral cavity, the urinary tract, and the skin (Sinkiewicz *et al.*, 2010). This bacterium is known for its probiotic effects and plays an important role in food fermentation and therefore can be found in a variety of dairy products (Giraffa *et al.*, 2010). The treatment of individuals with *L. reuteri,* to establish a probiotic benefit from the bacterium, has been conducted in many studies with

adults, children and immune suppressed patients (Hoy-Schulz *et al.*, 2016; Valeur *et al.*, 2004; Weizman & Alsheikh, 2006; B. W. Wolf *et al.*, 1998). It appears that the oral administration of the bacterium promotes good health, improves the absorption of nutrients, minerals and vitamins, promotes gut mucosal integrity and protection against pathogenic overgrowth or pathogenic translocation in the gut, *e.g.* against *Helicobacter pylori* (Hou *et al.*, 2015; Spinler *et al.*, 2008; Tubelius *et al.*, 2005). Additionally it was reported that two *L. reuteri* strains from rat and human increased the thickness of the inner mucus layer in a mouse model where animals were challenged with chemically induced colitis (Ahl *et al.*, 2016). *L. reuteri*, like other *Lactobacillus* spp., can produce substances that are beneficial for the host, such as antimicrobial compounds (reuterin), vitamins B12 and B9 and histamine (Diaz *et al.*, 2016; Linares *et al.*, 2017; Talarico & Dobrogosz, 1989). The probiotic effect of *L. reuteri* is well characterized, and the bacterium seems to be beneficial in defending against invading pathogens.

The protective mucus layers of the gastrointestinal tract of mammals

3.1.8 Mucins and their distribution in the intestine

Mucins are a large group of proteins characterized by their high amount of O-glycans (M. E. V. Johansson & Hansson, 2016). These O-linked glycans are covering the mucin domains and have a high affinity to water, which gives the mucins the gel-like quality and makes them act as lubricant (Swidsinski *et al.*, 2008). Mucin proteins are produced by all mucosal surfaces, including the airways and the intestinal tract (Ridley & Thornton, 2018). The mucus layers are the first line of defence produced by the host against environmental microbes (M. E. V. Johansson *et al.*, 2013; Pelaseyed *et al.*, 2014). Intestinal mucins are separated in two groups: transmembrane mucins and gel forming mucins. The members of the transmembrane mucins have different lengths and are found for example on the apical surfaces of enterocytes in the ileum. The extracellular domain of the transmembrane mucins is cleaved or released

from the membrane by mechanical force, whereas the intracellular domain is involved in signal transduction (Hattrup & Gendler, 2008). Enterocytes are the most common cell type of the intestinal epithelium and the transmembrane mucins (MUC3 mostly in the duodenum, MUC12 mainly in the colon, MUC17 in the small intestine and duodenum) anchored in the enterocyte membranes expand into the lumen of the intestine, generating a local glycan-rich protection barrier, the glycocalyx (Hattrup & Gendler, 2008). The gel-forming mucins are secreted by a specific cell type in the intestinal tract, the goblet cells. The mucins multimerize via disulfide bonds and thereby form the net structure of the mucus layer. The predominant gel-forming mucin in the intestine is MUC2, which is found mostly in the colon (M. E. V. Johansson *et al.*, 2008). The distribution of MUC2 differs in the different parts of the gastrointestinal tract (Figure 10). In the ileum the mucus is organized in patches, in the cecum only parts of the epithelial cells are covered by a thin mucus layer, whereas in the colon a tick mucus layer covers all epithelial cells.
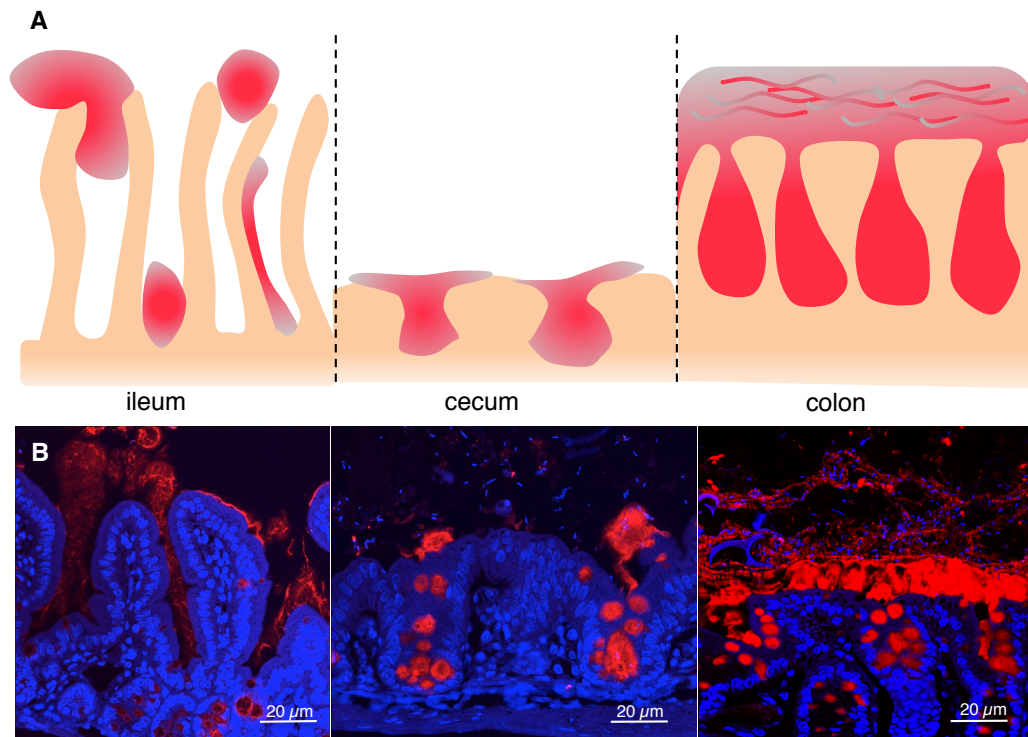
Figure 10: MUC2 mucin distribution in the gastrointestinal tract.

The upper panel A shows a schematic of the MUC2 distribution. In the lower panel B representative images of intestinal sections of *C. albicans*-monocolonized mice are shown. MUC2 is produced in the goblet cells. In the ileum, these cells are located on the very bottom of the villi. By releasing the MUC2 proteins from the cells, the mucin forms patches that move towards the lumen. Most of the epithelium of the ileum is not covered with mucus. The tissue of the cecum is thin and harbours shallow crypts that release mucin into the lumen. Like in the ileum, the epithelium is not completely covered with mucin. The mucus distribution is distinct in the colon: the mucin-producing goblet cells are located in the side walls of the crypts and constantly secrete mucin towards the lumen, where it forms a dense impenetrable layer. Towards the lumen, this mucus layer, which consists of stacked complex sheets of MUC2 mucins, gets more loose and harbours the microbiota. In the colon, the whole epithelium is covered with mucus. The contact of the microbiota with the colon epithelium is a proxy for infection.

In the ileum, the MUC2 producing goblet cells are located at the bottom of the villi. In the colon, most goblet cells are found in the upper parts of the crypts. The goblet cells release the densely packed mucins at a constant rate into the crypts, and by releasing the mucins into the lumen, the large, multimeric, net-like insoluble molecules, that can be visualized as mucus layers, are formed

(M. E. V. Johansson, Holmén Larsson, *et al.*, 2011; M. E. V. Johansson, Larsson, *et al.*, 2011). The expansion of the mucus from the granules of the goblet cells into the intestinal lumen is driven by the massive capability of the mucins to absorb water. The combination of low pH and high levels of Ca^{2+} in the granules of the goblet cells prevent the expansion inside the granules (Ambort *et al.*, 2012). Released from the granules, the MUC2 mucins unfold into large sheets with a dense net-like structure. Due to the constant production of new mucin, the layers are shed towards the lumen of the intestinal tract. Traveling towards the lumen, the net of the mucins gets more wide and the mucins are less densely packed. This mechanism is thought to be driven, among other things, by the increased availability of water towards the lumen, proteolytic weakening of the bonds between the mucins, mechanical force during the digestion process and the microbiota that colonizes the outer more loose mucus layers (Ambort *et al.*, 2012). By this mechanism, the microbiota, which is found in and on the outer mucin layer, is constantly pushed away from the epithelium of the colon and although some bacteria can penetrate the mucus layer, in healthy individuals, the inner mucus layer covering the whole colon epithelium is devoid of bacteria (M. E. V. Johansson *et al.*, 2008).

3.1.9 MUC2 mucin and the microbiota

The distribution of the most prominent mucin, MUC2, differs in various parts of the intestine. In the ileum, the distribution of MUC2 is rather patchy, the mucins are released from the bottom of the villi and in these mucin patches a high amount of microbes can be found (M. E. V. Johansson, Larsson, *et al.*, 2011). In the colon dense layers of mucin sheets are shed towards the lumen keeping the microbiota away from the epithelium. The differential expression of the MUC2 mucin in the ileum and colon is building different niches, which can be colonized by various microbes (M. E. V. Johansson *et al.*, 2008). The loose mucin patches that can be found in the ileum are penetrable by

microbes and therefore these patches are highly colonized by the microbiota (Loonen *et al.*, 2014; Vaishnava *et al.*, 2011). Other than in the colon, the epithelium of the ileum is not completely covered with a protective mucus layer (Figure 10). Therefore especially in the small intestine, the amount of defensins and IgA that are secreted from the epithelium are particularly high. Additionally it was reported that the flexible mucin patches that originate at the bottom of the ileal villi have a cleansing effect when they make their way into to lumen. When the mucin is moving from the bottom of the intestinal villi towards the lumen, microbes and cell debris of the gastrointestinal content that was trapped in the depth of the villi attaches to the mucin and is transported into the ileal lumen (Loonen *et al.*, 2014; Vaishnava *et al.*, 2011).

While the inner mucin layers of the colon are impenetrable and covering the surface of all epithelial cells, the outer mucus layer of the colon, where the dense net-like structure of the mucins is loosened, the mucin is densely colonized with microbes.

The gel-like structure of the mucin absorbs small solvable nutritional particles and the exposed glycans of the mucin chains allow attachment of microbes. Some bacteria can glycosylate the mucins and thereby provide a stable source of nutrients. Many bacterial species have adapted to the niche of the colonic mucus layers like *Akkermansia muciniphila* and *Mucispirillum* spp (H. Li *et al.*, 2015b). Several studies have revealed that although most members of the microbiota prefer the undigested food-related polysaccharides, some species, like *Bacteroides thetaiotaomicron*, can use the host-produced mucins as a carbon source (Bjursell *et al.*, 2006; Sonnenburg *et al.*, 2005b). On the other hand, the metabolites that are produced by the bacteria that colonize the outer mucus layer, like short-chain fatty acids, can be absorbed by the host epithelium. In nutrient deficient parts of the intestine, like the distal colon, it is especially important for the host to gain all available nutrients and the short-chain fatty acids or the by bacteria digested glycans are a welcome source of additional nutrients (Gaudier *et al.*, 2004).

The disruption or penetration of the intestinal barrier or an insufficient production of MUC2 is a cause of major infections. In gnotobiotic animals that

were raised sterile the mucin production is greatly decreased and it has been shown that the presence of the microbiota and even single bacterial species can stimulate the production of mucus in the colon. It is believed that the bacteria communicate with the host cells via second messenger molecules to accelerate the rate of mucus production (Jakobsson *et al.*, 2015). The intact mucus layer in the colon is essential for the health of the host. Animal experiments using *muc2$^{-/-}$* mice showed high sensitivity to induced colitis, colon cancer, and infections in mice with defective mucin production (M. E. V. Johansson *et al.*, 2008; Van der Sluis *et al.*, 2006; Velcich *et al.*, 2002). To overcome the natural barrier of the mucus layer, invading pathogens like *Salmonella enterica* serovar Typhimurium, *Shigella flexneri* and *Vibrio cholerae* have to be able to actively swim against the mucus flow coming from the epithelium. Additionally, expression of mucin-degrading proteases help the bacteria to make their way through the mucin towards the epithelium (Navarro-Garcia *et al.*, 2010; A. J. Silva *et al.*, 2003; Stecher *et al.*, 2004). The interactions between the microbiota and the host-derived mucins are complex but likely contribute to the homeostasis of the intestine.

3.2 Results

Co-colonization of *C. albicans* and the bacteria *B. thetaiotaomicron* and *L. reuteri*

3.2.1 The fungus *Candida albicans* establishes intestinal co-colonization with single bacterial species in gnotobiotic mice

To study the inter-kingdom interactions of fungi and bacteria, several gnotobiotic mouse models were established. Germfree NMRI mice were gavaged with the fungus *C. albicans* or one of the bacterial species *Bacteroides thetaiotaomicron* or *Lactobacillus reuteri* (Figure 11 A). All of the three microorganisms established stable colonization levels (Figure 11 B) for 21 days (duration of the experiment). The colony forming units (cfu) were monitored every week. The bacterium *L. reuteri* was detected with an abundance of 1×10^8 cfu/g feces, whereas the *B. thetaiotaomicron* strain was able to colonize with numbers three logs higher, with around 1×10^{11} cfu/g feces. The recovered cfu for the microbes are consistent with previous observations by other groups (Bloom *et al.*, 2011; Walter, 2008; White *et al.*, 2007). Additionally co-colonization models were established, where mice were first colonized with *C. albicans* and then, seven days later, with the bacterium. The recovered counts for all microbes in the co-colonized models were consistent with the cfu from the monocolonized models (*C. albicans* 5×10^7 cfu/g feces, *B. thetaiotaomicron* 1×10^{11} cfu/g feces, *L. reuteri* 5×10^8 cfu/g feces). The presence of the fungus seems to have no impact on the ability of the microbes to colonize the gut of mice or vice versa.
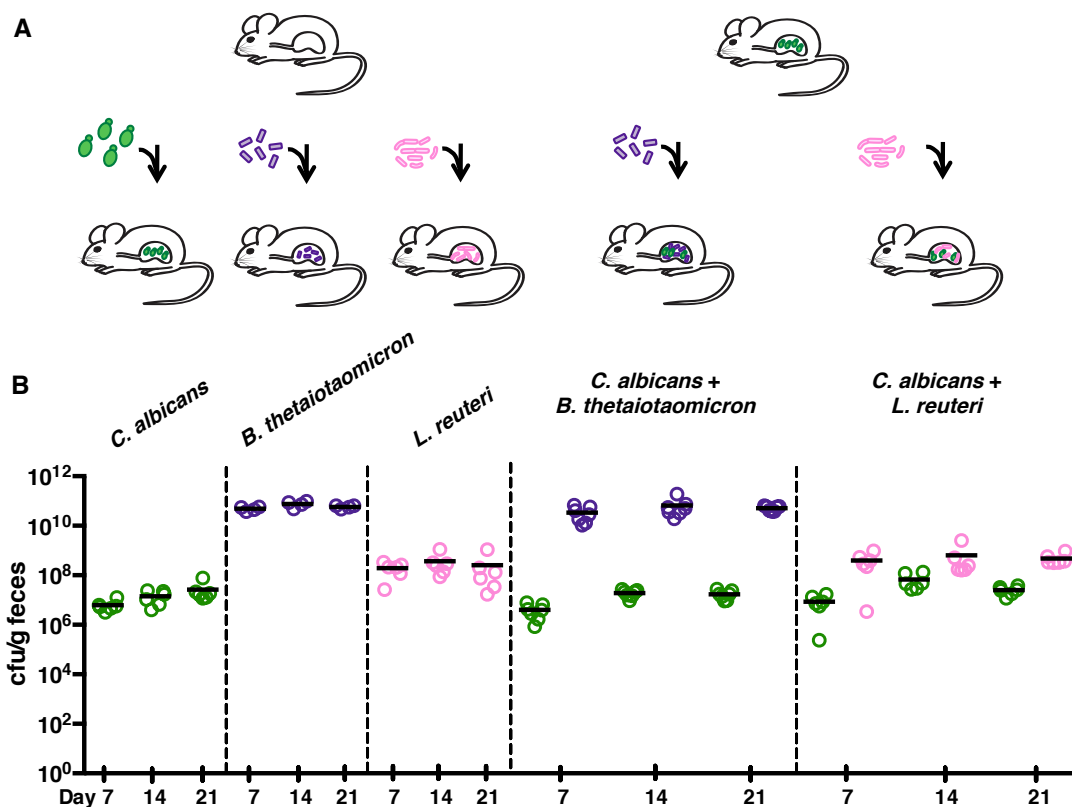
Figure 11: Mono- and co-colonization of gnotobiotic animals.

The gnotobiotic animals of this study were colonized as indicated in the schematic plan (A). Mice were either monocolonized with one organism (*C. albicans* (green), *B. thetaiotaomicron* (purple) or *L. reuteri* (pink)) or first colonized with the fungus *C. albicans* and then, in a second gavage, one bacterial species was added (*B. thetaiotaomicron* or *L. reuteri*). The colonization of the animals was observed at different time points by monitoring the cfu numbers recovered from their stool samples (B) (Eckstein *et al.*, 2020).

To make sure the colonization levels are not depending on the sequence of the gavaged microbe, the order of colonization was inverted in separate experiments. The animals were colonized first with *B. thetaiotaomicron* and 7 days later with the fungus. The *C. albicans* numbers were slightly lower over the time course of 21 days ($\sim 5 \times 10^6$ cfu/g feces compared to *C. albicans* 5×10^7 cfu/g feces in animals first colonized with *C. albicans*) and the numbers of *B. thetaiotaomicron* were marginally higher ($\sim 1 \times 10^{12}$ cfu/g feces) when *B. thetaiotaomicron* was inoculated first. Although this slight shift in colonization

is detectable we do not consider this shift to affect the stability of the co-colonization (Figure 12 A).

Additionally, the morphology of *C. albicans* was monitored during the co-colonization experiments. In the mouse models co-colonized with *C. albicans* and either *B. thetaiotaomicron* or *L. reuteri* the morphology of the fungus was monitored in the ileum, cecum and colon. In all evaluated samples the yeast morphology was predominant (Figure 12 B and C), as was observed before in the monocolonization experiments. Therefore, the presence of a single bacterial species (*B. thetaiotaomicron* (Figure 12 B) or *L. reuteri* (Figure 12 C) has no impact on fungal cell morphology in the investigated parts of the gastrointestinal tract. The morphology of the fungus is an important indicator of the lifestyle of *C. albicans*. Extensive studies showed that in the pathogenic lifestyle the fungus adopts the hyphal form (Jacobsen *et al.*, 2014; Kumamoto & Vinces, 2005). In our colonization models we predominantly find the yeast morphology of the fungus, this points out that the fungus resides as a commensal in the gastrointestinal tract of these mammals.
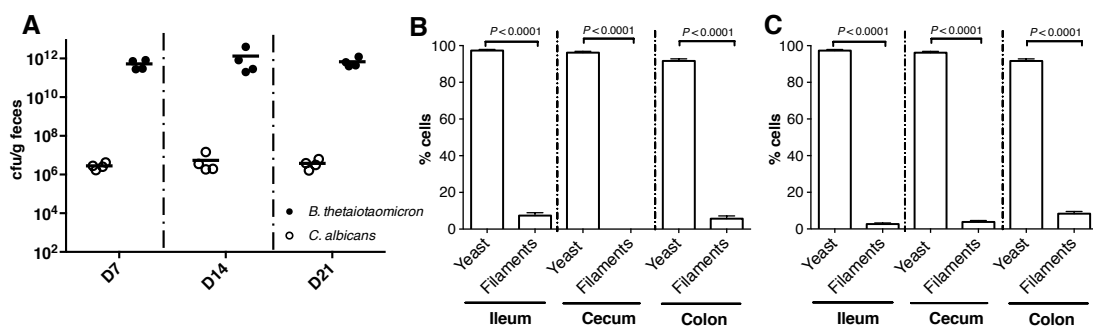
Figure 12: Cell count and morphology of *C. albicans* in the presence of *B. thetaiotaomicron* and *L. reuteri*.

The order of colonization has no impact on the stability of the co-colonized system of *C. albicans* and *B. thetaiotaomicron* (A). Cfu counts gained from fecal samples of 4 animals at the indicated time points. The presence of neither *B. thetaiotaomicron* (B) nor *L. reuteri* (C) has an impact on the predominatnt yeast morphology of the fungus *C. albicans*. For each condition 5 pictures were analysed of at least 3 animals; statistical analysis was performed using Student´s t-test (Eckstein *et al.*, 2020).

3.2.2 Localization of *B. thetaiotaomicron*, *L. reuteri*, and *C. albicans* in the intestine of monocolonized mice

To evaluate the localization of the microbes in the intestine of gnotobiotic animals, tissue samples of the gastrointestinal tract were removed, processed and stained with FISH probes. In conventional mice, that harbour a diverse microbiota, many bacterial strains colonize a niche of the gastrointestinal tract that suits their abilities. The gram-negative saccharolytic *B. thetaiotaomicron*, for example, is mostly found in the colon. Here, the bacterial load and diversity is highest in general, as is the load of polysaccharides that have not been degraded by the host, providing a constant source of nutrition for *B. thetaiotaomicron* (Vercellotti *et al.*, 1977). Lactobacilli have been reported to be most abundant in the small intestine of conventional animals, however this tendency has not been reported in gnotobiotic mice (S. Da Silva *et al.*, 2015). In our colonization models all three species, *C. albicans*, *B. thetaiotaomicron* and *L. reuteri*, were found throughout the length of the mouse intestine. As expected the microbial density in the ileum was lower compared to the density in the cecum and colon (Figure 13). In all colonization models the bacterium *B. thetaiotaomicron* reached the highest cfu counts (Figure 11 B). Supporting this finding, *B. thetaiotaomicron* cells were visibly more abundant in the pictures taken from the colon (Figure 13 B) compared to the visual numbers of *C. albicans* and *L. reuteri* (Figure 13). In the colon, all microbes are distinctly separated from the epithelium by the sterile mucus layer (indicated in Figure 13 as white dashed lines). In the ileum, where the epithelium is not physically separated from the lumen by a mucus layer, cells of all three species could be visualized in very close proximity or even in direct contact with epithelial cells (borders of the ileal epithelium indicated with white dotted lines in Figure 13). In the colon, where the protective mucus barrier covers the epithelium, the microbes were found equally distributed in the lumen or associated with the outer mucus layer, but never in direct contact with the epithelium. The density of microbes visualized in the ileum was similar in all colonization models

(Figure 13 F-J) and especially lower than other compartments of the gut. While the colonization density and localization differs strongly among different species and regions of the gut, bacteria and *C. albicans* do not affect each other`s colonization in these regards.
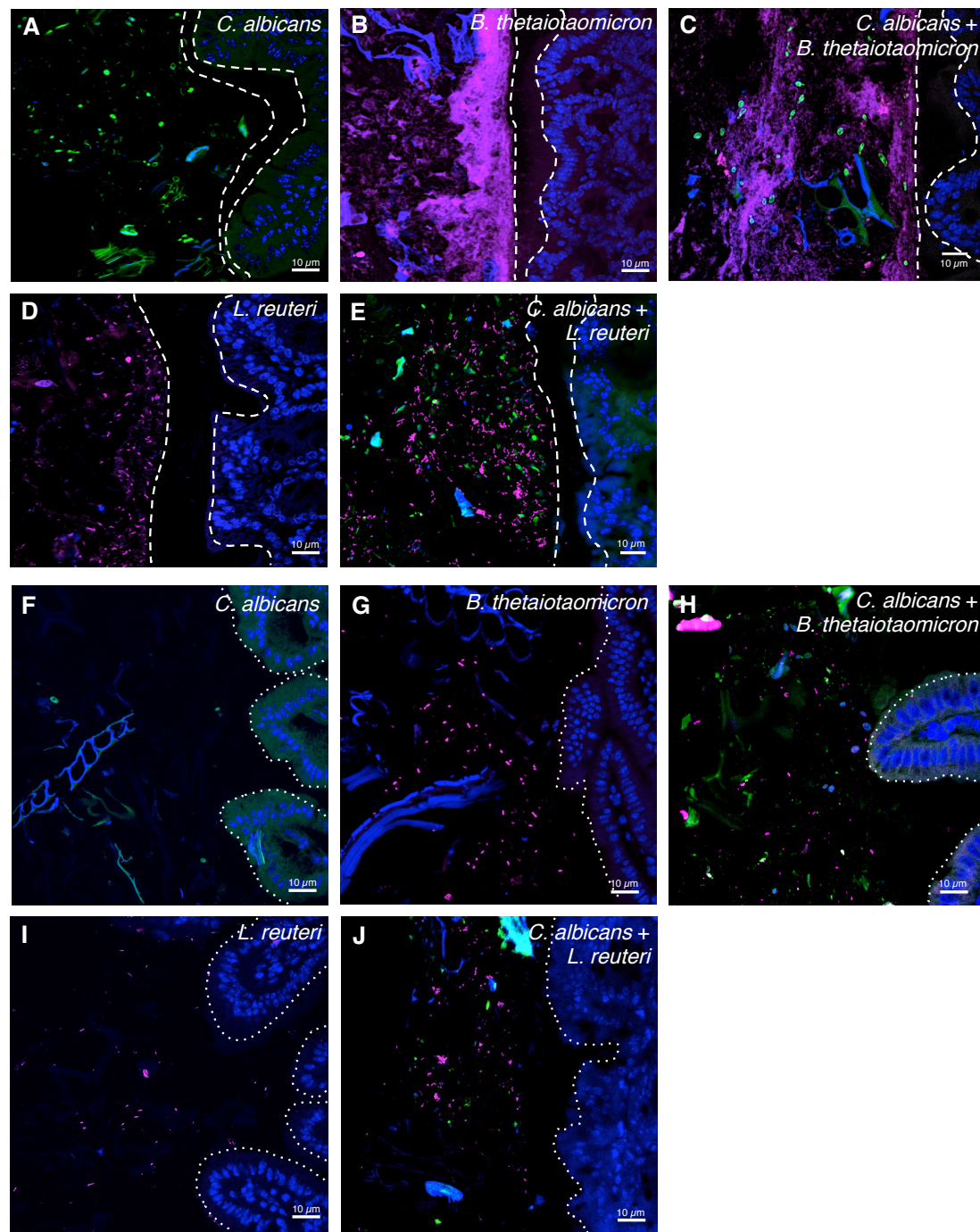
Figure 13: Spatial distribution of *C. albicans*, *B. thetaiotaomicron*, **and** *L. reuteri* **in the gut of gnotobiotic mice.**

The distribution of the three indicated microbes in the gut of gnotobiotic mice is visualized using FISH. The position of the inner sterile mucus layer in the colon is indicated by the dashed line (A-E). The border of the ileal epithelium is indicated by the dotted lines (F-J), nuclei of the host cells are stained in blue (DAPI), bacterial species are visualized in pink and *C. albicans* cells in green (Eckstein *et al.*, 2020).

Colonization and growth in the presence of mucus

3.2.3 Single microbes can shape the mucus layers of the colon

While analysing the FISH-stained sections of the intestines of mice, we noticed, that the outer mucus layer, which is visual in *B. thetaiotaomicron* colonized animals is absent in the *C. albicans* or *L. reuteri* monocolonized animals. It was surprising, that the presence of a single bacterium can shape its own environment within the host therefore we wanted to further investigate this finding. Additionally to monitoring the cfu and the spatial distribution of the microbes in the gastrointestinal tract, we examined the mucin layers of the colon in the colonized animals. It has been established before that the mucin layers of the colon are different in germfree mice compared to conventional animals (Schroeder, 2019a). In germfree animals the mucin layers have been described as less prominent, as well as less protective against microbial invasion, compared to mice harbouring a conventional microbiota (M. E. V. Johansson *et al.*, 2015; M. E. V. Johansson, Larsson, *et al.*, 2011).

So far it has not been described what effect the fungus *C. albicans* has on the colonic mucus layer. To address this question, colon tissue sections of *C. albicans* monocolonized mice were stained with FISH probes to monitor the fungus, while an anti-Muc2 antibody was used to visualize colonic mucin. In monocolonized mice, *C. albicans* cells were found either in the lumen or adjacent to the mucus layer (Figure 13 A and 14 A), but never found to penetrate this layer. The mucus layer in *C. albicans* monocolonized animals is covering the colon epithelium, therefore no contact of fungal and host cells was observed. There is no visual difference comparing the mucus layers of *C. albicans* monocolonized animals to the mucus layers of germfree animals.

To better understand, which microbes affect the mucus layer tissue sections of all the different animal models were stained. The colonization of the gut of gnotobiotic mice with *L. reuteri* did not lead to changes in the mucus layers (Figure 14 C and D). They show similar mucus patterns as animals monocolonized with *C. albicans* or germfree animals. Interestingly in the presence of *B. thetaiotaomicron*, the mucin layers differed from other

colonization models (Figure 14 E and F). While the sterile inner mucin layer appears similar for all colonization types, a prominent outer mucus layer appeared only in the presence of *B. thetaiotaomicron* (Figure 14 E and F). In this outer mucus layer, the bacterium thrives. This secondary mucus layer that is detected in the presence of *B. thetaiotaomicron* is comparable with the mucin layer that can be observed in conventionally raised animals (M. E. V. Johansson, Larsson, *et al.*, 2011).
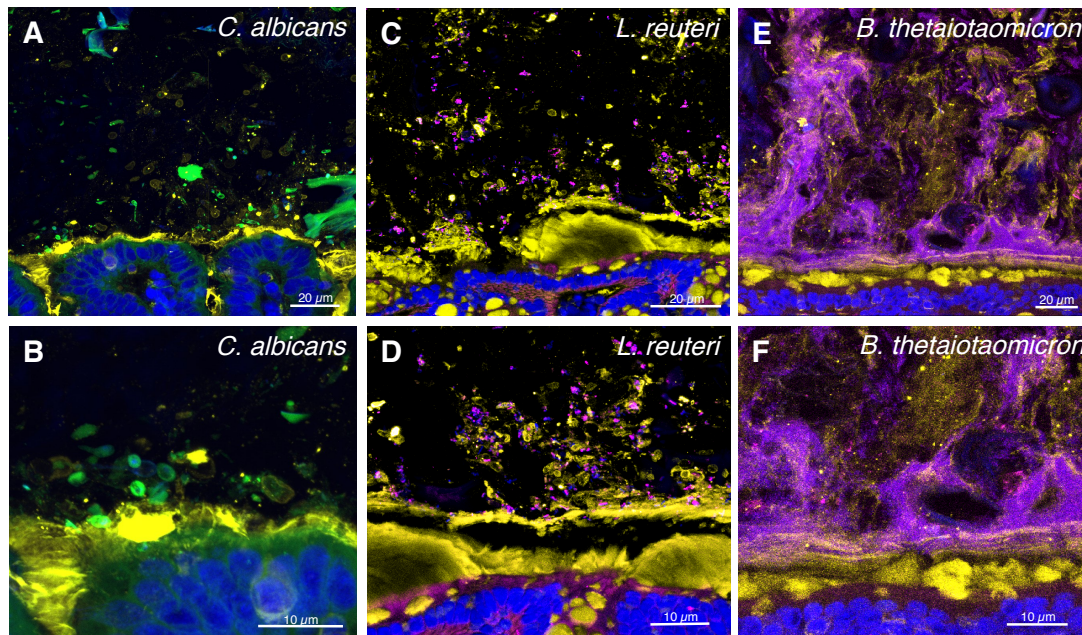
Figure 14: The secondary outer mucus layer is depending on the presence of *B. thetaiotaomicron*.

The distribution of MUC2 mucin (yellow) in the proximal colon of mice is shown. Animals were monocolonized with *C. albicans* (A and B), *L. reuteri* (C and D) and *B. thetaiotaomicron* (E and F). Fungal cells (green) and bacteria (purple) were stained with FISH probes. The Muc2 mucin was stained using an anti-MUC2 antibody (yellow). Nuclei of the epithelial cells were stained with DAPI (Eckstein *et al.*, 2020).

In order to better quantify the differences in mucus quantity, we measured the thickness of both mucus layers at three different positions per picture in at least 10 pictures per colonization type (Figure 15 A). The presence of the outer mucin layer significantly depends on the presence of *B. thetaiotaomicron*. The average thickness of the outer mucin layer of 70 *µ*m is around 30 % less than other measurements taken by different research

groups in conventional mice. It seems that the single species *B. thetaiotaomicron* is sufficient to establish an outer mucin layer, which is usually found in conventional mice, albeit to a lesser extent. In our animals co-colonized with *B. thetaiotaomicron* and fungus *C. albicans* the mice developed an outer mucus layer similar to the one in *B. thetaiotaomicron* monocolonized animals. The presence of the fungus seems to have no impact on the mucus layer thickness. The thin outer mucin layer observed in monocolonized animals with *C. albicans* or *L. reuteri* is not different to the situation in gnotobiotic animals (Figure 15 A). The presence of a thick secondary outer mucus layer that is comparable to that described in conventionally colonized animals, can in our experimental setup only be visualized in the presence of the bacterium *B. thetaiotaomicron*.

Additionally we did a time course analysis to find out when the secondary outer mucus layer is produced. We took samples to measure the mucus layer thickness in animals 3, 7, 14 and 21 days post colonization of the animals with *B. thetaiotaomicron*. The measurements were taken from two mice per time point and at 3 different positions in at least 10 pictures per animal and compared to the measurements taken from germfree animals. Already at our earliest time point, after 3 days of colonization, the outer mucus layer is significantly different from the un-colonized controls, although the outer mucus layer is around 20 % thinner in the early time points compared to the thickness of the layer after 21 days of colonization (Figure 15 B). The mucus thickness measurement 3 days post colonization demonstrates that the production of this outer mucus layer is already on a stable rate in the early days of gut colonization with *B. thetaiotaomicron* and indicates that the production of the outer mucus layer starts immediately after colonization of the gut.

A

B
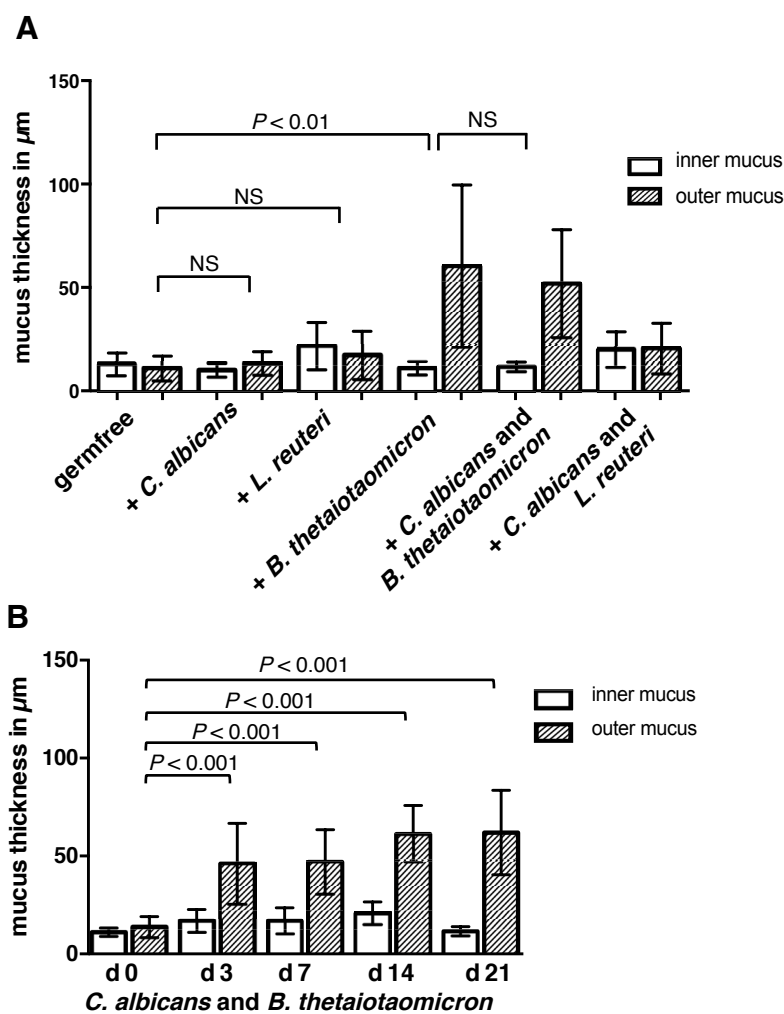
Figure 15: Measurement of the outer mucus layer in colonized animals.

The thickness of the inner and outer mucus layers was quantified in the proximal colon of germfree, mono- and co-colonized mice (21 days post-gavage (A). Additionally the thickness of the mucus layers were measured in *C. albicans* and *B. thetaiotaomicron* co-colonized animals at different time points throughout the experiment (B). For each group > 10 sections derived from at least 3 mice were evaluated. Shown are the means ± SD. Statistical analysis by one-way ANOVA followed by Tukey's post hoc test (Eckstein *et al.*, 2020).

The bacterium *B. thetaiotaomicron* promotes the production of an outer mucus layer. To investigate the distribution of fungal *C. albicans* cells, samples of co-colonized animals were stained with FISH probes and an anti-MUC2 antibody. In animals colonized with *B. thetaiotaomicron* and *C. albicans* the fungal cells colonize in the outer mucus layer that is depending on the presence of the

bacterium. The fungal cells seem to easily occupy this *B. thetaiotaomicron*-dependent niche (Figure 16 A). The fungal and bacterial cells persist in close proximity to each other in the outer mucin layer but never penetrate the sterile inner mucin layer. The number of *Candida* cells found in the lumen and in the outer mucus layer of the distal colon were about the same (Figure 16 B).
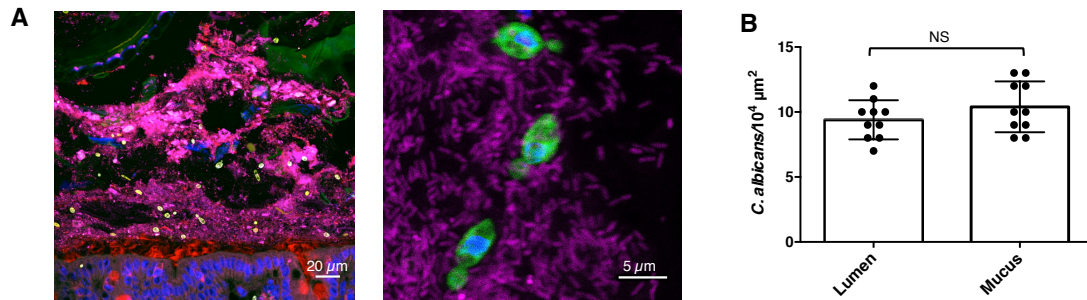
Figure 16: In the outer mucus layer that is promoted by *B. thetaiotaomicron*, fungal and bacterial cells thrive in close proximity.

Images of the proximal colon of mice co-colonized with *C. albicans* (green) and *B. thetaiotaomicron* (purple) are shown (A). In the left panel, mucin is stained in red and mouse nuclei in blue (DAPI). A higher magnification is shown in the right panel to visualize microbial cells. The numbers of *C. albicans* cells occupying either the lumen or the outer mucus layer in proximal colon are equally distributed (B). Cell distribution was observed in 5 pictures for 10 animals; bars represent means ± SD. Statistical analysis by Student's t-test (Eckstein *et al*., 2020).

We next explored whether *C. albicans* could rely on mucin as the only carbon source. YNB medium was supplemented with either untreated mucin (from porcine stomach, Sigma-Aldrich), mucin that was preincubated with *B. thetaiotaomicron* or *L. reuteri,* mucin that was preincubated with the enzyme β-glucanase, with PBS incubated with *B. thetaiotaomicron* or without any supplements, as negative control. The differently supplemented media were inoculated with *C. albicans* and incubated for 48 h at 30 °C. Samples were taken twice a day. The results showed that the fungal cells can grow on mucins as carbohydrate source up to an optical density OD_{600nm} of around 1.6 and a number of 1×10^8 cells/ml (Figure 17 A and B). The best growth rates were observed for the cultures supplemented with the mucin that was

enzymatically predigested by β-glucanase enzyme from *Trichoderma longibrachiatum*. The cultures that were supplemented with the mucin that was incubated with a *B. thetaiotaomicron* culture before the growth experiment showed significantly more growth (in OD_{600nm} and cfu) compared to the untreated mucin or the mucin incubated with *L. reuteri*. By including the negative control of PBS pretreated with *B. thetaiotaomicron* it can be excluded that the growth effect of *C. albicans* is promoted by particles or nutrients secreted by the bacterial. It appears that *C. albicans* can use mucin that was predigested by the bacterium *B. thetaiotaomicron* more efficiently for its own growth. These results suggest that the proliferation of the fungus may be preferentially fuelled by bacteria-processed mucin over intact mucin.
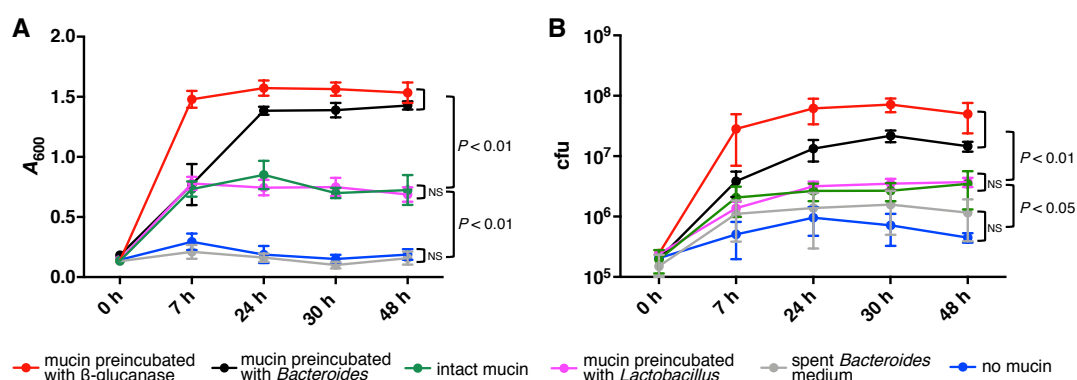
Figure 17: *C. albicans* growth is promoted by *B. thetaiotaomicron*-preincubated mucin.

Growth of *C. albicans* in minimal medium supplemented with the indicated substances. Culture density (A_{600nm}) and cfu counts are shown in (A) and (B), respectively. Plotted are the means ± SD from three independent experiments conducted in technical triplicates. Statistical analysis by ANOVA followed by Tukey's post hoc test (Eckstein *et al.*, 2020).

In the colon of *B. thetaiotaomicron*-colonized animals, we see an increased mucus layer thickness. To determine if the bacterium is able to digest these polysaccharides and use them as a carbon source, an *in vitro* growth assay was conducted. Here a defined Bacteroides minimal media was supplemented with either mucin or left without carbon source to be inoculated with *B. thetaiotaomicron*. The cultures were incubated in the anaerobic chamber at 37 °C for 48 h (Figure 18). The bacteria grew significantly better in

media that was supplemented with mucin compared to the negative control (Figure 18), which is consistent with the notion that *B. thetaiotaomicron* can utilize gastrointestinal mucins *in vivo* (Roberton & Stanley, 1982; Schwalm *et al.*, 2017).
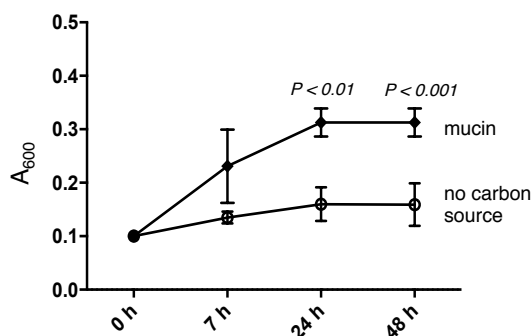
Figure 18: *B. thetaiotaomicron* growth on mucin

The growth of *B. thetaiotaomicron* was observed measuring the OD_{600nm} over the period of 48 h. In minimal media containing porcine stomach mucin, the growth of the bacterium was increased in comparison to the media control without supplementation of carbohydrates (Eckstein *et al.*, 2020).

3.2.4 *C. albicans* adheres to intestinal mucin

In the animal experiments using mono- and co-colonized mouse models, we visualized *C. albicans* cells in close proximity to the mucus layers of the host. To find out more about the interactions of the fungus and the intestinal mucus we established an *in vitro* model. We used the human colorectal adenocarcinoma cell line HT29-MTX-E12 because of its mucin producing property (Navabi *et al.*, 2013). Cells of the HT29 cell line release mucin after a culturing time of 21 days. We conducted an attachment assay to observe the attachment of fungal cells to the human cells. After the cell line cells start secreting mucin the cells of a *C. albicans* culture (MOI 1) were added and incubated together with the human cell line. To evaluate the attachment, the cell line cells were stained with DAPI and the fungal cells and the mucin were stained with antibodies. The released mucin is visual as patches on the cell line layer, not covering the entire cell layer but rather building big three-

dimensional mucin clouds (Figure 19 A). The fungal cells can almost exclusively be found in these mucin patches, only a minority of single fungal cells are found attached directly to the cells of the cell line (Figure 19 A and B).

In an additional assay the mucin that is released from the HT29 cell line was collected and used to supplement a growth curve of *C. albicans*. The cell growth of *C. albicans* in minimal media supplemented with the HT29-produced mucin is very similar to the growth of the fungus in media supplemented with mucin from porcine stomach (Figure 19 B). Predigestion of the HT29 mucin also increased its positive effect on the growth of *C. albicans*, as was also observed for the porcine mucus. The decisive factor that promotes fungal cell growth appears to be the preincubation of the mucins with the saccharolytic bacterium *B. thetaiotaomicron*, rather than the origin of the mucus.
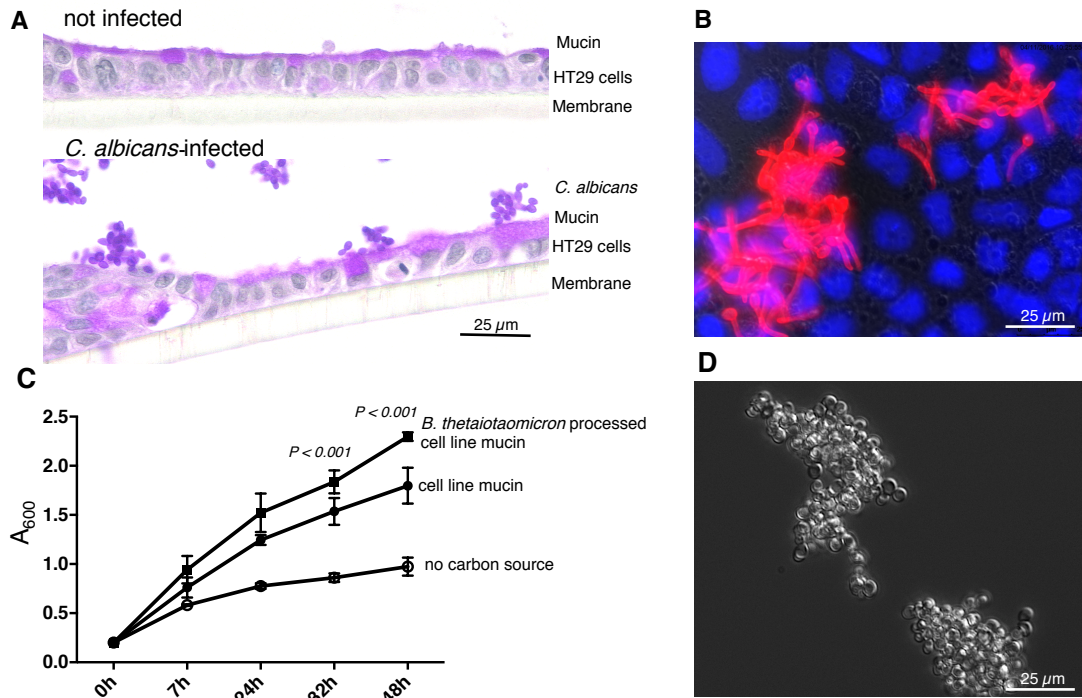
Figure 19: *C. albicans* attachment and aggregation in the presence of mucin

Mucus produced by the colon cell line HT29 forms patches on top of the cell layer and induces fungal cells to attach as aggregates ((A) horizontal cut through the cell layer, periodic-acid-Schiff-stained, (B) top view onto the cell layer, cell line nuclei stained with DAPI (blue) and fungal cells with an antibody (red)). *C. albicans* can utilize the cell line produced mucin (C), while growing in mucin-supplemented media the fungal cells form big aggregates detectable with light-microscopy (D).

3.2.5 Mucin induces yeast cell aggregation

During the *in vitro* growth assays, we observed that the fungal cells form aggregates when they grow in minimal media supplemented with mucin (Figure 19 D). Aggregation of fungal *C. albicans* cells can be observed under several conditions. Usually this aggregation is due to the hyphal morphology of the cells. In this state, the cells produce significantly more adhesins to attach to host cells as well as to each other. The formation of hyphae can be induced, among other things, by exposing cells to high temperatures or serum. Interestingly, the big aggregates of fungal cells that are formed when *C. albicans* is inoculated in minimal media supplemented with mucin consist

exclusively of cells of the round yeast morphology and not hyphae. This cell aggregation in yeast morphology was not observed in minimal media supplemented with glucose. The formation of aggregates in the yeast morphology has not been reported so far under any tested condition for *C. albicans* cells. The presence of mucin in the growth media appears to lock the fungus in its yeast morphology. Although we don't see aggregation of fungal cells in the *in vivo* colonization experiments we did report predominantly yeast shaped cells in the gastrointestinal tract of the colonized animals (see 2.2.1).

3.2.6 Transcriptome analysis of *C. albicans* response to mucin

We performed a transcriptome analysis (RNA-Seq) to investigate the response of fungal cells to incubation with mucin. In an *in vitro* experiment, YNB minimal media was supplemented either with glucose, mucin (from porcine stomach) or left without supplements and then inoculated with *C. albicans* and incubated at 37 °C under anaerobic conditions to mimic the colon environment, which is largely devoid of oxygen (Donaldson *et al.*, 2015; Thursby & Juge, 2017). After 24 hours, the fungal cells were harvested and the RNA was extracted and analysed by RNA-sequencing. With a principal component analysis, a first overview over the data was obtained. The graph of the PCA (Figure 20) shows the clustering of the sample duplicates and leads to the first conclusion that the gene expression pattern in cells grown with mucin and in cells grown in media without supplements is roughly the same, whereas the samples obtained from cells grown in minimal YNB media that was supplemented with glucose cluster very differently.
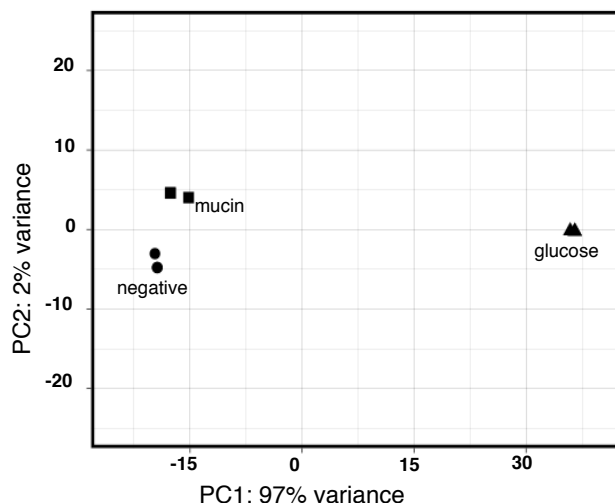
Figure 20: Principal component analysis of the comparative transcriptomics of *C. albicans* grown with different carbon sources.

PCA comparing the transcriptomic profiles of *C. albicans* cells grown in minimal media with and without glucose or with the addition of mucin as the sole carbon source. Expression patterns of cells grown with mucin or without any supplementation in YNB minimal media under anaerobic conditions are comparable, whereas the gene expression pattern in cells grown in media supplemented with glucose under anaerobic conditions was different (Eckstein *et al.*, 2020).

To further analyse the transcriptomic profiles of the different samples, a direct comparison between the cells grown with glucose or mucin and the control samples grown in media without supplements was conducted in R studio using the DESeq2 package (Love *et al.*, 2014). As the PCA already suggested, the *p*-values and $\log_2$ fold changes in the glucose/control-comparison were much higher than the values in the mucin/control-comparison. Indicating that the gene expression pattern is very different in the glucose containing samples compared to the control samples and the mucin-containing samples. In the glucose/control-comparison 1443 genes were significantly differentially regulated with a $\log_2$ fold change cut off of ±2 and *p*-value lower than 0.01 (Supplementary Data 6.1). In the same comparison, the mucin/control-analysis showed only 94 differently expressed genes with a $\log_2$ fold change cut off of ±1 and *p*-value below 0.01 (Supplementary Data 6.2).

These differences in the expression patterns are reflected in the axis scales of the volcano plots below (Figure 21). In samples that were supplemented with glucose, several glycolysis enzymes were up-regulated, for example pyruvate kinase *CDC19*, enolase *ENO1*, phosphoglycerate mutase *GPM1*, glucose-6-phosphate isomerase *PGI1*, while, simultaneously, mitochondrial genes known to be involved in respirative growth (*e.g. QCE1, PET9, NUO4*) were down-regulated. Comparing cells grown with mucin to the control samples revealed that ribosomal genes were overrepresented in the list of mucin-induced transcripts, whereas putative glucose transporters (*HGT2/6/12/19*) were overrepresented in the list of mucin-repressed genes. Although the transcriptome datasets provide a lot of information they have not jet revealed a conclusive mechanism on how *C. albicans* utilization of mucin is different from the digestion of glucose as a carbon source.
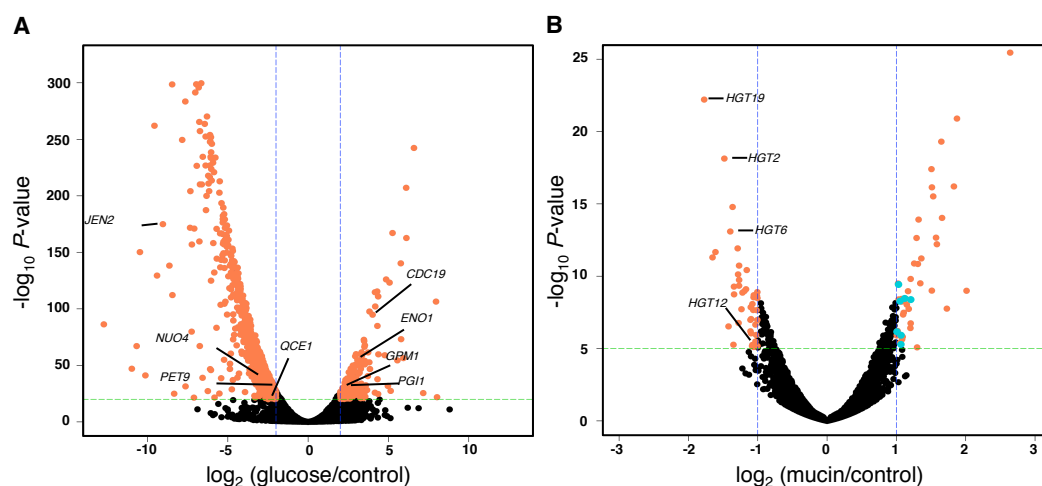
Figure 21: Volcano plots depicting the comparison of the transcriptomes of cells grown in glucose/control and mucin/control.

In the glucose/control comparison (A), genes of the glycolysis were up-regulated whereas mitochondrial genes were found in the down-regulated dataset (find selected gene names in the graph). In the mucin/control comparison (B), genes highlighted in turquoise are ribosome associated and more abundant in the dataset of the overexpressed genes, whereas putative glucose transporters (see selected names in the graph) are more abundant in the dataset of the down-regulated genes. All significantly different genes are depicted in orange (Eckstein *et al.*, 2020).

The reads that had been mapped to the correct positions within the genome were visualized using the Mochiview gene viewer (Homann & Johnson, 2010). Three major candidates were chosen to further investigate in their importance during fungal growth on mucin: the transcription factor *TEC1*, the aldo-keto reductase *IFD6,* and the hyphal cell wall protein *HYR1*. The coloured tracks (Figure 22) show the number of reads mapped to the genes` open reading frames. All of these three genes showed higher expression in cells grown in mucin when compared to the negative control and the glucose grown samples, suggesting that these genes are important for the fungus when proliferating in mucin.
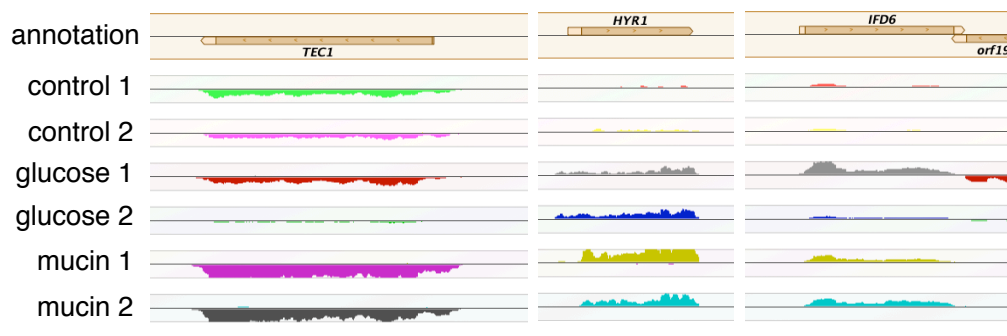
Figure 22: Selected mucin-induced transcripts are visualized using Mochiview.

Transcriptomic analysis is displayed in duplicates; the sequenced transcripts are visualized as tracks using the Mochiview software. To validate the mapping position of the reads, the annotation of three genes from the *Candida albicans* genome are depicted at the top showing the size and direction of the open reading frame. The peaks of the three of the genes that were detected as significantly up-regulated in the presence of mucin (in comparison to the control), *TEC1, HYR1,* and *IFD6,* are depicted.

3.2.7 Evaluating the role(s) of the *C. albicans* genes *TEC1*, *IFD6*, and *HYR1* in the presence of mucin

Based on the transcriptome analysis of *C. albicans* grown in mucin, we selected three genes that showed some of the highest expression induction due to mucin: the transcription factor *TEC1*, the aldo-keto reductase *IFD6* and the hyphal cell wall protein *HYR1*. For the TEC1 gene a deletion mutant of *C. albicans* was already available in our laboratory (Homann *et al.*, 2009). This experiment has already been conducted for the transcription factor mutant *tec1Δ/Δ* by the lab of Suzanne Noble (Witchley *et al.*, 2019b). These authors found that the *tec1Δ/Δ* mutant is hyperfit in colonizing the gastrointestinal tract and outcompetes the control strain in the course of 21 days. For IFD6 and HYR1 deletion mutants were constructed using the standard protocol of gene deletion with auxotrophic markers (Hernday *et al.*, 2010). None of the three deletion mutants show a growth deficiency under laboratory growth conditions. So we conducted the additional competition assays, inoculating conventional animals pretreated with antibiotics with the *hyr1Δ/Δ* or *ifd6Δ/Δ* mutant strains and the wild type control strain and monitored the cfu of the strains over the time course of 21 days. The fungal load of the animals is, with around 5 x 10^6 cfu/g feces, slightly lower than in gnotobiotic animals, the competitor strains are not outcompeting each other (Figure 23 A and B). Although the composition of the fungal community is not 1:1 (mutant:wild type) anymore, the change in the abundance of the single strains seem to be caused by individual effects of the animals rather than fitness defects of the inoculated strains (Figure 23 A and B). Therefore, these results indicate that neither gene plays a significant role in intestinal colonization.

We observed that *C. albicans* cells form aggregates when incubated under anaerobic conditions in media supplemented with mucin. To investigate whether any of the three genes has a role in this phenotype, we cultivated the deletion mutants in YNB minimal media supplemented with mucin as the sole carbon source under anaerobic conditions. Similar to the wild type, the mutants form big cell clumps out of yeast shaped cells in media supplemented

with mucin (Figure 23 C). The deleted genes are consequently not required for the aggregate formation observed under the tested *in vitro* conditions.

To find out if the *TEC1*, *IFD6*, and *HYR1* genes contribute to the attachment to mucus, we used our established *in vitro* cell culture based model with the mucin producing HT29-MTX-E12 cell line. The HT29 cell lawn with the secreted mucin on top was inoculated with the *C. albicans* deletion mutants and the corresponding wild type in separate wells. The attachment of the fungal cells to the human cell line and the produced mucin was evaluated using immunofluorescent staining. The numbers of attached *C. albicans* cells were counted in each picture and compared to the amount of attached cells of the wild type (Figure 23 D). The *tec1Δ/Δ* mutant showed slightly lower attachment rates compared to the wild type, whereas attachment of the *ifdΔ/Δ* deletion strain was slightly higher. The attachment of the *hyr1Δ/Δ* strain seemed fairly similar to the corresponding wild type strain. Overall the attachment of fungal cells to the HT29 cell line was not mutant-specific. The deleted genes seem to not play a major role in the attachment to mucin *in vitro*.
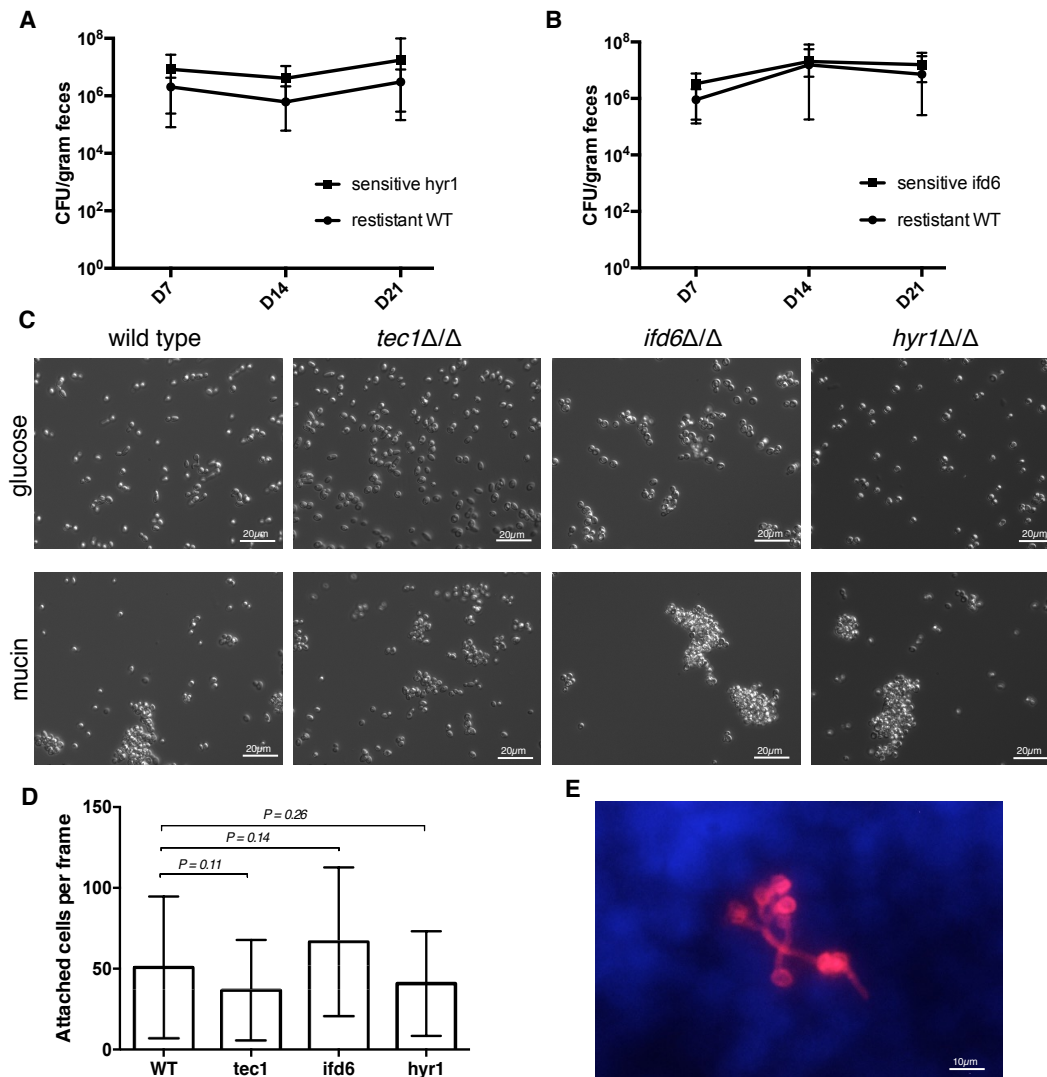
Figure 23: *C. albicans* deletion mutants do not show different behaviour than the wilt type strain.

For the mutants *hyr1Δ/Δ* and *ifd6Δ/Δ* a competition assay was conducted in conventional mice. The cfu of the wild type strain and either of the mutants (A and B) were not altered during the course of the experiment. In *C. albicans* cultures in minimal media supplemented with mucin grown in the anaerobic chamber the morphology of the fungus predominantly adopted the yeast shape, the cells formed dense clusters that were not dependent on any of the three genes (C). The three *C. albicans* mutants *hyr1Δ/Δ*, *ifd6Δ/Δ* and *tec1Δ/Δ* were used in a mucin attachment assay. The attachment rates were similar to the wild type (D) and the attachment to the mucin producing cell line was visually similar as well (E cell line cells stained with DAPI in blue and fungal cells in red).

Co-colonization of mice with *C. albicans* and a defined microbiota

3.2.8 The Oligo12-Mouse Microbiota provides colonization resistance to *C. albicans*

In our experiments, *C. albicans* and *B. thetaiotaomicron* could coexist stably within the mouse gut. The presence of a conventional microbiota, however, provides colonization resistance to *C. albicans*, it is unknown how or what microbes of the commensal microbiota mediate this resistance. The usage of a minimal consortium of bacteria can help dissect the biology of *C. albicans* in the presence of a microbiota. The Oligo12-Mouse Microbiota was designed to mimic the complex intestinal microbiota of a conventional mouse by the representation of twelve bacterial species. Young germfree NMRI mice were co-housed with a donor animal harbouring the OMM[12] for four weeks to transfer microbiota. The animals were then inoculated with *C. albicans* and the fungal and bacterial load was monitored over the time course of 21 days (Figure 24). The fungal load recovered from the stool samples is lower than in the germfree animal model. After seven days of colonization, the fungal cfu ranged from 10^6 down to 10^4 per gram stool (detection limit around 10^3 cfu/g feces). After 21 days the fungal numbers decreased even further. In many animals harbouring the OMM[12] the cfu of the fungus dropped under the limit of detection already after 7 days of colonization. We performed two colonization experiments (N = 6 or 10 animals) with mice harbouring the OMM[12] microbiota (Figure 24). In the first experiment we saw a decreased fungal colonization in the mice over the time course of 21 days, whereas in the second experiment the fungal cfu in many animals dropped below the limit of detection already at early time points. The OMM[12] mediates a colonization resistance to the fungus *C. albicans*, and although this resistance is not immediate, the usage of the OMM[12] appears to be inapplicable to study the biology of *C. albicans*, but is rather suited to elucidate which components of the microbiota are responsible for the colonization resistance of a conventionally grown mouse to *C. albicans*. With our experiments we could

show that *B. thetaiotaomicron* or *L. reuteri* alone are not sufficient, while 12 or less species are sufficient.
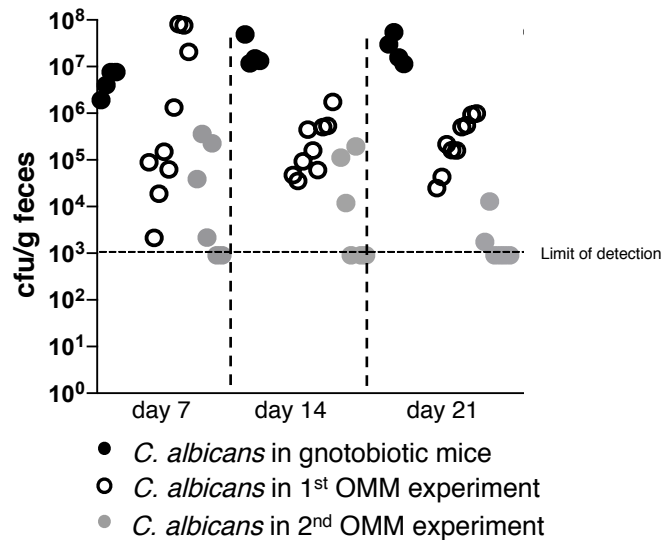
Figure 24: The presence of the OMM[12] decreases the recovered fungal cfu from feces.

In animals harbouring the OMM[12] minimal microbiota, the colonization of *C. albicans* was decreased. Fecal samples were plated weekly to monitor fungal cell counts. The average *C. albicans* numbers are lower in mice carrying the OMM[12] compared to germfree animals. In the two experiments with the exact same execution, the cfu numbers of *C. albicans* are distinctly different. This can be caused by a dynamic OMM[12] composition.

To detect changes in the composition of the OMM[12] over the time period of 21 days, the abundance of all the 12 bacterial species were quantified using a quantitative PCR approach (qPCR testing was conducted by the lab of Bärbel Stecher, Munich (Brugiroux *et al.*, 2016)). We investigated if the OMM[12] composition shifted in the presence of *C. albicans*. Although the OMM[12] is supposed to establish a stable colonization we could detect changes, up to 5-fold, for some of the species in the OMM[12] composition even before the addition of *C. albicans.* The experiment was conducted twice (N = 6 or 10 animals), and although in the first round of the experiment an increased number of gram-positive bacteria were detected in the OMM, namely *Clostridium innocuum*, *Lactobacillus reuteri*, and *Blautia coccoides* (Figure 25 A), no such trend towards an increased number of gram-positive bacteria was

observed in the second round of the experiment (Figure 25 B). The variability of the microbial community itself was too high to relate any of the detected changes to the presence of the fungus. Additionally the fungal numbers were strongly decreased in the presence of the OMM[12], in many animals even below the limit of detection, possibly the colonization resistance that is observed in conventional animals is already developed in animals harbouring the less diverse minimal microbiota. Due to the poor fungal load in the colonized animals the system was not suitable to study the biology of *C. albicans* in the presence of a minimal microbiota.
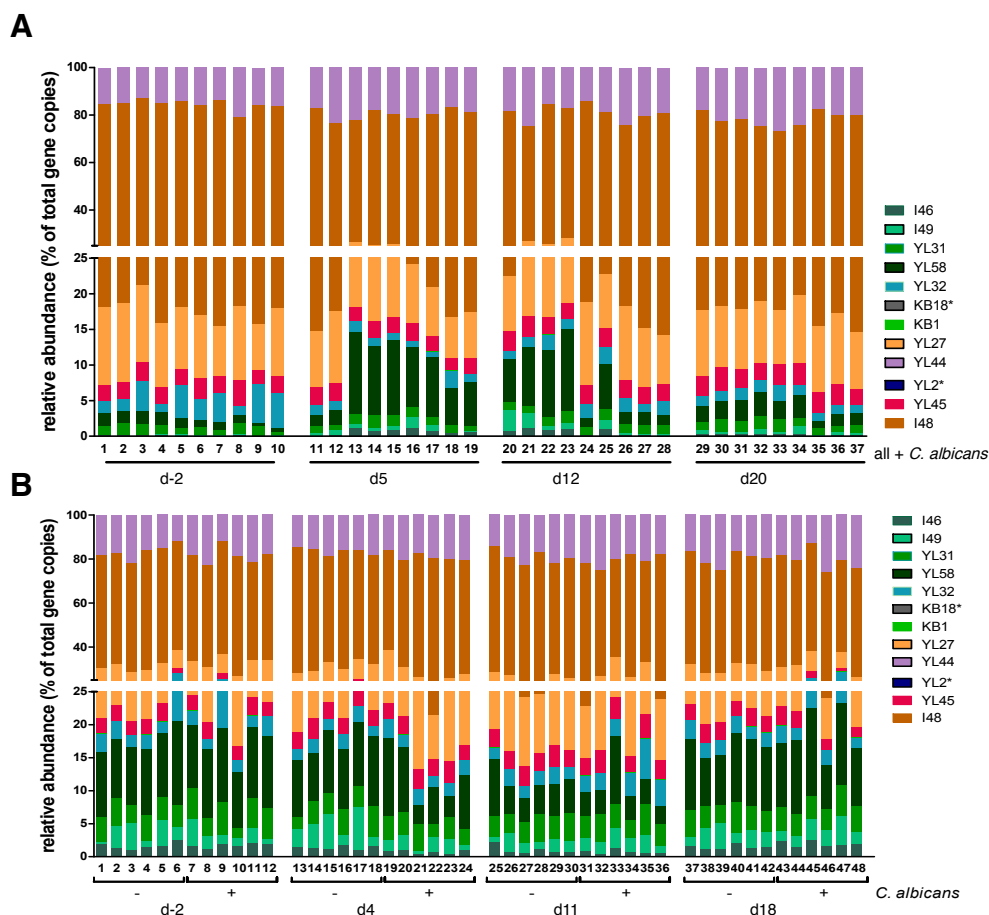
Figure 25: Composition of the minimal mouse microbiota over the course of 21 days with and without *C. albicans*.

The composition of the minimal microbiota was monitored using quantitative PCR using primers for each of the bacterial strains. The composition is very dynamic, even without the addition of other species. In the first experiment (A) an increase in *Lactobacillus reuteri, Blautia coccoides,* and *Clostridium innocuum* was detected in the presence of *C. albicans*. In the second experiment (B) no shifts of the minimal microbiota that was detected that could be traced back to the presence of the fungus *C. albicans* (Quantification experiments were performed by Claudia Eberl, LMU).

3.3 Discussion

In this chapter of my dissertation I expanded the *C. albicans* monocolonization model to include single bacterial members of the gut microbiota and a defined community of 12 bacteria. Stable co-colonization was achieved with *C. albicans* and the commensal gram-negative *Bacteroides thetaiotaomicron* or the commensal gram-positive *Lactobacillus reuteri*, I monitored the spatial distribution and abundance of each microbe in different parts of the mouse intestine. A key finding from this analysis is the establishment that, in the colon, *C. albicans* cells localized in a *B. thetaiotaomicron*-promoted outer mucus layer. The outer mucus layer is a compartment distinct from the adjacent lumen (H. Li *et al.*, 2015b). Therefore, our finding indicates that gut bacteria shape the intestinal microhabitats occupied by the fungus.

The colonization models that were established in this work using gnotobiotic mice are stable systems to study the gastrointestinal colonization of fungi and bacteria. The colonization rates of the single microbes we observed are in agreement with previous reports (*C. albicans* 1 x 10^7 cells/g feces, *B. thetaiotaomicron* 1 x 10^{11} cells/g feces, *L. reuteri* 1 x 10^8 cells/g feces). Interestingly the cfu numbers of all the microbes did not change over time and did not exceed the species specific threshold. The microbial density in our colonization models is higher in the colon and cecum compared to the small intestine. This is in line with other reports that have looked at other components of the gut microbiota (Barko *et al.*, 2018; Bowcutt *et al.*, 2014; Power *et al.*, 2014). *C. albicans* has been described to colonize all parts of the gastrointestinal tract (Koh, 2013), which is what we observed in our data. *B. thetaiotaomicron* has been described to mostly colonize the large intestine (Martens *et al.*, 2008). Consistent with this notion, we observed the highest density for this bacterial species in the colon of mono- and co-colonized animals. *Lactobacillus* species, however, are common colonizers of the small intestine at least in conventional animals (Herías *et al.*, 1999). For gnotobiotic rodents no such prevalence was described (S. Da Silva *et al.*, 2015) and evaluating our tissue sections we could detect a similar high abundance of *L.*

reuteri in the colon and ileum of colonized animals. One of the reasons *L. reuteri* is not limited to the ileum in gnotobiotic animals might be the missing competition. In conventional raised animals the microbial density is the highest in the colon and therefore colonization may be very competitive, whereas in germfree animals all niches are free and can be colonized.

In all colonization models the morphology of the fungus *C. albicans* was examined in the ileum, cecum and colon. We observed the round yeast morphology (Figure 12 B and C) in all gnotobiotic mouse models of this work. The yeast morphology of *C. albicans* is connected to the commensal lifestyle of the fungus (Neville *et al.*, 2015; Pérez, 2019), supporting the hypothesis that the fungus resides as a commensal in our colonization models. The *C. albicans* morphology in the gut of these mice does not seem to be altered by the presence of bacterial commensals.

On the host side of the colonization models applied in this work we focused on the overall appearance of the intestinal mucus. In all the colon sections we could observe that the microbes were clearly separated from the colonic epithelium. In the ileum, by contrast, we could observe patches of mucin that are colonized by microbes as well as parts of the epithelium without any adjacent mucus. In the latter parts, single bacterial and fungal cells were found in direct contact with the epithelium. This colonization pattern is commonly found in the small intestine (M. E. V. Johansson *et al.*, 2015). The role of the mucin layer in the colon is different. Johansson *et al.* have shown that there is an inner mucus layer which is normally devoid of bacteria; therefore, the direct contact of microbes with colon tissue is typically associated with pathogenesis (Malin E V Johansson *et al.*, 2014; Richard *et al.*, 2018).

In our model system, the mucus layer of the colon was also devoid of any fungal (*C. albicans*) cells. Our findings indicated that, like bacteria, *C. albicans* is also only present on top of the mucin layer and does not penetrate the inner layer. Of particular interest to this work, we found that the monocolonization of the gut by *C. albicans* does not promote the formation of an outer mucin layer, which is found in conventionally raised animals (M. E. V. Johansson *et al.*,

2008). The outer mucin layer was promoted in the presence of *B. thetaiotaomicron*, as expected (Bjursell *et al.*, 2006; Sonnenburg *et al.*, 2005b; Xu *et al.*, 2003). The colonization of the gut with *L. reuteri*, or *L. reuteri* and *C. albicans* showed no promotion of the outer mucus layer. The thickness of the outer mucin layer has been measured by several groups so far (Earle *et al.*, 2015) and our measurements of ~ 70 *µ*m with a model using gnotobiotic mice is around 30 % less of the previously described measurements for conventionally colonized mice (M. E. V. Johansson *et al.*, 2008). The thickness of the inner mucin layer was measured in all models of this work. The measured thickness of this inner sterile layer of ~ 20 *µ*m corresponds well to measurements of previous studies in mice (Jakobsson *et al.*, 2015; H. Li *et al.*, 2015b). The inner mucus layer is defined by the absence of microbes (M. E. V. Johansson *et al.*, 2008). Malin Johansson *et al.*, (2016) reported that the integrity of the inner mucus layer in gnotobiotic mice is not stabilized until six weeks past bacterial colonization. This conclusion was drawn from the results that before the six weeks threshold bacterial sized particles were able to penetrate into the inner mucus layer. All samples of this study were taken at earlier time points than the six weeks threshold established by Johansson *et al.*, but in all our analysed samples we see an intact impenetrable mucus layer already after a colonization period of 21 days.

We found that the outer mucus layer, which is promoted by the presence of *B. thetaiotaomicron*, could be occupied by the fungus *C. albicans*. Thus, although the fungus itself cannot promote the production of a secondary outer mucin layer, it colonizes this niche if it is available (Figure 26).

C. albicans has previously been reported to digest mucin under certain *in vitro* growth conditions (A R Colina *et al.*, 1996). Under our experimental conditions, the fungus could utilize intact mucin as a carbon source to a limited extent; however, mucin that was previously digested by other bacteria or enzymes, like *B. thetaiotaomicron* or β-glucanase, supported higher levels of fungal proliferation. We speculate that by occupying the *B. thetaiotaomicron*-promoted outer mucin layer, *C. albicans* may have access to significant amounts of digested mucin. Although in the presence of *B.*

thetaiotaomicron the fungus occupied a particular microniche (i.e. the outer mucin layer), the overall cfu numbers of *C. albicans* did not vary between mono- and co-colonized animals. This might be explained by the complexity of the gut, due to factors that might still be unknown which mask a shift in fungal cfu or the changes are simply too minor to detect them with our quantification method.

In conventional animals the outer mucin layer has been described as a popular niche, favoured by many intestinal bacteria even non-mucolytic species (H. Li *et al*., 2015a). Possibly the abundance of *C. albicans* colonizing this niche and due to the rich growth conditions in this environment, regardless of the availability of mucins. In *in vitro* assays of this work as well as in a previous study (Ana Rosa Colina *et al*., 1996), it can be observed that the fungus is able to grow on mucin as carbon source. Colina *et al*. 1996 attributes the mucin degradation to the secretory aspartyl proteinases (SAP) encoded by *C. albicans*. Coming to the conclusion that the fungus prefers glucose as a carbon source but is able to digest highly glycosylated mucins for its growth (Figure 17).

Additionally we could observe in several *in vitro* assays that *C. albicans* has the ability to attach to mucin. This affiliation of the fungus to mucin corresponds to the localization of the fungus. In the colon of mice *C. albicans* is found with a high prevalence in the outer mucin layer. *In vitro* the fungal cells form strongly attached aggregates without forming filaments when the cells are grown on mucin as a carbon source, so far this behaviour has not been described for *C. albicans* under any condition.
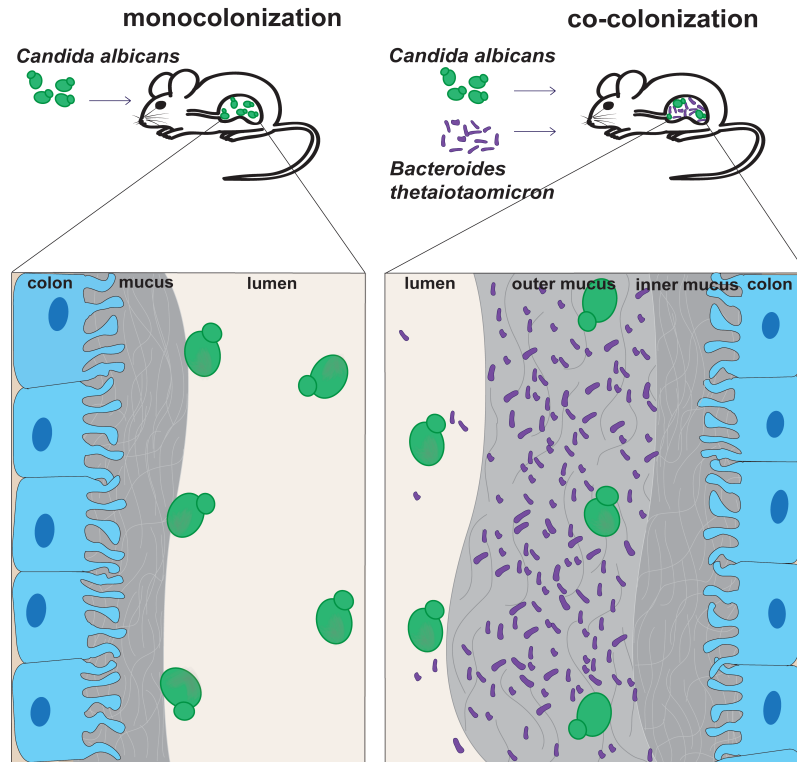
Figure 26: *C. albicans* colonizes the outer mucin layer that is promoted by the presence of *B. thetaiotaomicron in vivo*.

Illustration depicting the mono- and co-colonization model of gnotobiotic animals with *C. albicans* and *B. thetaiotaomicron* and the location of the fungal and bacterial cells in the colon of these animals. In co-colonized animals the fungus can colonize the niche of the outer mucus layer, which is promoted by the presence of *B. thetaiotaomicron* in the gut of mice.

In commensal mice the gastrointestinal microbiota prevents colonization with *C. albicans,* therefore we used a gnotobiotic animal model in this work. The most ideal animal model to study fungal bacterial interactions in the gastrointestinal tract should include a commensal microbiota and the fungus. Therefore the usage of the minimal microbiota OMM^{12} consisting of 12 bacterial mouse-derived species was adapted to create an environment comparable to a commensal microbiota. The colonization of the gut of gnotobiotic animals with the OMM^{12} mediated a colonization resistance (Figure 24). The presence of this minimal microbiota has been previously reported to establish a colonization resistance against pathogenic bacterial species, like *Salmonella* spp. (Brugiroux *et al.*, 2016), similar to a commensal

microbiota. Is appears that although *C. albicans* solely displayed the behaviour of a commensal in this work the presence of a commensal microbiota permits the colonization of the gut by the fungus.

In this second chapter of my dissertation I revealed that the fungus *C. albicans* and the commensal gut bacteria *B. thetaiotaomicron* and *L. reuteri* can colonize the gastrointestinal tract of gnotobiotic animals in mono- and co-colonized systems in a stable way, that *C. albicans*, *B. thetaiotaomicron* and *L. reuteri* have different effects on the mucus structure in the colon of colonized animals, and that *C. albicans* can colonize the loose outer mucus layer in the that is promoted by *B. thetaiotaomicron* in the gastrointestinal tract of colonized animals.

4. Conclusions and Outlook

The gastrointestinal tract of mammals contains a diverse and dynamic community of microbes. While most studies to date have focused on the bacterial portion of the gut microbiota, here I have investigated several aspects of intestinal colonization by the fungus *Candida albicans*. Specifically, I have addressed the interactions between the fungus and single bacterial species or a small assembly of bacteria. I have also started to define the host response of intestinal tissue to fungal colonization. Using a monocolonized mouse model, I have established that not only the bacterial microbiota (Sommer & Bäckhed 2015) but also the fungus *C. albicans* induces the production of reactive oxygen species (involving the enzyme DUOX2) in the intestinal epithelium. The mechanism(s) that lead to the activation of this particular response, *e.g.* which fungal moieties or secreted molecules act as stimuli, remains to be determined. Additional investigations with immunodeficient mice, *e.g. Duoxa*$^{-/-}$ mice (Grasberger *et al.* 2012), could also reveal whether the oxidative stress response of the host plays any significant role in keeping the fungus in the commensal state in the gut.

Circadian clock genes have also previously been reported to be regulated by the presence of the gastrointestinal microbiota (Wang *et al.*, 2017). The results described in this dissertation, however, reveal for the first time that a single fungal species, *C. albicans,* may be sufficient to activate the expression of genes of the circadian clock circuitry, as well as the distribution of these proteins within epithelial cells of the gastrointestinal tract. The physiological consequences of the regulation of this pathway by the fungus is unclear. Circadian clock genes are involved in the regulation of many metabolic and physiologic pathways (*e.g.* cell division and lipid uptake and storage) (Causton *et al.*, 2015; Tu *et al.*, 2005). The composition of the gut microbiota can also contribute a great share of the metabolic activity in the gastrointestinal tract (Chen & Wang 2019, Smirnov *et al.* 2016). Whether the presence of *C. albicans* in the intestine has any impact on the metabolic profile of the host by the regulation of circadian clock genes is something that

could be addressed experimentally in the future (*e.g.* through metabolomics analyses).

To obtain a more complex animal model we expanded the *C. albicans*-monocolonized mouse model by the addition of single bacterial species. The common gut bacteria *B. thetaiotaomicron* or *L. reuteri* were gavaged to animals that were already harbouring the fungus. In the two co-colonization models the fungal and the bacterial colonizer both reached stable colonization rates. While visualizing the distribution of the microbes in the gastrointestinal tract, we observed a distinct difference in the mucus layers of the colon of the colonized animals. We noticed that the presence of *B. thetaiotaomicron,* a bacterium that is known to induce mucin production and to be able to utilize polysaccharides, led to the production of a thick loose outer mucus layer in the colon. Only a very thin outer mucus layer could be detected in animals that were colonized with *L. reuteri* and *C. albicans*. And while it has been reported that *B. thetaiotaomicron*-presence in the gastrointestinal tract of mice induces the production of larger amounts of mucins (Wrzosek 2013), it is not understood how this is achieved. Whether *B. thetaiotaomicron* directly affects the mucus-producing cells by direct stimulation or if the epithelium senses the presence of the bacterium indirectly needs further investigation. One possible mechanism by which host senses the bacterium is the secretion of messenger molecules originating from *B. thetaiotaomicron*, like it has previously been reported by Andrew Koh (Fan *et al.*, 2015). Alternatively or additionally, the host might be able to recognize the utilization of the outer mucins by *B. thetaiotaomicron*. It is also unclear what products are left behind by *B. thetaiotaomicron* when it utilized these host-produced mucins. We could detect an increased growth rate of the fungus *C. albicans* in mucin that was previously treated with *B. thetaiotaomicron.* These findings and the observation that fungal cells are able to colonize the *B. thetaiotaomicron*-promoted mucus layer in co-colonized animals in our experimental setup suggest that the saccharolytic bacterium is able to subsist from the mucins. It further implies that, while digesting the long mucin chains for its own use, the bacteria might leave shorter mucin chains behind, which are more accessible

for other species, like the fungus *C. albicans*. The genome of *B. thetaiotaomicron* harbours a great variety of genetic tools to utilize the mucin of the gastrointestinal tract (Flint *et al.*, 2012; Rogers *et al.*, 2013). In order to identify the genes that are involved in these processes, the use of a *B. thetaiotaomicron* mutant library could provide novel insights. The question of how the *B. thetaiotaomicron*-treated mucin differs from undigested mucin and if it is in fact consisting of shorter glycan chains, might be addressed by using an HPLC- or mass spectrometry-based approach.

The bacterium *B. thetaiotaomicron* is able to shape its own environment; visual for us by the abundance of the loose outer mucus layer present in the colon of colonized mice. For the fungus *C. albicans* we could not observe this kind of active intervention on the gastrointestinal environment. However, the fungus efficiently colonizes this new microniche of the outer mucus layer that is produced in the presence of the bacterium. To gain insights into the mechanism(s) the fungus is using to colonize the mucus layer, a colonization approach using a *C. albicans* deletion mutant library could reveal relevant genes and thereby processes and mechanisms of this colonization.

In all experimental setups of this work, *in vivo* and *in vitro*, the *C. albicans* cells predominantly kept their round yeast morphology, which is commonly connected to the commensal lifestyle of the fungus. *In vitro* the fungal cells aggregated in the presence of mucin and formed firm clusters, while all cells of these clusters remained in yeast morphology. Usually the aggregation of fungal cells can be monitored for example at infection sites (Meir *et al.*, 2018) or in the presence of serum (this work 2.2.1). Under these mentioned conditions the fungal cells are consistently found as hyphae. The aggregates found in this study in the presence of mucin are distinctly different from the hyphal clusters that are commonly observed. Why the fungal cells keep their yeast morphology during the formation of the aggregates will need further investigation. To address the question which regulatory pathways might mediate the cluster formation of the fungus, a comparative transcriptome analysis in the presence or absence of mucin or hyphae-cluster-stimulating agents, such as serum, could be helpful. Additionally, one might investigate *C.*

albicans deletion mutants of adhesins and other proteins known to be overexpressed in cells of the hyphal morphology.

While the fungus *C. albicans* was able to stably colonize the gastrointestinal tract of mice in the presence of a single bacterial strain in our experiments, the presence of a minimal consortium of bacteria mediated a colonization resistance to the fungus, very similar to the situation that is found in conventionally raised mice. To gain more information about this colonization resistance that is mediated either by the minimal consortium as a whole, or possibly by single members, the establishment of separate colonization models might be of great use. By inoculating a smaller bacterial consortium of bacteria or single species for the co-colonization experiments with the fungus, insights on the colonization resistance and how it is mediated might be revealed. By expanding the co-colonization experiments it would also be possible to investigate further how bacteria shape their environment, for example by affecting the mucus production by the host.

Fungal-bacterial interactions have so far been mostly studied in *in vitro* systems such as mixed-species biofilms. Obtained information on inter-kingdom interactions, withtin the natural niche, in which the two microbes cohabitate, are rare. The model I used in this dissertation of mono- and co-colonized gnotobiotic mice, using single bacterial and fungal strains, proved to be an effective tool to dissect host-fungal and bacterial-fungal interactions within the gastrointestinal tract. In this work I could describe the host response to the monocolonization of the gastrointestinal tract by the fungus *C. albicans,* including the activation of a reactive oxygen species-related defence mechanism and the induction of regulators of the circadian clock circuitry. And by using co-colonized mouse models I could observe that the outer mucus layer is promoted by the bacterium *B. thetaiotaomicron* and that the fungus *C. albicans* colonizes this *B. thetaiotaomicron*-dependent microhabitat when it is available. The co-colonization models will continue to be helpful in the future to investigate the interactions taking place between fungi and bacteria in the gut and can be developed further to address many arising open questions.

5. Material and Methods

5.1 Cultivation of eukaryotic cells and bacteria

5.1.1 Cultivation of *Candida albicans*

If not indicated differently, the fungus was cultured in YPD (Yeast Glucose media) at 30 °C under aerobic conditions. Liquid cultures (20 ml) were placed on a shaker with 160 rmp or 3 ml cultures in tubes in a rotation wheel. For growth on solid media, *C. albicans* was streaked or plated on YPD agar (15 g/l) plates.

5.1.2 Cultivation of *Bacteroides thetaiotaomicron*

B. thetaiotaomicron is an aerotolerant anaerobic bacterium, growing only in the absence of oxygen. Therefore, liquid cultures or agar plates containing *B. thetaiotaomicron* were always kept in the Don Whitley Scientific anaerobic chamber with an atmosphere of 80 % N_2, 10 % CO_2 and 10 % H_2. To grow *B. theta*, either BHI media supplemented with 10 % defibrinated horse blood (Fisher Scientific) or Tryptophan Yeast Glucose media (TYG), both either liquid or solid, were used.

5.1.3 Cultivation of *Lactobacillus reuteri*

L. reuteri is a microaerophilic bacterium growing only in an atmosphere with reduced amounts of oxygen. Therefore, liquid cultures or agar plates containing *L. reuteri* were always kept in incubators with an atmosphere containing 5 % O_2. To grow *L. reuteri*, either BHI media supplemented with 10 % defibrinated horse blood or MRS media (De Man, Rogosa and Sharpe media) was used.

5.1.4 Cultivation of human cell lines

Cell lines used in this work were purchased from the ECACC (European Collection of Authenticated Cell Cultures, Sigma-Aldrich, UK) (C99 and HT29-MTX-E12) or kindly provided by Prof. Dr. Cynthia Sharma (CaCo2). Cells were stored in cryotubes in liquid nitrogen for long term storage and were thawed prior to usage in a 37 °C water bath and then cultured in corresponding media (Table 4) supplemented with 20 % fetal bovine serum (Thermo Fischer) in a 37 °C incubator with a 5 % CO_2 atmosphere. Cells were passaged at least twice but no more than 20 times before the usage of the cells in experiments.

Table 4: Cell lines and their growth media and supplements.

Cell line	Media	Supplements
CaCo2	MEM	10 % fetal bovine serum
C99	IMDM	10 % fetal bovine serum, 2 mM glutamine
HT29-MTX-E12	DMEM	10 % fetal bovine serum, 2mM non-essential amino acids, 2 mM glutamine

All cell culture media and supplements were purchased from Thermo Fischer

5.1.5 Preparation of mucin for *in vitro* growth experiments

The commercially available mucin from porcine stomach, Type III (Sigma-Aldrich) was prepared as previously described by Roberton & Stanley, 1982. In brief, 0.33 g of the mucin were solved in 30 ml of ddH_2O and sterilized by autoclaving. The solution was then dialyzed (molecular weight cut of 14,000, D9777, Sigma-Aldrich) for 24 h at 4 °C and filter sterilized (pore size 0.45 µm). The pretreated mucin was incubated with *B. thetaiotaomicron* or *L. reuteri* prior to the experiments. For this purpose, the bacteria were grown under the conditions described above for 30 h. This dense culture was then washed twice in PBS and added to 10 ml of already dialyzed and filtered porcine stomach mucin. After an incubation period of 24 h under the ideal growth

conditions of the bacteria, the solution was filter sterilized to remove the bacterial cells. To account for the effect of molecules that are secreted by *B. thetaiotaomicron* during the incubation with the mucin, a negative control using PBS that was incubated with *B. thetaiotaomicron* for 24 h was prepared and used for growth experiments.

5.1.5.1 β-glucanase treatment of mucin

To enzymatically digest mucin, 100 mg β-glucanase from *Trichoderma longibrachiatum* (Sigma-Aldrich) was mixed with 1 ml PBS and then 500 μl of this β-glucanase solution was used to inoculate 10 ml of dialyzed and filtered mucin from porcine stomach. The mucin was incubated for 2 h at 37 °C and afterwards filter sterilized.

5.1.5.2 Preparation of mucin from HT29-MTX-E12 cells

The human adenocarcinoma cell line HT29-MTX-E12 was cultivated in an atmosphere with 10 % CO_2 at 37 °C. Cells were seeded into 6 well plates in a density of 1 x 10^5 cells/ml. Media was changed twice per week- After 21 days of cultivation, the cells start to secrete visual amounts of mucus. Secreted mucus was collected by removing the media from the well and then isolated by filtering through a cell strainer (100 μm nylon mesh). Isolated mucin was then filter sterilized (pore size 0.45 μm). Similar to the mucin from porcine stomach, the mucin collected from the cell line was incubated with *B. thetaiotaomicron* prior experiments.

5.1.6 *C. albicans* growth in mucin-supplemented media

An overnight culture of *C. albicans* was washed twice in PBS and used to inoculate YNB minimal media supplemented with different pretreated mucins. The minimal media was supplemented with 10 % of either porcine stomach mucin (Sigma-Aldrich), mucin that was preincubated with bacteria (*L. reuteri* or *B. thetaiotaomicron*), PBS preincubated with B. theta or without additives.

The different media were inoculated with the washed *C. albicans* culture and set to an OD_{600nm} of 0.2 and incubated for 48 h at 30 °C. On five different time points, the OD_{600nm} was measured and samples were taken and plated onto YPD agar plates to monitor the Candida cfu during the incubation time. To investigate the morphology of the fungus during the growth in minimal media supplemented with mucin, minimal media supplemented with mucin from porcine stomach (10 % v/v) or *B. thetaiotaomicron*-digested mucin (10 % v/v) was inoculated with a single colony of *C. albicans* and incubated at 30 °C over night. On the following day, 1 ml of the Candida culture was washed in 1 ml sterile PBS and stained with propidium iodide or left unstained and embedded on a microscope slide to be observed under the fluorescent microscope (Leica, DMI 6000B)

5.1.7 *B. thetaiotaomicron* growth in mucin-supplemented media

The growth of *B. thetaiotaomicron* on mucin as a carbon source was monitored in minimal media for *Bacteroides* spp. The media was supplemented with either 10 % mucin from porcine stomach or left without any carbohydrate. A saturated *B. thetaiotaomicron* culture that was grown for 30 h in rich TYG media in the anaerobic chamber was washed twice in PBS and then used to inoculate the prepared minimal media with an OD_{600nm} of 0.1. The growth of *B. thetaiotaomicron* was monitored at different time points by optical density as well as recovered cfu data.

5.2 Mouse experiments

5.2.1 Gastrointestinal tract colonization

To colonize the gut of germfree mice with *Candida albicans*, an oral gavage was performed. Therefore, an overnight culture of *C. albicans* was grown at 37 °C in YPD media, 1 ml of this ON culture was washed twice with PBS and set to a total number of 1 x 10^8 cells/ml using the haemocytometer. 100 μl of this stock solution was used to infect germfree mice with a total number of 1 x

10^7 Candida cells per NMRI mouse using a gavage needle. Colonization status was monitored by plating fecal pellets on YPD plates. Similarly, colonization of the gastrointestinal tract by the bacterial species *Bacteroides thetaiotaomicron* and *Lactobacillus reuteri* were obtained by oral gavage of 1 x 10^8 bacterial cells per mouse. In co-colonization experiments, mice were gavaged twice, a minimum of 6 days were kept in between the two infections to let the mice rest and the already gavaged organism proliferate. To monitor the colonization levels of the different microbes, feces pellets were collected for each mouse twice per week and frozen in 10 % glycerol to be plated on agar plates suitable for the microbe, the mice were infected with. Additionally, control samples were always taken before the initial gavage to test for sterility of the animals. The input culture was always plated to ensure the correct gavage numbers.

5.2.2 Co-housing of mice

The Oligo^{12}-Mouse-Microbiota was designed by the lab of Prof. Dr. Bärbel Stecher at the LMU Munich. The OMM^{12} consortium of bacteria was gavaged to germfree C57BL/6 mice and the mice were maintained in a sterile environment to keep the original composition over generations. To colonize other breeds of mice with this OMM^{12} consortium, up to four female germfree NMRI animals were co-housed with one female C57BL/6 OMM^{12}-colonized donor animal in a germfree cage for 28 days. After the co-housing period, mice were gavaged like described before in 4.2.1, to count *C. albicans* cfu in fecal samples from OMM^{12} animals the pellets were plated onto YPD agar plated containing (15 mg/ml gentamicin and 50 mg/ml ampicillin). To monitor the composition of the OMM^{12} during colonization, feces samples were taken and analysed using qPCR. Analysis of the OMM^{12} composition was performed by the group of Bärbel Stecher, Munich; see Brugiroux *et al.*, 2016.

5.2.3 Sacrifice of the animals and sample collection

At the end of each mouse experiment, usually 14 or 21 days post the first gavage; the mice were sacrificed using CO_2 followed by cerebral dislocation or final blood sampling. Whole blood was collected and centrifuged to isolate the serum, which was kept frozen at -80 °C. Samples of the intestinal content coming from ileum, cecum, and colon were collected in 1.5 ml Eppendorf tubes containing 500 μl of sterile 10 % (v/v) glycerol and stored at -80 °C to be used for cfu observation. Tissue samples (approx. 1 cm of intestine) for cytokine measurement or RNA extraction were taken from ileum and colon, the intestinal content was removed and the tissue immediately frozen at - 80 °C. For histology samples of ileum, cecum, and colon, approximately 1 cm of tissue was collected still containing the fecal content. The samples were placed in methacarn solution (60 % methanol, 30 % chloroform, 10 % acetic acid, all Roth Germany) immediately. Like previously described (M. E. V. Johansson, Larsson, *et al.*, 2011), the tissue samples were fixed to maintain an intact mucus layer. After incubation of the samples for 24 h at 4 °C in methacarn, the samples were washed twice in 100 % methanol for 30 min, followed by a 35 min washing step in 100 % ethanol. For long term storage, the samples were embedded in paraffin with a paraffin embedding machine (Leica EG 1160) using the standard program, which, after several washing steps in increasing ethanol concentrations, and a xylene bath, replaces all liquid of the samples with 62 °C warm melted paraffin. Later, the tissue samples were embedded in melted paraffin blocks, stored at room temperature and later cut in 3-5 μm thin sections.

5.2.4 Gastrointestinal colonization of SPF mice

Specific pathogen free female NMRI mice were ordered from Charles River Laboratories, Sulzfeld, Germany. The water of the animals was supplemented with Gentamicin (666 μl / l H_2O of a 150 mg/ml stock) and Oxytetracyclin (5 ml/l H_2O of a 200 mg/ml stock) one week before starting the infection. The antibiotics supplemented water was changed twice per week with fresh

antibiotic supplemented water, over the whole three weeks of colonization. To determine the fitness of different mutants in the gastrointestinal tract of mice, the *C. albicans* mutant and the parental strain of the mutant were orally gavaged into the mice in a 1:1 ratio. In total, 1×10^7 *Candida* cells were given to the mice in 100 μl of PBS. The parental *C. albicans* strain was tagged with a SAT-cassette, which made this strain resistant to Nourseothricin (NAT). The mice were colonized with the strain mix and stool samples were taken once per week from each mouse over a time period of 3 weeks. The stool samples were plated on YPD agar plates and YPD agar plates supplemented with NAT. This procedure allowed monitoring the population of both strains in the intestine of the mice. After 21 days of colonization, the animals were sacrificed.

5.2.5 Ethics statement

The animal studies and protocols (permission numbers 16/2307, 16/2372) were approved by the local government of lower Saxony (Niedersächsisches Landesamt für Verbraucherschutz und Lebensmittelsicherheit), Germany. All animal studies were performed in strict accordance with the guidelines for animal care and experimentation of the German Animal Protection Law and EU directive 2010/63/EU.

5.3 Microscopy methods

5.3.1 Fluorescence *In Situ* Hybridization (FISH)

Paraffin embedded sections were cut in 3-5 μm thick sections and applied on SuperFrost Slides (Hartenstein Laborversand). In order to remove the paraffin, a descending ethanol series was prepared. The samples were dipped in xylene for 10 min twice, then in 96 % EtOH for 5 min each, followed by 70 % EtOH and 50 % EtOH for 5 min each. The samples were then rested in ddH$_2$O for up to 5 min. For FISH staining fluorescently labelled probes (100 pmol) were diluted 1:1500 in hybridization buffer. The samples were covered

with the hybridization buffer containing the probes and incubated for 16 h at 55 °C. After hybridization, the samples were always kept in the dark while being washed twice in wash buffer for 10 min. Slides were transferred to a humidified dark chamber to stain the tissue with DAPI (5 μg/ml in PBS) for 1 h at 4 °C. Later the samples were washed again twice with PBS, while kept in the dark. After the washing steps, the samples were mounted in Diamond Antifade Mountingsolution (Thermo Fischer) and kept in the dark at 4 °C until visualization under the microscope.

For the staining of gram-positive bacteria with a FISH probe, a treatment with lysozyme was necessary prior the hybridization to achieve sufficient fluorescent staining. Therefore, samples were covered with lysozyme solution (0.05 g/ml in PBS) and incubated in a humid chamber at 37 °C for 30 min. Then, the staining procedure was continued as described above.

Hybridization buffer

200 μl   Tris-HCl (1 M, pH 7.2)

1.8 ml   NaCl (5 M)

100 μl   SDS (10 % w/v)

Adjust to 10 ml with ddH$_2$O

Wash buffer

1.6 ml   Tris-HCl (1 M, pH 7.2)

14.4 ml   NaCl (5 M)

Adjust to 80 ml with ddH$_2$O

Table 5: FISH probes used in this work ordered from Eurofins Scientific

Probe name	Label	Sequence
Pan Yeast	Cy3	CTCTGGCTTCACCCTTATTC
Pan Bacteria	Cy5	GCTGCCTCCCGTAGGAGT

5.3.2 Immunofluorescent staining

The paraffin was removed from the samples as described above with a descending ethanol series. After the 5 min incubation of the samples in ddH$_2$O, the samples were transferred to PBS-T for 3 min and then placed in a tray containing citrate buffer and boiled at 95 °C for 20 min using a water bath. The slides were allowed to cool down in PBS-T for 30 min and with the help of a Dako Pen (Agilent), a hydrophobic barrier was drawn around the samples on the slides. To block any unspecific binding, samples were covered with BSA Fraction V (5 mg/ml in PBS, Sigma-Aldrich) in a humid chamber at 4 °C for 30 min. After removal of the BSA, the samples were incubated with the primary antibody diluted 1:100 in Antibody-Diluent (Carl Roth) overnight at 4 °C. To remove unbound antibodies, the samples were washed 3 times in PBS for 10 min. The secondary antibody was diluted 1:400 in Antibody-Diluent (Carl Roth) and placed on the slides for 1 h at 4 °C. After 3 washing steps with PBS for 10 min each, the samples were mounted in Diamond Antifade Mounting Solution (Thermo Fischer) and kept in the dark at 4 °C until visualization under the microscope. All primary and secondary antibodies used in this work are listed in Table 6.

5.3.3 FISH and immunofluorescent staining

To visualize *C. albicans*, bacteria, and the host produced murine mucus on the same sample, a combination of FISH and immunofluorescent staining was performed. The tissue samples were prepared as described above and the paraffin removed with the descending ethanol series. First the FISH probes (Pan Yeast/Pan Bacteria) were hybridized to the tissue sample as describes in the paragraph above and after the two washing steps with wash buffer, the slides were transferred to a humidified box and blocked by incubating the samples with BSA Fraction V (5 mg/ml in PBS, Sigma-Aldrich) at 4 °C for 30 min. The blocking reagent was removed and then the primary antibody (anti-Muc2 produced in rabbit, Santa Cruz) diluted 1:400 in blocking reagent was left on the samples for 2-12 h at 4 °C in the humidified chamber. After removal

of the primary antibody and three washing steps, each for 10 min, the secondary anti-rabbit Alexa-594 antibody was diluted 1:400 and DAPI dye (5 µg/ml) was diluted 1:100 in blocking reagent and incubated on the samples for 1 h at 4 °C. After the final three washes with PBS, each wash for 10 min, the samples were mounted in Diamond Antifade Mounting Solution (Thermo Fischer) and stored at 4 °C for 1 h and then immediately visualized with the Leica confocal microscope.

Table 6: Antibodies used in this work.

Primary antibodies			
Target	Origin	Usage	Vendor
MUC2	rabbit	WB, IF	Santa Cruz Biotechnology
Candida albicans	rabbit	IF	Abcam
Actin	rabbit	WB	Sigma-Aldrich
DUOX2	rabbit	WB	Invitrogen
NFIL3	rabbit	IF	Bioss Antibodies
REV-ERBα	rabbit	IF	Abcam
DBP	rabbit	IF	Abcam
Secondary antibodies			
Target	Conjugation	Usage	Vendor
rabbit Ig-G	Alexa 594	IF	Thermo Fischer
rabbit Ig-G	HRP	WB	Sigma-Aldrich

IF: Immunofluorescent staining, WB: Western blot

4.3.4 Fluorescent *in situ* hybridization for RNA targets

To localize the expression of single RNA transcripts in cells, we used the method of the RNAscope® Multiplex Fluorescent Assay V2 (ADC, a Bio-Techne Brand). This method uses specifically designed probes to bind exclusively to target RNA molecules. The probes are then detected with antibodies and visualized by the binding of an Opal™ fluorophore (Akoya

Biosciences). With this method it is possible to detect up to three different RNA targets simultaneously in one sample. We used the probes mM-DUOX2-C1, mM-DBP-C2, and mM-DUOX2A-C3 assigned to the fluorophores Opal™ 520, Opal™ 570 and Opal™ 690 and followed the proposed workflow of the RNAscope manual precisely. Samples were then evaluated with the Leica confocal microscope.

5.3.5 Confocal microscopy

High-resolution microscopy was performed using a laser scanning confocal microscope (Leica, TCS SP5). The microscope is equipped with four lasers: Leica UV diode (405nm), argon (488 nm), DPSS (561 nm) and HeNe (633 nm) which were used for fluorescence excitation. All confocal images were captured using Leica microsystem CMS software (LAS AF v.2.0.2), the excitation and emission (Ex/Em) of the fluorescent signals were monitored as follows: DAPI staining for cell nuclei (Ex/Em 405/410-460 nm), Cys3-labeled probes (Ex/EM 514/520-550 nm), Alexa fluor 594 conjugated antibody (Ex/Em 561/600-630 nm) and Cys5-labeled probes (Em/Ex 633/640-720 nm). The data was exported from LAS AF software and processed with the FIJI (https://fiji.sc/) imaging tool.

5.4 RNA-based methods

5.4.1 RNA extraction from colon tissue for transcriptome analysis

For RNA extraction, pieces of colon tissue were homogenized in Trizol (Sigma-Aldrich) using the MP Biomedical FastPrep-24™ Classic Instrument and Lysis Matrix D tubes (MP Biomedicals), settings were set to 40 sec at 6.5 m/sec. To each tube containing homogenized tissue, 500 µl of Phenol:Chlorofom:Isoamylalcohol (25:24:1, Sigma-Aldrich) was added and inverted several times prior to a 10 min centrifugation step at 15,000 rpm at 4 °C. The upper aqueous phase was transferred to a new reaction tube and overlayed with 400 µl of ice-cold isopropanol, slowly inverted and left at -20 °C

for 2 h or overnight to precipitate the RNA. Afterwards, the precipitated RNA was pelleted down and washed twice with 70 % ethanol (Laborhaus Scheller), air dried and then the RNA pellet was solved in 100 μl ddH$_2$O and stored at -80 °C. A DNase treatment was performed as described in 4.4.4 and the RNA was send to GATC Biotec AG, Konstanz Germany for sequencing. The single-end Illumina sequencing produced between five and 15 million reads per sample. The 50 bp long reads were clipped (Trimmomatic tool, Bolger *et al.*, 2014) and mapped to the mouse genome (STAR align tool, Dobin & Gingeras, 2015), count files for the analysis were generated using HTSeq (Anders *et al.*, 2015) and the analysis was performed using the DESeq2 (Love *et al.*, 2014) package in R studio. Two biological replicates per condition were analysed.

5.4.2 RNA extraction from cell lines

For the extraction of RNA from cell line cells, the cells were seeded in 6 well plates and grown and treated according to the experimental set up. Then, the cell culture medium was removed and the cells were washed with PBS twice for 2 min. To each well of cells, 500 μl Trizol was added and cells were scraped off the culture plates using a cell scraper. The cell suspension was then transferred to a Lysis Matrix D tube (MP Biomedicals). The RNA extraction was performed like described under 5.4.1 described above. The extracted RNA was then DNase treated and used for qPCR as described in 5.4.4 and 5.

5.4.3 RNA extraction from yeast cells for transcriptome analysis

For the transcriptome analysis, RNA from *C. albicans* yeast cells was extracted. The fungal cells were cultivated in yeast nitrogen base (YNB) minimal media (Becton and Dickinson) at 37 °C under anaerobic conditions. The minimal media was supplemented with either 10 % glucose, 10 % mucin (from Porcine stomach, Sigma-Aldrich), 10 % mucin which was previously digested by *B. thetaiotaomicron* or left without supplements as a negative

control. To 20 ml of this media containing these different carbon sources, 800 μl of a saturated washed *C. albicans* culture (5 x 10^8 cells/ml) was added and left to grow for 24 h in the anaerobic chamber. After the incubation time, the cells were harvested and the RNA extraction was performed using the RiboPure™ RNA-Extraction Kit for yeast (Thermo Fischer) following the manufacturer`s instructions.

With the extracted RNA, Illumina library preparation and paired-end sequencing was performed by Novogene (Cambridge, UK) following the standard operating procedures. Illumina read processing, mapping and differential gene expression analysis were carried out as described before (del Olmo Toledo *et al.*, 2018). Briefly, we obtained ~23 million reads per sample. Illumina adaptor sequences were removed using the Trimmomatic tool (Bolger *et al.*, 2014). Trimmed reads were aligned to the *C. albicans* reference genome assembly 21 (www.candidagenome.org) using STAR (Dobin & Gingeras, 2015). Count files were generated using HTSeq (Anders *et al.*, 2015). Raw read counts were loaded into R and analysed with the DESeq2 package (Love *et al.*, 2014). Visualization of the reads was performed by loading wig files into the Mochiview gene viewer (Homann & Johnson, 2010). Two biological replicates of each growth condition were analysed.

5.4.4 DNase treatment and cDNA transcription for qPCR

To remove residual DNA after RNA extraction, the Invitrogen Turbo™ DNase kit (Thermo Fischer) was used. To determine the amount of RNA that needs to be transcribed in cDNA, the samples were measured at the NanoDrop™ (DeNovix). To produce cDNA, the Superscript II reverse transcriptase (Invitrogen, Thermo Fischer) was used. Same amounts of RNA were incubated with 2 μl of 10 x cDNA mix (containing random primer 5´ NNN NNN NNN NNN´3, dATP, dTTP, dGTP, dCTP) at 60 °C and then 4 μl 5 x first strand buffer, 2 μl DTT and 1 μl of Superscript II was added to each sample. Synthesis of cDNA was performed in the Eppendorf Mastercycler using a program that first incubates the samples at 25 °C for 10 min, then for 50 min

at 42 °C, and lastly for 15 min at 70 °C. Samples were then stored at -20 °C until usage for qPCR.

5.4.5 Quantitative PCR

To quantify the expression of specific genes quantitative real time PCR was performed. To monitor the levels of dsDNA in the reaction, the fluorescent dye SYBR Gold™ (Thermo Fischer) was used. For the qPCR, the Taq Polymerase (New England Biolabs) was used in 25 μl reactions with an additional 1.2 μl of DMSO and 0.05 μl of SYBR Gold. As a template, 1 μl of the cDNA was used. All genes were measured in duplicates and compared to the house-keeping gene GAPDH.

Table 7: qPCR primers used in this work.

Name	Description	Sequence 5´-3
JCP_2427	GAPDH for	CAACTCCCACTCTTCCACCT
JCP_2428	GAPDH rev	GAGTTGGGATAGGGCCTCTC
JCP_2746	DUOX2 for	ACGCAGCTCTGTGTCAAAGGT
JCP_2747	DUOX2 rev	TGATGAACGAGACTCGACAGC

Sequences of DUOX2 for/rev have been published by Lipinski *et al.*, 2009.

5.5 Other methods

5.5.1 Cytokine measurement with the Luminex® assay

To determine the amount of cytokines in mouse derived samples we used the Luminex® assay R&D Systems Inc., Minneapolis, USA) according to the manufacturer's instructions in a Bio-Plex® MAGPIX™ Multiplex Reader (Bio‑Rad, USA). Tissue samples of colonized distal mouse colon were homogenized using the MP Biomedical FastPrep-24™ Classic Instrument and Lysis Matrix D tubes (MP Biomedicals), settings were set to 40 sec at 6.5 m/sec. Lysate of the homogenized tissue or blood serum was used in the assay following the instructors manual. For each sample two technical

replicates were performed and in each well the amount of mouse IL-1α, IL-1β, IL-6, IL-17α, CXCL1, CXCL2 and G-CSF was measured.

5.5.2 Attachment of fungal cells to intestinal cell line cells

The intestinal cell line HT29-MTX-E12 was cultured as described above (4.1.4) and seeded in to 96-well plates (100 μl per well) with the density of 5 x 10^5 cells/ml. The media was changed twice per week and after 21 days media without serum was used. Each well was then infected with a MOI of *1 C. albicans* cells in media without serum. After 1 h of incubation in a 10 % CO_2 incubator at 37 °C, medium was removed and epithelial cells were washed 3 times with PBS to remove no-adherent *C. albicans* cells. After fixation with 4% paraformaldehyde, cells were incubated overnight with a primary rabbit anti‑Candida antibody. The next day, cells were washed again with PBS and stained with a secondary Alexa Fluor 594‑conjugated goat anti‑rabbit antibody. Images were acquired with a Leica DMI 6000B microscope (Leica, Germany) using a filter set to detect Alexa Fluor 594. The number of adhered fungal cells was quantified in 25 fields per strain.

4% Paraformaldehyde

0.4 g   paraformaldehyde

Heat up to 60°C, stir until dissolved

Adjust pH to 6.9 and volume to 10 ml with 1x PBS

5.5.3 Gene deletion in *C. albicans*

To delete a gene in the diploid fungus, the chemical method with lithium acetate was used. In short, homologous regions of the surrounding gene were amplified in a PCR and then fused upstream and downstream to a nutritional marker cassette (HIS-1 or LEU-2). First, one fragment was used in the transformation to be integrated by homologous recombination into the genome of *C. albicans.* And after approval by PCR, a second round of transformation was performed using the fragment containing the other nutritional marker cassette. After the second round of transformation, the

strain should then have no residual copies of the targeted gene. Transformations were performed following the protocol established by Hernday *et al.*, 2010.

Table 8: Primers used for gene deletion in this work.

Name	Description	Sequence 5´-3
JCP_2919	5´end IFD6 for	CGGTAAATAACTATGTCGGGCA
JCP_2930	5´end IFD6 rev	CAC GGC GCG CCT AGC AGC GG CAACAACAACAACAACAACAACA
JCP_2931	3´end IFD6 for	GTC AGC GGC CGC ATC CCT GC ATCACGCCAAAGATTTAGCAAA
JCP_2932	3´end IFD6 rev	AGTTGTGTTTATCTCCCCAATGA
JCP_2933	internal IFD6 for	TGCTACGACAATGGTTTCCG
JCP_2934	internal IFD6 rev	CAGAATCTTCAACAGCAGCCA
JCP_2935	5´end HYR1 for	CTGCACCACTGGATGATATGT
JCP_2936	5´end HYR1 rev	CAC GGC GCG CCT AGC AGC GG ACTGGAGCAATTTCAAGAAGGA
JCP_2937	3´end HYR1 for	GTC AGC GGC CGC ATC CCT GC ACAGAACAACCACGGCAAAA
JCP_2938	3´end HYR1 rev	TGGTGATCAACATGGTTTTGGA
JCP_2939	internal HYR1 for	GGTTCTGGCTCTCAAACTGG
JCP_2940	internal HYR1 rev	GAACCAGAGTGTGAACCTGC
JCP_1111	universal primer 2	CCGCTGCTAGGCGCGCCGTGACCAGTGTGATGGATATCTGC
JCP_1112	universal primer 5	GCAGGGATGCGGCCGCTGACAGCTCGGATCCACTAGTAACG

5.5.4 Western blot from cell line lysates

Intestinal epithelial cell line cells were trypsinated and counted in a haemocytometer chamber to be seeded in 6 well plates in appropriate supplemented media and incubated at 37 °C and 5 % CO_2 atmosphere for 7 days (C99 cell line) or 3 days (CaCo2 and HT29 cell lines). Cells were then treated with Mannan (1 mg/ml, Sigma-Aldrich), heat killed *Candida albicans* cells, 5-aminosalicylic acid (20 mM, Sigma-Aldrich) or living *Candida albicans* cells. After different time points, the media of the wells was removed and the cell lawn was washed carefully with PBS. After the removal of all liquid, 300 μl of 1 x sample buffer was added to each well. The cells were scraped of the well using a cell scraper and together with the sample buffer transferred to a 1.5 ml Eppendorf tube. To lyse the cells, the samples were treated with ultrasound using a sonicator with the intensity of 30 % for 15 sec per sample. After disruption, samples were frozen at -20 °C or stored on ice. Samples were boiled at 100 °C for 10 min followed by a 1 min cooling period on ice.

The same amount of each sample was loaded onto a NuPAGE Bis-Tris 4%-12% gel (Thermo Fischer), and then run with 1 x MOPS buffer (Thermo Fischer) for 2 h at 120 V. Afterwards, the proteins were transferred onto a PVDF membrane (pore size 0.45 µm, Carl Roth) for 2 h at 30 V. After the transfer, the membrane was washed in ddH$_2$O and then blocked in 5 % milk powder in TBS-T (1 x TBS +0.1% Tween) for 1 h. The primary antibody was diluted 1:5000 in the milk solution and incubated on the blot overnight at 4 °C. The secondary antibody (HRP-labelled anti-rabbit, VWR) was diluted 1:10,000 in 1 x TBS-T + 5 % milk powder and added to the membrane after 2 washing steps with TBS-T. After incubating the secondary antibody, the membrane was washed 3 times with TBS-T and then the bands were imaged using the LAS4000 system and the SuperSignal™ West Femto Maximum Sensitivity Substrate Kit (Thermo Fischer). All antibodies used in this work are listed in Table 6.

Sample buffer (3x)

0.002 g	bromphenol blue
0.6 g	SDS
3 ml	glycerol
3.9 ml	0.5 mM Tris pH 6.8
1.5 ml	β-mercaptoethanol

Adjust to 10 ml with ddH$_2$O store at -20 °C

Transfer buffer (1x)

14.5 g	glycine
3 g	Tris base
100 ml	methanol
400 ml	ddH$_2$O

TBS buffer (10x)

24.11 g	Tris base
72.6 g	NaCl

Adjust to 1 l with ddH$_2$O pH 7.4

5.5.5 Statistical analysis of mucin layer thickness

To evaluate the mucin layers of the mouse colon, samples were stained with the anti-Muc2 antibody and pictures were taken using a laser scanning confocal microscope (Leica, TCS SP5). Samples from differently colonized mice were processed simultaneously. For each colonization condition at least 10 pictures each from 3 different mice were taken. In all the pictures, the inner and outer mucus layer was measured in 3 different locations using FIJI (https://fiji.sc/). The significance of the measurements was evaluated by Student´s t-test (two-tailed, unpaired). The inner mucus layer can be evaluated very precisely, due to its absence of microbes and intestinal debris and the specific staining of the Muc2 antibody. For the outer mucus layer, the borders are not as clear but the signal of the specific Muc2 antibody can be visualized even if the mucin is mixed with microbes and debris.

5.5.6 Statistical analysis of *C. albicans* morphology

The morphology of *C. albicans* is an indicator of its virulence and therefore we investigated the shape of the fungus in the ileum, cecum, and colon of mice colonized only with *C. albicans*, but also in mice co-colonized with *C. albicans* and bacteria. At least 3 different mice were analysed per condition and from each mouse around 5 pictures were taken to count the total amount of *C. albicans* cells per picture, as well as the amount of elongated hyphae and round yeast shaped cells. Statistical analysis was performed using the Student´s t-test (two-tailed, unpaired).

6. Supplementary Data

6.1 Transcriptome Data Glucose/Control

Results of the transcriptome analysis comparing *C. albicans* cells grown in minimal medium supplemented with glucose to fungal cells grown in minimal media without carbon source. The experimental procedure is described in 5.4.3. 1443 genes were significantly differentially regulated with a log2 fold change cut off of ±2 and pvalue lower than 0.01, adapted form Eckstein *et al.* 2020.

Systematic Name	Alias	Assembly 19 Identifier	log2 (glucose/control)	P-value	Annotation
C3_01540W_A		orf19.1691	8.812254501	3.43E-11	Plasma-membrane-localized protein
C6_00470C_A	FET99	orf19.4212	8.02812628	8.53E-22	Multicopper oxidase family protein
C4_00450C_A	PGA10	orf19.5674	7.964411076	1.32E-105	GPI anchored membrane protein
C1_12720C_A		orf19.6350	7.167997829	2.44E-25	Ortholog of C. dubliniensis CD36
CR_04440C_A	RBR1	orf19.535	6.879222773	2.78E-12	Glycosylphosphatidylinositol
C4_04320W_A	FRE10	orf19.1415	6.590771284	7.08E-241	Major cell-surface ferric reductase
C1_12000C_A		orf19.5266	6.2035506	1.21E-12	Planktonic growth-induced gene
CR_08510W_A	PGA13	orf19.6420	6.119908106	1.52E-161	GPI-anchored cell wall protein
C1_06610C_A	HAK1	orf19.6249	6.106236398	8.33E-206	Putative potassium transporter
C4_05780C_A	CFL2	orf19.1264	5.933109853	5.80E-56	Oxidoreductase
C2_02910W_A		orf19.5814.1	5.789613889	1.49E-72	Protein of unknown function
C1_05960W_A	PGA45	orf19.2451	5.770877418	2.91E-139	Putative GPI-anchored cell wall protein
C2_06970W_A	AAH1	orf19.2251	5.558153272	5.93E-54	Adenine deaminase
C3_02150C_A	ERG6	orf19.1631	5.255870336	5.97E-166	Delta(24)-sterol C-methyltransferase
C4_01800W_A		orf19.4612	5.140625928	3.06E-27	Protein with a dienelactone hydrolase domain
C4_00990W_A		orf19.4690	5.124369286	9.44E-04	NRAMP metal ion transporter domain
C1_09080C_A	PGA6	orf19.4765	5.070244589	2.72E-122	GPI-anchored cell wall adhesin-like protein
C3_02060W_A		orf19.1641	4.967294884	1.50E-31	Ortholog(s) have extracellular region localization
C3_01270W_A		orf19.1724	4.912219162	1.58E-05	Protein of unknown function
C2_10160W_A		orf19.1765	4.858230326	4.27E-125	Secreted protein
C1_07480C_A		orf19.2797	4.803028278	1.52E-10	Has domain(s) with predicted ATP binding
C3_04310C_A		orf19.5874	4.779160312	2.09E-06	Ortholog of C. dubliniensis CD36
C7_03300C_A	LIP8	orf19.1345	4.771637025	1.87E-58	Secreted lipase
C4_00980C_A	MRV1	orf19.4691	4.45111366	1.09E-19	Ortholog of *Candida albicans* WO-1
C5_02460C_A	ECM33 1	orf19.4255	4.376420734	2.84E-59	GPI-anchored protein
C6_00440C_A	FET34	orf19.4215	4.36163702	3.96E-110	Multicopper ferroxidase
C1_04650W_A	DUR3	orf19.781	4.356460317	1.59E-24	High affinity spermidine transporter
C5_03520W_A		orf19.6661	4.345379574	8.17E-17	Predicted ORF from Assembly 19
C7_04340C_A		orf19.7127.1	4.342567087	2.98E-04	Putative protein of unknown function
C1_07330W_A	RME1	orf19.4438	4.321654601	1.90E-37	Zinc finger protein

C4_02720C_A		orf19.2726	4.313669103	3.42E-84	Putative plasma membrane protein
C2_05660W_A	PNG2	orf19.6877	4.298889183	1.58E-114	Putative peptide:N-glycanase
C4_03500C_A		orf19.3378	4.252557198	9.68E-10	Protein of unknown function
C1_14130W_A	FTR1	orf19.7219	4.179949501	2.46E-101	High-affinity iron permease
C5_00600C_A		orf19.929	4.168055299	1.77E-08	Protein of unknown function
C1_00220W_A	PHR2	orf19.6081	4.16499709	7.33E-114	Glycosidase
CR_01930C_A	BIO2	orf19.2593	4.160870091	1.02E-25	Putative biotin synthase
C3_02330C_A		orf19.1611	4.144921562	3.86E-09	Protein of unknown function
C3_05330C_A		orf19.6970	4.026948229	2.46E-11	Ortholog of C. dubliniensis
C2_05460W_A	CDC19	orf19.3575	4.013667611	4.61E-94	Pyruvate kinase at yeast cell surface
C6_04620C_A	NAG4	orf19.2160	3.956045559	8.97E-06	Putative transporter
C2_08360C_A	OPT5	orf19.5121	3.895546215	2.00E-03	Oligopeptide transporter
C1_04450C_A	FMA1	orf19.6837	3.89477816	4.01E-14	Putative oxidoreductase
C6_03250W_A	BMT4	orf19.5612	3.850127639	2.15E-46	Beta-mannosyltransferase
C3_05710W_A	RCT1	orf19.7350	3.821795106	6.86E-97	Fluconazole-induced protein
C3_04660C_A	ARG11	orf19.5926	3.812096655	2.53E-18	Putative ornithine transporter
C2_09400C_A	ERG24	orf19.1598	3.80846976	2.88E-52	C-14 sterol reductase
C2_06340W_A	EFH1	orf19.5498	3.785297267	2.85E-05	APSES transcription factor
CR_04970C_A		orf19.634	3.748842996	5.56E-05	Ortholog of C. dubliniensis CD36
C1_05950C_A		orf19.2452	3.73615876	6.33E-61	Protein of unknown function
C1_10710C_A		orf19.2350	3.717975181	3.67E-40	Protein similar to S. cerevisiae Yor378w
C3_07970C_A	TLO8	orf19.6191	3.67247789	7.61E-16	Member of a family of telomere-proximal genes
C2_09590C_A		orf19.1395	3.667207972	5.50E-28	copper ion transmembrane transporter activity
C5_03530C_A		orf19.6662	3.638170844	2.53E-11	Putative coenzyme Q (ubiquinone) binding protein
C1_13440C_A	OFI1	orf19.4972	3.601636695	3.22E-06	Putative transcription factor
CR_07220C_A		orf19.6148	3.595339966	3.59E-32	Homolog of nuclear distribution factor NudE
C3_04200W_A	AFP99	orf19.5862	3.594675777	3.34E-13	Protein related to arginases
C6_04320C_A		orf19.1090	3.578050743	2.54E-10	Ortholog of C. dubliniensis CD36
C3_07590W_A		orf19.6731	3.558024537	2.95E-22	Protein of unknown function
C6_01680C_A		orf19.3418	3.547854547	1.10E-13	Has domain(s) with predicted hydrolase activity
C2_09220W_A	DDR48	orf19.4082	3.532568149	3.79E-67	Immunogenic stress-associated protein
CR_06550C_A		orf19.711	3.528978071	1.48E-53	Protein of unknown function
C2_02590W_A	ZRT2	orf19.1585	3.525150576	2.09E-50	Zinc transporter
C3_01570W_A		orf19.1686	3.524060838	2.44E-26	Has domain(s) with predicted phosphotransferase
C4_04770C_A	MNN22	orf19.3803	3.505439148	7.33E-66	Alpha-1,2-mannosyltransferase
C2_06940C_A	ARE2	orf19.2248	3.488101827	6.46E-71	Acyl CoA:sterol acyltransferase
C4_02410C_A	AHP1	orf19.2762	3.474553291	5.28E-72	Alkyl hydroperoxide reductase
C1_09480W_A	PPT2	orf19.4812	3.452067579	6.39E-21	Phosphopantetheinyl transferase (PPTase)
C1_04440W_A		orf19.6833.2	3.440261123	1.63E-12	Ortholog of Candida albicans WO-1
C6_03090W_A		orf19.5592	3.435020899	1.19E-03	Ortholog of C. dubliniensis CD36
C1_02670C_A	MNN43	orf19.2957	3.399200949	6.25E-07	Protein required for transfer of mannosylphosphate
C1_04030W_A		orf19.4478	3.397715463	1.37E-12	Ortholog(s) have aspartate-tRNA ligase activity
C1_06160W_A		orf19.2429	3.388862725	4.34E-07	Protein of unknown function

C3_00600W_A	IFF11	orf19.5399	3.382614055	1.31E-04	Secreted protein
C6_03610W_A	FGR17	orf19.5729	3.371967085	1.77E-16	Putative DNA-binding transcription factor
C6_04610C_A	NAG3	orf19.2158	3.371962968	2.93E-26	Putative MFS transporter
C1_11450C_A	SAM2	orf19.657	3.351836672	3.36E-58	S-adenosylmethionine synthetase
C2_03710W_A	MNN41	orf19.849	3.338488446	2.05E-18	Ortholog(s) have enzyme activator activity
C2_06100W_A	PMT4	orf19.4109	3.330485851	5.51E-61	Protein mannosyltransferase
C2_04450W_A		orf19.4507	3.328267645	4.03E-10	Protein of unknown function
C1_11470C_A	DPP1	orf19.656	3.326779066	3.52E-11	Putative diacylglycerol pyrophosphate phosphatase
C1_09300C_A		orf19.4789	3.320120215	1.17E-07	Has domain(s) predicted metal ion binding activity
C7_00490C_A		orf19.7069	3.315365062	1.02E-30	Putative AdoMet-dependent proline methyltransferase
C2_08520C_A		orf19.3626.1	3.313850159	3.53E-02	Ortholog of C. parapsilosis CDC317
C2_10020C_A		orf19.1780	3.310043987	2.79E-07	Has domain(s) with predicted catalytic activity
C6_03590C_A		orf19.5727	3.305315182	1.13E-33	Ortholog of C. dubliniensis CD36
C4_00390W_A		orf19.5666	3.279764629	1.73E-46	Ortholog(s) have chromatin binding activity
C4_00720W_A	CSP2	orf19.4170	3.276624439	3.43E-10	Putative cell wall associated protein
C6_01990W_A	PLB1	orf19.689	3.273887176	3.72E-05	Phospholipase B
C7_01190W_A		orf19.6901	3.268856644	8.25E-21	Ortholog(s) have RNA 7-methylguanosine cap binding, exoribonuclease activator activity
C2_07290W_A		orf19.2286	3.260595225	3.39E-53	Putative deoxyhypusine hydroxylase
CR_04220C_A		orf19.510	3.249646294	8.08E-32	Protein of unknown function
C2_08610W_A	ERG9	orf19.3616	3.246558545	2.86E-51	Putative farnesyl-diphosphate farnesyl transferase
C1_05710C_A	UGA4	orf19.2479	3.220857212	1.71E-12	Putative gamma-aminobutyric acid/polyamine permease
C1_10560C_A		orf19.1002	3.218492222	5.31E-17	Protein of unknown function
C7_03140W_A		orf19.5141	3.2173711	6.72E-13	Ortholog of Candida albicans WO-1
C5_00710W_A	IFF8	orf19.570	3.21477977	7.13E-09	Putative GPI-anchored adhesin-like protein
C2_02220C_A		orf19.1539	3.212554183	3.07E-06	Protein of unknown function
C6_01120C_A		orf19.119	3.20826902	1.91E-13	Ortholog(s) have protein C-terminal S-isoprenylcysteine carboxyl O-methyltransferase activity
C2_04430W_A		orf19.4509	3.204287465	1.97E-02	Protein of unknown function
C5_02520W_A		orf19.4264	3.202260084	5.64E-51	Protein of unknown function
C1_05560W_A	RIB4	orf19.410.3	3.201382532	4.43E-43	Lumazine synthase
C6_02480W_A		orf19.5517	3.198900073	1.56E-22	Similar to alcohol dehydrogenases
C6_02950C_A		orf19.5573	3.190151224	5.03E-13	Protein of unknown function
C2_07910C_A		orf19.2191.1	3.179303877	1.08E-19	Ortholog of C. dubliniensis CD36
C1_08010W_A	DPM1	orf19.5073	3.148542465	2.68E-42	Dolichol-phosphate mannose
CR_01920W_A	BIO3	orf19.2591	3.097643814	7.02E-04	Putative adenosylmethionine-8-amino-7-oxononanoate transaminase
C3_02250C_A		orf19.1620	3.09340881	2.57E-02	Protein of unknown function
C2_01040W_A		orf19.2018.1	3.090516692	6.09E-06	PProtein of unknown function
C2_01250W_A		orf19.1999	3.089785757	3.43E-31	Protein of unknown function
C1_08500C_A	ENO1	orf19.395	3.072601827	3.17E-54	Enolase
C1_13870W_A	MET3	orf19.5025	3.070319665	1.47E-49	ATP sulfurlyase
C7_00680W_A		orf19.7051	3.057231423	1.91E-10	Maf-like protein
C1_07900W_A	COI1	orf19.5063	3.048594341	5.95E-51	Secreted protein
CR_02920C_A	AQY1	orf19.2849	3.038698726	8.44E-27	Aquaporin water channel

127

C1_10930C_A	UBA4	orf19.2324	3.038370197	2.29E-32	Putative ubiquitin activating protein
C6_04420W_A		orf19.2125	3.035859457	1.23E-50	Protein of unknown function
C1_07570C_A		orf19.2788	3.027613972	3.75E-18	Has domain(s) with predicted RNA binding
C1_13590W_A		orf19.4995	3.025986172	1.01E-06	Ortholog of C. dubliniensis CD36
C6_00460C_A	FET3	orf19.4213	3.022380416	3.08E-27	Multicopper oxidase
C2_08530C_A		orf19.3626	3.005997633	2.67E-18	Has domain(s) with predicted asparagine synthase
C2_10270W_A	PUS7	orf19.1753	2.992691945	1.38E-38	Pseudouridine synthase
C2_07790C_A		orf19.2202	2.990494817	7.61E-12	Protein of unknown function
C1_12200W_A	MCD4	orf19.5244	2.989017851	1.27E-26	Mannose-ethanolamine phosphotransferase
C6_02210W_A		orf19.3461	2.987937085	6.08E-13	Protein of unknown function
CR_00910W_A		orf19.3264.1	2.98620277	2.04E-59	Protein of unknown function
C3_01280W_A		orf19.1723	2.977332216	6.11E-26	Ortholog(s) have role in response to purine-containing compound
C4_02680C_A		orf19.2731	2.970501623	5.50E-12	Ortholog of Debaryomyces hansenii CBS767 58603
CR_06580W_A		orf19.693	2.939507167	6.92E-02	Protein of unknown function
C3_04060C_A	HEM13	orf19.2803	2.936983429	1.42E-57	Coproporphyrinogen III oxidase
C4_03960W_A		orf19.787.1	2.93576519	4.03E-50	Protein of unknown function
C4_00730C_A		orf19.4169	2.92780857	1.34E-05	Ortholog of C. dubliniensis CD36
C1_05010C_A		orf19.55	2.925370169	6.48E-36	Ortholog(s) have role in cellular zinc ion homeostasis
C3_05340W_A	DIE2	orf19.6971	2.925221967	8.75E-05	Ortholog(s) have dolichyl pyrophosphate Glc2Man9GlcNAc2 alpha-1,2-glucosyltransferase activity
CR_09330C_A		orf19.7328	2.924991454	5.18E-44	Protein with a Staphylococcal nuclease domain
C3_00640W_A		orf19.5393	2.921069184	6.62E-35	Putative cysteine sulfinate decarboxylase
C6_03710W_A	ALS9	orf19.5742	2.918382511	8.63E-29	ALS family cell-surface glycoprotein
C3_02140C_A		orf19.1632	2.906691803	7.19E-19	Has domain(s) with predicted catalytic activity
C4_02750W_A	HIT1	orf19.2723	2.904271974	4.96E-18	Ortholog of S. cerevisiae Hit1
C6_03110C_A		orf19.5596	2.89240147	3.03E-15	Ortholog of S. cerevisiae
C6_02650C_A		orf19.5535	2.885990226	2.77E-29	Predicted membrane transporter
C2_06700W_A	AMO2	orf19.3152	2.884211733	1.90E-30	Protein similar to A. niger predicted peroxisomal copper amino oxidase
CR_03920C_A	TPO4	orf19.473	2.878049216	2.91E-48	Putative sperimidine transporter
C1_03890W_A		orf19.4463	2.865702056	7.78E-02	Ortholog of *Candida albicans* WO-1
C4_02270C_A	BFR1	orf19.4560	2.862825435	5.46E-44	Protein involved in the maintenance of normal ploidy
C3_06480C_A	ECM15	orf19.7436.1	2.859714985	2.60E-30	Protein of unknown function
C1_05940W_A	PHO87	orf19.2454	2.855378296	8.32E-33	Putative phosphate permease
CR_01910C_A	BIO4	orf19.2590	2.854069766	1.82E-06	Putative dethiobiotin synthetase
C3_07330W_A		orf19.6758	2.846808677	5.15E-19	Predcted glucose 1-dehydrogenase
C5_02630C_A	MNN1	orf19.4279	2.845061761	1.82E-37	Putative alpha-1,3-mannosyltransferase
C5_03970W_A		orf19.3214	2.840199254	1.10E-28	Alpha/beta-HydrolasE superfamily protein
C5_04390C_A		orf19.3925	2.837836175	4.52E-08	Putative protein of unknown function
C1_13940W_A	SIM1	orf19.5032	2.832495929	3.60E-32	Adhesin-like protein
CR_04120C_A		orf19.496	2.819771916	6.18E-28	Ortholog(s) have DNA-dependent ATPase activity
C3_07240W_A		orf19.6777	2.81464361	1.30E-07	Ortholog of *Candida albicans* WO-1
CR_09890C_A	BET2	orf19.7563	2.809534349	1.30E-22	Putative Type II geranylgeranyltransferase

C6_01090C_A		orf19.115	2.806165453	5.17E-08	Ortholog of Candida tropicalis _05252
C7_01050W_A		orf19.7009	2.789251918	4.24E-08	Has domain(s) with predicted catalytic activity
C1_08590C_A	ERG1	orf19.406	2.788189364	1.95E-49	Squalene epoxidase
C4_06340W_A	AGO1	orf19.2903	2.786404061	4.65E-31	Putative Argonaute protein involved in RNA silencing
C4_01280C_A		orf19.4659	2.76811696	1.13E-39	Ortholog(s) have RNA binding activity
C5_00430W_A	MET14	orf19.946	2.765318408	1.53E-15	Putative adenylylsulfate kinase
C3_05310W_A	USO6	orf19.6967	2.764590913	1.21E-34	Putative vesicular transport protein
C2_07600C_A	MSC7	orf19.1865	2.759051096	2.24E-37	S. cerevisiae ortholog Mcs7 has a role in reciprocal meiotic recombination
C3_02070C_A		orf19.1639	2.75685353	1.61E-07	Has domain(s) with predicted oxidoreductase activity and role in oxidation-reduction process
C2_03160C_A	RNR1	orf19.5779	2.752975724	5.09E-47	Ribonucleotide reductase large subunit
C6_01080C_A		orf19.114	2.752255199	5.25E-10	Ortholog of C. dubliniensis CD36
C1_04940C_A		orf19.750	2.747585426	9.45E-04	Protein of unknown function
C1_04900W_A	MNN15	orf19.753	2.739596081	1.05E-39	Putative alpha-1,3-mannosyltransferase
C1_00120C_A	TRP1	orf19.6096	2.738444537	2.50E-37	Phosphoribosylanthranilate isomerase
C4_00290C_A		orf19.5655	2.736457089	8.30E-08	Has domain(s) with predicted 2 iron
C2_07240C_A		orf19.2281	2.73351092	4.27E-16	Has domain(s) with predicted CoA-transferase activity
C4_06320C_A		orf19.2905	2.728473956	1.34E-03	Ortholog of Candida albicans WO-1
C3_06130W_A		orf19.7395	2.726884574	9.61E-02	Ortholog of Candida albicans WO-1
C5_00870C_A	GIT4	orf19.1980	2.715673989	1.05E-09	Glycerophosphocholine transporter
C2_02690W_A	SER2	orf19.5838	2.711800001	1.01E-24	Ortholog(s) have phosphoserine phosphatase
C2_04390W_A		orf19.4515	2.708201911	3.41E-07	Predicted protein with similarity to cell wall proteins
C6_00420W_A	DPM2	orf19.1203.1	2.704611843	3.30E-25	Dolichol-phosphate mannose synthase subunit enzyme activity
C4_05550C_A	GVP36	orf19.1236	2.703368761	2.19E-40	BAR domain protein
C2_03830W_A		orf19.839	2.681908383	2.22E-23	Putative endoribonuclease
C7_04210C_A		orf19.7152	2.681684689	1.46E-34	Protein similar to Aspergillus CYSK assimilation
C1_09580C_A	LIP1	orf19.4821	2.678734504	1.14E-05	Secreted lipase
CR_05160C_A		orf19.639	2.677758398	2.52E-11	S. cerevisiae ortholog YDR370C
C1_12210W_A	TRP3	orf19.5243	2.676080677	1.06E-26	Putative bifunctional enzyme
C1_11160C_A		orf19.2299	2.669003434	2.04E-25	Ortholog(s) have protein tag activity
C3_02080W_A		orf19.1638	2.6640677	2.53E-26	Has domain(s) with predicted zinc ion binding activity
C4_02590C_A		orf19.2740	2.662925891	5.10E-24	Ortholog(s) have 5'-flap endonuclease activity
C2_01260W_A		orf19.1998	2.661748323	7.54E-15	Orthologof C. dubliniensis CD36
C1_13860C_A	GND1	orf19.5024	2.658162444	1.09E-46	6-phosphogluconate dehydrogenase
C5_03700C_A		orf19.1124.2	2.656505489	9.74E-19	Ortholog(s) have diphthine synthase activity and role in peptidyl-diphthamide biosynthetic process from peptidyl-histidine
C3_06870W_A	TDH3	orf19.6814	2.656019227	1.88E-36	NAD-linked glyceraldehyde-3-phosphate dehydrogenase
C5_00280C_A		orf19.967	2.650977871	3.92E-24	Major mitochondrial nuclease
C1_03000W_A	HOL1	orf19.2991	2.650916849	4.88E-09	Putative MFS transporter
C4_01830C_A		orf19.4610	2.647896145	7.15E-22	Predicted metallocarboxypeptidase
C2_06630C_A		orf19.36.1	2.645902597	5.94E-13	Ortholog of C. parapsilosis CDC317
CR_02290W_A	PGA22	orf19.3738	2.633536847	1.57E-03	Putative GPI-anchored protein
C7_02830C_A	LIP5	orf19.5179	2.630845044	4.84E-12	Cold-activated secreted lipase

C7_03470W_A		orf19.6704	2.628506738	1.37E-07	Protein of unknown function
C2_02630W_A		orf19.1589	2.625871514	9.96E-22	Putative transcription factor component of the core factor rDNA transcription factor complex
C2_02930C_A		orf19.5812	2.624734448	3.47E-40	Ortholog of S. cerevisiae Ett1
C3_01050C_A		orf19.2509	2.620135914	6.01E-03	Ortholog of C. dubliniensis CD36 :
C3_02680C_A	SLD1	orf19.260	2.618497932	1.14E-37	Sphingolipid delta-8 desaturase
CR_00280C_A		orf19.7506	2.617225316	9.40E-30	Ortholog(s) have ATPase activity
C4_06550C_A	IFF5	orf19.2879	2.616340491	4.23E-34	Putative GPI-anchored protein
C2_06080C_A		orf19.4112	2.61596144	2.22E-27	Ortholog(s) have 8-oxo-dGDP phosphatase activity
C4_01690C_A	HRT2	orf19.4624	2.615803771	1.08E-20	described as having a role in Ty3 transposition
C4_05010W_A		orf19.3778	2.609545662	9.09E-28	Protein with a predicted role in ribosome biogenesis
C4_06270C_A	ERG26	orf19.2909	2.609177583	3.07E-29	C-3 sterol dehydrogenase
C1_05260C_A	SDH1	orf19.440	2.599060885	7.99E-23	Putative mitochondrial succinate dehydrogenase
C1_12190W_A	BUL4	orf19.5245	2.598121005	4.18E-14	Protein with a predicted BUL1 N-terminal and C-terminal domains
C4_06280C_A		orf19.2908	2.594970655	1.45E-11	Predicted oxidoreductase
CR_02720C_A	RPC31	orf19.2831	2.592181898	1.64E-20	Putative RNA polymerase III subunit C31
C1_05480C_A		orf19.416	2.591512754	6.75E-10	Ortholog of C. dubliniensis CD36
CR_01530C_A		orf19.2539	2.59069865	1.17E-01	Protein of unknown function
C1_09720W_A	URA1	orf19.4836	2.589336516	5.22E-35	Dihydroorotate dehydrogenase
C7_00620W_A	GUS1	orf19.7057	2.587838836	5.23E-35	Putative glutamine-tRNA ligase
C2_06950C_A		orf19.2249	2.584515694	3.59E-16	Putative metalloprotease of the mitochondrial inner membrane
C4_05250W_A		orf19.6864	2.581410157	8.93E-07	Putative ubiquitin-protein ligase
C2_00860C_A		orf19.2038	2.576485773	1.96E-15	Protein of unknown function
C1_04880C_A	MRPL37	orf19.755	2.574659882	1.55E-11	Putative mitochondrial large subunit ribosomal protein
C3_06750W_A		orf19.6828.1	2.57398766	2.91E-27	Ortholog(s) have P-P-bond-hydrolysis-driven protein transmembrane transporter activity
C1_00690W_A	RIC1	orf19.6036	2.568769309	3.10E-15	Ortholog of S. cerevisiae Ric1 guanyl-nucleotide exchange factor
C2_04110W_A		orf19.810	2.561783004	8.63E-12	Ortholog(s) have DNA helicase activity
C6_02350C_A		orf19.3477	2.55533204	1.67E-25	Putative pseudouridine synthase
CR_03300C_A		orf19.2394	2.555075211	1.71E-02	Ortholog(s) have aldehyde dehydrogenase (NAD+) activity
C1_04430C_A		orf19.5194.1	2.545943969	3.41E-16	Putative protein of unknown function
C2_10240W_A	GPD1	orf19.1756	2.54431184	1.01E-25	Glycerol-3-phosphate dehydrogenase
C1_08870C_A	JIP5	orf19.4746	2.543929789	3.75E-26	Ortholog of S. cerevisiae Jip5
C4_02050W_A	HGH1	orf19.4587	2.54108568	7.34E-26	Putative HMG1/2-related protein
C1_14140C_A	SET3	orf19.7221	2.536806609	1.52E-43	NAD-dependent histone deacetylase
C7_01560C_A	NUP	orf19.6570	2.535099785	7.27E-04	Nucleoside permease
C5_05260W_A	PSY4	orf19.4019	2.534525284	2.44E-14	Regulatory subunit of protein phosphatase PP4
C3_00720W_A	PMA1	orf19.5383	2.525804539	1.51E-32	Plasma membrane H(+)-ATPase
C4_01360W_A	PGA53	orf19.4651	2.525103237	1.49E-22	GPI-anchored cell surface protein unknown function
C3_04190W_A		orf19.5861.1	2.519759057	1.99E-09	Protein of unknown function
C6_00860W_A	GPX1	orf19.87	2.518757216	4.64E-11	Putative thiol peroxidase
C6_00680C_A		orf19.4192.1	2.511366498	1.05E-20	Ortholog of C. dubliniensis CD36
C2_10430C_A	FGR29	orf19.5316	2.509962554	6.46E-13	Protein lacking an ortholog in S. cerevisiae

130

C3_01560W_A		orf19.1687	2.506935811	1.67E-29	Ortholog of S. cerevisiae Prp43
C2_08970C_A	DFG10	orf19.209	2.506742911	3.22E-11	Ortholog(s) have role in dolichol biosynthetic process
C4_06160W_A	PAC2	orf19.2921	2.503991543	7.96E-13	Ortholog(s) have alpha-tubulin binding activity
C7_04220W_A		orf19.7151	2.497760545	1.33E-01	Ortholog of *Candida albicans* WO-1
C7_00750W_A	ACB1	orf19.7043.1	2.497125678	3.46E-34	Protein similar to a region of acyl-coenzyme-A-binding protein
CR_04990C_A		orf19.654	2.491657487	2.09E-04	Predicted protein only found in *C. albicans* and C. dubliniensis
CR_05620C_A	MTG2	orf19.6653	2.486361584	2.55E-18	Putative Obg family GTPase member
C1_02250W_A	CWH8	orf19.3682	2.483766031	5.30E-21	Putative dolichyl pyrophosphate (Dol-P-P) phosphatase
C1_00850W_A	IHD2	orf19.6021	2.471137273	1.25E-20	Protein of unknown function
C2_01380W_A	PLB4.5	orf19.1442	2.468691867	1.64E-28	Phospholipase B
CR_06300C_A	FGR50	orf19.3884	2.45979313	2.42E-08	Protein lacking an ortholog in S. cerevisiae
CR_05520W_A	NOC2	orf19.5850	2.459445679	3.42E-32	Putative nucleolar complex protein
C4_02260C_A		orf19.4563	2.459440823	6.38E-22	Protein of unknown function
C1_04870W_A	SAP7	orf19.756	2.455625406	7.12E-02	Pepstatin A-insensitive secreted aspartyl protease
C1_10500W_A		orf19.993	2.455527956	6.55E-08	Protein of unknown function
C2_01570W_A		orf19.1465	2.455416805	4.65E-06	Has domain(s) with predicted N-acetyltransferase activity
C6_04260C_A		orf19.1083	2.454346569	2.38E-11	Putative protein of unknown function
C2_00550W_A		orf19.2072	2.453629975	1.20E-12	Ortholog(s) have (R)-carnitine transmembrane transporter activity
CR_06310W_A		orf19.3885	2.453441142	4.32E-04	Has domain(s) with predicted N-acetyltransferase activity
C4_02580W_A		orf19.2742	2.447452976	3.85E-09	Ortholog of C. parapsilosis CDC317
C1_01510W_A		orf19.3337	2.446108923	5.28E-14	Protein of unknown function
C4_02090C_A		orf19.4582	2.442576946	2.01E-22	Ortholog(s) have role in U1 snRNA 3'-end processing
C4_01010C_A	DAG7	orf19.4688	2.43916829	8.04E-16	Secretory protein
C1_03040W_A		orf19.2995	2.438427384	1.87E-17	Protein of unknown function
C4_04470W_A	SAP10	orf19.3839	2.436072242	5.77E-25	Secreted aspartyl protease
C3_05200W_A	RPS19 A	orf19.5996.1	2.431721523	6.36E-36	Putative ribosomal protein S19
C2_09140C_A	MET10	orf19.4076	2.431275699	3.86E-38	Sulfite reductase
CR_03570C_A	YVH1	orf19.4401	2.430056661	5.46E-19	Putative dual specificity phosphatase
C2_07420W_A		orf19.1889	2.427064162	1.59E-24	Putative phosphoglycerate mutase family protein
C1_04770C_A	ERG3	orf19.767	2.425309371	3.78E-26	C-5 sterol desaturase
C2_03170W_A		orf19.5777	2.423811085	8.11E-16	Protein of unknown function
C2_05550W_A		orf19.6867	2.417064245	1.67E-24	Protein with a predicted cytochrome b5-like heme/steroid binding domain
C2_01970C_A	ROD1	orf19.1509	2.416603326	2.75E-23	Protein similar to S. cerevisiae Rod1
C5_03440W_A		orf19.2638.1	2.40939083	2.36E-22	Protein of unknown function
C1_03680W_A	ENG1	orf19.3066	2.407771921	4.62E-22	Endo-1,3-beta-glucanase
C1_09800C_A	TVP18	orf19.4845	2.400900614	7.79E-20	Putative integral membrane protein
C4_02180C_A	ZCF26	orf19.4573	2.399573237	3.59E-11	Zn2-Cys6 transcription factor of unknown function
C3_01040C_A	PRM9	orf19.2508	2.398481162	3.66E-06	Protein described a similar to S. cerevisiae Prm9
C4_03950C_A		orf19.787	2.398201453	5.83E-17	Protein of unknown function
C4_01000C_A	PGA57	orf19.4689	2.397298636	5.31E-08	Putative GPI-anchored protein
C4_00480W_A	DUR4	orf19.5677	2.3953582	6.23E-14	Putative urea permease

C3_07340W_A	GCY1	orf19.6757	2.391583302	2.54E-24	Aldo/keto reductase
C3_06830C_A		orf19.6818	2.386028885	7.69E-23	Has domain(s) with predicted ATP binding, helicase activity
C4_05650W_A		orf19.1250	2.377328997	2.71E-25	Ortholog(s) have role in maturation of SSU-rRNA from tricistronic rRNA transcript and nucleolus localization
C1_11040W_A	RPL29	orf19.2310.1	2.376398642	1.08E-32	Ribosomal protein L29
C1_03030W_A	RPS16 A	orf19.2994.1	2.373397572	3.30E-32	Putative 40S ribosomal subunit
C3_05800W_A		orf19.7361	2.369834992	2.76E-19	Ortholog(s) have tRNA-intron endonuclease activity
C2_10640C_A	MTR2	orf19.5342.1	2.369775548	9.68E-22	Nuclear export protein
C4_04780W_A	PMT6	orf19.3802	2.368514685	1.20E-27	Protein mannosyltransferase
C1_01640W_A	RPS42	orf19.3354	2.365435454	1.78E-32	Predicted ribosomal protein S4
C6_04330W_A	NOP8	orf19.1091	2.361813975	1.31E-24	Ortholog of S. cereviiae Nop8
C1_10520W_A		orf19.996	2.361459106	5.11E-09	Protein with a predicted leucine-rich repeat domain
C3_02300W_A	FGR23	orf19.1616	2.360448944	1.34E-20	Protein of unknown function
CR_00990W_A		orf19.3259	2.36018175	3.63E-18	Ortholog(s) have peptidase activity
C1_07050C_A		orf19.6199	2.354427015	5.94E-19	Ortholog(s) have 5'-3' DNA helicase activity and DNA helicase A complex
C3_01450C_A	MET18	orf19.1706	2.353867768	2.62E-14	Putative protein with a predicted role in nucleotide excision repair (NER) and RNA polymerase II (RNAP II) transcription
C1_13020C_A	SPC3	orf19.4930	2.352095431	2.02E-18	Essential protein
C3_02340W_A		orf19.1610	2.352094674	3.76E-04	Putative protein of unknown function
C4_03510C_A	HWP2	orf19.3380	2.351621699	3.83E-02	GPI-anchored, glycosylated cell wall protein
C1_09330W_A		orf19.4793	2.35113282	7.43E-17	Putative ribosome-associated protein
C3_00060W_A	TLO7	orf19.5467	2.350766611	6.66E-09	Member of a family of telomere-proximal genes of unknown function
C2_04440W_A		orf19.4508	2.346757233	6.12E-05	Ortholog of Candida albicans WO-
C2_09560C_A		orf19.1400	2.34496469	2.56E-19	Ortholog of C. dubliniensis
C7_00140C_A		orf19.7109	2.339799403	2.69E-24	Ortholog of S. cerevisiae
C1_12020W_A		orf19.5264	2.339520637	1.62E-01	Dubious open reading frame
CR_06340C_A	PGI1	orf19.3888	2.338849303	1.73E-31	Glucose-6-phosphate isomerase
C2_06350C_A		orf19.5499	2.337960497	6.59E-02	Ortholog(s) have 4-hydroxyphenylpyruvate dioxygenase activity and role in aromatic amino acid family biosynthetic process
CR_09360W_A	FCY24	orf19.7331	2.336520305	9.46E-14	Putative transporter
C7_00630C_A		orf19.7056	2.335631625	6.71E-02	Putative protein of unknown function
C2_09640C_A	PMI1	orf19.1390	2.334538835	1.61E-20	Phosphomannose isomerase
C1_04590W_A		orf19.6852.1	2.330645791	6.80E-37	Protein of unknown function
C2_07110C_A		orf19.2266	2.328844725	1.22E-16	Ortholog(s) have ATPase activity
CR_02400W_A	PHO11 2	orf19.3727	2.32842318	1.02E-06	Phytase
C4_06310C_A	PGA41	orf19.2906	2.326676359	6.56E-07	Putative GPI-anchored protein
C1_04580C_A		orf19.6852	2.316830799	4.41E-25	Ortholog of Rmd6 involved in S. cerevisiae sporulation
C2_02360C_A		orf19.1557	2.316619424	1.73E-13	Ortholog(s) have S-adenosylmethionine-dependent methyltransferase activity and role in protein methylation
C5_00740W_A	CTF8	orf19.576	2.315768702	1.53E-06	Putative kinetochore protein with a predicted role in sister chromatid cohesion
C4_03250C_A	RHD2	orf19.2668	2.314757564	3.91E-05	Predicted ORF in retrotransposon Tca4 with similarity to the Gag region encoding nucleocapsid-like protein
C3_02010C_A		orf19.1647	2.314725097	6.63E-02	Ortholog(s) have role in ascospore wall

					assembly
C6_03040C_A		orf19.5586	2.314297837	9.96E-13	Ortholog(s) have phosphatidylinositol-3,5-bisphosphate 5-phosphatase activity
C7_01670W_A		orf19.6557	2.312895342	2.67E-15	Protein with a predicted fatty acid amide hydrolase I domain
C5_00010W_A	TLO11	orf19.5700	2.309489594	1.16E-18	Member of a family of telomere-proximal genes of unknown function
C4_06240W_A		orf19.2914	2.306170349	6.12E-13	Ortholog of C. dubliniensis
C6_03320W_A		orf19.5620	2.305262753	2.22E-29	Stationary phase enriched protein
CR_01700C_A		orf19.2563	2.301487231	1.47E-21	Ortholog(s) have U6 snRNA binding
C2_04420W_A	IFA4	orf19.4510	2.298081044	8.67E-08	Protein of unknown function
C3_01780C_A		orf19.1667.1	2.297528008	3.95E-12	Ortholog(s) have role in mitochondrial cytochrome c oxidase assembly
C4_04880W_A	FGR10	orf19.3791	2.294625145	1.31E-10	Putative asparaginase
C3_02180C_A		orf19.1626	2.294566492	1.62E-20	Deoxyhypusine synthase
C4_02280W_A	IDI1	orf19.2775	2.293535666	1.16E-29	Ortholog(s) have isopentenyl-diphosphate delta-isomerase activity and role in farnesyl diphosphate biosynthetic process
C2_06110W_A		orf19.4107	2.29184367	1.91E-12	Exopolyphosphatase, hydrolyzes inorganic polyphosphate (poly P) into Pi residues
C4_05270C_A	RAD59	orf19.2630	2.287400803	1.17E-14	Protein involved in homologous recombination and DNA breaks repair
C3_00760W_A	ERG4	orf19.5379	2.283680988	6.43E-29	Protein similar to sterol C-24 reductase
C5_00660C_A	ERG11	orf19.922	2.282109008	2.23E-34	Lanosterol 14-alpha-demethylase
C3_06760W_A		orf19.6828	2.280288416	7.56E-23	Ortholog(s) have role in rRNA processing and preribosome
C1_00070W_A	MVD	orf19.6105	2.276966016	7.12E-28	Mevalonate diphosphate decarboxylase
C7_03650W_A		orf19.6699	2.276648465	2.89E-11	Ortholog(s) have histidinol-phosphatase activity and role in histidine biosynthetic process
C1_11720W_A		orf19.1146	2.275192197	2.23E-03	Ortholog of Candida albicans WO-1
C2_03210W_A		orf19.909.1	2.272471228	1.16E-07	Ortholog of C. dubliniensis
C3_04350C_A		orf19.5879	2.270464729	3.01E-10	Has domain(s) with predicted oxidoreductase activity and role in metabolic process
CR_02770C_A		orf19.2835	2.268182201	6.56E-13	Ortholog(s) have SUMO activating enzyme activity
C1_05070C_A	GPI7	orf19.4064	2.265410673	5.19E-16	Protein involved in attachment of GPI-linked proteins to cell wall
C5_01350W_A		orf19.1933	2.264491443	1.64E-16	Ortholog(s) have role in ER-dependent peroxisome organization
CR_05500C_A		orf19.5852	2.264212388	1.52E-12	Protein of unknown function
C2_06770W_A		orf19.2228	2.2612021	1.79E-08	Ortholog(s) have actin filament binding
C4_05880W_A	GAT1	orf19.1275	2.260122462	9.79E-19	GATA-type transcription factor
C2_07590W_A	VMA10	orf19.1866	2.258937975	8.77E-24	Subunit G of the V1 peripheral membrane domain of the vacuolar H+-ATPase
C2_10010C_A		orf19.1782	2.254453871	2.65E-19	Membrane-localized protein of unknown function
CR_04740C_A	ADE6	orf19.6317	2.2543655	2.23E-28	5-Phosphoribosylformyl glycinamidine synthetase
C6_02960W_A		orf19.5574	2.250505703	9.79E-14	Ortholog of S. cerevisiae : MCY1
CR_10720W_A	HMI1	orf19.7661	2.24341736	3.60E-20	ATP-dependent 3' - 5' helicase involved in maintenance of mitochondrial DNA
C7_01000C_A		orf19.7014	2.242476424	5.36E-02	Putative protein of unknown function
C4_00650W_A	HIS5	orf19.4177	2.240981715	3.14E-19	Putative histidinol-phosphate aminotransferase
C7_03130C_A	DFR1	orf19.5142	2.238578649	9.64E-12	Trimethoprim resistant dihydrofolate reductase (DHFR
CR_08500W_A		orf19.6418	2.237409074	1.73E-23	Ortholog(s) have unfolded protein binding activity and role in protein import into nucleus
C1_05720W_A		orf19.2478.1	2.234768066	1.37E-26	60S ribosomal protein L7

C1_07790C_A		orf19.5049	2.234628694	2.45E-16	Putative U3-containing 90S preribosome processome complex subunit
C4_05450C_A	CBR1	orf19.1801	2.234180285	1.80E-27	Putative cytochrome B5 reductase
C3_05860C_A		orf19.7366	2.228892909	7.24E-20	Ortholog(s) have S-adenosylmethionine-dependent methyltransferase activity
C3_07580W_A		orf19.6731.1	2.226120584	1.17E-21	Ortholog of C. dubliniensis CD36
C2_06200C_A		orf19.5483	2.225436688	4.49E-19	Ortholog(s) have GTPase activity, mitochondrial ribosome binding activity
C1_11790W_A		orf19.1137	2.221601481	3.50E-11	Thymidylate kinase of unknown role
C2_09650W_A		orf19.1389	2.221032851	2.05E-29	Ortholog(s) have poly(A) binding activity
C1_13720W_A		orf19.5009	2.218306166	2.50E-18	Ortholog of S. cerevisiae : KEL3
C2_03030W_A	LIG4	orf19.5798	2.217408885	3.00E-26	DNA ligase
C3_01440C_A		orf19.1707	2.215724218	2.26E-04	Ortholog of Candida albicans WO-1
C3_07490W_A		orf19.6739	2.211767943	3.57E-24	Ortholog(s) have phosphopentomutase activity and role in guanosine catabolic process
C4_01530C_A	ERG251	orf19.4631	2.210797006	1.87E-30	C-4 sterol methyl oxidase
C2_05480C_A		orf19.3577.1	2.209265811	1.69E-08	Ortholog(s) have mitochondrial intermembrane space localization
C1_07510W_A		orf19.2794	2.209046777	1.13E-15	Putative non-specific single-domain racemase
C1_00630W_A		orf19.6043	2.20861907	7.63E-15	Has domain(s) with predicted UDP-N-acetylmuramate dehydrogenase activity
C6_01260W_A		orf19.134	2.204490029	7.00E-10	Protein of unknown function
C2_02750C_A		orf19.5831	2.203940852	1.91E-02	Ortholog of C. dubliniensis CD36
C2_10830W_A		orf19.5365.1	2.201114344	7.35E-20	Ortholog of C. dubliniensis CD36
C7_04240C_A		orf19.7149	2.200499729	1.17E-24	Putative GTPase inhibitor
CR_04110W_A		orf19.494	2.198969102	9.58E-21	Putative RNA-binding protein
CR_00080W_A	MIS12	orf19.7534	2.196893983	4.35E-26	Mitochondrial C1-tetrahydrofolate synthase precursor
C2_02900W_A	ERI1	orf19.5814	2.196859484	4.11E-08	Protein of unknown function
C3_03140C_A	DAL4	orf19.313	2.195167266	2.35E-08	Putative allantoin permease
C1_07060C_A		orf19.6198.1	2.186649038	2.50E-16	Ortholog of S. cerevisiae : YIL156W-B
C6_02000W_A	PLB2	orf19.690	2.18369001	5.60E-10	Putative phospholipase B
CR_10550W_A	DRS1	orf19.7635	2.1799632	6.23E-25	Putative nucleolar DEAD-box protein
C4_05230C_A		orf19.6862	2.179336212	4.11E-17	Hap43-induced gene
C2_03270W_A	GPM1	orf19.903	2.178367635	2.94E-29	Phosphoglycerate mutase
CR_10530W_A		orf19.7632	2.177815423	6.45E-14	Ortholog of C. dubliniensis
C1_06900C_A	MMD1	orf19.6220.3	2.177035188	2.63E-17	Mitochondrial protein
C4_02190C_A		orf19.4571	2.17431921	6.88E-04	CoA-transferase family protein
C1_09040C_A		orf19.4760	2.173065988	4.42E-18	Putative protein-histidine N-methyltransferase
CR_01760C_A	FRS1	orf19.2573	2.171495067	6.59E-28	Phenylalanyl-tRNA synthetase
CR_05630W_A	DBP8	orf19.6652	2.167137209	3.75E-19	Protein similar to S. cerevisiae Dbp8p
C1_11740W_A		orf19.1143	2.164577835	6.34E-14	Ortholog of Pichia stipitis Pignal : PICST_30878
C5_00040C_A		orf19.5693	2.162446623	1.10E-24	Subunit of the GPI protein transamidase complex
C4_03310C_A		orf19.1440.1	2.160890301	1.64E-01	Protein of unknown function
C6_02220W_A	SAR1	orf19.3462	2.159344767	9.94E-25	Functional homolog of S. cerevisiae Sar1
C2_02800W_A		orf19.5825.1	2.158186183	5.84E-16	Ortholog(s) have role in endoplasmic reticulum to Golgi vesicle-mediated transport and COPII-coated ER to Golgi transport vesicle
CR_01380W_A		orf19.2521	2.157461951	6.64E-17	Ortholog of C. dubliniensis CD36
C2_00170C_A	HMA1	orf19.2115	2.153675927	2.17E-24	Putative molybdopterin-converting factor

134

C3_00390W_A		orf19.5428	2.153375704	1.97E-07	Putative Golgi membrane protein with a predicted role in manganese homeostasis
C1_12940C_A		orf19.4923.1	2.152951669	1.54E-02	Ortholog of C. parapsilosis
CR_04730W_A		orf19.6318	2.152706978	3.24E-25	Has domain(s) with predicted membrane localization
C5_05510C_A		orf19.4055	2.152358159	2.06E-03	Protein similar to S. cerevisiae Ybr075wp
C2_05830C_A		orf19.5206	2.152122381	1.66E-15	Putative chaperone protein
C1_00150C_A	RIM8	orf19.6091	2.150616216	1.30E-27	Beta-arrestin-like protein
CR_01550C_A		orf19.2541	2.147000066	2.80E-14	Ortholog(s) have 3'-5'-exodeoxyribonuclease activity
C1_04130W_A	ERB1	orf19.1047	2.141534429	3.44E-24	Protein with a predicted role in ribosomal large subunit biogenesis
C7_00990W_A	RPP0	orf19.7015	2.141327307	1.33E-29	Putative ribosomal protein
C3_03360W_A	FCY2	orf19.333	2.138605293	3.07E-16	Purine-cytosine permease of pyrimidine salvage
C4_06480C_A	CEK1	orf19.2886	2.135768876	1.80E-22	ERK-family protein kinase
CR_01950W_A		orf19.2594	2.133082556	4.70E-23	Ortholog(s) have RNA polymerase I activity and role in nucleolar large rRNA transcription by RNA polymerase I
C3_04740C_A		orf19.5934	2.132850909	2.67E-16	Ortholog(s) have DNA topoisomerase activity, DNA topoisomerase type I activity
C5_00290W_A	DUS4	orf19.966	2.130385429	1.68E-19	Ortholog(s) have tRNA dihydrouridine synthase activity and role in tRNA modification
C2_00630C_A		orf19.2065	2.128904377	4.73E-07	Ortholog(s) have allantoicase activity and role in allantoin catabolic process
C4_04860W_A		orf19.3793	2.127030727	3.03E-10	Protein of unknown function
C4_06100W_A	CWH41	orf19.4719	2.126714714	4.11E-18	Processing alpha glucosidase I
C3_04460W_A		orf19.5897	2.125938313	4.55E-17	Ortholog(s) have role in positive regulation of TORC1 signaling and Seh1-associated complex
C3_04670C_A	RPS15	orf19.5927	2.125850408	6.32E-28	Putative ribosomal protein
C4_05790W_A		orf19.1265	2.124975701	5.76E-14	Ortholog(s) have Rab guanyl-nucleotide exchange factor activity
C3_05530W_A	OST1	orf19.6988	2.124263066	1.21E-21	Alpha subunit of the oligosaccharyltransferase complex of the ER lumen
CR_03400W_A		orf19.2382	2.120401868	2.65E-14	Protein similar to isoleucyl-tRNA synthetase
C5_05150C_A		orf19.4007	2.119824245	1.65E-11	Ortholog(s) have protein-lysine N-methyltransferase activity
C5_00120W_A		orf19.5684.1	2.117414087	1.71E-09	Ortholog of Candida tropicalis: CTRG1_CGOB_00063
C2_05470W_A	COQ5	orf19.3577	2.115818782	1.99E-19	Putative methyltransferase of ubiquinone biosynthesis
C4_06290W_A		orf19.2907.1	2.113132036	1.19E-06	Ortholog(s) have chromatin DNA binding activity
C7_01570C_A		orf19.6569	2.111825279	3.21E-10	Predicted transmembrane transporter
C1_06270W_A		orf19.1823	2.111312595	1.09E-14	Predicted membrane protein
C4_03840C_A	RRP42	orf19.5039	2.106723875	4.82E-15	Putative exosome non-catalytic core component
C3_01940C_A		orf19.1654	2.106107759	1.31E-22	Predicted membrane protein
C4_04270W_A		orf19.1421	2.104838851	1.91E-08	Ortholog(s) have ureidoglycolate lyase activity
C1_12310C_A	CSI2	orf19.5232	2.104374282	1.08E-17	Putative 66S pre-ribosomal particle component
C4_04440W_A		orf19.3843	2.104142612	1.24E-22	Ortholog(s) have protein transmembrane transporter activity and role in filamentous growth
C7_03850W_A		orf19.7197	2.101545991	2.85E-22	Putative intranuclear transport and DNA replication mediator
C4_00130W_A	RBT5	orf19.5636	2.10085016	2.88E-22	GPI-linked cell wall protein
C2_10820C_A		orf19.5365	2.099973101	4.60E-21	S. cerevisiae ortholog YMR259C interacts with Trm7 for 2'-O-methylation of C32 of substrate tRNAs
C2_03070C_A	SMP3	orf19.5792	2.098372198	1.38E-10	Mannosyltransferase of

135

					glycosylphosphatidylinositol (GPI) biosynthesis
C5_02540C_A	SPR28	orf19.4266	2.096992373	1.74E-06	Septin
CR_06170W_A		orf19.3872	2.0931216	1.05E-12	Protein of unknown function
C3_02020W_A		orf19.1646	2.090105897	9.60E-24	Ortholog(s) have rRNA primary transcript binding activity
C2_10810W_A		orf19.5364	2.089546851	2.11E-18	Putative pre-mRNA splicing factor
C5_03640W_A		orf19.6676	2.089516988	1.65E-07	Has domain(s) with predicted diphthine synthase activity
C2_10150W_A		orf19.1766	2.089185625	2.83E-13	Secreted protein
C3_05290C_A		orf19.6008	2.087990313	5.35E-07	S. cerevisiae ortholog YLL032C interacts with ribosomes
C3_07300W_A	NOP13	orf19.6766	2.087615583	3.30E-23	Ortholog of S. cerevisiae Nop13
C1_12670C_A		orf19.6356	2.086850787	5.92E-14	Ortholog(s) have role in mRNA splicing, via spliceosome and U4/U6 snRNP
C1_06690W_A	CYK3	orf19.6242	2.085788282	5.74E-07	Essential protein involved in cytokinesis
C1_10410W_A		orf19.4911	2.084485337	2.59E-06	BED zinc finger protein
C4_03730C_A		orf19.1305	2.083994736	3.89E-14	Ortholog(s) have tRNA (guanine-N1-)-methyltransferase activity
C4_06860C_A		orf19.3123.2	2.079949353	1.01E-06	Ortholog(s) have cytidine deaminase activity
C3_03320W_A	RUB1	orf19.330.1	2.075343048	3.55E-13	Ubiquitin-related protein with similarity to mammalian NEDD8
C4_02600C_A		orf19.2739	2.073903089	3.95E-17	Ortholog(s) have histone binding activity
C7_03920C_A	RPP1B	orf19.7188	2.069544373	2.85E-24	Conserved acidic ribosomal protein
C4_02840C_A	MED20	orf19.2711.1	2.06844964	1.46E-12	Subunit of the RNA polymerase II mediator complex
C2_09780C_A		orf19.1372	2.066406795	3.63E-20	Protein of unknown function
C6_02150C_A		orf19.3455	2.065576837	4.15E-08	Putative mitochondrial inner membrane magnesium transporter
C5_02580W_A		orf19.4271	2.062995709	1.71E-13	Predicted ORF from Assembly 19
C3_05770C_A	SAM50	orf19.7358	2.062719747	9.85E-09	Predicted component of the SAM complex involved in mitochondrial protein import
C1_08900W_A		orf19.4749	2.06092791	5.33E-16	Protein of unknown function
C4_01430C_A		orf19.4642	2.060792611	7.58E-16	Protein of unknown function
C2_10780C_A	PSO2	orf19.5362	2.060665404	1.62E-06	Putative DNA cross-link repair protein
C2_03120W_A	AMO1	orf19.5784	2.057556592	9.95E-10	Putative peroxisomal copper amine oxidase
C2_02540W_A		orf19.1578	2.056884568	8.55E-19	Ortholog of S. cereviaie Rrp5
C1_01370C_A	RPS21B	orf19.3325.3	2.056737444	1.79E-22	Ribosomal protein S21
C5_01110W_A		orf19.1959	2.056134056	1.86E-13	Ortholog of S. cerevisiae : OTU2
C1_03240W_A		orf19.3016	2.053911302	4.51E-16	Ortholog of C. dubliniensis CD36
C7_00500W_A		orf19.7070	2.04995607	2.26E-01	Ortholog of Candida guilliermondii ATCC 6260
CR_01830C_A	PTR2	orf19.2583	2.046331488	1.55E-01	Oligopeptide transporter involved in uptake of di-/tripeptides
C2_05890C_A	IDP1	orf19.5211	2.044613313	5.32E-22	Putative isocitrate dehydrogenase
CR_02690W_A		orf19.2828	2.042317066	9.26E-13	Ortholog(s) have alpha-tubulin binding
C1_04280C_A		orf19.1063	2.041305852	1.06E-07	Ortholog(s) have alpha-1,6-mannosyltransferase activity
C4_03720C_A		orf19.1306	2.040500971	2.44E-15	Has domain(s) with predicted 2-oxoglutarate-dependent dioxygenase activity and role in oxidation-reduction process
C7_00960W_A	RPS18	orf19.7018	2.040225738	5.15E-24	Predicted ribosomal protein
C3_06040W_A		orf19.7385	2.038954419	4.79E-10	CCCH zinc finger protein
C2_08550C_A	MSU1	orf19.3624	2.038636011	6.93E-17	Ortholog(s) have exoribonuclease II activity
C1_09460W_A	ERG12	orf19.4809	2.037148986	7.27E-19	Ortholog(s) have mevalonate kinase activity and role in ergosterol biosynthetic process

C4_02660W_A		orf19.2734	2.036348923	3.86E-07	Protein with a glucose/ribitol dehydrogenase family domain
CR_07680C_A		orf19.6282	2.035468378	7.01E-10	Ortholog of C. dubliniensis
C2_08870C_A	PIR1	orf19.220	2.034956306	4.77E-21	1,3-beta-glucan-linked cell wall protein
C6_01040C_A		orf19.107	2.034670222	1.10E-19	DEAH-box ATP-dependent RNA helicase
C2_01500W_A		orf19.1456	2.034188667	4.85E-07	Ortholog of Candida albicans WO-1
C2_05080C_A		orf19.3539	2.032910594	1.92E-14	Predicted nucleolar S-adenosylmethionine-dependent rRNA methyltransferase
C7_00560C_A	THG1	orf19.7063	2.030101657	5.99E-11	tRNA guanylyltransferase
C4_04890C_A	RPL24A	orf19.3789	2.029051644	1.16E-22	Predicted ribosomal protein
C6_00100C_A	HET1	orf19.6327	2.02850154	4.05E-23	Putative sphingolipid transfer protein
C5_05090W_A		orf19.4001	2.028431421	1.37E-06	Ortholog(s) have role in protein insertion into mitochondrial inner membrane from matrix and extrinsic component of mitochondrial inner membrane
C2_08040C_A	RPS10	orf19.2179.2	2.028058368	4.79E-25	Ribosomal protein S10
C1_00730C_A	CMP1	orf19.6033	2.025509338	1.80E-21	Catalytic subunit of calcineurin (Ca^{2+}-calmodulin-regulated S/T protein phosphatase)
C7_01390W_A		orf19.6920	2.025314844	6.40E-10	Protein of unknown function
C1_03790C_A		orf19.1030	2.023592314	3.30E-20	Putative peptidyl-prolyl cis-trans isomerase
C2_03810C_A	RPL21A	orf19.840	2.023388845	7.41E-25	Putative ribosomal protein
C6_02880W_A		orf19.5564	2.019800115	8.04E-10	Ortholog(s) have RNA-DNA hybrid ribonuclease activity
CR_00270C_A		orf19.7507	2.018986208	1.43E-12	Ortholog of C. dubliniensis CD36
C7_04170W_A		orf19.7157	2.017473841	1.22E-04	Protein with a tubulin binding cofactor C domain
C1_01870C_A	CYS4	orf19.4536	2.014537947	1.02E-22	Cystathionine beta-synthase
C6_03080C_A	ADO1	orf19.5591	2.014462689	9.80E-17	Adenosine kinase
CR_01970C_A	VMA4	orf19.2598	2.013671538	1.89E-23	H+ transporting ATPase E chain
CR_02710W_A	RRP9	orf19.2830	2.013196392	5.67E-17	Ribosomal protein
C1_10320W_A		orf19.4903	2.01272415	7.80E-11	Ortholog(s) have N-acetylglucosaminylphosphatidylinositol deacetylase activity
C1_11910W_A		orf19.5276	2.012103211	2.16E-07	Putative nuclear pore-associated protein
C7_04190C_A	UTP18	orf19.7154	2.011628717	6.27E-19	Putative U3 snoRNA-associated protein
C3_02960C_A	KRE5	orf19.290	2.011445973	9.90E-19	UDP-glucose:glycoprotein glucosyltransferase
C1_08180C_A		orf19.5095	2.009046304	9.22E-26	Putative oxysterol-binding protein
C1_09060C_A		orf19.4763	2.00880645	3.33E-09	Protein of unknown function
C7_02840C_A	ERG5	orf19.5178	2.007709034	1.89E-26	Putative C-22 sterol desaturase
C2_04380C_A		orf19.4516	2.006798185	1.13E-13	Ortholog(s) have tetrahydrofolylpolyglutamate synthase activity
C6_02250W_A		orf19.3466	2.006781389	1.28E-09	Predicted methyltransferase
C6_04650W_A		orf19.2163	2.00664706	1.85E-24	Has domain(s) with predicted peptidase activity and role in proteolysis
CR_03040C_A	HGT18	orf19.2425	2.005314138	1.11E-12	Putative glucose transporter of the major facilitator superfamily
C5_02140C_A		orf19.4220	2.002496795	1.81E-18	Predicted pyridoxal 5'-phosphate synthase
C6_04300W_A		orf19.1087	2.001250738	5.30E-14	Ortholog of C. dubliniensis CD36
C2_01940C_A		orf19.1506	-2.00109658	2.34E-01	Ortholog of Candida albicans WO-1 : CAWG_03962
C1_05860W_A	PRN2	orf19.2463	-2.003666172	2.17E-21	Protein similar to pirin
C2_03770C_A	STE11	orf19.844	-2.004471336	3.40E-26	Protein similar to S. cerevisiae Ste11p
C5_03210C_A		orf19.2657	-2.00565086	2.19E-09	Protein of unknown function
CR_07540C_A		orf19.2624	-2.005702196	1.83E-03	Protein of unknown function

C7_00880C_A		orf19.7027	-2.007097164	2.10E-16	Protein of unknown function
C1_04490W_A		orf19.6843	-2.009114449	5.08E-24	Ortholog(s) have role in CENP-A containing nucleosome assembly
C3_00670C_A	FKH2	orf19.5389	-2.010560594	2.30E-21	Forkhead transcription factor
C2_09610W_A		orf19.1393	-2.012021338	1.11E-12	Ortholog(s) have NAD transmembrane transporter activity
C1_13930W_A	SSK1	orf19.5031	-2.013869895	2.14E-23	Response regulator of two-component system
CR_09750C_A		orf19.7547	-2.014284917	4.65E-19	Ortholog(s) have phosphatidylinositol-3-phosphate binding
C6_00260W_A		orf19.1185	-2.015310487	3.38E-25	Ortholog(s) have ubiquitin protein ligase activity
C1_07580C_A	PRY1	orf19.2787	-2.016876002	5.02E-02	Pry family pathogenesis-related protein
CR_09430C_A		orf19.7340	-2.017994307	2.29E-01	Protein of unknown function
C5_00540C_A	AGA1	orf19.935	-2.019983777	2.26E-01	Protein with some similarity to agglutinin subunit
C4_04250W_A		orf19.1424	-2.020322855	6.88E-20	Predicted membrane transporter
C2_10000C_A		orf19.1782.1	-2.027080882	6.67E-05	Ortholog of C. parapsilosis CDC317
C6_03760C_A	SHM2	orf19.5750	-2.029251627	2.28E-27	Cytoplasmic serine hydroxymethyltransferase
C6_03920W_A	SNF4	orf19.5768	-2.030268793	7.50E-25	Putative subunit of the AMP-activated Snf1p kinase
C7_03770C_A	YAF9	orf19.5501	-2.032071469	3.79E-20	YEATS domain-containing protein involved in transcription regulation
CR_00810W_A		orf19.3275	-2.033335359	6.64E-20	Ortholog of C. dubliniensis CD36
CR_03130W_A		orf19.2412	-2.03385755	3.19E-16	Ortholog(s) have role in late endosome to vacuole transport via multivesicular body sorting pathway and Vps55/Vps68 complex
C2_00700W_A		orf19.2057	-2.038318565	9.64E-28	Ortholog(s) have ATP binding
C1_06320W_A		orf19.177	-2.038675041	1.43E-17	Has domain(s) with predicted phosphatidylinositol binding activity and role in cell communication
CR_06520C_A		orf19.714	-2.044111734	1.46E-17	Ortholog(s) have GTPase activity
C1_03810C_A	ELA1	orf19.1028	-2.044522602	1.81E-15	Elongin A
C1_06250W_A		orf19.1825	-2.044691755	1.17E-12	Protein of unknown function
C7_00420C_A		orf19.7078	-2.046413661	3.50E-18	Ortholog of S. cerevisiae : YCL012C
CR_09990W_A		orf19.7574	-2.048489068	2.63E-27	Ortholog(s) have ubiquitin ligase complex localization
C2_07880W_A	APM4	orf19.2194	-2.050123569	1.59E-23	Cargo-binding subunit of the clathrin associated protein complex (AP-2)
C1_10040W_A	ERO1	orf19.4871	-2.051996155	1.14E-28	Ortholog of S. cerevisiae Ero1
C7_03040W_A		orf19.5157	-2.05628494	2.00E-09	Protein with a protein tyrosine phosphatase-like protein domain
C1_13840W_A		orf19.5022	-2.056585642	3.62E-22	Ortholog(s) have inorganic cation transmembrane transporter activity and role in cellular cobalt ion homeostasis
C4_01420W_A		orf19.4643	-2.056596908	1.70E-23	Ortholog of C. dubliniensis CD36
CR_04180C_A		orf19.504	-2.058706429	1.28E-28	Ortholog(s) have 3'-5' DNA helicase activity
C2_03430W_A	NBN1	orf19.878	-2.059242811	8.31E-22	Subunit of the NuA4 histone acetyltransferase complex
C5_02110W_A		orf19.4216	-2.061885956	4.91E-23	Putative heat shock protein
C3_00930W_A	ATO2	orf19.2496	-2.061983698	1.27E-25	Putative fungal-specific transmembrane protein
C5_01280C_A	NUF2	orf19.1941	-2.065598745	5.01E-22	Kinetochore component
C4_04180C_A		orf19.5291	-2.067581662	1.45E-18	Ortholog(s) have role in phospholipid biosynthetic process
C1_03520W_A	RPN3	orf19.3054	-2.068657053	4.78E-24	Putative non-ATPase regulatory subunit of the 26S proteasome lid
CR_01470W_A	CSP37	orf19.2531	-2.069029527	3.09E-26	Hyphal cell wall protein
C5_00570W_A		orf19.932	-2.069806544	1.29E-24	Putative aminophospholipid translocase (flippase)

C2_08940C_A	VPS28	orf19.212	-2.070602867	4.47E-20	ESCRT I protein sorting complex subunit
C2_04540C_A	GDT1	orf19.4496	-2.077727345	2.99E-23	Golgi Ca2+/H+ exchanger
CR_06660W_A	SEO1	orf19.700	-2.078698541	6.05E-18	Protein with similarity to permeases
CR_05280W_A		orf19.1009	-2.080337737	1.80E-01	Ortholog of *Candida albicans* WO-1
C5_02800C_A		orf19.4305	-2.081621329	2.21E-05	Ortholog of C. dubliniensis CD36
C1_08330C_A	ADH2	orf19.5113	-2.08164859	4.77E-23	Alcohol dehydrogenase
C2_09520C_A	CCT2	orf19.1402	-2.081680099	7.54E-29	Chaperonin of the cytosolic TCP1 ring complex
C2_01010W_A	HGT8	orf19.2021	-2.081753667	1.04E-17	High-affinity glucose transporter of the major facilitator superfamily
C6_01710C_A	PTK2	orf19.3415	-2.083560622	2.44E-27	Putative protein kinase of polyamine import
C7_00890C_A	MCM1	orf19.7025	-2.083966428	1.77E-25	Transcription factor
C7_01410C_A	NBP2	orf19.6588	-2.08647102	1.36E-22	Protein containing an SH3 domain
CR_06530W_A		orf19.713	-2.088217717	2.70E-26	Ortholog(s) have role in hydrogen peroxide-mediated programmed cell death
C1_06780W_A	NPR1	orf19.6232	-2.092017604	1.04E-27	Predicted serine/threonine protein kinase, involved in regulation of ammonium transport
CR_06940W_A	DSL1	orf19.2370	-2.094885881	6.13E-22	Protein similar to S. cerevisiae Dsl1p
C5_04360C_A		orf19.3922	-2.097813296	2.47E-25	Possible pyrimidine 5' nucleotidase
C3_00850C_A		orf19.6160	-2.100000245	5.20E-27	Ortholog(s) have role in eisosome assembly and eisosome
C1_08680C_A		orf19.4726	-2.100860734	3.47E-25	Ortholog(s) have 1-phosphatidylinositol 4-kinase activator activity
C6_00600C_A	YHM2	orf19.4197	-2.106969823	2.34E-26	Predicted carrier protein
C1_12150C_A		orf19.5249	-2.108277608	1.15E-12	Ortholog(s) have role in autophagosome assembly
C2_01690W_A		orf19.1480	-2.113941558	5.52E-27	Putative succinate dehydrogenase
C3_04860W_A	SFP1	orf19.5953	-2.114461548	1.49E-27	C2H2 transcription factor involved in regulation of biofilm formation
C1_00660C_A		orf19.6039	-2.115613096	7.68E-25	Ortholog(s) have SNAP receptor activity
C1_13320C_A		orf19.4959	-2.116223857	7.56E-26	Protein of unknown function
C1_13140C_A	TYE7	orf19.4941	-2.120015016	1.19E-17	bHLH transcription factor
C5_04080C_A		orf19.1281	-2.124799397	1.12E-26	Putative splicing factor required for the first step of pre-mRNA splicing
C6_02890C_A	HPD1	orf19.5565	-2.125488467	1.23E-09	3-hydroxypropionate dehydrogenase
C3_03850C_A	SOL1	orf19.6930	-2.129869375	8.95E-23	Cell cycle regulator
C1_01270W_A	CTA9	orf19.3315	-2.129946603	1.48E-23	Protein required for normal filamentous growth
CR_08120C_A	DCP2	orf19.6373	-2.130261412	3.58E-30	Ortholog(s) have chromatin binding
C7_01940C_A		orf19.6527	-2.136169826	6.19E-22	Pheromone-regulated protein (Prm10) of S. cerevisiae
C7_01770W_A		orf19.6547	-2.140939215	6.20E-02	Ortholog of *Candida albicans* WO-1
C3_01960C_A	POX1-3	orf19.1652	-2.141583589	3.50E-25	Predicted acyl-CoA oxidase
C5_02190C_A		orf19.4225.1	-2.143177168	6.80E-24	Ortholog(s) have oxoglutarate dehydrogenase (succinyl-transferring) activity
CR_03240C_A		orf19.2399	-2.143566912	6.34E-27	Putative transcription factor with zinc finger DNA-binding motif
C2_06070W_A	FAA2-1	orf19.4114	-2.144004425	4.37E-21	Predicted long chain fatty acid CoA ligase
CR_07120C_A		orf19.9	-2.145990377	8.30E-10	Ortholog of C. dubliniensis CD36
C6_02600W_A	NAB3	orf19.5530	-2.148155224	4.51E-27	Putative nuclear polyadenylated RNA-binding protein
C3_02640C_A	ZCF1	orf19.255	-2.14920308	1.74E-19	Zn(II)2Cys6 transcription factor
C1_00580W_A		orf19.6048	-2.152789338	2.76E-17	Protein of unknown function
C3_03250W_A		orf19.323	-2.153002735	2.36E-24	Putative haloacid dehalogenase
C3_00680C_A		orf19.5390	-2.15496839	1.13E-15	Ortholog of *Candida albicans* WO-1

CR_07700W_A		orf19.1985	-2.155130235	1.10E-15	Has aminoglycoside phosphotransferase and protein kinase domains
C1_10760W_A	VPS23	orf19.2343	-2.155519665	6.58E-18	ESCRT I protein sorting complex protein
C2_08730W_A	MFG1	orf19.3603	-2.155627684	4.51E-27	Regulator of filamentous growth
C1_11620W_A		orf19.1158	-2.158809882	7.45E-12	Ortholog of S. cerevisiae Yft2 required for normal ER membrane biosynthesis
C7_02380C_A	CYP1	orf19.6472	-2.162698687	3.30E-33	Peptidyl-prolyl cis-trans isomerase
C5_04090C_A	SUI1	orf19.1280	-2.166066602	3.01E-31	Putative translation initiation factor
CR_08840C_A	NIT2	orf19.7279	-2.167886808	2.38E-15	Putative carbon-nitrogen hydrolase
C5_02020C_A		orf19.3169	-2.16982788	6.63E-30	Ortholog(s) have role in establishment of mitotic sister chromatid cohesion
C2_04680W_A	TIM17	orf19.150	-2.170901668	5.22E-29	Predicted component of the Translocase of the Inner Mitochondrial membrane (TIM23 complex)
C2_05070W_A	FRE9	orf19.3538	-2.176359769	2.47E-26	Ferric reductase
C1_06820W_A		orf19.6227	-2.178233657	3.81E-26	Ortholog of C. dubliniensis
C1_14400C_A	MLH3	orf19.7257	-2.179901033	6.09E-24	Ortholog(s) have role in meiotic mismatch repair
C1_10360C_A		orf19.4907	-2.185015879	6.32E-30	Putative protein of unknown function
C1_05440C_A		orf19.419	-2.18515712	6.57E-27	Protein of unknown function
C7_00080C_A	SAC7	orf19.7115	-2.18981802	5.22E-30	Putative GTPase activating protein (GAP) for Rho1
C1_11990W_A		orf19.5267	-2.191146583	7.38E-06	Putative cell wall adhesin-like protein
CR_00790C_A		orf19.3277	-2.19144951	1.01E-01	Ortholog of *Candida albicans* WO-1
C4_01960C_A		orf19.4596	-2.19497876	1.28E-24	Protein of unknown function
C2_04050C_A	DCK1	orf19.815	-2.196531657	1.22E-30	Putative guanine nucleotide exchange factor
C1_13250W_A		orf19.4952	-2.19951856	4.48E-30	Protein of unknown function
C1_05350W_A	YPT53	orf19.430	-2.201236209	9.98E-28	Rab-family GTPase involved in vacuolar trafficking
C2_06980W_A		orf19.2252	-2.20141473	1.90E-01	Protein of unknown function
C5_04500W_A		orf19.3935	-2.20141473	1.90E-01	Ortholog of *Candida albicans* WO-1
C7_01910C_A		orf19.6530	-2.203106834	6.51E-20	Similar to bacterial DnaJ
C1_10580C_A		orf19.1830	-2.20372413	1.24E-15	Protein of unknown function
CR_07130C_A	ALK8	orf19.10	-2.20553259	2.34E-05	Alkane-inducible cytochrome P450
C1_06660W_A		orf19.6245	-2.205559332	7.42E-31	Protein of unknown function
C2_01140C_A		orf19.2010	-2.206473009	1.68E-01	Ortholog of C. dubliniensis CD36
C1_01220C_A		orf19.3310	-2.206633218	6.13E-26	Protein of unknown function
C5_00590W_A	PET9	orf19.930	-2.207587725	2.92E-30	Mitochondrial ADP/ATP carrier protein involved in ATP biosynthesis
C3_06310C_A	ISW2	orf19.7401	-2.209555461	6.04E-28	Ortholog of S. cerevisiae Isw2
C3_04110C_A	MBP1	orf19.5855	-2.210094907	6.82E-31	Putative component of the MBF transcription complex involved in G1/S cell-cycle progression
C7_03220C_A	ZCF29	orf19.5133	-2.212908381	2.05E-31	Zn(II)2Cys6 transcription factor
CR_00110W_A		orf19.7527	-2.214078674	1.58E-26	Ortholog of C. dubliniensis CD36 : Cd36_25130
C5_04540C_A		orf19.3940	-2.217307375	1.00E-17	Ortholog of C. dubliniensis CD36 : Cd36_54170
C4_03700W_A		orf19.1308	-2.218114191	1.32E-24	Predicted membrane transporter
C5_03090W_A	VPS4	orf19.4339	-2.219401775	2.07E-21	AAA-ATPase involved in transport from MVB to the vacuole and ESCRT-III complex disassembly
C1_00340W_A	HBR1	orf19.6074	-2.22024768	4.27E-32	Essential protein involved in regulation of MTL gene expression
C6_00480C_A	FET31	orf19.4211	-2.222736342	9.47E-07	Putative multicopper oxidase

C7_00370W_A	DCC1	orf19.7083	-2.232044011	1.27E-20	Protein with a predicted role in sister chromatid cohesion and telomere length maintenance
CR_00520C_A	CRM1	orf19.7483	-2.232345116	7.60E-32	Functional homolog of S. cerevisiae Crm1
C1_05370C_A		orf19.428	-2.234020727	2.47E-25	Putative serine/threonine kinase
C2_00400C_A		orf19.2091	-2.237401831	2.66E-26	Putative NADH dehydrogenase
CR_07770C_A	PTC6	orf19.3705	-2.239374386	3.67E-28	Mitochondrial protein phosphatase of the Type 2C-related family (serine/threonine-specific
C2_05260W_A	BUD14	orf19.3555	-2.241209394	5.73E-30	Putative SH3-domain-containing protein
C2_09800C_A		orf19.1370	-2.24174049	1.82E-01	Protein of unknown function
C1_09210C_A		orf19.4779	-2.242331282	3.49E-29	Putative transporter
C5_02030W_A	RPN8	orf19.3168	-2.242343469	4.42E-33	Putative regulatory subunit of the 26S proteasome
C1_03410W_A		orf19.3042	-2.242929756	5.13E-16	Protein of unknown function
C5_02790C_A	GAP1	orf19.4304	-2.243076165	1.45E-23	Amino acid permease
C4_00360C_A	RCH1	orf19.5663	-2.243222186	3.49E-24	Plasma membrane protein
C7_01370W_A	QCE1	orf19.6918	-2.24446278	2.23E-26	Mitochondrial protein required for expression of respiratory chain complex III
C1_13130C_A		orf19.4940	-2.244997403	9.63E-27	Putative histidine permease
C3_06580W_A	JEN1	orf19.7447	-2.246708693	4.74E-03	Lactate transporter
C5_02180C_A	LEU3	orf19.4225	-2.249226894	1.04E-32	Zn(II)2Cys6 transcription factor
CR_08410W_A		orf19.6407	-2.25226004	2.35E-31	Ortholog(s) have role in ribosomal large subunit biogenesis
C1_05890W_A		orf19.2460	-2.254741495	9.46E-02	Protein of unknown function
C7_04060W_A		orf19.7173	-2.258705536	3.51E-12	Ortholog of C. dubliniensis CD36 : Cd36_73730
C3_00030C_A		orf19.5469	-2.261090447	6.03E-21	Protein with a predicted DEAD-like DNA/RNA helicase domain
CR_03210C_A	SSU72	orf19.2402	-2.261254847	2.21E-29	Ortholog(s) have RNA polymerase II CTD heptapeptide repeat phosphatase activity
C2_05990C_A		orf19.4121	-2.262726208	5.54E-17	Predicted thioesterase/thiol ester dehydrase-isomerase
C3_01130C_A		orf19.2515	-2.263567417	2.63E-27	ZZ-type zinc finger protein
C6_00620W_A	FCA1	orf19.4195.1	-2.265529207	6.44E-16	Cytosine deaminase
C6_04150W_A		orf19.77.1	-2.266619777	1.78E-01	Protein of unknown function
C2_04620W_A		orf19.4488	-2.267426199	8.92E-36	Predicted ortholog of S. cerevisiae Swi3
C1_14000C_A	DOA4	orf19.7207	-2.267798453	7.21E-30	Ortholog of S. cerevisiae Doa4
C5_04410C_A		orf19.3928	-2.273419393	2.01E-25	Putative transcription factor with zinc finger DNA-binding motif
C5_03870C_A		orf19.1107	-2.274324927	1.55E-31	Protein of unknown function
CR_01670W_A		orf19.2558	-2.275029635	5.71E-27	Has domain(s) with predicted zinc ion binding activity and host cell nucleus
C3_05640W_A		orf19.6999	-2.275858865	7.76E-02	Predicted oxidoreductase
C1_02160W_A		orf19.3673	-2.276764295	1.91E-22	Ortholog(s) have Rab guanyl-nucleotide exchange factor activity and role in chromosome organization
C3_05680W_A		orf19.7347	-2.280225972	3.31E-30	Ortholog(s) have ubiquitin-protein transferase activity, role in protein monoubiquitination
C5_02200W_A		orf19.4227	-2.282047352	3.41E-18	Ortholog of C. dubliniensis CD36 : Cd36_52020
C1_09520C_A		orf19.4816	-2.2822552	2.17E-31	Protein of unknown function
CR_10300W_A	PUP1	orf19.7605	-2.284576478	7.22E-36	Putative beta 2 subunit of the 20S proteasome
C7_03320C_A	MED16	orf19.1343	-2.287099968	3.71E-33	Putative RNA polymerase II mediator complex subunit
C5_05110C_A	TIP20	orf19.4003	-2.289096153	4.19E-32	Protein interacting with Sec20p
C2_00390C_A		orf19.2092	-2.289201454	8.03E-30	Putative peroxisomal cystathionine beta-lyase
C2_00710W_A	NPL6	orf19.2055	-2.28993093	4.56E-33	Putative nuclear protein localization factor

C1_05810W_A	GIM5	orf19.2471	-2.291455089	2.29E-29	Putative heterohexameric cochaperone prefoldin complex subunit
CR_09100C_A		orf19.7306	-2.292488765	2.27E-33	Aldo-keto reductase
C2_00290W_A		orf19.2104	-2.296341306	7.60E-21	Ortholog(s) have ATPase activator activity
C1_03310W_A		orf19.3027	-2.297863618	8.49E-32	Putative DNA translocase
CR_08980C_A		orf19.7295	-2.303266464	1.21E-25	Ortholog(s) have protein phosphatase 1 binding activity
C1_04640W_A		orf19.782	-2.303806006	8.96E-24	Ortholog(s) have hydrolase activity
C4_02510W_A		orf19.2751	-2.308371315	7.08E-27	Predicted membrane transporter
C1_01260C_A	TRS20	orf19.3314	-2.308649367	6.37E-19	Ortholog(s) have role in cellular protein-containing complex assembly
C2_09900C_A	TIM23	orf19.1361	-2.309540761	1.30E-27	Protein involved in mitochondrial matrix protein import
C6_01440C_A	FRP5	orf19.3440	-2.312650322	6.49E-06	Protein with a GPR1/FUN34/yaaH family domain
C7_01150W_A		orf19.6898	-2.31325201	5.19E-22	Protein similar to S. pombe SPBC1709.16c a predicted aromatic ring-opening dioxygenase
C2_05060C_A		orf19.3537	-2.315847245	2.53E-23	Putative sulfiredoxin
C2_04180C_A		orf19.804	-2.315904993	4.85E-23	Putative mitochondrial carrier family transporter
CR_01580C_A	DOT6	orf19.2545	-2.316298295	1.51E-33	Protein with a predicted role in telomeric gene silencing and filamentation
C5_00170W_A		orf19.5680	-2.317882376	1.68E-30	Protein with predicted hydrolase domains
C3_01370C_A	PGA44	orf19.1714	-2.321933315	4.89E-02	Putative GPI-anchored protein
C4_06540W_A	MNN4	orf19.2881	-2.325014578	4.55E-29	Regulator of mannosylphosphorylation of N-linked mannans to cell wall proteins
C4_05720W_A		orf19.1257	-2.327630612	1.66E-01	Ortholog of Candida albicans WO-1 : CAWG_03251
C5_05240C_A		orf19.4017	-2.328225525	4.54E-07	Ortholog of C. dubliniensis CD36 : Cd36_54840
C7_02330W_A	YCF1	orf19.6478	-2.328259318	1.40E-36	Putative glutathione S-conjugate transporter
C5_03020W_A	CCC2	orf19.4328	-2.330050993	2.07E-28	Copper-transporting P-type ATPase of Golgi
C6_00670W_A	CDC14	orf19.4192	-2.333400444	1.50E-23	Protein involved in exit from mitosis and morphogenesis
C7_03480W_A		orf19.6705	-2.334666905	1.95E-36	Putative guanyl nucleotide exchange factor with Sec7 domain
CR_00100C_A	EPL1	orf19.7529	-2.338054846	3.20E-37	Subunit of the NuA4 histone acetyltransferase complex
C6_03400C_A	QCR7	orf19.5629	-2.339455405	4.30E-34	Putative ubiquinol-cytochrome-c reductase, subunit 7
C2_00360C_A		orf19.2095	-2.341166882	1.16E-36	Ortholog(s) have role in negative regulation of transcription from RNA polymerase II promoter in response to iron and cytosol localization
C1_04370C_A		orf19.5201	-2.34175819	6.32E-34	Ortholog(s) have structural constituent of ribosome activity and mitochondrial small ribosomal subunit localization
C2_07580W_A		orf19.1867	-2.344897001	6.78E-20	Putative malate permease
C1_02810W_A	RAD16	orf19.2969	-2.346282931	1.41E-34	Ortholog of S. cerevisiae Rad16
C5_01380W_A	CFL5	orf19.1930	-2.347121118	3.79E-02	Ferric reductase
C3_05060W_A		orf19.5976	-2.348966156	3.43E-22	Protein of unknown function
C1_08340C_A		orf19.5114	-2.35156032	3.02E-30	Sorting nexin
C2_05370C_A	RXT3	orf19.3568	-2.356580309	5.32E-26	Putative transcriptional repressor
C6_01650C_A	FMP27	orf19.3422	-2.363792178	5.90E-30	Putative mitochondrial protein
C4_03090W_A		orf19.2682	-2.365213622	1.63E-28	Ortholog(s) have TBP-class protein binding
CR_10790W_A	MAL2	orf19.7668	-2.366454758	2.79E-29	Alpha-glucosidase
C5_03590W_A	LAP4	orf19.6671	-2.366547972	6.22E-34	Protein similar to aminopeptidase I
C7_03860W_A		orf19.7196	-2.367957894	5.94E-38	Putative vacuolar protease
CR_00150C_A	POT1	orf19.7520	-2.370386978	1.78E-28	Putative peroxisomal 3-oxoacyl CoA thiolase

142

C1_02840W_A	PDE2	orf19.2972	-2.374563446	1.45E-33	High affinity cyclic nucleotide phosphodiesterase
C6_00590W_A	SLY41	orf19.4199	-2.375003019	5.15E-31	Protein involved in ER-to-Golgi transport
C1_06510C_A		orf19.6263	-2.378272173	8.91E-36	Predicted MFS membrane transporter
C4_05680W_A	PHO4	orf19.1253	-2.378461636	4.49E-27	bHLH transcription factor of the myc-family
CR_01250C_A		orf19.3229	-2.379636679	1.49E-01	Protein of unknown function
C2_03460C_A		orf19.874	-2.38046056	6.06E-33	Predicted mitochondrial i-AAA protease supercomplex
C2_10360C_A	HEM3	orf19.1742	-2.383328123	1.87E-32	Hydroxymethylbilane synthase
C2_08920W_A		orf19.215	-2.385626804	5.76E-23	Component of a complex containing the Tor2p kinase
C2_00240C_A	SOD6	orf19.2108	-2.38582943	4.47E-23	Copper-containing superoxide dismutase
CR_08920W_A		orf19.7288	-2.391714458	1.02E-25	Protein with predicted oxidoreductase and dehydrogenase domains
CR_06590C_A	RGS2	orf19.695	-2.392878958	3.81E-28	Protein of RGS superfamily
C2_00680C_A	SOD5	orf19.2060	-2.396233442	3.27E-05	Cu-containing superoxide dismutase
C2_03240C_A	ROM2	orf19.906	-2.396874619	8.59E-39	Putative GDP/GTP exchange factor
C2_08100W_A		orf19.2175	-2.397152458	2.15E-23	Mitochondrial apoptosis-inducing factor
C3_07840C_A		orf19.6179	-2.399741989	6.17E-03	Ortholog of *Candida albicans* WO-1 : CAWG_03090
C7_03760W_A		orf19.5502	-2.399829941	1.13E-26	Ortholog of C. dubliniensis CD36 : Cd36_73420
C2_00480C_A	PHHB	orf19.2079	-2.402132803	5.60E-27	Putative 4a-hydroxytetrahydrobiopterin dehydratase
CR_10810C_A		orf19.7672	-2.402475889	3.83E-26	Ortholog(s) have protein-containing complex binding activity and role in endoplasmic reticulum unfolded protein response
CR_09440C_A		orf19.7341	-2.403859973	5.02E-37	Protein of unknown function
C1_12100C_A	PXA2	orf19.5255	-2.404284548	1.72E-18	Putative peroxisomal, half-size adrenoleukodystrophy protein subfamily ABC transporter
C2_00220C_A		orf19.2111	-2.404352306	6.72E-36	Ortholog(s) have RNA polymerase II complex binding activity
CR_10230W_A		orf19.7598	-2.411899658	1.52E-36	Ortholog(s) have histone acetyltransferase activity, role in histone acetylation
C3_02370C_A	ALR1	orf19.1607	-2.413430857	2.92E-35	Putative transporter of divalent cations
C4_05670W_A	YME1	orf19.1252	-2.417103093	1.07E-40	Ortholog(s) have ATP-dependent peptidase activity
C3_00810C_A	FOX2	orf19.1288	-2.419857956	7.17E-30	3-hydroxyacyl-CoA epimerase
C6_00940C_A		orf19.95	-2.423568685	3.85E-12	Ortholog of S. cerevisiae : PRM5
C2_03790C_A	ASR3	orf19.842	-2.427498644	6.46E-40	Adenylyl cyclase and stress responsive protein
C7_02020W_A	RAD14	orf19.6517	-2.42857738	8.37E-28	Putative DNA repair protein
C2_06260W_A		orf19.5488	-2.428689019	3.63E-26	Ortholog(s) have mitochondrial inner membrane
C5_01890W_A		orf19.3183	-2.429738654	2.14E-34	Protein with a role in insertion of tail-anchored proteins into the ER membrane
C4_01330W_A		orf19.4654	-2.43417602	7.72E-02	Protein of unknown function
C3_05910W_A	ZCF35	orf19.7371	-2.434942523	6.56E-38	Zn(II)2Cys6 transcription factor
C1_01890C_A		orf19.4534	-2.436379732	7.69E-39	Putative UBX-domain (ubiquitin-regulatory domain) protein
C6_02330W_A		orf19.3475	-2.438797638	1.95E-33	Described as a Gag-related protein
CR_10680W_A	RPO21	orf19.7655	-2.441537913	8.48E-34	RNA polymerase II
C7_03780C_A		orf19.7204	-2.442588282	6.68E-19	Has domain(s) with predicted catalytic activity
C4_04260C_A	FZO1	orf19.1422	-2.444621777	4.95E-39	Mitochondrial biogenesis protein
CR_10110W_A	CHT3	orf19.7586	-2.456467793	2.04E-08	Major chitinase
C7_00730W_A	MET28	orf19.7046	-2.458407054	1.90E-39	Predicted bZIP domain-containing transcription factor

143

CR_06860C_A	ARO10	orf19.1847	-2.458976437	1.31E-30	Aromatic decarboxylase
C2_10570W_A	SGS1	orf19.5335	-2.459173906	2.54E-38	RecQ-related DNA helicase
C1_07010W_A		orf19.6205	-2.460539407	4.71E-22	Ortholog of C. dubliniensis CD36 : Cd36_06550
CR_09460C_A		orf19.7341.1	-2.46077641	2.92E-33	Protein of unknown function
C1_05330C_A		orf19.432	-2.461172954	4.27E-34	Predicted SCF ubiquitin ligase complex protein
C1_02120C_A	SHA3	orf19.3669	-2.466709888	1.18E-27	Putative ser/thr kinase involved in glucose transport
C6_02320C_A	IPL1	orf19.3474	-2.467103877	1.56E-31	Putative Aurora kinase
C3_03870C_A	SAP9	orf19.6928	-2.468209066	1.74E-35	Secreted aspartyl protease
C2_08020C_A		orf19.2180	-2.471646074	1.57E-30	Ortholog(s) have calcium ion binding
C1_12060C_A		orf19.5259	-2.471777637	1.73E-17	Ortholog of C. dubliniensis CD36 : Cd36_11290
CR_09830W_A		orf19.7554	-2.475942524	9.55E-25	Transporter
C3_01640C_A		orf19.1679	-2.476938332	7.87E-03	Ortholog of C. dubliniensis CD36 : Cd36_81550
C2_10080W_A	RAP1	orf19.1773	-2.484633508	4.22E-26	Transcription factor
C6_00880W_A	PEX7	orf19.89	-2.485191529	5.48E-20	Ortholog(s) have peroxisome matrix targeting signal-2 binding activity
CR_00560W_A	NTH1	orf19.7479	-2.494809218	3.85E-33	Neutral trehalase
C1_04960C_A		orf19.50	-2.496291875	1.13E-36	Ortholog(s) have role in SCF-dependent proteasomal ubiquitin-dependent protein catabolic process
C1_09160W_A	AOX1	orf19.4774	-2.498361485	4.80E-32	Alternative oxidase
C1_03940W_A		orf19.4468	-2.50072847	5.54E-37	Putative succinate dehydrogenase
C1_10860C_A	ADA2	orf19.2331	-2.50135138	1.56E-22	Zinc finger and homeodomain transcriptional coactivator
CR_01160W_A		orf19.3238	-2.501637617	1.68E-08	Ortholog of Candida albicans WO-1 : CAWG_01469
C2_00380C_A	RFA1	orf19.2093	-2.502200199	6.50E-43	Putative DNA replication factor A
C1_14220C_A	FTR2	orf19.7231	-2.504752058	4.11E-23	High-affinity iron permease
C7_01490W_A		orf19.6580	-2.507913329	7.15E-35	Protein of unknown function
C2_10530C_A	KIN3	orf19.5325	-2.52146528	7.34E-38	Protein similar to S. cerevisiae Kin3p
C2_10540W_A	MIG2	orf19.5326	-2.523387853	4.25E-36	Transcription factor with zinc finger DNA-binding motif
C4_02220C_A	ZCF25	orf19.4568	-2.525117716	8.94E-26	Putative Zn(II)2Cys6 transcription factor
CR_04830C_A		orf19.6310	-2.525807315	9.50E-24	Has domain(s) with predicted myosin binding activity
C1_00290W_A	POL93	orf19.6078	-2.526864257	6.50E-38	Predicted ORF in retrotransposon Tca8 with similarity to the Pol region of retrotransposons encoding reverse transcriptase
CR_08690C_A	ECI1	orf19.6445	-2.528422828	1.11E-35	Protein similar to S. cerevisiae Eci1p
C2_08790W_A	JEM1	orf19.3592	-2.530545311	1.10E-40	Functional homolog of S. cerevisiae Jem1p
C5_00210C_A	BRE1	orf19.976	-2.53168839	1.03E-42	Putative transcription factor with C3HC4 zinc finger DNA-binding motif
C2_08030W_A		orf19.2181	-2.53352322	7.15E-11	Ortholog of Spathaspora passalidarum NRRL Y-27907 : spas_CGOB_00067 and Candida albicans WO-1 : CAWG_05895
C4_02020W_A	CAT2	orf19.4591	-2.537248859	2.69E-30	Major carnitine acetyl transferase
C3_01060W_A		orf19.2509.1	-2.537365011	7.98E-06	Ortholog of C. dubliniensis CD36 : Cd36_29340
C7_02450W_A		orf19.6464	-2.539982572	5.70E-38	Protein of unknown function
C3_07060W_A	FESUR1	orf19.6794	-2.544166041	1.59E-38	Putative ubiquinone reductase
CR_00290W_A		orf19.7504	-2.546559016	1.16E-36	Ortholog of S. cerevisiae Rts3
C3_05750C_A		orf19.7356	-2.549156571	8.16E-24	Ortholog of C. parapsilosis CDC317 : CPAR2_807080

C4_05400C_A		orf19.1797	-2.552524392	2.91E-34	D-arabinose 5-phosphate isomerase
C7_00410C_A		orf19.7079	-2.55531569	1.61E-31	Ortholog(s) have Rho guanyl-nucleotide exchange factor activity
C2_00140W_A	NDT80	orf19.2119	-2.555437758	3.79E-41	Ortholog of Ndt80
CR_06870C_A		orf19.1844	-2.556660284	5.84E-06	Protein similar to ferric reductase Fre10p
CR_03870W_A		orf19.4358	-2.560325742	1.10E-39	Putative protein of unknown function
C2_09250W_A		orf19.4086	-2.56367896	7.30E-32	Has domain(s) with predicted protein tyrosine phosphatase activity
CR_05220C_A	GUT1	orf19.558	-2.564318562	1.03E-33	Putative glycerol kinase
C3_07460W_A		orf19.6742	-2.567800864	3.50E-42	Ortholog(s) have RNA polymerase II CTD heptapeptide repeat phosphatase activity
C2_05330C_A		orf19.3563	-2.570562976	1.09E-27	Ortholog of C. dubliniensis CD36 : Cd36_19810
C2_07070W_A		orf19.2262	-2.570984715	4.69E-40	Protein similar to quinone oxidoreductases
C1_09010W_A	NAR1	orf19.4757	-2.578672486	3.74E-41	Putative cytosolic iron-sulfur (FeS) protein assembly machinery protein
C1_00410C_A		orf19.6066	-2.584110372	2.03E-30	Hexadecenal dehydrogenase
C3_00010C_A		orf19.5474	-2.588098888	7.42E-21	Protein of unknown function
C1_00330C_A		orf19.6075	-2.588216699	1.75E-40	Putative CCR4-Not complex transcription factor
C3_07430W_A		orf19.6747	-2.588420384	4.20E-43	Ortholog(s) have acid phosphatase activity and role in dephosphorylation
C6_04130C_A	ALS4	orf19.4555	-2.590376276	4.06E-26	GPI-anchored adhesin
C5_01880C_A		orf19.3184	-2.591933238	3.89E-37	Has domain(s) with predicted role in vesicle-mediated transport
C2_00530W_A		orf19.2074	-2.592783915	4.32E-06	Ortholog of Candida albicans WO-1 : CAWG_03833
C3_07200C_A	ZFU2	orf19.6781	-2.596781368	1.96E-34	Zn(II)2Cys6 transcription factor
C1_06840C_A		orf19.6225.1	-2.600281737	2.01E-27	Ortholog(s) have role in mitochondrial cytochrome c oxidase assembly and extrinsic component of matrix side of mitochondrial inner membrane
CR_04860C_A		orf19.6307	-2.602729786	3.37E-35	Ortholog of C. dubliniensis CD36 : Cd36_30250
C7_03240W_A		orf19.5131	-2.605009432	1.05E-40	Ortholog of S. cerevisiae Gid7, a GID complex protein
C3_04020C_A	ZCF16	orf19.2808	-2.609649886	2.53E-35	Predicted Zn(II)2Cys6 transcription factor
C4_06780C_A	OYE32	orf19.3131	-2.613725609	3.98E-45	NAD(P)H oxidoreductase family protein
C1_02070W_A	HSP31	orf19.3664	-2.618042643	6.65E-07	Putative 30 kda heat shock protein
CR_02160W_A	UGT51C1	orf19.2616	-2.619387973	1.82E-44	UDP-glucose:sterol glucosyltransferase
C2_09230C_A	KIS1	orf19.4084	-2.625486777	5.93E-45	Snf1p complex scaffold protein
C1_08050W_A	NUO4	orf19.5077	-2.626660554	9.30E-40	Subunit of mitochondrial respiratory chain complex I
C4_00960W_A	PTC8	orf19.4698	-2.629057211	2.99E-33	Predicted type 2C protein phosphatase, ser/thr-specific
C4_04240C_A		orf19.1426	-2.630276263	6.47E-43	Ortholog of S. cerevisiae Skg6
C7_01760C_A	ISU1	orf19.6548	-2.632995803	5.05E-45	Protein with similarity to NifU
C1_08690W_A		orf19.4727	-2.634189877	7.42E-35	Ortholog(s) have role in mitochondrial respiratory chain complex II assembly
C6_00170C_A		orf19.6319	-2.634303098	4.74E-45	Ortholog(s) have mRNA binding, thiol-dependent ubiquitin-specific protease activity
C2_04090W_A		orf19.812	-2.635271763	4.98E-08	Ortholog of C. dubliniensis CD36 : Cd36_18730
C4_01710C_A		orf19.4623	-2.635911955	1.73E-43	Protein of unknown function
C5_00200C_A	BDF1	orf19.978	-2.638097874	5.66E-46	Essential chromatin-binding bromodomain protein
C6_02530C_A		orf19.5522	-2.638213112	1.74E-32	Ortholog of C. dubliniensis CD36 : Cd36_62760
C4_02910W_A		orf19.2704	-2.640506694	1.14E-01	Ortholog of Candida albicans WO-1 : CAWG_03507

C7_00900W_A		orf19.7024	-2.640506694	1.14E-01	Ortholog of *Candida albicans* WO-1 : CAWG_05448
C1_06550W_A	GLT1	orf19.6257	-2.64143194	4.86E-42	Putative glutamate synthase
C2_09970C_A		orf19.1355	-2.644621491	2.87E-46	Putative protein of unknown function
C1_07680W_A	HAP2	orf19.1228	-2.645839148	7.58E-37	CCAAT-binding transcription factor
C2_09710C_A		orf19.1381	-2.646022739	5.54E-37	Ortholog of S. cerevisiae/S. pombe Lsb5
C6_00800C_A		orf19.3644	-2.649806919	1.66E-42	Protein of unknown function
C3_02540C_A	OXR1	orf19.243	-2.650118972	4.76E-39	Ortholog(s) have role in cellular response to oxidative stress and mitochondrion localization
C4_03460C_A		orf19.3373	-2.654866427	2.18E-18	Putative protein of unknown function
C6_01400W_A		orf19.3444	-2.655631346	5.86E-21	Predicted membrane transporter, member of the drug:proton antiporter
CR_06930W_A		orf19.178	-2.661127894	8.18E-36	Ortholog of C. dubliniensis CD36 : Cd36_32460
C2_00510W_A		orf19.2076	-2.662152932	2.57E-30	Protein of unknown function
C4_07230C_A	VID21	orf19.3077	-2.674048336	8.38E-39	Subunit of the NuA4 histone acetyltransferase complex
CR_04850C_A		orf19.6308	-2.678402826	7.25E-34	Ortholog of *Candida albicans* WO-1 : CAWG_01818
C3_01420C_A		orf19.1709	-2.678415963	2.90E-34	Sterol carrier domain protein
C4_01720C_A		orf19.4622	-2.679465581	2.87E-48	Ortholog(s) have role in cellular response to DNA damage stimulus
CR_08160W_A	PTC5	orf19.6376	-2.679895743	4.35E-42	Mitochondrial protein phosphatase of the Type 2C-related
C2_09960W_A		orf19.1356	-2.679986659	2.48E-25	Ortholog(s) have thiosulfate sulfurtransferase activity and role in tRNA wobble position uridine thiolation
CR_10350C_A	TRX1	orf19.7611	-2.681128168	9.89E-44	Thioredoxin
C4_03330W_A	IPK1	orf19.1439	-2.684029721	1.33E-45	Ortholog of S. cerevisiae/S. pombe Ipk1
C7_02390W_A	AHP2	orf19.6470	-2.686686901	1.14E-45	Putative thiol-specific peroxiredoxin
C4_01340W_A		orf19.4653	-2.693327401	2.94E-02	Protein similar to GPI-linked cell-wall proteins
C5_01870W_A		orf19.3185	-2.693479482	5.58E-47	Ortholog(s) have acetyltransferase activator activity
C4_03890W_A	PTP2	orf19.5045	-2.695359611	3.37E-35	Predicted protein tyrosine phosphatase
CR_00780C_A	GSY1	orf19.3278	-2.6967569	3.23E-49	Glycogen synthase (UDP glucose/starch glucosyltransferase)
C4_00080C_A		orf19.376	-2.702459008	7.21E-30	Protein of unknown function
C2_00780W_A	POT1-2	orf19.2046	-2.703969223	3.00E-40	Putative peroxisomal 3-ketoacyl CoA thiolase
C1_08540C_A		orf19.399	-2.712061338	1.19E-49	Putative serine/threonine protein kinase
C1_13400C_A	AGC1	orf19.4966	-2.714748494	3.14E-36	Putative mitochondrial carrier protein
C6_00910C_A		orf19.92	-2.717603344	9.06E-50	Protein with a predicted thioredoxin-like domain
C6_04220C_A	HBR2	orf19.1078	-2.722203961	1.25E-43	Putative alanine glyoxylate aminotransferase
CR_02100C_A		orf19.2610	-2.731253562	2.90E-36	Putative tRNA binding protein
CR_01680C_A	CDC4	orf19.2559	-2.736527404	4.36E-50	F-box subunit of SCF(CDC4) ubiquitin ligase
C1_04330W_A	RPN4	orf19.1069	-2.738804488	1.78E-44	C2H2 transcription factor
C6_02800W_A		orf19.5553	-2.742413967	4.05E-33	Ortholog(s) have methionine-R-sulfoxide reductase activity and role in cellular response to oxidative stress
C1_01840C_A		orf19.4539	-2.744445163	2.78E-36	Protein with a Rho GDP-dissociation inhibitor domain
C1_02890C_A		orf19.2978	-2.745210579	1.15E-33	Protein of unknown function
C2_00130W_A		orf19.1906	-2.749502682	1.59E-04	Protein of unknown function
C3_02920W_A		orf19.285	-2.749907638	6.41E-49	Ortholog of S. cerevisiae Igo2
CR_02260C_A		orf19.3743	-2.751927015	2.17E-31	Ortholog of C. dubliniensis CD36 : Cd36_27230

C2_03320W_A	CHK1	orf19.896	-2.756123757	1.05E-34	Histidine kinase
C2_10600W_A		orf19.5339	-2.758937147	3.34E-43	Ortholog of S. cerevisiae Spg5
C6_01720C_A	SUR7	orf19.3414	-2.759556108	2.56E-42	Protein required for normal cell wall
C5_04560C_A	CUP1	orf19.3940.1	-2.759713489	3.80E-38	Metallothionein
C3_07360W_A	DLD2	orf19.6755	-2.767414184	1.39E-13	Ortholog(s) have D-lactate dehydrogenase (cytochrome) activity
C3_07080W_A	RRD1	orf19.6792	-2.768435028	1.48E-36	Putative peptidyl-prolyl cis/trans-isomerase
C1_14180W_A		orf19.7225	-2.77089887	4.48E-38	Ortholog of C. dubliniensis CD36 : Cd36_13150
C1_07070C_A	DHH1	orf19.6197	-2.777630898	8.77E-29	Putative RNA helicase
C5_03880C_A		orf19.1106	-2.77871148	1.94E-07	Protein with Mob2p-dependent hyphal regulation
C2_09240C_A		orf19.4085	-2.780034527	4.99E-30	Protein of unknown function
C3_01090W_A		orf19.2511.2	-2.780041176	7.91E-25	Ortholog of C. parapsilosis CDC317 : CPAR2_103040
C2_09870W_A		orf19.1364	-2.78018962	2.00E-41	Ortholog of S. pombe Stm1 G-protein coupled receptor
CR_08300C_A		orf19.6396	-2.785038536	1.79E-52	Putative patatin-like phospholipase
C2_00740C_A		orf19.2050	-2.785645689	1.39E-50	Ortholog(s) have sterol esterase activity
C4_01890C_A	ARL1	orf19.4603	-2.790453298	1.92E-45	Putative GTPase in the late Golgi involved in regulation of polarized growth and secretion
C1_02320C_A		orf19.3689	-2.795298636	9.03E-47	Putative protein similar to 6-phosphofructo-2-kinase/fructose-2,6-bisphosphatase
C4_04550C_A	OMA1	orf19.3827	-2.79539313	9.77E-39	Putative metalloendopeptidase of mitochondrial inner membrane
C1_08620W_A	CTR2	orf19.4720	-2.797141534	2.16E-36	Putative low-affinity copper transporter of the vacuolar membrane
C2_04170C_A		orf19.804.1	-2.802885391	9.16E-52	Ortholog of S. cerevisiae : YPR010C-A
CR_08310C_A		orf19.6398	-2.804291886	3.57E-08	S. pombe ortholog SPBC460.04c
CR_06780W_A		orf19.1856	-2.805411198	5.09E-48	Ortholog(s) have histone deacetylase activity
CR_06980W_A		orf19.2367	-2.805917774	2.63E-39	Putative protein of unknown function
C7_01070C_A		orf19.7006	-2.810846996	2.45E-50	Ortholog(s) have role in reciprocal meiotic recombination
C2_06430C_A		orf19.21	-2.815607083	4.00E-33	Ortholog(s) have role in ethanol metabolic process and mitochondrial inner membrane localization
C2_04030C_A	ACP12	orf19.819	-2.815627527	1.92E-48	Putative mitochondrial acyl carrier protein
C5_03980W_A		orf19.3213	-2.818590751	1.46E-42	Protein of unknown function
C1_09870W_A	HCM1	orf19.4853	-2.822076487	4.61E-37	Protein with forkhead domain
C4_00150C_A	PEX5	orf19.5640	-2.829898314	4.77E-52	Pex5p family protein
C1_03820W_A	PDR16	orf19.1027	-2.832526879	1.99E-48	Phosphatidylinositol transfer protein
C5_04550W_A		orf19.3939	-2.843242019	3.78E-42	Ortholog(s) have ER membrane protein complex localization
C4_05150W_A	VAC8	orf19.745	-2.845981728	5.30E-55	Protein involved in vacuolar inheritance
CR_02560C_A	ASG1	orf19.166	-2.85058123	2.86E-51	Gal4p family zinc-finger transcription factor with similarity to S. cerevisiae Asg1p
C3_05900W_A		orf19.7370	-2.852394478	2.02E-47	Possible G-protein coupled receptor
C1_01140C_A		orf19.3302	-2.854459647	3.43E-50	Putative type-1 protein phosphatase targeting subunit
CR_05170C_A	FDH1	orf19.638	-2.855049416	1.13E-36	Formate dehydrogenase
C4_01170C_A	BMT9	orf19.4673	-2.858256941	2.13E-19	Beta-mannosyltransferase
C3_00020W_A		orf19.5475	-2.86645426	4.79E-02	Sef1p-, Sfu1p-, and Hap43p-regulated gene
C7_02200W_A	WHI3	orf19.6494	-2.872063217	4.96E-49	Putative RNA binding protein
C2_05130W_A		orf19.3544	-2.87216217	2.33E-31	Putative protein of unknown function
CR_02510W_A		orf19.173	-2.877357182	2.37E-50	C2H2 transcription factor

CR_08040W_A		orf19.592	-2.880003733	1.14E-51	Ortholog of S. cerevisiae YNL092W and S. pombe SPBC1778.07
C3_04940W_A		orf19.5963	-2.88499877	6.04E-51	Putative prenyltransferase
C2_01110C_A	BCY1	orf19.2014	-2.886073041	1.02E-57	Protein kinase A regulatory subunit
C6_04140C_A		orf19.4553	-2.88804791	1.28E-44	Ortholog of C. dubliniensis CD36 : Cd36_64990
C1_06200W_A		orf19.2663	-2.888228245	9.74E-46	Ortholog of Pichia stipitis Pignal : PICST_29216 and Candida albicans WO-1 : CAWG_00788
C3_01710C_A	PPT1	orf19.1673	-2.89092703	2.20E-50	Putative serine/threonine phosphatase
C7_01130C_A		orf19.6897	-2.891890276	6.37E-02	Protein of unknown function
C3_06000W_A	AHR1	orf19.7381	-2.891915326	4.40E-37	Zn(II)2Cys6 transcription factor
C7_01060W_A		orf19.7007	-2.892860014	6.41E-02	Ortholog of C. dubliniensis CD36 : Cd36_70990 and Candida albicans WO-1 : CAWG_05464
C7_01500W_A		orf19.6579	-2.894524295	3.65E-41	Ortholog of C. dubliniensis CD36 : Cd36_71340
C2_03500W_A		orf19.871	-2.894853304	9.17E-55	Ortholog(s) have GTPase activator activity
C5_01620C_A	VPS22	orf19.6296	-2.896922528	5.54E-47	ESCRT-II complex protein with a role in multivesicular body (MVB) trafficking
C7_00380W_A		orf19.7082	-2.901249915	1.07E-40	S-adenosylmethionine transporter of the mitochondrial inner membrane
C5_03270W_A	TEF4	orf19.2652	-2.903249731	4.35E-06	Putative translation elongation factor
C2_08380C_A		orf19.1434	-2.903928978	2.26E-45	Ortholog(s) have DNA polymerase binding
C4_06760W_A	GUT2	orf19.3133	-2.906178202	2.03E-35	Glycerol-3-phosphate dehydrogenase
C2_05250C_A	AAT1	orf19.3554	-2.906194497	4.16E-41	Aspartate aminotransferase
C1_08170C_A	BUL1	orf19.5094	-2.906471111	1.64E-46	Protein similar but not orthologous to S. cerevisiae Bul1
C1_05910W_A	SIP5	orf19.2458	-2.906700873	7.27E-55	Protein of unknown function
C2_03310C_A	VPS20	orf19.897	-2.908015666	5.22E-39	ESCRT III complex protein
CR_10480W_A	PGA1	orf19.7625	-2.916773593	1.67E-43	Putative GPI-anchored protein
C3_06900W_A	ISA2	orf19.6811	-2.918167033	2.99E-46	Protein required for maturation of mitochondrial proteins
CR_08440W_A		orf19.6413	-2.923333749	5.48E-37	Protein of unknown function
C6_04180W_A		orf19.73	-2.925594337	5.42E-56	Putative metalloprotease
C4_01230C_A		orf19.4666	-2.927536722	1.44E-35	Protein of unknown function
C5_01490C_A		orf19.4144	-2.927635443	7.15E-46	Predicted protein kinase
C3_00210C_A		orf19.5449	-2.92848252	1.56E-17	Predicted integral membrane protein
CR_05920C_A	MHP1	orf19.6621	-2.928881209	3.27E-56	Protein similar to S. cerevisiae Mhp1p
C6_02300C_A		orf19.3471	-2.931279529	1.41E-16	Protein with a predicted anaphase-promoting complex APC subunit 1 CDC26 domain
C5_03060C_A	TNA1	orf19.4335	-2.952541051	9.81E-15	Putative nicotinic acid transporter
C5_01850C_A	ZNC1	orf19.3187	-2.959543571	1.47E-57	Zn(2)-Cys(6) transcription factor
C2_06930C_A		orf19.2247	-2.960271105	2.55E-18	Ortholog of C. dubliniensis CD36 : Cd36_21220
C7_01430C_A		orf19.6586	-2.962994779	1.24E-30	Protein of unknown function
C3_03470W_A		orf19.345	-2.966632918	1.11E-39	Succinate semialdehyde dehydrogenase
C5_01830C_A	HAL9	orf19.3190	-2.969048898	2.00E-50	Putative Zn(II)2Cys6 transcription factor
C6_01590W_A		orf19.3428	-2.969411536	2.49E-55	Protein of unknown function
C4_02500C_A	ADR1	orf19.2752	-2.978803713	1.22E-43	C2H2 transcription factor
C4_02530W_A	ARG83	orf19.2748	-2.978828836	3.36E-41	GAL4-like Zn(II)2Cys6 transcription factor
C1_03560C_A	SUA71	orf19.3059	-2.980439632	2.62E-60	Transcription factor TFIIB
C5_02940C_A	MIG1	orf19.4318	-2.980440807	8.23E-38	C2H2 transcription factor

C1_08770W_A		orf19.4735	-2.981454004	2.92E-39	Ornithine cyclodeaminase family protein
C5_05120W_A	CCT3	orf19.4004	-2.983642576	2.38E-60	Putative cytosolic chaperonin Cct ring complex subunit
C7_00340C_A		orf19.7086	-2.987233283	1.38E-56	Ortholog(s) have nuclear import signal receptor activity
C4_06610C_A	SDH12	orf19.2871	-2.988804286	1.13E-58	Succinate dehydrogenase
C3_05610W_A	MNN14	orf19.6996	-2.999814093	7.49E-31	Predicted alpha-1,3-mannosyltransferase activity with a role in protein glycosylation
C1_06120C_A		orf19.2433	-3.002511256	5.40E-27	Has domain(s) with predicted flap-structured DNA binding activity and role in double-strand break repair via single-strand annealing
C2_04560W_A	KTR2	orf19.4494	-3.003445531	2.29E-42	Mannosyltransferase
CR_05450C_A		orf19.3516	-3.005334044	2.69E-32	Protein of unknown function
C1_03380W_A	TPS2	orf19.3038	-3.006433363	2.39E-57	Trehalose-6-phosphate (Tre6P) phosphatase
C1_08850C_A	AFG1	orf19.4743	-3.010881321	1.72E-35	Putative mitochondrial ATPase of the AAA family
C7_03890C_A		orf19.7193	-3.012192212	1.43E-61	Specificity factor required for ubiquitination
C1_05850W_A	POL32	orf19.2465	-3.012656476	7.22E-57	Putative subunit of DNA polymerase delta
C6_02500C_A	GCV1	orf19.5519	-3.016157913	1.89E-45	Putative T subunit of glycine decarboxylase
C1_10220C_A	TPK1	orf19.4892	-3.021264367	4.90E-40	cAMP-dependent protein kinase catalytic subunit
CR_02440W_A		orf19.3721	-3.023005189	1.02E-04	Protein of unknown function
C2_00720C_A	FGR15	orf19.2054	-3.026415445	1.41E-50	Putative transcription factor with zinc finger DNA-binding motif
C4_04660C_A		orf19.3815	-3.027219053	1.05E-59	Ortholog(s) have thiol-dependent ubiquitin-specific protease activity and role in protein deubiquitination
C5_02680W_A		orf19.4286	-3.030307731	1.13E-47	Protein of unknown function
C4_02300W_A	HOS3	orf19.2772	-3.031958183	2.39E-54	Histone deacetylase
C7_00660W_A	GAC1	orf19.7053	-3.037857545	7.25E-45	Putative regulatory subunit of ser/thr phosphoprotein phosphatase 1
CR_10280W_A		orf19.7603	-3.041586663	2.42E-55	Protein with a predicted role in cytochrome c oxidase assembly
C6_00810C_A		orf19.3643	-3.042071035	1.03E-22	Protein of unknown function
C3_07120W_A		orf19.6788	-3.042392647	8.51E-25	Protein with a predicted role in cotranslational protein targeting to membrane
C1_08790W_A	TPO3	orf19.4737	-3.046044063	6.29E-45	Putative polyamine transporter
C5_00690C_A	TFB3	orf19.567	-3.047651113	1.12E-48	Putative C3HC4 zinc finger transcription factor
C3_02030W_A		orf19.1643	-3.049696696	2.31E-57	Ortholog(s) have serine-type endopeptidase activity
C1_06980C_A		orf19.6209	-3.051238205	2.68E-51	Predicted membrane transporter
C3_06610W_A		orf19.7450	-3.052291027	5.09E-56	Ortholog(s) have myosin II tail binding
C1_14100W_A	YPT52	orf19.7216	-3.055725017	7.75E-57	Rab-family GTPase involved in vacuolar trafficking
C2_03930C_A	SNF6	orf19.831	-3.063975264	7.63E-58	Subunit of SWI/SNF chromatin remodeling complex
C2_00520W_A	DFG5	orf19.2075	-3.067390852	1.17E-61	N-linked mannoprotein of cell wall and membrane
CR_10290C_A		orf19.7604	-3.069124492	1.09E-60	Ortholog(s) have Rab guanyl-nucleotide exchange factor activity
C1_06540C_A		orf19.6259	-3.073499627	2.94E-46	Exosome non-catalytic core component
C5_05440C_A		orf19.4043	-3.074212134	1.85E-59	Protein with a predicted pleckstrin homology domain
C1_13620W_A	ROB1	orf19.4998	-3.074732923	1.51E-62	Zn(II)2Cys6 transcription factor
C2_00150W_A	LEU5	orf19.2117	-3.077423628	7.49E-47	Putative mitochondrial carrier protein
CR_00300W_A	CDA2	orf19.7503	-3.07847858	4.93E-30	Putative chitin deacetylase
C6_02590C_A	MOB1	orf19.5528	-3.078494045	4.36E-50	Putative mitotic exit network component
CR_07250C_A		orf19.6143	-3.085593522	4.91E-56	Predicted long-chain-alcohol oxidase

149

C1_13150W_A		orf19.4942	-3.085680167	2.59E-03	Ortholog of *Candida albicans* WO-1 : CAWG_00134
CR_06440C_A	BCR1	orf19.723	-3.086250785	3.11E-45	Transcription factor
C2_04660C_A	YAK1	orf19.147	-3.100494853	6.13E-55	Predicted serine-threonine protein kinase
C2_01270W_A	CHA1	orf19.1996	-3.10078589	4.08E-46	Similar to catabolic ser/thr dehydratases
C2_10100W_A	CWC22	orf19.1771	-3.105250391	6.74E-58	Predicted spliceosome-associated protein
C6_01870C_A		orf19.3395	-3.106938297	3.65E-53	Predicted MFS membrane transporter, member of the drug:proton antiporter family
C2_02390W_A		orf19.1562	-3.108011476	6.09E-59	Protein of unknown function
CR_07920W_A		orf19.606	-3.108406072	1.01E-61	Protein of unknown function
C5_05390C_A	PGA4	orf19.4035	-3.11294627	1.73E-61	GPI-anchored cell surface protein
CR_09960C_A	UGA3	orf19.7570	-3.123810022	3.90E-50	Zn(II)2Cys6 transcription factor
C2_01700C_A	HAP42	orf19.1481	-3.128430413	2.62E-56	Predicted transcription factor
C2_01180W_A	COX17	orf19.2006.1	-3.129451639	4.94E-62	Putative copper metallochaperone
C4_06580W_A	CBF1	orf19.2876	-3.131816387	2.28E-63	Transcription factor
C3_00940W_A		orf19.2498	-3.137610001	5.27E-63	Predicted ubiquitin-protein ligase
CR_09410W_A		orf19.7337	-3.138788457	3.27E-52	Protein with a nischarin related domain and leucine rich repeats
C2_00600C_A		orf19.2067	-3.145313614	1.03E-59	Protein with a predicted role in mitochondrial iron metabolism
C1_07970C_A	IRE1	orf19.5068	-3.150090713	3.37E-65	Putative protein kinase
CR_00330C_A	PXA1	orf19.7500	-3.151146804	1.13E-52	Putative peroxisomal, half-size adrenoleukodystrophy protein (ALD or ALDp) subfamily ABC family transporter
CR_08870W_A	PEX13	orf19.7282	-3.159962219	4.81E-51	Protein required for peroxisomal protein import mediated by PTS1 and PTS2 targeting sequences
C2_02570W_A		orf19.1582	-3.16280953	5.34E-36	Predicted membrane transporter
C3_04730C_A		orf19.5933	-3.164374464	1.00E-11	Protein of unknown function
C1_01620C_A		orf19.3352	-3.165485995	1.46E-35	Has domain(s) with predicted oxidoreductase activity and role in metabolic process
C1_04810W_A	TCO89	orf19.761	-3.168981391	3.64E-60	Putative homolog of S. cerevisiae Tco89p
C1_14200W_A		orf19.7228	-3.170715107	4.30E-57	Possible Golgi membrane protein
C3_07070C_A		orf19.6793	-3.176036758	4.13E-53	Protein of unknown function
C1_04360C_A		orf19.5201.1	-3.179654256	5.55E-63	Has domain(s) with predicted ATPase inhibitor activity
C3_03700C_A		orf19.6949	-3.190804088	1.77E-02	Ortholog of *Candida albicans* WO-1 : CAWG_02687
C3_04870W_A		orf19.5954	-3.193526295	5.19E-02	Ortholog(s) have ubiquitin ligase activator activity
CR_06140W_A		orf19.3869	-3.194196759	1.16E-44	Protein of unknown function
C4_03280W_A	MSN5	orf19.2665	-3.195839925	3.26E-70	Predicted karyopherin involved in nuclear import and export of proteins
CR_09620C_A		orf19.6600	-3.199285839	9.04E-62	Ortholog(s) have phosphatidic acid transfer activity and role in cardiolipin metabolic process
C1_14150C_A	PAM16	orf19.7222	-3.203164779	4.29E-56	Putative maltase
C1_01630W_A		orf19.3353	-3.204743308	3.06E-49	Protein similar to a mitochondrial complex I intermediate-associated protein
C2_08340C_A		orf19.1349	-3.206609761	2.31E-12	Ortholog of C. dubliniensis CD36 : Cd36_22470
C3_04920C_A		orf19.5961	-3.21651534	2.20E-61	Ortholog(s) have proteasome regulatory particle binding activity
C1_10090C_A		orf19.4878	-3.217857362	1.54E-66	Protein of unknown function
C6_02340W_A	HRR25	orf19.3476	-3.219230695	3.90E-71	Predicted protein serine/threonine kinase
C1_02440C_A		orf19.2933	-3.226738958	6.65E-60	Ortholog(s) have thiol-dependent ubiquitin-specific protease activity and role in protein deubiquitination

C3_04530C_A	TEC1	orf19.5908	-3.23101161	6.07E-60	TEA/ATTS transcription factor
C4_01910W_A		orf19.4601	-3.236100516	2.50E-53	Putative RNA polymerase III transcription initiation factor complex (TFIIIC) subunit
C6_03240W_A		orf19.5611	-3.24125922	2.19E-33	Predicted 3-methylbutanol:NAD(P) oxidoreductase and methylglyoxal reductase (NADPH-dependent)
C3_06790W_A	TRY6	orf19.6824	-3.243206851	8.31E-33	Helix-loop-helix transcription factor
C7_01860W_A		orf19.6534	-3.243694695	2.97E-09	Ortholog of *Candida albicans* WO-1 : CAWG_05537
C1_05510C_A	RPS27A	orf19.413.1	-3.2599268	3.69E-69	Ribosomal protein S27
C2_08830W_A		orf19.3586	-3.263801767	2.87E-63	Ortholog(s) have role in chitin localization
C7_01440W_A		orf19.6585	-3.264693724	2.99E-46	Ortholog(s) have role in protein maturation by [4Fe-4S] cluster transfer and mitochondrial matrix localization
C1_10160W_A	MIR1	orf19.4885	-3.266729319	7.40E-58	Putative mitochondrial phosphate transporter
CR_01390W_A	MGE1	orf19.2524	-3.266783801	3.64E-68	Putative mitochondrial matrix cochaperone
C6_01740C_A	ATG15	orf19.3412	-3.269194416	4.03E-66	Putative lipase
C1_07360W_A		orf19.4435	-3.269498099	2.77E-69	Ortholog(s) have beta-tubulin binding
C2_03520C_A	ADAEC	orf19.868	-3.278719587	4.51E-62	Protein of unknown function
C3_03480C_A	ALT1	orf19.346	-3.292844694	1.30E-58	Putative alanine transaminase
C1_08070W_A	CDR4	orf19.5079	-3.29326279	7.23E-76	Putative ABC transporter superfamily
C3_07830W_A	FBP1	orf19.6178	-3.295677566	1.01E-65	Fructose-1,6-bisphosphatase
CR_04610C_A		orf19.552	-3.295995117	2.12E-21	Ortholog of a S. cerevisiae Atg22
CR_06000W_A	SOK1	orf19.451	-3.297484758	3.82E-51	Protein kinase required for degradation of Nrg1p
C5_03240W_A	BUB3	orf19.2655	-3.299150462	1.28E-68	Protein similar to S. cerevisiae Bub3
C2_00250W_A	STF2	orf19.2107.1	-3.302494984	3.85E-68	Protein involved in ATP biosynthesis
C1_01710W_A		orf19.3360	-3.305571805	2.10E-68	Protein of unknown function
C4_05120C_A		orf19.741	-3.305793703	4.11E-09	Dubious open reading frame
C2_08390W_A		orf19.1433	-3.308625644	3.66E-59	Protein of unknown function
C1_01130W_A		orf19.3301	-3.310397685	4.79E-46	Putative ubiquitin ligase complex component
C1_05200C_A		orf19.446	-3.315558569	4.21E-64	Protein of unknown function
C1_13630W_A	CYB2	orf19.5000	-3.320535133	4.26E-41	Putative cytochrome b2 precursor
C3_02800W_A	ADH4	orf19.271	-3.322237082	2.61E-02	Predicted 3-hydroxyacyl-CoA dehydrogenase
C5_01790C_A		orf19.3196	-3.325853183	3.50E-04	Ortholog of *Candida albicans* WO-1 : CAWG_04564
C4_03080W_A		orf19.2684	-3.333667459	7.84E-69	Protein of unknown function
C4_01200C_A	AAT22	orf19.4669	-3.338170244	2.60E-36	Aspartate aminotransferase
CR_06460W_A	GST3	orf19.720	-3.341495215	5.19E-23	Glutathione S-transferase
C4_05170C_A	NBP35	orf19.747	-3.343071237	1.67E-65	Similar to nucleotide-binding proteins
C2_04970W_A	ABP2	orf19.3529	-3.346355513	2.53E-19	Putative alpha-actinin-like protein
CR_08030C_A	FGR32	orf19.593	-3.352637249	5.43E-75	Protein similar to S. cerevisiae Swa2p
C7_01780W_A	LPI9	orf19.6544	-3.355174882	1.01E-71	Protein phosphatase type 1 regulator
C3_07790W_A	STD1	orf19.6173	-3.359171156	1.44E-66	Putative transcription factor
C1_09850C_A		orf19.4850	-3.367167479	4.54E-66	Ortholog of S. cerevisiae : CUB1
C1_09780C_A		orf19.4843	-3.371198216	1.14E-57	Putative iron/copper reductas
C7_03020C_A	DUG3	orf19.5159	-3.377889026	3.38E-72	Putative glutamine amidotransferase (GATase II)
CR_00630W_A	VHR1	orf19.7468	-3.378064051	1.61E-72	Transcriptional activator of genes involved in biotin metabolism
C2_09350W_A	TAZ1	orf19.4096	-3.38094605	6.32E-53	Putative lyso-phosphatidylcholine acyltransferase

CR_05730C_A		orf19.6639	-3.388094474	1.11E-65	Ortholog of S. cerevisiae Mdm36
C2_05950C_A	TES15	orf19.5215	-3.393604261	1.35E-40	Putative acyl-CoA thioesterase
C1_11950W_A		orf19.5270	-3.395124839	1.16E-12	Protein of unknown function
C1_11350C_A	TOS4	orf19.668	-3.403011705	2.82E-55	Putative fork-head transcription factor
C1_02690C_A		orf19.2959	-3.403434265	3.63E-02	Predicted ORF from Assembly 19
C1_05800C_A		orf19.2472	-3.411542402	6.92E-63	Ortholog of S. pombe replication termination factor Rtf2
C5_03500W_A	GAP6	orf19.6659	-3.414255681	5.01E-59	Broad-specificity amino acid permease
C4_05900C_A		orf19.1277	-3.424893095	3.64E-75	Protein of unknown function
C1_04950C_A	RPM2	orf19.48	-3.428142081	5.90E-75	Mitochondrial RNase P subunit
C1_03320C_A	EHD3	orf19.3029	-3.429256423	2.06E-51	Predicted 3-hydroxyisobutyryl-CoA hydrolase
CR_02810W_A	CIRT4B	orf19.2839	-3.432165956	3.13E-76	Cirt family transposase
C3_00730W_A		orf19.5381	-3.432708079	9.69E-69	Ortholog(s) have mRNA binding activity
C1_13670W_A	OSM2	orf19.5005	-3.433714258	2.60E-43	Putative mitochondrial fumarate reductase
CR_02800C_A		orf19.2838	-3.435020842	2.11E-65	Protein of unknown function
C3_00860W_A	CSE4	orf19.6163	-3.440461715	9.25E-43	Centromeric histone H3 variant
CR_02750C_A	PGA34	orf19.2833	-3.459728813	6.59E-13	Putative GPI-anchored protein
C7_02000C_A		orf19.6520	-3.471221568	2.13E-06	Putative allantoate permease
C6_00290W_A		orf19.1189	-3.473541727	5.45E-52	Protein of unknown function
C2_07370W_A		orf19.1897	-3.473954104	9.45E-73	Ortholog of C. dubliniensis CD36 : Cd36_21640
C2_03980C_A	MED1	orf19.826	-3.482886497	1.91E-60	RNA polymerase II mediator complex subunit
C3_01320C_A	SGA1	orf19.1719	-3.48751932	4.27E-66	Putative glucoamylase
C4_01350W_A		orf19.4652	-3.510400701	9.68E-03	Protein of unknown function
C2_04810W_A	HIS3	orf19.183	-3.510629382	6.55E-40	Imidazoleglycerol-phosphate dehydratase
C4_01220C_A		orf19.4668	-3.511127311	9.68E-40	Protein with a glycoside hydrolase domain
C5_05430W_A	PEX4	orf19.4041	-3.512586945	7.29E-63	Putative peroxisomal ubiquitin conjugating enzyme
C4_02520C_A		orf19.2749	-3.521081529	7.79E-68	BTB/POZ domain protein
CR_09780C_A	IFA14	orf19.7550	-3.526537669	2.01E-53	Putative LPF family protein
C2_05690C_A	YTH1	orf19.6881	-3.528507022	1.84E-77	Putative mRNA cleavage and polyadenylation specificity factor
C3_04240C_A		orf19.5866	-3.53113854	5.18E-04	Ortholog of Candida albicans WO-1 : CAWG_02737
C4_02920W_A		orf19.2703	-3.539942158	1.20E-75	Specificity factor required for ubiquitination and sorting of specific cargo proteins at the multivesicular body
CR_08890C_A	ASR2	orf19.7284	-3.542855912	2.45E-56	Adenylyl cyclase and stress responsive protein
C4_07140W_A		orf19.3089	-3.556850431	2.30E-68	Predicted mitochondrial intermembrane space protein
CR_06090W_A		orf19.3862	-3.557026701	2.45E-84	Putative intracellular transport protein
C1_12080W_A	LCB4	orf19.5257	-3.557883186	1.81E-75	Putative sphingosine kinase
C2_05960C_A		orf19.5216	-3.558506004	1.89E-06	Ortholog of C. dubliniensis CD36 : Cd36_20380
CR_07400C_A	LPD1	orf19.6127	-3.559517472	4.21E-62	Putative dihydrolipoamide dehydrogenase
C2_09750W_A	LEU42	orf19.1375	-3.561428656	2.17E-78	Putative alpha-isopropylmalate synthase
CR_09790W_A	ALO1	orf19.7551	-3.579616111	5.83E-81	D-Arabinono-1,4-lactone oxidase involved in biosynthesis of dehydro-D-arabinono-1,4-lactone
C7_03340C_A	PRR2	orf19.1341	-3.580162719	3.20E-47	Putative serine/threonine protein kinase
C6_00280W_A	CPH2	orf19.1187	-3.585775675	6.73E-85	Myc-bHLH transcription factor
C3_03990C_A	AAP1	orf19.2810	-3.586133164	8.15E-60	Putative amino acid permease

C1_06970C_A		orf19.6211	-3.596301869	6.89E-74	Protein of unknown function
C7_00390W_A	SPL1	orf19.7081	-3.610058513	8.17E-90	Protein similar to S. cerevisiae Spl1p
CR_03120W_A		orf19.2414	-3.610833859	8.03E-87	Ortholog of S. cerevisiae Mpm1
C2_10210C_A	RAS1	orf19.1760	-3.619273275	3.91E-87	RAS signal transduction GTPase
C1_04480C_A	TUS1	orf19.6842	-3.628462376	1.29E-86	Putative guanine nucleotide exchange factor
C5_01400W_A	SEF2	orf19.1926	-3.631032303	8.63E-76	Zn(II)2Cys6 transcription factor
C1_13880C_A		orf19.5026	-3.633862209	9.55E-74	C2H2 transcription factor
C3_04080W_A		orf19.913.2	-3.63452372	9.45E-72	Ortholog of subunit 6 of the ubiquinol cytochrome-c reductase complex
C7_02010C_A		orf19.6518	-3.637399772	7.31E-46	Predicted aldehyde dehydrogenase [NAD(P)+]
C3_02630C_A		orf19.254	-3.647562896	1.67E-58	Protein of unknown function
CR_10660W_A	CKA1	orf19.7652	-3.648378584	7.54E-79	Putative alpha subunit (catalytic subunit) of protein kinase CK2
C1_10280C_A		orf19.4898	-3.651564892	2.17E-75	Putative protein of unknown function
C2_08120W_A	MAF1	orf19.2173	-3.651781818	1.14E-74	Putative negative regulator of RNA polymerase III
C4_06890W_A	ARR3	orf19.3122	-3.658816137	2.74E-79	Ortholog of S. cerevisiae Arr3
C1_02140C_A		orf19.3671	-3.661504185	2.17E-03	Dubious open reading frame
C2_09890W_A	SMM1	orf19.1362	-3.670014435	1.44E-75	Putative dihydrouridine synthase
C1_08610C_A		orf19.409	-3.673887328	9.07E-64	Ortholog of S. cerevisiae Aim38/Rcf2, cytochrome c oxidase subunit
C3_03570C_A		orf19.355	-3.674189747	2.89E-12	Has domain(s) with predicted oxidoreductase activity and role in oxidation-reduction process
C1_00880W_A		orf19.6017	-3.675357632	1.65E-42	Protein of unknown function
C2_08050C_A	SIT1	orf19.2179	-3.680690337	1.06E-60	Transporter of ferrichrome siderophores, not ferrioxamine B
C1_08400C_A	GCV2	orf19.385	-3.689221467	1.27E-84	Glycine decarboxylase P subunit
C3_05450C_A		orf19.6983	-3.693929207	1.32E-73	Protein of unknown function
C2_08950W_A		orf19.211	-3.695192608	1.83E-72	Predicted homeodomain-like transcription factor
C5_01360W_A	CFL4	orf19.1932	-3.695696992	2.13E-06	C-terminus similar to ferric reductases
C4_01070W_A	HGT17	orf19.4682	-3.700064066	6.40E-11	Putative MFS family glucose transporter
C5_00880C_A	GIT3	orf19.1979	-3.708110533	2.28E-82	Glycerophosphocholine permease
CR_09530C_A		orf19.6608	-3.709494665	5.39E-93	Predicted DDE superfamily endonuclease domain
C2_00770W_A		orf19.2047	-3.712588604	3.18E-79	Putative protein of unknown function
C1_10060C_A		orf19.4873	-3.725245836	4.65E-65	Protein of unknown function
CR_09210W_A	SUC1	orf19.7319	-3.725988328	2.41E-80	Zinc-finger transcription factor
C5_04830W_A	SFL2	orf19.3969	-3.728647947	1.03E-53	Transcription factor involved in regulation of morphogenesis
C1_02040C_A		orf19.3661	-3.745515264	7.54E-76	Putative deubiquitinating enzyme
C1_13350W_A	STP2	orf19.4961	-3.747904311	2.37E-92	Amino-acid-regulated transcription factor
C1_06350W_A		orf19.6276	-3.757291719	3.95E-68	Protein of unknown function
C4_02540W_A	RGT1	orf19.2747	-3.76083781	2.71E-79	Zn(II)2Cys6 transcription factor
C5_02380W_A		orf19.4246	-3.761605946	1.62E-86	Protein with similarity to S. cerevisiae Ykr070w
CR_08290W_A		orf19.6393	-3.763817468	6.27E-74	Putative Arf3p GTPase activating protein
C6_00980C_A		orf19.100	-3.764178654	2.15E-81	Alpha/beta hydrolase and lipase domain protein
C4_06910W_A		orf19.3120	-3.765314059	9.65E-13	PDR-subfamily ABC transporter (half-size)
C6_02020C_A		orf19.692	-3.767675843	1.47E-79	Protein of unknown function
C4_02770C_A		orf19.2721	-3.767818925	2.56E-86	Ortholog(s) have ATP binding
CR_06510W_A		orf19.715	-3.777477838	8.81E-74	Protein of unknown function

153

CR_00550W_A		orf19.7480	-3.787258967	2.31E-04	Putative protein of unknown function
CR_02490W_A	OPT4	orf19.176	-3.787317196	1.34E-65	Oligopeptide transporter
C6_03930W_A	OPT8	orf19.5770	-3.78854887	1.24E-84	Oligopeptide transporter
C7_03280C_A		orf19.5125	-3.789435846	1.86E-81	Protein of unknown function
C5_02000C_A	ACH1	orf19.3171	-3.791432249	2.47E-77	Acetyl-coA hydrolase
C1_01780C_A	HOL4	orf19.4546	-3.803037502	1.58E-80	Putative ion transporter
C1_07220W_A		orf19.4445	-3.804154718	1.67E-57	Protein of unknown function
CR_03730C_A		orf19.4372	-3.804453021	6.99E-90	Predicted transmembrane transporter
C1_09150W_A	AOX2	orf19.4773	-3.827627106	2.65E-07	Alternative oxidase
C1_07980C_A		orf19.5069	-3.831294466	4.84E-57	Ortholog of S. cerevisiae Sae3
CR_03280W_A	IFR2	orf19.2396	-3.845188723	6.25E-100	Zinc-binding dehydrogenase
C1_11690W_A		orf19.1150	-3.851354329	3.75E-76	GATA-like transcription factor
C3_02610C_A	GLX3	orf19.251	-3.851498063	1.04E-103	Glutathione-independent glyoxalase
C6_00840W_A	GPX2	orf19.85	-3.855399013	5.65E-94	Similar to glutathione peroxidase
C2_06440C_A		orf19.22	-3.85924048	7.13E-84	Protein with homology to peroxisomal membrane proteins
C1_02980W_A	GOR1	orf19.2989	-3.864536686	3.59E-93	Ortholog(s) have glyoxylate reductase activity
C3_07180C_A	BMT1	orf19.6782	-3.864699524	3.84E-80	Beta-mannosyltransferase
C1_09700W_A		orf19.4834	-3.870100676	8.60E-08	Ortholog of C. dubliniensis CD36 : Cd36_09140
C1_09420W_A	LIP2	orf19.4804	-3.870789416	3.39E-06	Secreted lipase
C1_06140C_A		orf19.2431	-3.873042196	1.77E-13	Dubious open reading frame, only conserved in Candida dubliniensis
C1_06110C_A	NPL4	orf19.2434	-3.877553231	2.99E-98	Putative ubiquitin-binding protein
C5_01990W_A		orf19.3172	-3.893485032	1.07E-09	Ortholog of C. dubliniensis CD36 : Cd36_51840
C1_11670W_A		orf19.1152	-3.896576276	2.60E-104	Protein of unknown function
C6_03770C_A	ORM1	orf19.5751	-3.901619919	1.83E-98	Putative endoplasmic reticulum membrane protein
C7_01960W_A		orf19.6525	-3.903721377	1.16E-83	S. cerevisiae ortholog Inp1 is a peripheral membrane protein of peroxisomes involved in peroxisomal inheritance
C6_00830C_A	CAN3	orf19.84	-3.903836979	1.06E-99	Predicted amino acid transmembrane transporter
C3_06620W_A	FUN31	orf19.7451	-3.916074753	2.45E-103	Putative PAS kinase involved in cell wall damage response
CR_00360C_A	LEU1	orf19.7498	-3.918148866	5.50E-79	3-isopropylmalate dehydratase
C2_01200C_A	REG1	orf19.2005	-3.918844455	4.25E-90	Putative protein phosphatase regulatory subunit
C1_02880C_A	MIA40	orf19.2977	-3.925946201	3.96E-81	Predicted component of the mitochondrial intermembrane space import machinery
C4_01990W_A		orf19.4593.1	-3.928110858	3.08E-26	Protein with a predicted role in mitochondrial respiratory chain complex II assembly
C3_07730W_A	WOR4	orf19.6713	-3.929791673	4.05E-70	Predicted C2H2 zinc finger protein, involved in transcriptional regulation of white-opaque phenotypic switching
C1_03990W_A		orf19.4474	-3.933049974	1.97E-84	Ortholog(s) have proteasome binding activity and role in cellular response to arsenic-containing substance
C6_00330C_A	GNP1	orf19.1193	-3.944911492	1.75E-73	Similar to asparagine and glutamine permease
C7_00290C_A	HGT13	orf19.7093	-3.956313185	2.01E-60	Predicted sugar transporter
C2_01750C_A		orf19.1486	-3.962683001	1.18E-86	Protein with a life-span regulatory factor domain
C1_12880C_A		orf19.4918	-3.964609906	4.50E-85	Has domain(s) with predicted DNA binding, nucleic acid binding activity
C2_08820C_A	SPO11	orf19.3589	-3.966596975	5.47E-17	DNA endonuclease
C5_04460C_A		orf19.3931.2	-3.973626845	4.15E-03	Protein of unknown function

C7_02220C_A		orf19.6492	-3.976593735	2.32E-87	Predicted protein serine/threonine kinase and/or protein tyrosine kinase
C2_01210C_A	HNM1	orf19.2003	-3.979630245	5.47E-96	Putative choline/ethanolamine transporter
C4_05130C_A	ALD6	orf19.742	-3.983329663	1.33E-74	Putative aldehyde dehydrogenase
C1_10180C_A	ECM21	orf19.4887	-3.991792215	2.97E-77	Predicted regulator of endcytosis of plasma membrane proteins
C3_00880W_A	KGD1	orf19.6165	-3.996349308	3.54E-98	Putative 2-oxoglutarate dehydrogenase
C2_00990W_A		orf19.2024	-4.011035056	1.58E-10	Ortholog of Candida albicans WO-1 : CAWG_03878
CR_06500C_A		orf19.716	-4.01164364	5.54E-70	Protein of unknown function
C1_13090W_A		orf19.4936	-4.013134183	2.12E-09	Dubious open reading frame
C1_01920W_A	ROA1	orf19.4531	-4.018339757	6.53E-104	Putative PDR-subfamily ABC transporter involved in sensitivity to azoles
C4_06620C_A		orf19.2870	-4.020025828	6.34E-71	Protein of unknown function
C2_03760C_A		orf19.846	-4.032367814	4.39E-105	Predicted protein kinase similar to S. cerevisiae Nnk1
C2_05380W_A		orf19.3569	-4.041742443	3.27E-96	Protein of unknown function
C3_04070C_A	CDR11	orf19.918	-4.053759158	5.99E-111	Putative transporter of PDR subfamily of ABC family
C1_13480W_A	HSP70	orf19.4980	-4.055609184	2.05E-03	Putative hsp70 chaperone
C2_10110W_A	CYC1	orf19.1770	-4.059712524	6.74E-102	Cytochrome c
C1_03270W_A		orf19.3021	-4.06127109	2.64E-101	Putative protein of unknown function
C1_01250W_A		orf19.3312	-4.081757771	1.36E-101	Protein of unknown function
C1_06090C_A		orf19.2436	-4.087843071	7.47E-108	Predicted protein serine/threonine kinase
C6_00990W_A	RIM9	orf19.101	-4.09050751	2.76E-100	Protein required for alkaline pH response via the Rim101 signaling pathway
C7_03030W_A		orf19.5158	-4.095810867	4.84E-105	Protein with similarity to a human gene associated with colon cancer and to orf19.5158
C2_08330W_A		orf19.1350	-4.10845665	1.58E-94	Protein with a thioredoxin domain
C3_01480C_A	RKI1	orf19.1701	-4.115217891	1.11E-59	Ortholog(s) have ribose-5-phosphate isomerase activity and role in pentose-phosphate shunt
C5_00510W_A		orf19.938	-4.129131236	1.44E-12	Ortholog of C. dubliniensis CD36 : Cd36_50520
CR_03860C_A		orf19.4357	-4.129830361	7.81E-106	Putative protein similar to S. cerevisiae Mgr3p
CR_08860W_A	PDK2	orf19.7281	-4.130651959	2.38E-93	Putative pyruvate dehydrogenase kinase
C5_03130W_A	SUT1	orf19.4342	-4.131905917	2.86E-81	Zn2Cys6 transcription factor involved in sterol uptake
C5_01810W_A	FCR3	orf19.3193	-4.135655575	5.65E-95	bZIP transcription factor
CR_05610C_A	SRR1	orf19.5843	-4.140271118	4.23E-80	Two-component system response regulator
C4_03160C_A		orf19.2674	-4.148184248	1.06E-61	Protein of unknown function
C1_09840C_A		orf19.4849	-4.1571369	1.56E-109	Protein required for localizing proteasomes to the nucleus
C3_05620W_A	ATO5	orf19.6997	-4.158181966	4.47E-08	Putative fungal-specific transmembrane protein
C1_10010C_A	SWE1	orf19.4867	-4.161968764	3.81E-108	Putative protein kinase with a role in control of growth and morphogenesis
C6_03810W_A		orf19.5755	-4.181116091	1.03E-85	Ortholog(s) have cyclin-dependent protein serine/threonine kinase regulator activity
C1_01970W_A		orf19.4528.1	-4.182320338	2.01E-03	Protein of unknown function
C6_02840C_A	RBF1	orf19.5558	-4.195964567	4.06E-96	Transcription factor
C2_03250W_A	AVT7	orf19.905	-4.205852709	8.43E-117	Ortholog of S. cerevisiae Avt7 transporter
C1_01240W_A	IFD3	orf19.3311	-4.206690315	8.54E-81	Putative aldo/keto reductase
CR_09180W_A	CDG1	orf19.7314	-4.213108297	4.94E-119	Putative cysteine dioxygenases
C1_05340C_A	ZCF2	orf19.431	-4.219284229	1.79E-118	Zn(II)2Cys6 transcription factor

155

C6_01500C_A	TRY5	orf19.3434	-4.219661786	1.59E-76	Zn(II)2Cys6 transcription factor
C1_11310C_A	PSP1	orf19.671	-4.223915227	4.69E-115	Protein repressed during the mating process
C2_01120W_A	KAR2	orf19.2013	-4.232246468	4.24E-121	Similar to Hsp70 family chaperones
C6_02510C_A	ASG7	orf19.5520	-4.278207906	5.52E-03	a-cell specific protein of unknown function
CR_08260C_A		orf19.6390	-4.278207906	5.52E-03	Protein of unknown function
C1_06810W_A	CAT1	orf19.6229	-4.278612637	6.94E-114	Catalase
C1_12850W_A	BLP1	orf19.4914.1	-4.284124355	2.19E-116	Protein of unknown function, serum-induced
C7_00770W_A		orf19.7042	-4.286821515	1.14E-99	Protein of unknown function
C2_09880C_A		orf19.1363	-4.302045319	2.40E-97	Putative protein of unknown function
C3_01930W_A	PXP2	orf19.1655	-4.303275443	1.93E-42	Putative acyl-CoA oxidase
C1_03740W_A	WAR1	orf19.1035	-4.306192701	1.00E-116	Zn(II)2Cys6 transcription factor
C6_00760W_A		orf19.3649	-4.317350989	4.19E-113	Ortholog(s) have adenyl-nucleotide exchange factor activity
C1_14190C_A		orf19.7227	-4.322014511	1.03E-112	Protein phosphatase inhibitor
C7_00360W_A	DFI1	orf19.7084	-4.324483381	1.75E-117	Cell-surface associated glycoprotein
C5_04420W_A		orf19.3929	-4.339920229	1.01E-109	Ortholog(s) have role in cellular response to heat
C6_00150W_A	ARD	orf19.6322	-4.342874273	1.82E-130	D-arabitol dehydrogenase, NAD-dependent
CR_06060W_A		orf19.3858	-4.348444291	1.28E-116	Protein of unknown function
C5_04960W_A		orf19.3984	-4.360040127	6.83E-112	Protein of unknown function
C1_06850W_A	PCL7	orf19.6225	-4.360130673	2.50E-100	Putative cyclin-like protein
C6_00610C_A		orf19.4196	-4.361230687	1.04E-03	Dubious open reading frame
CR_07420W_A	KGD2	orf19.6126	-4.362783864	1.67E-121	Putative dihydrolipoamide S-succinyltransferase
C7_00280W_A	HGT12	orf19.7094	-4.362929662	4.73E-03	Glucose, fructose, mannose transporter
C4_01900C_A	MDH1-1	orf19.4602	-4.364592409	8.60E-126	Predicted malate dehydrogenase precursor
C2_04280W_A		orf19.791	-4.368761954	5.23E-83	Ortholog(s) have protein serine/threonine kinase activity
C3_00230C_A		orf19.5446	-4.372718041	5.66E-06	Putative protein of unknown function
C1_07870C_A	SMI1	orf19.5058	-4.376029548	3.55E-126	Cell wall biosynthesis protein
C1_09170W_A	CTA8	orf19.4775	-4.377245402	4.60E-114	Essential transcription factor
CR_05180C_A	SDH2	orf19.637	-4.390078782	2.24E-119	Succinate dehydrogenase, Fe-S subunit
C2_07380W_A	SSC1	orf19.1896	-4.390683287	1.83E-135	Heat shock protein
C2_10170C_A		orf19.1764	-4.393646999	2.30E-127	Protein of unknown function
C1_10050W_A		orf19.4872	-4.401721368	7.63E-39	Protein of unknown function
C7_02500C_A	DPP3	orf19.6459	-4.413742469	2.10E-100	Protein similar to S. cerevisiae pyrophosphate phosphatase Dpp1
C1_14090W_A		orf19.7215.3	-4.417626385	1.03E-106	Ortholog(s) have chaperone binding
C2_09340W_A		orf19.4095	-4.421391853	7.87E-04	Ortholog of C. dubliniensis CD36 : Cd36_23460
C1_08350C_A		orf19.5114.1	-4.426023716	1.85E-113	Ortholog of C. dubliniensis CD36 : Cd36_02630
C2_04080W_A		orf19.813	-4.4338109	5.77E-113	Protein of unknown function
C4_06630C_A		orf19.2869	-4.446988883	3.50E-03	Ortholog of C. dubliniensis CD36 : Cd36_46110
C1_12910W_A		orf19.4921.1	-4.449410498	3.96E-67	Protein of unknown function
C1_13470W_A	KNS1	orf19.4979	-4.481167323	9.24E-127	Protein kinase involved in negative regulation of PolIII transcription
C1_10140C_A		orf19.4883	-4.485262815	1.19E-125	Protein of unknown function
CR_03500W_A	CIT1	orf19.4393	-4.486342184	1.53E-135	Citrate synthase
C3_03710W_A	CCC1	orf19.6948	-4.487656156	7.42E-110	Manganese transporter

C2_09010W_A	STB3	orf19.203	-4.490156441	3.29E-120	Putative SIN3-binding protein 3 homolog
CR_07810W_A	YHB5	orf19.3710	-4.504460179	2.48E-130	Flavohemoglobin-related protein
C1_00190C_A		orf19.6084	-4.535555775	7.24E-82	Protein of unknown function
C1_14350W_A		orf19.7250	-4.565260274	4.96E-124	Protein of unknown function
C6_01860C_A	HCH1	orf19.3396	-4.584985431	1.78E-140	Ortholog of S. cerevisiae Hch1, a regulator of heat shock protein Hsp90
C6_01730W_A	FGR37	orf19.3413	-4.589668961	2.35E-03	Protein lacking an ortholog in S. cerevisiae
C4_01100C_A	AGP2	orf19.4679	-4.60338887	2.34E-76	Amino acid permease
CR_06070W_A		orf19.3859	-4.621003716	3.41E-141	Putative microsomal beta-keto-reductase
C6_02780C_A	MIF2	orf19.5551	-4.621822871	9.50E-141	Centromere-associated protein
C3_05630W_A	GTT1	orf19.6998	-4.639517895	3.10E-04	Putative glutathione S-transferase
C6_00930C_A		orf19.94	-4.645312336	2.00E-125	Protein of unknown function
C1_11480W_A	PHO84	orf19.655	-4.656364631	1.08E-111	High-affinity phosphate transporter
CR_04870C_A		orf19.6306	-4.656872697	6.27E-89	Trimethylaminobutyraldehyde dehydrogenase
C6_00160W_A	PGA48	orf19.6321	-4.665248351	2.04E-94	Putative GPI-anchored adhesin-like protein
C6_03740W_A		orf19.5748	-4.666792772	2.43E-72	Ortholog of C. dubliniensis CD36 : Cd36_64250
C6_03790C_A	HGT10	orf19.5753	-4.66794569	2.67E-19	Glycerol permease involved in glycerol uptake
C2_00690W_A		orf19.2059	-4.684201881	1.04E-36	Protein with homology to magnesium-dependent endonucleases and phosphatases
C3_04930C_A	HGT4	orf19.5962	-4.685542775	3.18E-127	Glucose and galactose sensor
CR_09240C_A		orf19.7322	-4.692435204	3.70E-150	Protein of unknown function
C1_10190W_A		orf19.4888	-4.693094917	3.91E-135	Has domain(s) with predicted nucleic acid binding, nucleotide binding activity
C5_03150W_A		orf19.4347	-4.700323892	4.14E-120	Putative serine/threonine protein kinase
C2_09980W_A		orf19.1785	-4.706154834	4.30E-151	Protein with a PI31 proteasome regulator domain
CR_02650C_A	DRE2	orf19.2825	-4.714765976	2.91E-152	Putative cytosolic Fe-S protein assembly protein
C7_02280W_A		orf19.6484	-4.723350238	9.02E-07	Ortholog of C. parapsilosis CDC317 : CPAR2_808370
C2_10350C_A	ACS1	orf19.1743	-4.728757865	6.72E-139	Acetyl-CoA synthetase
C5_01250W_A	GPR1	orf19.1944	-4.730364334	8.96E-142	Plasma membrane G-protein-coupled receptor of the cAMP-PKA pathway
C2_03720W_A	PGA16	orf19.848	-4.74753593	1.85E-04	Putative GPI-anchored protein
CR_07270C_A	HGT16	orf19.6141	-4.750153193	1.38E-28	Putative glucose transporter of the major facilitator superfamily
C6_02790C_A		orf19.5552	-4.791405145	6.93E-146	Putative transcriptional regulator of ribonucleotide reductase genes
C6_01450C_A		orf19.3439	-4.796713873	2.03E-116	Protein of unknown function
CR_07530C_A	ECM22	orf19.2623	-4.79693681	2.72E-109	Zn(II)2Cys6 transcription factor
C1_02700C_A		orf19.2959.1	-4.801406261	3.87E-131	Gene induced by hypoxia and ketoconazole
C1_10020W_A	SFU1	orf19.4869	-4.813453757	1.21E-138	GATA-type transcription factor
C7_01690W_A		orf19.6555	-4.815758248	6.72E-60	Ortholog(s) have zinc ion binding activity
CR_08280W_A		orf19.6392	-4.840088739	5.77E-128	Ortholog of C. dubliniensis CD36 : Cd36_33870
C3_03580C_A	GTT13	orf19.356	-4.864263139	5.04E-51	Putative glutathione S-transferase
C1_07170C_A	ZCF23	orf19.4450	-4.864888028	2.50E-137	Predicted Zn(II)2Cys6 transcription factor
C5_04480C_A		orf19.3932.1	-4.869173534	2.06E-46	Has domain(s) with predicted nucleic acid binding
C2_07900W_A	GDH2	orf19.2192	-4.899883077	2.15E-117	Putative NAD-specific glutamate dehydrogenase
C3_02220W_A	CAP1	orf19.1623	-4.929829327	4.85E-168	AP-1 bZIP transcription factor
C7_00650W_A		orf19.7054	-4.958460657	5.40E-06	Dubious open reading frame

C2_04190C_A	UGA1	orf19.802	-4.964314667	5.00E-160	Putative GABA transaminase
C6_03370W_A		orf19.5626	-4.966855826	7.53E-128	Protein of unknown function
C2_03750W_A	YIM1	orf19.847	-4.980272921	5.14E-155	Protein similar to protease of mitochondrial inner membrane
C5_03890C_A		orf19.1105.3	-4.996112549	5.27E-05	Protein of unknown function
C5_03730W_A		orf19.1122	-5.006256707	2.66E-10	Protein of unknown function
C4_04400C_A		orf19.1409.3	-5.01449867	2.42E-11	Protein of unknown function
C6_03670C_A		orf19.5735.3	-5.044288117	3.45E-94	Protein of unknown function
C5_04980W_A		orf19.3988	-5.054951108	1.16E-157	Putative adhesin-like protein
C2_04020C_A	SDS22	orf19.820	-5.054995344	7.47E-154	Putative regulatory subunit of the PP1 phosphatase Glc7p
C6_03750C_A	SBA1	orf19.5749	-5.057892883	1.22E-172	Similar to co-chaperones
C2_05770W_A		orf19.6888	-5.069199302	1.97E-163	Zn(II)2Cys6 domain transcription factor
CR_03250C_A		orf19.2398	-5.072641083	1.26E-148	Protein of unknown function
C3_02480C_A	CCP1	orf19.238	-5.12728848	1.22E-158	Cytochrome-c peroxidase N terminus
C4_06900W_A	GST1	orf19.3121	-5.142480353	2.31E-12	Putative glutathione S-transferase
C2_04010C_A	HSP21	orf19.822	-5.152160413	1.50E-105	Small heat shock protein
C2_06680W_A	FRP3	orf19.1224	-5.172969405	1.94E-170	Putative ammonium transporter
C1_07350C_A	GPX3	orf19.4436	-5.179114971	2.28E-164	Putative glutathione peroxidase involved in Cap1p-dependent oxidative stress response
C2_05180W_A	WH11	orf19.3548.1	-5.182925714	8.25E-160	White-phase yeast transcript
C6_02610C_A	CDC37	orf19.5531	-5.191541332	6.42E-178	Chaperone for Crk1p
C3_02720W_A		orf19.264	-5.196871768	7.39E-142	Has domain(s) with predicted protein kinase binding activity
C7_01700W_A		orf19.6554	-5.210023781	3.70E-135	Regulator of calcineurin
CR_00200W_A	PCK1	orf19.7514	-5.212970938	1.04E-103	Phosphoenolpyruvate carboxykinase
CR_02350C_A	GEF2	orf19.3734	-5.216515131	8.14E-156	Member of the voltage chloride channel family
C5_00890C_A	GIT2	orf19.1978	-5.23045323	1.56E-182	Putative glycerophosphoinositol permease
C6_01490C_A		orf19.3435	-5.232349177	1.82E-54	Ortholog of *Candida albicans* WO-1 : CAWG_05215
C7_02370W_A		orf19.6474	-5.266665804	2.55E-158	Protein with chitin synthesis regulation
C1_09120W_A	IPT1	orf19.4769	-5.270528385	3.61E-148	Inositol phosphoryl transferase
C6_00920W_A		orf19.93	-5.283119606	2.47E-188	Putative mitochondrial intermembrane space protein
CR_03260W_A		orf19.2397.3	-5.297034734	1.46E-156	Putative aminotransferase
CR_10670W_A	CPR6	orf19.7654	-5.302511336	4.13E-181	Putative peptidyl-prolyl cis-trans isomerase
CR_08820C_A	TAR1	orf19.6834.10	-5.306918271	3.50E-178	Ortholog of S. cerevisiae Tar1p
C1_08370W_A	SDS24	orf19.5118	-5.313156438	3.92E-175	Protein similar to S. cerevisiae Sds24 involved in cell separation during budding
CR_07170W_A		orf19.732	-5.328367394	1.47E-146	Possible dehydrogenase
C3_04000C_A	CTN3	orf19.2809	-5.34815603	3.82E-165	Peroxisomal carnitine acetyl transferase
CR_06960W_A		orf19.2369	-5.393272177	2.77E-192	Ortholog(s) have ATP binding, DNA replication origin binding activity
C7_02250W_A		orf19.6488	-5.393735545	1.43E-04	Ortholog of C. dubliniensis CD36 : Cd36_72050
C5_01800C_A	HIP1	orf19.3195	-5.413449696	2.90E-142	Amino acid permeases
C1_10170W_A		orf19.4886	-5.414429168	2.47E-38	Putative adhesin-like protein
C3_03490W_A	RSN1	orf19.347	-5.421141956	1.15E-165	Protein of unknown function
C4_02930W_A		orf19.2701	-5.447008137	8.13E-103	Protein of unknown function
C6_02620C_A		orf19.5532	-5.467632701	9.25E-136	Protein of unknown function
C5_00670C_A	HMS1	orf19.921	-5.478654328	1.45E-165	hLh domain Myc-type transcript factor

CR_06490C_A	HSP60	orf19.717	-5.5043115	1.61E-211	Heat shock protein
C7_02030W_A	HSP90	orf19.6515	-5.525163388	1.71E-201	Essential chaperone
C1_05830W_A		orf19.2468	-5.526398166	5.85E-25	Ortholog(s) have trans-aconitate 3-methyltransferase activity and cytosol localization
C1_06860W_A		orf19.6224	-5.590475901	6.14E-16	RTA domain protein
C1_04310C_A	GIG1	orf19.1066	-5.68667899	2.22E-143	Protein induced by N-acetylglucosamine (GlcNAc)
CR_08990C_A	SLP3	orf19.7296	-5.698736199	1.30E-169	Plasma membrane protein implicated in stress response
C5_04370C_A	PGA37	orf19.3923	-5.706201842	1.46E-82	Putative GPI-anchored protein
C1_06100C_A	MSI3	orf19.2435	-5.775248444	2.01E-232	Essential HSP70 family protein
CR_00530W_A		orf19.7482	-5.817701545	3.03E-07	Ortholog of C. dubliniensis CD36 : Cd36_25640
C1_02520W_A	SCW4	orf19.2941	-5.828173523	1.74E-21	Putative cell wall protein
CR_08830W_A		orf19.7279.1	-5.843675217	3.55E-131	Protein of unknown function
C4_05110C_A	HAP41	orf19.740	-5.861812709	1.51E-219	Putative Hap4-like transcription factor
CR_06100C_A		orf19.3863	-5.904127846	4.47E-157	Ortholog of C. dubliniensis CD36 : Cd36_31580
C4_04530C_A	PHR1	orf19.3829	-5.922026772	6.21E-228	Cell surface glycosidase
C2_04000C_A		orf19.823	-5.922092391	2.64E-06	Protein of unknown function
CR_04200W_A	YDJ1	orf19.506	-5.996056608	1.57E-244	Putative type I HSP40 co-chaperone
C1_14340C_A	RIM101	orf19.7247	-6.008993124	3.13E-212	Transcription factor
C6_01620W_A		orf19.3425	-6.029586428	2.42E-222	RING/FYVE/PHD zinc finger protein
C1_11850W_A		orf19.5282	-6.039153514	4.66E-237	Protein of unknown function
C3_05810C_A	SKN1	orf19.7362	-6.045627547	5.27E-124	Protein with a role in beta-1,6-glucan synthesis
C1_09690W_A	MLS1	orf19.4833	-6.051454411	2.33E-250	Malate synthase
C4_04050C_A	RHD3	orf19.5305	-6.052416261	1.88E-45	GPI-anchored yeast-associated cell wall protein
CR_10270C_A	AHA1	orf19.7602	-6.057498999	3.44E-232	Putative Hsp90p co-chaperone
C5_04220W_A	MRV5	orf19.3905	-6.06109307	4.51E-08	Planktonic growth-induced gene
CR_08210C_A	ACO1	orf19.6385	-6.067400961	5.16E-233	Aconitase
C1_02130C_A	GAL1	orf19.3670	-6.090890526	1.01E-246	Galactokinase
C6_03600C_A		orf19.5728	-6.098714067	2.65E-46	Putative cytochrome P450
C1_02150W_A	GAL10	orf19.3672	-6.099981983	5.09E-252	UDP-glucose 4-epimerase
C1_02170C_A	GAL102	orf19.3674	-6.104803989	1.76E-225	UDP-glucose 4,6-dehydratase
C5_03600W_A	MDJ1	orf19.6672	-6.106040304	2.75E-246	Putative member of the HSP40 (DnaJ) family of chaperones
C5_02860C_A	GRP2	orf19.4309	-6.110671082	2.58E-252	NAD(H)-linked methylglyoxal oxidoreductase involved in regulation of methylglyoxal and pyruvate levels
C5_04970C_A	PPR1	orf19.3986	-6.1242067	3.52E-215	Transcription factor with zinc cluster DNA-binding motif involved in regulation of purine catabolism
C6_03850C_A	IHD1	orf19.5760	-6.164835815	7.18E-203	GPI-anchored protein
C2_04940C_A	ITR1	orf19.3526	-6.200973816	1.54E-209	MFS inositol transporter
C6_01060C_A	CAN2	orf19.111	-6.217709643	1.87E-216	Basic amino acid permease
C7_03740C_A		orf19.5503	-6.245253756	4.49E-27	Putative protein of unknown function
C5_01820W_A	STI1	orf19.3192	-6.296967013	1.50E-268	Protein that interacts with Cdc37 and Crk1 in two-hybrid
C1_05880W_A	PRN4	orf19.2461	-6.326118198	1.14E-198	Protein with similarity to pirins
CR_00050W_A	INO2	orf19.7539	-6.360108218	4.31E-186	Transcriptional activator that forms a heterodimer with Ino4p
C7_01510W_A		orf19.6578	-6.380265045	6.48E-251	Predicted membrane transporter

CR_07790C_A	YHB1	orf19.3707	-6.381263783	1.95E-225	Nitric oxide dioxygenase
C1_05160C_A		orf19.449	-6.437024869	4.89E-262	Putative phosphatidyl synthase
C1_06230C_A	MDM34	orf19.1826	-6.559556488	4.35E-233	Putative zinc finger transcription factor
C5_04380C_A		orf19.3924	-6.571806366	1.10E-38	Ortholog of *Candida albicans* WO-1 : CAWG_04810
C1_07160C_A		orf19.4450.1	-6.623752357	8.73E-209	Protein conserved among the CTG-clade
C1_02530C_A	DIP5	orf19.2942	-6.657829734	7.27E-298	Dicarboxylic amino acid permease
CR_00540C_A	MDH1	orf19.7481	-6.732242115	8.30E-209	Mitochondrial malate dehydrogenase
CR_09920W_A		orf19.7566	-6.73512572	1.11E-255	Predicted amino acid transport domain
C2_01450C_A		orf19.1449	-6.747491873	1.57E-66	Protein of unknown function
C3_00220W_A	HGT19	orf19.5447	-6.771521238	1.67E-158	Putative MFS glucose/myo-inositol transporter
C1_02800W_A		orf19.2968	-6.773837249	9.20E-264	Protein of unknown function
C1_00390W_A	ENA2	orf19.6070	-6.817484241	3.68E-294	Putative sodium transporter
C1_13080W_A	OP4	orf19.4934	-6.888448437	2.51E-11	Ala- Leu- and Ser-rich protein
C5_04440C_A	SFC1	orf19.3931	-6.934652953	3.69E-225	Putative succinate-fumarate transporter
C2_00760C_A		orf19.2048	-6.962370253	5.02E-297	Proten of unknown function
C3_05580C_A	GAP2	orf19.6993	-7.026391774	8.47E-290	General broad specificity amino acid permease
C7_03560W_A		orf19.6688	-7.09341259	7.88E-170	Protein of unknown function
C4_04020C_A		orf19.5308	-7.110384663	2.17E-21	Protein of unknown function
C1_09250W_A	CRP1	orf19.4784	-7.164775147	1.07E-26	Copper transporter
CR_06080W_A	SIS1	orf19.3861	-7.216450982	4.49E-13	Putative Type II HSP40 co-chaperone
C1_09240C_A		orf19.4783	-7.238172757	7.41E-156	Protein of unknown function
C5_04190W_A	MRV2	orf19.3902	-7.254288524	3.59E-79	Protein of unknown function
C4_03570W_A	HWP1	orf19.1321	-7.331117791	7.45E-203	Hyphal cell wall protein
C2_08260W_A		orf19.2220	-7.348881031	1.47E-170	Protein of unknown function
C5_02600W_A	PUT1	orf19.4274	-7.351607628	9.79E-05	Putative proline oxidase
C1_13100W_A		orf19.4936.1	-7.40734598	3.64E-61	Putative adhesin-like protein
C1_05870W_A	PRN3	orf19.2462	-7.414341408	1.89E-10	Protein similar to pirin
CR_02270C_A		orf19.3742	-7.458580924	3.01E-17	Protein of unknown function
C2_03390C_A	HSP78	orf19.882	-7.485617889	1.12E-12	Heat-shock protein
C6_03700W_A	ALS1	orf19.5741	-7.63431688	3.50E-31	Cell-surface adhesin
C1_05840W_A	PRN1	orf19.2467	-7.64688194	8.02E-282	Protein with similarity to pirins
CR_07440W_A	ACE2	orf19.6124	-7.731321476	3.34E-09	Transcription factor
C1_11320C_A		orf19.670.2	-7.841591224	5.72E-248	Protein of unknown function
CR_08250C_A	HSP104	orf19.6387	-7.971498652	1.95E-06	Heat-shock protein
CR_06950C_A	ATX1	orf19.2369.1	-8.038051241	4.08E-32	Putative cytosolic copper metallochaperone
CR_08420W_A		orf19.6408	-8.272452897	7.54E-01	Putative DnaJ-like heat shock/chaperone
C1_02180W_A	GAL7	orf19.3675	-8.319119521	3.43E-18	Putative galactose-1-phoshphate uridyl transferase
C5_04210C_A	MRV4	orf19.3904	-8.34132585	8.37E-25	Protein of unknown function
C4_03470C_A	ECE1	orf19.3374	-8.450029219	2.43E-111	Candidalysin, cytolytic peptide toxin essential for mucosal infection
C4_01940W_A	PHO89	orf19.4599	-8.466705753	6.96E-297	Putative phosphate permease
C1_02110C_A	HGT2	orf19.3668	-8.544165236	1.00E+07	Putative MFS glucose transporter
C5_04930C_A	MAL31	orf19.3981	-8.638670045	3.04E-137	Putative high-affinity maltose transporter
C6_02520W_A	ISA1	orf19.5521	-8.859239098	1.46E-144	Putative mitochondrial iron-sulfur protein

C1_04500W_A	ICL1	orf19.6844	-8.905741519	1.26E-134	Isocitrate lyase
CR_05340C_A	IFE2	orf19.5288	-8.95304617	6.34E-13	Putative alcohol dehydrogenase
C4_04030W_A	JEN2	orf19.5307	-9.043392794	1.02E-173	Dicarboxylic acid transporter
C4_01160W_A	CRD2	orf19.4674.1	-9.406727037	1.73E-128	Metallothionein
C1_01740W_A	CTN1	orf19.4551	-9.569009749	1.98E-260	Carnitine acetyl transferase
CR_02360W_A	IDP2	orf19.3733	-9.851050583	1.22E-144	Isocitrate dehydrogenase
C5_02870C_A		orf19.4310	-10.13294759	8.91E-41	Dubious open reading frame
C1_01980W_A	HGT1	orf19.4527	-10.29028007	2.71E-65	High-affinity MFS glucose transporter
C1_04300C_A	SSA2	orf19.1065	-10.33836029	3.36E-28	HSP70 family chaperone
C7_00350C_A		orf19.7085	-10.44467584	7.79E-54	Protein of unknown function
CR_08270W_A		orf19.6391	-10.47376303	3.77E-149	Protein of unknown function
C4_04080C_A	PGA31	orf19.5302	-10.67825609	1.74E-66	Cell wall protein
C3_00920W_A	ATO1	orf19.6169	-10.97913772	1.26E-46	Putative fungal-specific transmembrane protein
C3_05050W_A	TRY4	orf19.5975	-12.72064272	1.40E-85	C2H2 transcription factor

6.2 Transcriptome Data Mucus/Control

Results of the transcriptome analysis comparing *C. albicans* cells grown in minimal medium supplemented with mucin (Sigma-Aldrich) to fungal cells grown in minimal media without carbon source. The experimental procedure is described in 5.4.3. 94 genes were significantly differentially regulated with a log2 fold change cut off of ±1 and pvalue lower than 0.01, adapted form Eckstein *et al.* 2020.

Systematic Name	Alias	Assembly 19 Identifier	log2 (mucin/control)	P-value	Annotation
C1_13450W_A	HRY1	orf19.4975	2.640926538	1.75E-22	GPI-anchored hyphal cell wall protein
C6_00790C_A	CTR1	orf19.3646	1.873855721	2.10E-18	Copper transporter; transcribed in low copper
C6_03170C_A	MRD1	orf19.5604	1.829697647	4.43E-14	Plasma membrane MDR/MFS multidrug efflux pump
C1_06280C_A	UME6	orf19.1822	1.727788832	1.55E-06	Zn(II)2Cys6 transcription factor
C4_03470C_A	ECE1	orf19.3374	1.65854609	4.20E-12	Candidalysin
C1_14130W_A	FTR1	orf19.7219	1.648274296	6.18E-17	High-affinity iron permease
C4_04320W_A	FRE10	orf19.1415	1.584134302	1.91E-10	Multicopper ferroxidase
C1_04020C_A	CSH1	orf19.4477	1.571807167	7.51E-11	Aldo-keto reductase
C6_00440C_A	FET34	orf19.4215	1.531172886	1.68E-13	Multicopper ferroxidase
C4_00360C_A	RCH1	orf19.5663	1.512550134	4.45E-14	Plasma membrane protein
C7_00430W_A	FRE7	orf19.7077	1.511153066	1.49E-07	Putative ferric reductase
CR_09370W_A	ELF1	orf19.7332	1.505879794	3.28E-15	Putative mRNA export protein
C4_03540C_A	ECM38	orf19.1325	1.359690111	1.47E-09	Putative gamma-glutamyltransferase
C1_04010C_A	IFD1/6	orf19.4476	1.344927975	5.44E-08	Protein with a NADP-dependent oxidoreductase domain
C1_11210C_A	HAP43	orf19.681	1.32013895	5.03E-12	CCAAT-binding factor-dependent transcription factor
C4_06120W_A	GDH3	orf19.4716	1.309629401	3.22E-09	NADP-glutamate dehydrogenase
CR_04940W_A		orf19.1806	1.298752759	2.28E-04	Ortholog of *C. dubliniensis CD36*: Cd36_30340
C3_04530C_A	TEC1	orf19.5908	1.290742446	7.51E-11	TEA/ATTS transcription factor
C3_02310W_A	MEP1	orf19.1614	1.256951016	3.11E-09	Ammonium permease
C1_00170W_A	LEU4	orf19.6086	1.206015676	1.10E-05	Putative 2-isopropylmalate synthase
CR_09830W_A		orf19.7554	1.205494635	2.95E-08	Transporter; similar to the Sit1 siderophore transporter
C1_04660W_A	DUR1/2	orf19.780	1.201853815	2.03E-05	Urea amidolyase; hydrolyzes urea to CO2
C1_00780C_A	HGC1	orf19.6028	1.178044484	1.59E-06	Hypha-specific G1 cyclin-related protein
CR_02980C_A	SRP40	orf19.2859	1.167924939	1.54E-07	Putative chaperone of small nucleolar ribonucleoprotein particles
C3_07150C_A	RPS12	orf19.6785	1.150319052	9.00E-07	Acidic ribosomal protein S12
C1_04140W_A	IFD6	orf19.1048	1.144040002	8.13E-03	Aldo-keto reductase
C1_06470W_A		orf19.6264.4	1.134165727	4.05E-07	Ortholog of S. cerevisiae Rpl39
C1_11040W_A	RPL29	orf19.2310.1	1.105150235	2.59E-06	Ribosomal protein L29
CR_04100C_A	RPL15A	orf19.493	1.097082461	3.42E-06	Putative ribosomal protein
C1_09040C_A		orf19.4760	1.090418375	6.21E-05	Non-synonymous variation between alleles
C6_00480C_A	FET31	orf19.4211	1.085392353	7.66E-04	Putative multicopper oxidase induced
C1_06610C_A	HAK1	orf19.6249	1.082158106	3.16E-04	Putative potassium transporterpressed

C5_03060C_A	TNA1	orf19.4335	1.081696194	8.80E-05	Putative nicotinic acid transporter
C3_01150C_A	APD1	orf19.158	1.076249884	5.98E-07	Ortholog of S. cerevisiae Apd1
C5_05080W_A	GRF10	orf19.4000	1.072590982	4.07E-07	Putative homeodomain transcription factorNdt80 and Brg1
C7_00110W_A	SOD3	orf19.7111.1	1.053211162	1.35E-04	Cytosolic manganese-containing superoxide dismutase
C3_02320W_A	ILV2	orf19.1613	1.032966727	4.32E-07	Putative acetolactate synthase
C2_06810C_A	RPL11	orf19.2232	1.032229041	4.95E-05	Ribosomal protein
C3_04500C_A	RPL19A	orf19.5904	1.029780733	4.31E-05	Ribosomal protein L19
C1_09690W_A	MLS1	orf19.4833	1.024122939	5.44E-08	Malate synthase
C1_04470C_A		orf19.6840	1.016207662	3.06E-05	Protein of unknown function
CR_02330C_A	KAR4	orf19.3736	1.01264018	1.12E-03	Transcription factor
C1_01370C_A	RPS21	orf19.3325.3	1.004547341	5.18E-05	Ribosomal protein S21
C1_04710C_A		orf19.773	1.002341025	1.81E-03	Protein similar to S. cerevisiae
CR_06800C_A	HHF22	orf19.1854	-1.003590861	1.97E-04	Putative histone H4
C2_06680W_A	FRP3	orf19.1224	-1.004777165	3.76E-07	Putative ammonium transporter repressed
C1_02980W_A	GOR1	orf19.2989	-1.004971886	7.18E-06	Ortholog(s) have glyoxylate reductase activity
C1_11320C_A		orf19.670.2	-1.006077164	1.72E-07	Protein of unknown function
CR_08990C_A	SLP3	orf19.7296	-1.012048704	2.82E-07	Plasma membrane protein implicated in stress response
C2_08260W_A		orf19.2220	-1.016501796	1.77E-06	Protein of unknown function
C5_00540C_A	AGA1	orf19.935	-1.022016163	3.09E-03	Protein with some similarity to agglutinin subunit
C3_00920W_A	ATO1	orf19.6169	-1.022335134	3.37E-07	Putative fungal-specific transmembrane protein
C2_01270W_A	CHA1	orf19.1996	-1.023946936	4.88E-05	Similar to catabolic ser/thr dehydratases
CR_06810W_A	HHT2	orf19.1853	-1.024967913	2.05E-04	Putative histone H3
C7_00280W_A	HGT12	orf19.7094	-1.028762914	4.24E-03	Glucose, fructose, mannose transporter
C4_02330C_A		orf19.2770	-1.032446069	1.15E-04	Ortholog of C. dubliniensis CD36 : Cd36_42220
C3_01420C_A		orf19.1709	-1.03297549	1.29E-05	Sterol carrier domain protein
C1_04060W_A	IFI3	orf19.4482	-1.03751882	9.54E-04	Protein of unknown function
CR_06460W_A	GST3	orf19.720	-1.04971157	2.13E-03	Glutathione S-transferase
C1_09150W_A		orf19.4773	-1.056537745	2.61E-07	Alternative oxidase
C1_00880W_A		orf19.6017	-1.059244398	2.21E-04	Protein of unknown function
C2_10180W_A	IFR1	orf19.1763	-1.060064824	3.37E-07	Predicted oxidoreductase/dehydrogenase
C6_01410C_A	OYE2	orf19.3443	-1.064907515	1.77E-06	Putative NAPDH dehydrogenase
C1_09770W_A		orf19.4842	-1.076806939	8.28E-07	Protein of unknown function
C2_05990C_A		orf19.4121	-1.077692227	1.75E-04	Predicted thioesterase/thiol ester dehydrase-isomerase
C5_04480C_A		orf19.3932.1	-1.081909002	1.94E-04	Has domain(s) with predicted nucleic acid binding
C2_05130W_A		orf19.3544	-1.095142085	4.13E-05	Putative protein of unknown function
CR_08920W_A		orf19.7288	-1.096425702	6.45E-06	Protein with predicted oxidoreductase/dehydrogenase domains
C2_06930C_A		orf19.2247	-1.097014817	7.21E-04	Ortholog of C. dubliniensis CD36 : Cd36_21220
C4_02320C_A	SOD1	orf19.2770.1	-1.100528394	1.32E-06	Cytosolic copper- and zinc-containing superoxide dismutase
C6_01180C_A	EBP1	orf19.125	-1.105034402	3.17E-05	NADPH oxidoreductase
CR_00130C_A		orf19.7522	-1.105083309	7.17E-06	Protein with a pyridoxal phosphate-dependent transferase domain
C6_01490C_A		orf19.3435	-1.128805757	4.14E-04	Ortholog of Candida albicans WO-1 : CAWG_05215

C4_02360W_A	AMS1	orf19.2768	-1.158810479	7.78E-09	Putative alpha-mannosidase
C2_06720W_A	GRE2	orf19.3150	-1.169521707	1.23E-07	Putative reductase
C1_01630W_A		orf19.3353	-1.192581583	1.54E-07	Protein similar to a mitochondrial complex I intermediate-associated protein
C6_01500C_A	TRY5	orf19.3434	-1.220272235	1.83E-07	Zn(II)2Cys6 transcription factor
C1_13630W_A	CYB2	orf19.5000	-1.234658741	1.64E-06	Putative cytochrome b2 precursor
C5_00100C_A		orf19.5686	-1.268579429	3.34E-08	Protein of unknown function
C1_08330C_A	ADH2	orf19.5113	-1.269101364	3.98E-09	Alcohol dehydrogenase
C4_02930W_A		orf19.2701	-1.270020129	7.52E-08	Protein of unknown function
C6_03240W_A		orf19.5611	-1.27649869	1.05E-05	Predicted 3-methylbutanol:NAD(P) oxidoreductase
C4_02410C_A	AHP1	orf19.2762	-1.283684636	1.48E-08	Alkyl hydroperoxide reductase
C1_11660W_A	GAD1	orf19.1153	-1.289633788	3.48E-10	Putative glutamate decarboxylase repressed
C1_13670W_A	OSM2	orf19.5005	-1.341569886	2.34E-07	Putative mitochondrial fumarate reductase
C3_02680C_A	SLD1	orf19.260	-1.342960021	8.38E-08	Sphingolipid delta-8 desaturase
C3_00210C_A		orf19.5449	-1.350759983	1.70E-04	Predicted integral membrane protein
C4_06890W_A	ARR1	orf19.3122	-1.362999582	8.13E-13	Ortholog of S. cerevisiae Arr3
C2_01020W_A	HGT6	orf19.2020	-1.396345069	3.09E-11	Putative high-affinity MFS glucose transporter
C7_03310W_A		orf19.1344	-1.421398392	1.62E-05	Protein of unknown function
C1_02110C_A	HGT2	orf19.3668	-1.482037069	7.33E-16	Putative MFS glucose transporter a
CR_08880C_A		orf19.7283	-1.610086557	5.89E-10	Protein of unknown function
C3_01930W_A	PXP2	orf19.1655	-1.652364739	1.31E-09	Putative acyl-CoA oxidase
C3_00220W_A	HGT19	orf19.5447	-1.772624854	1.53E-19	Putative high-affinity MFS glucose transporter

7. References

Ahl, D., Liu, H., Schreiber, O., Roos, S., Phillipson, M., & Holm, L. (2016). *Lactobacillus reuteri* increases mucus thickness and ameliorates dextran sulphate sodium-induced colitis in mice. *Acta Physiologica*, *217*(4), 300–310. https://doi.org/10.1111/apha.12695

Akhtar, R. A., Reddy, A. B., Maywood, E. S., Clayton, J. D., King, V. M., Smith, A. G., Gant, T. W., Hastings, M. H., & Kyriacou, C. P. (2002). Circadian cycling of the mouse liver transcriptome, as revealed by cDNA microarray, is driven by the suprachiasmatic nucleus. *Current Biology*, *12*(7), 540–550. https://doi.org/10.1016/S0960-9822(02)00759-5

Ambort, D., Johansson, M. E. V., Gustafsson, J. K., Nilsson, H. E., Ermund, A., Johansson, B. R., Koeck, P. J. B., Hebert, H., & Hansson, G. C. (2012). Calcium and pH-dependent packing and release of the gel-forming MUC2 mucin. *Proceedings of the National Academy of Sciences of the United States of America*, *109*(15), 5645–5650. https://doi.org/10.1073/pnas.1120269109

Ameziane, R., Hassani, E., Benfares, N., Caillou, B., Talbot, M., Sabourin, J.-C., Belotte, V., Morand, S., Gnidehou, S., Agnandji, D., Ohayon, R., Kaniewski, J., Noël-Hudson, M.-S., Bidart, J.-M., Schlumberger, M., Virion, A., Dupuy, C., Hassani, A. El, Rabii, N., … Kaniewski, M.-S. N.-H. (2005). *Dual oxidase2 is expressed all along the digestive tract*. https://doi.org/10.1152/ajpgi.00198.2004.-The

Anders, S., Pyl, P. T., & Huber, W. (2015). HTSeq-A Python framework to work with high-throughput sequencing data. *Bioinformatics*, *31*(2), 166–169. https://doi.org/10.1093/bioinformatics/btu638

Antachopoulos, C., & Roilides, E. (2005). Cytokines and fungal infections. *British Journal of Haematology*, *129*(5), 583–596. https://doi.org/10.1111/j.1365-2141.2005.05498.x

Asher, G., & Sassone-Corsi, P. (2015). Time for food: The intimate interplay between nutrition, metabolism, and the circadian clock. In *Cell* (Vol. 161, Issue 1, pp. 84–92). Cell Press. https://doi.org/10.1016/j.cell.2015.03.015

Bäckhed, F., Ding, H., Wang, T., Hooper, L. V., Gou, Y. K., Nagy, A., Semenkovich, C. F., & Gordon, J. I. (2004). The gut microbiota as an environmental factor that regulates fat storage. *Proceedings of the National Academy of Sciences of the United States of America*, *101*(44), 15718–15723. https://doi.org/10.1073/pnas.0407076101

Barko, P. C., McMichael, M. A., Swanson, K. S., & Williams, D. A. (2018). The Gastrointestinal Microbiome: A Review. In *Journal of Veterinary Internal Medicine* (Vol. 32, Issue 1, pp. 9–25). Blackwell Publishing Inc. https://doi.org/10.1111/jvim.14875

Bedard, K., & Krause, K. H. (2007). The NOX family of ROS-generating NADPH oxidases: Physiology and pathophysiology. In *Physiological Reviews* (Vol. 87, Issue 1, pp. 245–313). Physiol Rev. https://doi.org/10.1152/physrev.00044.2005

Belkaid, Y., & Harrison, O. J. (2017). Homeostatic Immunity and the Microbiota. In *Immunity* (Vol. 46, Issue 4, pp. 562–576). Cell Press. https://doi.org/10.1016/j.immuni.2017.04.008

Bennett, R. J. (2015). The parasexual lifestyle of *Candida albicans*. In *Current Opinion in Microbiology* (Vol. 28, pp. 10–17). Elsevier Ltd. https://doi.org/10.1016/j.mib.2015.06.017

Biedermann, L., & Rogler, G. (2015). The intestinal microbiota: its role in health and disease. In *European Journal of Pediatrics* (Vol. 174, Issue 2, pp. 151–167). Springer Verlag. https://doi.org/10.1007/s00431-014-2476-2

Bjursell, M. K., Martens, E. C., & Gordon, J. I. (2006). Functional genomic and metabolic studies of the adaptations of a prominent adult human gut symbiont, *Bacteroides thetaiotaomicron*, to the suckling period. *Journal of Biological Chemistry*, *281*(47), 36269–36279. https://doi.org/10.1074/jbc.M606509200

Bloom, S. M., Bijanki, V. N., Nava, G. M., Sun, L., Malvin, N. P., Donermeyer, D. L., Dunne, W. M., Allen, P. M., & Stappenbeck, T. S. (2011). Commensal Bacteroides species induce colitis in host-genotype-specific fashion in a mouse model of inflammatory bowel disease. *Cell Host and Microbe*, *9*(5), 390–403. https://doi.org/10.1016/j.chom.2011.04.009

Böhm, L., Torsin, S., Tint, S. H., Eckstein, M. T., Ludwig, T., & Pérez, J. C. (2017). The yeast form of the fungus *Candida albicans* promotes persistence in the gut of gnotobiotic mice. *PLOS Pathogens*, *13*(10), e1006699-. https://doi.org/10.1371/journal.ppat.1006699

Bolger, A. M., Lohse, M., & Usadel, B. (2014). Trimmomatic: A flexible trimmer for Illumina sequence data. *Bioinformatics*, *30*(15), 2114–2120. https://doi.org/10.1093/bioinformatics/btu170

Bongomin, F., Gago, S., Oladele, R. O., & Denning, D. W. (2017). Global and multi-national prevalence of fungal diseases—estimate precision. In *Journal of Fungi* (Vol. 3, Issue 4). MDPI AG. https://doi.org/10.3390/jof3040057

Bougnoux, M. E., Diogo, D., François, N., Sendid, B., Veirmeire, S., Colombel, J. F., Bouchier, C., Van Kruiningen, H., D'Enfert, C., & Poulain, D. (2006). Multilocus sequence typing reveals intrafamilial transmission and microevolutions of *Candida albicans* isolates from the human digestive tract. *Journal of Clinical Microbiology*, *44*(5), 1810–1820.

https://doi.org/10.1128/JCM.44.5.1810-1820.2006

Bowcutt, R., Forman, R., Glymenaki, M., Carding, S. R., Else, K. J., & Cruickshank, S. M. (2014). Heterogeneity across the murine small and large intestine. In *World Journal of Gastroenterology* (Vol. 20, Issue 41, pp. 15216–15232). WJG Press. https://doi.org/10.3748/wjg.v20.i41.15216

Brandes, R. P., Weissmann, N., & Schröder, K. (2014). Nox family NADPH oxidases: Molecular mechanisms of activation. In *Free Radical Biology and Medicine* (Vol. 76, pp. 208–226). Elsevier Inc. https://doi.org/10.1016/j.freeradbiomed.2014.07.046

Brown, G. D., & Netea, M. G. (2012). Exciting developments in the immunology of fungal infections. In *Cell Host and Microbe* (Vol. 11, Issue 5, pp. 422–424). Cell Press. https://doi.org/10.1016/j.chom.2012.04.010

Brugiroux, S., Beutler, M., Pfann, C., Garzetti, D., Ruscheweyh, H. J., Ring, D., Diehl, M., Herp, S., Lötscher, Y., Hussain, S., Bunk, B., Pukall, R., Huson, D. H., Münch, P. C., McHardy, A. C., McCoy, K. D., MacPherson, A. J., Loy, A., Clavel, T., … Stecher, B. (2016). Genome-guided design of a defined mouse microbiota that confers colonization resistance against Salmonella enterica serovar Typhimurium. *Nature Microbiology*, *2*. https://doi.org/10.1038/nmicrobiol.2016.215

Burokas, A., Moloney, R. D., Dinan, T. G., & Cryan, J. F. (2015). Microbiota regulation of the mammalian gut-brain axis. *Advances in Applied Microbiology*, *91*, 1–62. https://doi.org/10.1016/bs.aambs.2015.02.001

Cabral, D. J., Penumutchu, S., Norris, C., Morones-Ramirez, J. R., & Belenky, P. (2018). Microbial competition between escherichia coli and *Candida albicans* reveals a soluble fungicidal factor. *Microbial Cell*, *5*(5), 249–255. https://doi.org/10.15698/mic2018.05.631

Canny, G. O., & McCormick, B. A. (2008). Bacteria in the intestine, helpful residents or enemies from within? In *Infection and Immunity* (Vol. 76, Issue 8, pp. 3360–3373). American Society for Microbiology Journals. https://doi.org/10.1128/IAI.00187-08

Carvalho, D. P., & Dupuy, C. (2013). Role of the NADPH Oxidases DUOX and NOX4 in Thyroid Oxidative Stress. *European Thyroid Journal*, *2*(3), 160–167. https://doi.org/10.1159/000354745

Castillo, L., MacCallum, D. M., Brown, A. J. P., Gow, N. A. R., & Odds, F. C. (2011). Differential Regulation of Kidney and Spleen Cytokine Responses in Mice Challenged with Pathology-Standardized Doses of *Candida albicans* Mannosylation Mutants . *Infection and Immunity*, *79*(1), 146–152. https://doi.org/10.1128/iai.01004-10

Causton, H. C., Feeney, K. A., Ziegler, C. A., & O'Neill, J. S. (2015). Metabolic cycles in yeast share features conserved among circadian rhythms.

Current Biology, *25*(8), 1056–1062.
https://doi.org/10.1016/j.cub.2015.02.035

Chehoud, C., Albenberg, L. G., Judge, C., Hoffmann, C., Grunberg, S., Bittinger, K., Baldassano, R. N., Lewis, J. D., Bushman, F. D., & Wu, G. D. (2015). Fungal signature in the gut microbiota of pediatric patients with inflammatory bowel disease. *Inflammatory Bowel Diseases*, *21*(8), 1948–1956. https://doi.org/10.1097/MIB.0000000000000454

Cheng, S.-C., Joosten, L. A. B., Kullberg, B.-J., & Netea, M. G. (2012). Interplay between *Candida albicans* and the Mammalian Innate Host Defense. *Infection and Immunity*, *80*(4), 1304–1313. https://doi.org/10.1128/iai.06146-11

Cho, D. Y., Nayak, J. V., Bravo, D. T., Le, W., Nguyen, A., Edward, J. A., Hwang, P. H., Illek, B., & Fischer, H. (2013). Expression of dual oxidases and secreted cytokines in chronic rhinosinusitis. *International Forum of Allergy and Rhinology*, *3*(5), 376–383. https://doi.org/10.1002/alr.21133

Colina, A R, Aumont, F., Deslauriers, N., Belhumeur, P., & de Repentigny, L. (1996). Evidence for degradation of gastrointestinal mucin by *Candida albicans* secretory aspartyl proteinase. *Infection and Immunity*, *64*(11).

Colina, Ana Rosa, Aumont, F., Deslauriers, N., Belhumeur, P., & De Repentigny, L. (1996). Evidence for degradation of gastrointestinal mucin by *Candida albicans* secretory aspartyl proteinase. *Infection and Immunity*, *64*(11), 4514–4519.

Costello, E. K., Lauber, C. L., Hamady, M., Fierer, N., Gordon, J. I., & Knight, R. (2009). Bacterial community variation in human body habitats across space and time. *Science*, *326*(5960), 1694–1697. https://doi.org/10.1126/science.1177486

Coussens, L. M., & Werb, Z. (2002). Inflammation and cancer. In *Nature* (Vol. 420, Issue 6917, pp. 860–867). Nature. https://doi.org/10.1038/nature01322

Cox, K. H., & Takahashi, J. S. (2019). Circadian clock genes and the transcriptional architecture of the clock mechanism. *Journal of Molecular Endocrinology*, *63*(4), R93–R102. https://doi.org/10.1530/JME-19-0153

Crampin, H., Finley, K., Gerami-Nejad, M., Court, H., Gale, C., Berman, J., & Sudbery, P. (2005). *Candida albicans* hyphae have a Spitzenkörper that is distinct from the polarisome found in yeast and pseudohyphae. *Journal of Cell Science*, *118*(13), 2935–2947. https://doi.org/10.1242/jcs.02414

Cryan, J. F., O'riordan, K. J., Cowan, C. S. M., Sandhu, K. V., Bastiaanssen, T. F. S., Boehme, M., Codagnone, M. G., Cussotto, S., Fulling, C., Golubeva, A. V., Guzzetta, K. E., Jaggar, M., Long-Smith, C. M., Lyte, J. M., Martin, J. A., Molinero-Perez, A., Moloney, G., Morelli, E., Morillas, E.,

… Dinan, T. G. (2019). The microbiota-gut-brain axis. *Physiological Reviews*, *99*(4), 1877–2013. https://doi.org/10.1152/physrev.00018.2018

Curvale-Fauchet, N., Botterel, F., Legrand, P., Guillot, J., & Bretagne, S. (2004). Frequency of intravascular catheter colonization by Malassezia spp. in adult patients. Haufigkeit der Besiedelung von intravaskularen Kathetern mit Malassezia spp. bei erwachsenen Patienten. *Mycoses*, *47*(11–12), 491–494. https://doi.org/10.1111/j.1439-0507.2004.01047.x

Cuskin, F., Lowe, E. C., Temple, M. J., Zhu, Y., Cameron, E. A., Pudlo, N. A., Porter, N. T., Urs, K., Thompson, A. J., Cartmell, A., Rogowski, A., Hamilton, B. S., Chen, R., Tolbert, T. J., Piens, K., Bracke, D., Vervecken, W., Hakki, Z., Speciale, G., … Gilbert, H. J. (2015). Human gut Bacteroidetes can utilize yeast mannan through a selfish mechanism. *Nature*, *517*(7533), 165–169. https://doi.org/10.1038/nature13995

Da Silva, S., Robbe-Masselot, C., Raymond, A., Mercade-Loubière, M., Salvador-Cartier, C., Ringot, B., Léonard, R., Fourquaux, I., Ait-Belgnaoui, A., Loubière, P., Théodorou, V., & Mercier-Bonin, M. (2015). Spatial localization and binding of the probiotic Lactobacillus farciminis to the rat intestinal mucosa: Influence of chronic stress. *PLoS ONE*, *10*(9). https://doi.org/10.1371/journal.pone.0136048

del Olmo Toledo, V., Puccinelli, R., Fordyce, P. M., & Pérez, J. C. (2018). Diversification of DNA binding specificities enabled SREBP transcription regulators to expand the repertoire of cellular functions that they govern in fungi. *PLoS Genetics*, *14*(12). https://doi.org/10.1371/journal.pgen.1007884

Delhaes, L., Monchy, S., Fréalle, E., Hubans, C., Salleron, J., Leroy, S., Prevotat, A., Wallet, F., Wallaert, B., Dei-Cas, E., Sime-Ngando, T., Chabé, M., & Viscogliosi, E. (2012). The airway microbiota in cystic fibrosis: A complex fungal and bacterial community-implications for therapeutic management. *PLoS ONE*, *7*(4). https://doi.org/10.1371/journal.pone.0036313

Dewhirst, F. E., Chien, C. C., Paster, B. J., Ericson, R. L., Orcutt, R. P., Schauer, D. B., & Fox, J. G. (1999). Phylogeny of the defined murine microbiota: Altered Schaedler flora. *Applied and Environmental Microbiology*, *65*(8), 3287–3292. https://doi.org/10.1128/aem.65.8.3287-3292.1999

Diamond, R. D., & Krzesicki, R. (1978). Mechanisms of attachment of neutrophils to *Candida albicans* pseudohyphae in the absence of serum, and of subsequent damage to pseudohyphae by microbicidal processes of neutrophils *in vitro*. *Journal of Clinical Investigation*, *61*(2), 360–369. https://doi.org/10.1172/JCI108946

Diaz, M., Ladero, V., Del Rio, B., Redruello, B., Fernández, M., Martin, M. C.,

& Alvarez, M. A. (2016). Biofilm-forming capacity in biogenic amine-producing bacteria isolated from dairy products. *Frontiers in Microbiology*, *7*(MAY). https://doi.org/10.3389/fmicb.2016.00591

Dinarello, C. A. (1997). Interleukin-1. In *Cytokine and Growth Factor Reviews* (Vol. 8, Issue 4, pp. 253–265). Elsevier Ltd. https://doi.org/10.1016/S1359-6101(97)00023-3

Dobin, A., & Gingeras, T. R. (2015). Mapping RNA-seq Reads with STAR. *Current Protocols in Bioinformatics*, *51*(1), 11.14.1-11.14.19. https://doi.org/10.1002/0471250953.bi1114s51

Donaldson, G. P., Lee, S. M., & Mazmanian, S. K. (2015). Gut biogeography of the bacterial microbiota. In *Nature Reviews Microbiology* (Vol. 14, Issue 1, pp. 20–32). Nature Publishing Group. https://doi.org/10.1038/nrmicro3552

Du, H., & Huang, G. (2016). Environmental pH adaption and morphological transitions in *Candida albicans*. In *Current Genetics* (Vol. 62, Issue 2, pp. 283–286). Springer Verlag. https://doi.org/10.1007/s00294-015-0540-8

Duez, H., van der Veen, J. N., Duhem, C., Pourcet, B., Touvier, T., Fontaine, C., Derudas, B., Baugé, E., Havinga, R., Bloks, V. W., Wolters, H., van der Sluijs, F. H., Vennström, B., Kuipers, F., & Staels, B. (2008). Regulation of Bile Acid Synthesis by the Nuclear Receptor Rev-erbα. *Gastroenterology*, *135*(2). https://doi.org/10.1053/j.gastro.2008.05.035

Dupuy, C., Pomerance, M., Ohayon, R., Noël-Hudson, M. S., Dème, D., Chaaraoui, M., Francon, J., & Virion, A. (2000). Thyroid oxidase (THOX2) gene expression in the rat thyroid cell line FRTL-5. *Biochemical and Biophysical Research Communications*, *277*(2), 287–292. https://doi.org/10.1006/bbrc.2000.3671

Earle, K. A., Billings, G., Sigal, M., Lichtman, J. S., Hansson, G. C., Elias, J. E., Amieva, M. R., Huang, K. C., & Sonnenburg, J. L. (2015). Quantitative Imaging of Gut Microbiota Spatial Organization. *Cell Host and Microbe*, *18*(4), 478–488. https://doi.org/10.1016/j.chom.2015.09.002

Eckburg, P. B., Bik, E. M., Bernstein, C. N., Purdom, E., Dethlefsen, L., Sargent, M., Gill, S. R., Nelson, K. E., & Relman, D. A. (2005). Microbiology: Diversity of the human intestinal microbial flora. *Science*, *308*(5728), 1635–1638. https://doi.org/10.1126/science.1110591

Egert, M., & Simmering, R. (2016). The microbiota of the human skin. In *Advances in Experimental Medicine and Biology* (Vol. 902, pp. 61–81). Springer New York LLC. https://doi.org/10.1007/978-3-319-31248-4_5

Fan, D., Coughlin, L. A., Neubauer, M. M., Kim, J., Kim, M. S., Zhan, X., Simms-Waldrip, T. R., Xie, Y., Hooper, L. V., & Koh, A. Y. (2015). Activation of HIF-1α and LL-37 by commensal bacteria inhibits *Candida*

albicans colonization. In *Nature Medicine* (Vol. 21, Issue 7, pp. 808–814). Nature Publishing Group. https://doi.org/10.1038/nm.3871

Findley, K., Oh, J., Yang, J., Conlan, S., Deming, C., Meyer, J. A., Schoenfeld, D., Nomicos, E., Park, M., Kong, H. H., & Segre, J. A. (2013). Topographic diversity of fungal and bacterial communities in human skin. *Nature*, *498*(7454), 367–370. https://doi.org/10.1038/nature12171

Flint, H. J., Scott, K. P., Louis, P., & Duncan, S. H. (2012). The role of the gut microbiota in nutrition and health. In *Nature Reviews Gastroenterology and Hepatology* (Vol. 9, Issue 10, pp. 577–589). Nat Rev Gastroenterol Hepatol. https://doi.org/10.1038/nrgastro.2012.156

Fontaine, C., Dubois, G., Duguay, Y., Helledie, T., Vu-Dac, N., Gervois, P., Soncin, F., Mandrup, S., Fruchart, J. C., Fruchart-Najib, J., & Staels, B. (2003). The orphan nuclear receptor Rev-Erbα is a peroxisome proliferator-activated receptor (PPAR) γ target gene and promotes PPARγ-induced adipocyte differentiation. *Journal of Biological Chemistry*, *278*(39), 37672–37680. https://doi.org/10.1074/jbc.M304664200

Forteza, R., Salathe, M., Miot, F., Forteza, R., & Conner, G. E. (2005). Regulated hydrogen peroxide production by duox in human airway epithelial cells. *American Journal of Respiratory Cell and Molecular Biology*, *32*(5), 462–469. https://doi.org/10.1165/rcmb.2004-0302OC

Frey-Klett, P., Burlinson, P., Deveau, A., Barret, M., Tarkka, M., & Sarniguet, A. (2011). Bacterial-fungal interactions: hyphens between agricultural, clinical, environmental, and food microbiologists. *Microbiology and Molecular Biology Reviews : MMBR*, *75*(4), 583–609. https://doi.org/10.1128/MMBR.00020-11

Fu, L., & Lee, C. C. (2003). The circadian clock: Pacemaker and tumour suppressor. In *Nature Reviews Cancer* (Vol. 3, Issue 5, pp. 350–361). Nature Publishing Group. https://doi.org/10.1038/nrc1072

Gachon, F., Olela, F. F., Schaad, O., Descombes, P., & Schibler, U. (2006). The circadian PAR-domain basic leucine zipper transcription factors DBP, TEF, and HLF modulate basal and inducible xenobiotic detoxification. *Cell Metabolism*, *4*(1), 25–36. https://doi.org/10.1016/j.cmet.2006.04.015

Garrett, W. S. (2015). Cancer and the microbiota. *Science*, *348*(6230), 80–86. https://doi.org/10.1126/science.aaa4972

Gaudier, E., Jarry, A., Blottière, H. M., De Coppet, P., Buisine, M. P., Aubert, J. P., Laboisse, C., Cherbut, C., & Hoebler, C. (2004). Butyrate specifically modulates MUC gene expression in intestinal epithelial goblet cells deprived of glucose. *American Journal of Physiology -*

Gastrointestinal and Liver Physiology, *287*(6 50-6).
https://doi.org/10.1152/ajpgi.00219.2004

Geiszt, M., & Leto, T. L. (2004). The Nox family of NAD(P)H oxidases: Host
defense and beyond. In *Journal of Biological Chemistry* (Vol. 279, Issue
50, pp. 51715–51718). American Society for Biochemistry and Molecular
Biology. https://doi.org/10.1074/jbc.R400024200

Geiszt, M., Witta, J., Baffi, J., Lekstrom, K., & Leto, T. L. (2003). Dual
oxidases represent novel hydrogen peroxide sources supporting mucosal
surface host defense. *The FASEB Journal : Official Publication of the
Federation of American Societies for Experimental Biology*, *17*(11), 1502–
1504. https://doi.org/10.1096/fj.02-1104fje

Giraffa, G., Chanishvili, N., & Widyastuti, Y. (2010). Importance of lactobacilli
in food and feed biotechnology. *Research in Microbiology*, *161*(6), 480–
487. https://doi.org/10.1016/j.resmic.2010.03.001

Gouba, N., & Drancourt, M. (2015). Digestive tract mycobiota: A source of
infection. In *Medecine et Maladies Infectieuses* (Vol. 45, Issues 1–2, pp.
9–16). Elsevier Masson SAS.
https://doi.org/10.1016/j.medmal.2015.01.007

Gow, N. A. R., Van De Veerdonk, F. L., Brown, A. J. P., & Netea, M. G.
(2012). *Candida albicans* morphogenesis and host defence:
Discriminating invasion from colonization. *Nature Reviews Microbiology*,
10(2), 112–122. https://doi.org/10.1038/nrmicro2711

Grasberger, H., & Refetoff, S. (2006). Identification of the maturation factor for
dual oxidase: Evolution of an eukaryotic operon equivalent. *Journal of
Biological Chemistry*, *281*(27), 18269–18272.
https://doi.org/10.1074/jbc.C600095200

Grice, E. A., Kong, H. H., Conlan, S., Deming, C. B., Davis, J., Young, A. C.,
Bouffard, G. G., Blakesley, R. W., Murray, P. R., Green, E. D., Turner, M.
L., & Segre, J. A. (2009). Topographical and temporal diversity of the
human skin microbiome. *Science*, *324*(5931), 1190–1192.
https://doi.org/10.1126/science.1171700

Griffin, E. A., Staknis, D., & Weitz, C. J. (1999). Light-independent role of
CRY1 and CRY2 in the mammalian circadian clock. *Science*, *286*(5440),
768–771. https://doi.org/10.1126/science.286.5440.768

Harbour, V. L., Weigl, Y., Robinson, B., & Amir, S. (2014). Phase differences
in expression of circadian clock genes in the central nucleus of the
amygdala, dentate gyrus, and suprachiasmatic nucleus in the rat. *PLoS
ONE*, *9*(7). https://doi.org/10.1371/journal.pone.0103309

Hastings, M. H., Maywood, E. S., & Brancaccio, M. (2018). Generation of
circadian rhythms in the suprachiasmatic nucleus. In *Nature Reviews*

Neuroscience (Vol. 19, Issue 8, pp. 453–469). Nature Publishing Group. https://doi.org/10.1038/s41583-018-0026-z

Hattrup, C. L., & Gendler, S. J. (2008). Structure and function of the cell surface (tethered) mucins. In *Annual Review of Physiology* (Vol. 70, pp. 431–457). Annu Rev Physiol. https://doi.org/10.1146/annurev.physiol.70.113006.100659

Herías, M. V., Hessle, C., Telemo, E., Midtvedt, T., Hanson, L. Å., & Wold, A. E. (1999). Immunomodulatory effects of Lactobacillus plantarum colonizing the intestine of gnotobiotic rats. *Clinical and Experimental Immunology*, *116*(2), 283–290. https://doi.org/10.1046/j.1365-2249.1999.00891.x

Hernday, A. D., Noble, S. M., Mitrovich, Q. M., & Johnson, A. D. (2010). Genetics and molecular biology in *Candida albicans*. *Methods in Enzymology*, *470*(C), 737–758. https://doi.org/10.1016/S0076-6879(10)70031-8

Herp, S., Brugiroux, S., Garzetti, D., Ring, D., Jochum, L. M., Beutler, M., Eberl, C., Hussain, S., Walter, S., Gerlach, R. G., Ruscheweyh, H. J., Huson, D., Sellin, M. E., Slack, E., Hanson, B., Loy, A., Baines, J. F., Rausch, P., Basic, M., … Stecher, B. (2019). Mucispirillum schaedleri Antagonizes Salmonella Virulence to Protect Mice against Colitis. *Cell Host and Microbe*, *25*(5), 681-694.e8. https://doi.org/10.1016/j.chom.2019.03.004

Hoffmann, C., Dollive, S., Grunberg, S., Chen, J., Li, H., Wu, G. D., Lewis, J. D., & Bushman, F. D. (2013). Archaea and Fungi of the Human Gut Microbiome: Correlations with Diet and Bacterial Residents. *PLoS ONE*, *8*(6). https://doi.org/10.1371/journal.pone.0066019

Hogan, D. A. (2006). Talking to themselves: Autoregulation and quorum sensing in fungi. In *Eukaryotic Cell* (Vol. 5, Issue 4, pp. 613–619). American Society for Microbiology (ASM). https://doi.org/10.1128/EC.5.4.613-619.2006

Hold, G. L., Smith, M., Grange, C., Watt, E. R., El-Omar, E. M., & Mukhopadhya, I. (2014). Role of the gut microbiota in inflammatory bowel disease pathogenesis: What have we learnt in the past 10 years? *World Journal of Gastroenterology*, *20*(5), 1192–1210. https://doi.org/10.3748/wjg.v20.i5.1192

Homann, O. R., Dea, J., Noble, S. M., & Johnson, A. D. (2009). A phenotypic profile of the *Candida albicans* regulatory network. *PLoS Genetics*, *5*(12). https://doi.org/10.1371/journal.pgen.1000783

Homann, O. R., & Johnson, A. D. (2010). MochiView: Versatile software for genome browsing and DNA motif analysis. *BMC Biology*, *8*, 49.

https://doi.org/10.1186/1741-7007-8-49

Hou, C., Zeng, X., Yang, F., Liu, H., & Qiao, S. (2015). Study and use of the probiotic *Lactobacillus reuteri* in pigs: A review. In *Journal of Animal Science and Biotechnology* (Vol. 6, Issue 1). BioMed Central Ltd. https://doi.org/10.1186/s40104-015-0014-3

Hoy-Schulz, Y. E., Jannat, K., Roberts, T., Zaidi, S. H., Unicomb, L., Luby, S., & Parsonnet, J. (2016). Safety and acceptability of *Lactobacillus reuteri* DSM 17938 and Bifidobacterium longum subspecies infantis 35624 in Bangladeshi infants: A phase I randomized clinical trial. *BMC Complementary and Alternative Medicine*, *16*(1). https://doi.org/10.1186/s12906-016-1016-1

Huang, G. (2012). Regulation of phenotypic transitions in the fungal pathogen *Candida albicans*. In *Virulence* (Vol. 3, Issue 3, pp. 251–261). Taylor and Francis Inc. https://doi.org/10.4161/viru.20010

Hube, B. (2004). From commensal to pathogen: Stage- and tissue-specific gene expression of *Candida albicans*. In *Current Opinion in Microbiology* (Vol. 7, Issue 4, pp. 336–341). Curr Opin Microbiol. https://doi.org/10.1016/j.mib.2004.06.003

Huttenhower, C., Gevers, D., Knight, R., Abubucker, S., Badger, J. H., Chinwalla, A. T., Creasy, H. H., Earl, A. M., Fitzgerald, M. G., Fulton, R. S., Giglio, M. G., Hallsworth-Pepin, K., Lobos, E. A., Madupu, R., Magrini, V., Martin, J. C., Mitreva, M., Muzny, D. M., Sodergren, E. J., … White, O. (2012a). Structure, function and diversity of the healthy human microbiome. *Nature*, *486*(7402), 207–214. https://doi.org/10.1038/nature11234

Huttenhower, C., Gevers, D., Knight, R., Abubucker, S., Badger, J. H., Chinwalla, A. T., Creasy, H. H., Earl, A. M., Fitzgerald, M. G., Fulton, R. S., Giglio, M. G., Hallsworth-Pepin, K., Lobos, E. A., Madupu, R., Magrini, V., Martin, J. C., Mitreva, M., Muzny, D. M., Sodergren, E. J., … White, O. (2012b). Structure, function and diversity of the healthy human microbiome. *Nature*, *486*(7402), 207–214. https://doi.org/10.1038/nature11234

Iliev, I. D., Funari, V. A., Taylor, K. D., Nguyen, Q., Reyes, C. N., Strom, S. P., Brown, J., Becker, C. A., Fleshner, P. R., Dubinsky, M., Rotter, J. I., Wang, H. L., McGovern, D. P. B., Brown, G. D., & Underhill, D. M. (2012). Interactions between commensal fungi and the C-type lectin receptor dectin-1 influence colitis. *Science*, *336*(6086), 1314–1317. https://doi.org/10.1126/science.1221789

Iliev, I. D., & Leonardi, I. (2017). Fungal dysbiosis: Immunity and interactions at mucosal barriers. In *Nature Reviews Immunology* (Vol. 17, Issue 10, pp. 635–646). Nature Publishing Group.

https://doi.org/10.1038/nri.2017.55

Itzkowitz, S. H., & Yio, X. (2004). Inflammation and cancer - IV. Colorectal cancer in inflammatory bowel disease: The role of inflammation. In *American Journal of Physiology - Gastrointestinal and Liver Physiology* (Vol. 287, Issues 1 50-1). American Physiological Society. https://doi.org/10.1152/ajpgi.00079.2004

Ivanov, I. I., Frutos, R. de L., Manel, N., Yoshinaga, K., Rifkin, D. B., Sartor, R. B., Finlay, B. B., & Littman, D. R. (2008). Specific Microbiota Direct the Differentiation of IL-17-Producing T-Helper Cells in the Mucosa of the Small Intestine. *Cell Host and Microbe*, *4*(4), 337–349. https://doi.org/10.1016/j.chom.2008.09.009

Jacobsen, I. D., Wilson, D., Wächtler, B., Brunke, S., Naglik, J. R., & Hube, B. (2014). *Expert Review of Anti-infective Therapy Candida albicans dimorphism as a therapeutic target*. https://doi.org/10.1586/eri.11.152

Jakobsson, H. E., Rodriguez-Pineiro, A. M., Schutte, A., Ermund, A., Boysen, P., Bemark, M., Sommer, F., Backhed, F., Hansson, G. C., & Johansson, M. E. (2015). The composition of the gut microbiota shapes the colon mucus barrier. *EMBO Reports*, *16*(2), 164–177. https://doi.org/10.15252/embr.201439263

Jiang, T. T., Shao, T. Y., Ang, W. X. G., Kinder, J. M., Turner, L. H., Pham, G., Whitt, J., Alenghat, T., & Way, S. S. (2017). Commensal Fungi Recapitulate the Protective Benefits of Intestinal Bacteria. *Cell Host and Microbe*, *22*(6), 809-816.e4. https://doi.org/10.1016/j.chom.2017.10.013

Johansson, M. E. V., & Hansson, G. C. (2016). Immunological aspects of intestinal mucus and mucins. In *Nature Reviews Immunology* (Vol. 16, Issue 10). https://doi.org/10.1038/nri.2016.88

Johansson, M. E. V., Holmén Larsson, J. M., & Hansson, G. C. (2011). The two mucus layers of colon are organized by the MUC2 mucin, whereas the outer layer is a legislator of host-microbial interactions. *Proceedings of the National Academy of Sciences of the United States of America*, *108*(SUPPL. 1), 4659–4665. https://doi.org/10.1073/pnas.1006451107

Johansson, M. E. V., Jakobsson, H. E., Holmén-Larsson, J., Schütte, A., Ermund, A., Rodríguez-Piñeiro, A. M., Arike, L., Wising, C., Svensson, F., Bäckhed, F., & Hansson, G. C. (2015). Normalization of host intestinal mucus layers requires long-term microbial colonization. *Cell Host and Microbe*, *18*(5), 582–592. https://doi.org/10.1016/j.chom.2015.10.007

Johansson, M. E. V., Phillipson, M., Petersson, J., Velcich, A., Holm, L., & Hansson, G. C. (2008). The inner of the two Muc2 mucin-dependent mucus layers in colon is devoid of bacteria. *Proceedings of the National Academy of Sciences of the United States of America, 105*(39), 15064–

15069. https://doi.org/10.1073/pnas.0803124105

Johansson, M. E. V., Sjövall, H., & Hansson, G. C. (2013). The gastrointestinal mucus system in health and disease. In *Nature Reviews Gastroenterology and Hepatology* (Vol. 10, Issue 6, pp. 352–361). Nat Rev Gastroenterol Hepatol. https://doi.org/10.1038/nrgastro.2013.35

Johansson, M. E. V., Larsson, J. M. H., & Hansson, G. C. (2011). The two mucus layers of colon are organized by the MUC2 mucin, whereas the outer layer is a legislator of host-microbial interactions. *Proceedings of the National Academy of Sciences*, *108*(Supplement_1), 4659–4665. https://doi.org/10.1073/pnas.1006451107

Johansson, Malin E V, Gustafsson, J. K., Holmen-Larsson, J., Jabbar, K. S., Xia, L., Xu, H., Ghishan, F. K., Carvalho, F. A., Gewirtz, A. T., Sjovall, H., & Hansson, G. C. (2014). Bacteria penetrate the normally impenetrable inner colon mucus layer in both murine colitis models and patients with ulcerative colitis. *Gut*, *63*(2), 281–291. https://doi.org/10.1136/gutjnl-2012-303207

Jones, R. M., Mercante, J. W., & Neish, A. S. (2012). Reactive oxygen production induced by the gut microbiota: pharmacotherapeutic implications. *Current Medicinal Chemistry*, *19*(10), 1519–1529. https://doi.org/10.2174/092986712799828283

Kamada, N., Seo, S. U., Chen, G. Y., & Núñez, G. (2013). Role of the gut microbiota in immunity and inflammatory disease. In *Nature Reviews Immunology* (Vol. 13, Issue 5, pp. 321–335). https://doi.org/10.1038/nri3430

Karantanos, T., Theodoropoulos, G., Pektasides, D., & Gazouli, M. (2014). Clock genes: Their role in colorectal cancer. *World Journal of Gastroenterology*, *20*(8), 1986–1992. https://doi.org/10.3748/wjg.v20.i8.1986

Kasubuchi, M., Hasegawa, S., Hiramatsu, T., Ichimura, A., & Kimura, I. (2015). Dietary gut microbial metabolites, short-chain fatty acids, and host metabolic regulation. In *Nutrients* (Vol. 7, Issue 4, pp. 2839–2849). MDPI AG. https://doi.org/10.3390/nu7042839

Kervezee, L., Shechter, A., & Boivin, D. B. (2018). Impact of Shift Work on the Circadian Timing System and Health in Women. In *Sleep Medicine Clinics* (Vol. 13, Issue 3, pp. 295–306). W.B. Saunders. https://doi.org/10.1016/j.jsmc.2018.04.003

Khan, I., Ullah, N., Zha, L., Bai, Y., Khan, A., Zhao, T., Che, T., & Zhang, C. (2019). Alteration of gut microbiota in inflammatory bowel disease (IBD): Cause or consequence? IBD treatment targeting the gut microbiome. In *Pathogens* (Vol. 8, Issue 3). MDPI AG.

https://doi.org/10.3390/pathogens8030126

Kim, J. H., Lyu, Y. S., & Kim, S. Y. (2020). Impact of social jetlag on weight change in adults: Korean national health and nutrition examination survey 2016–2017. *International Journal of Environmental Research and Public Health*, *17*(12), 1–12. https://doi.org/10.3390/ijerph17124383

Kim, J., & Sudbery, P. (2011). *Candida albicans*, a major human fungal pathogen. In *Journal of Microbiology* (Vol. 49, Issue 2, pp. 171–177). J Microbiol. https://doi.org/10.1007/s12275-011-1064-7

Klotz, S. A., Chasin, B. S., Powell, B., Gaur, N. K., & Lipke, P. N. (2007). Polymicrobial bloodstream infections involving Candida species: analysis of patients and review of the literature. *Diagnostic Microbiology and Infectious Disease*, *59*(4), 401–406. https://doi.org/10.1016/j.diagmicrobio.2007.07.001

Koch, B., Barugahare, A. A., Lo, T. L., Huang, C., Schittenhelm, R. B., Powell, D. R., Beilharz, T. H., & Traven, A. (2018). A Metabolic Checkpoint for the Yeast-to-Hyphae Developmental Switch Regulated by Endogenous Nitric Oxide Signaling. *Cell Reports*, *25*(8), 2244-2258.e7. https://doi.org/10.1016/j.celrep.2018.10.080

Koh, A. Y. (2013). Murine models of Candida gastrointestinal colonization and dissemination. In *Eukaryotic Cell* (Vol. 12, Issue 11, pp. 1416–1422). American Society for Microbiology (ASM). https://doi.org/10.1128/EC.00196-13

Koh, A. Y. (2017). Potential for monitoring gut microbiota for diagnosing infections and graft-versus-host disease in cancer and stem cell transplant patients. In *Clinical Chemistry* (Vol. 63, Issue 11, pp. 1685–1694). American Association for Clinical Chemistry Inc. https://doi.org/10.1373/clinchem.2016.259499

Koo, H., Andes, D. R., & Krysan, D. J. (2018). Candida–streptococcal interactions in biofilm-associated oral diseases. *PLOS Pathogens*, *14*(12), e1007342. https://doi.org/10.1371/journal.ppat.1007342

Kumamoto, C. A., Gresnigt, M. S., & Hube, B. (2020). The gut, the bad and the harmless: *Candida albicans* as a commensal and opportunistic pathogen in the intestine. In *Current Opinion in Microbiology* (Vol. 56, pp. 7–15). Elsevier Ltd. https://doi.org/10.1016/j.mib.2020.05.006

Kumamoto, C. A., & Vinces, M. D. (2005). Contributions of hyphae and hypha-co-regulated genes to *Candida albicans* virulence. In *Cellular Microbiology* (Vol. 7, Issue 11, pp. 1546–1554). Cell Microbiol. https://doi.org/10.1111/j.1462-5822.2005.00616.x

Kume, K., Zylka, M. J., Sriram, S., Shearman, L. P., Weaver, D. R., Jin, X., Maywood, E. S., Hastings, M. H., & Reppert, S. M. (1999). mCRY1 and

mCRY2 are essential components of the negative limb of the circadian clock feedback loop. *Cell*, *98*(2), 193–205. https://doi.org/10.1016/S0092-8674(00)81014-4

Lam, S., Zuo, T., Ho, M., Chan, F. K. L., Chan, P. K. S., & Ng, S. C. (2019). Review article: fungal alterations in inflammatory bowel diseases. In *Alimentary Pharmacology and Therapeutics* (Vol. 50, Issues 11–12, pp. 1159–1171). Blackwell Publishing Ltd. https://doi.org/10.1111/apt.15523

Lamont, R. J., & Hajishengallis, G. (2015). Polymicrobial synergy and dysbiosis in inflammatory disease. In *Trends in Molecular Medicine* (Vol. 21, Issue 3, pp. 172–183). Elsevier Ltd. https://doi.org/10.1016/j.molmed.2014.11.004

Lauer, A., Simon, M. A., Banning, J. L., André, E., Duncan, K., & Harris, R. N. (2007). Common cutaneous bacteria from the eastern red-backed salamander can inhibit pathogenic fungi. *Copeia*, *2007*(3), 630–640. https://doi.org/10.1643/0045-8511(2007)2007[630:CCBFTE]2.0.CO;2

Ley, R. E., Hamady, M., Lozupone, C., Turnbaugh, P. J., Ramey, R. R., Bircher, J. S., Schlegel, M. L., Tucker, T. A., Schrenzel, M. D., Knight, R., & Gordon, J. I. (2008). Evolution of mammals and their gut microbes. *Science*, *320*(5883), 1647–1651. https://doi.org/10.1126/science.1155725

Li, H., Limenitakis, J. P., Fuhrer, T., Geuking, M. B., Lawson, M. A., Wyss, M., Brugiroux, S., Keller, I., Macpherson, J. A., Rupp, S., Stolp, B., Stein, J. V., Stecher, B., Sauer, U., McCoy, K. D., & Macpherson, A. J. (2015a). The outer mucus layer hosts a distinct intestinal microbial niche. *Nature Communications*, *6*(May). https://doi.org/10.1038/ncomms9292

Li, H., Limenitakis, J. P., Fuhrer, T., Geuking, M. B., Lawson, M. A., Wyss, M., Brugiroux, S., Keller, I., Macpherson, J. A., Rupp, S., Stolp, B., Stein, J. V., Stecher, B., Sauer, U., McCoy, K. D., & Macpherson, A. J. (2015b). The outer mucus layer hosts a distinct intestinal microbial niche. *Nature Communications*, *6*. https://doi.org/10.1038/ncomms9292

Li, J., Chen, D., Yu, B., He, J., Zheng, P., Mao, X., Yu, J., Luo, J., Tian, G., Huang, Z., & Luo, Y. (2018). Fungi in Gastrointestinal Tracts of Human and Mice: from Community to Functions. In *Microbial Ecology* (Vol. 75, Issue 4, pp. 821–829). Springer New York LLC. https://doi.org/10.1007/s00248-017-1105-9

Li, X. V., Leonardi, I., & Iliev, I. D. (2019). Gut Mycobiota in Immunity and Inflammatory Disease. In *Immunity* (Vol. 50, Issue 6, pp. 1365–1379). Cell Press. https://doi.org/10.1016/j.immuni.2019.05.023

Limon, J. J., Skalski, J. H., & Underhill, D. M. (2017). Commensal Fungi in Health and Disease. In *Cell Host and Microbe* (Vol. 22, Issue 2, pp. 156–165). Cell Press. https://doi.org/10.1016/j.chom.2017.07.002

Linares, D. M., Gómez, C., Renes, E., Fresno, J. M., Tornadijo, M. E., Ross, R. P., & Stanton, C. (2017). Lactic Acid Bacteria and Bifidobacteria with Potential to Design Natural Biofunctional Health-Promoting Dairy Foods. In *Frontiers in Microbiology* (Vol. 8, Issue MAY, p. 846). Frontiers Media S.A. https://doi.org/10.3389/fmicb.2017.00846

Linden, S. K., Sutton, P., Karlsson, N. G., Korolik, V., & McGuckin, M. A. (2008). Mucins in the mucosal barrier to infection. In *Mucosal Immunology* (Vol. 1, Issue 3, pp. 183–197). Nature Publishing Group. https://doi.org/10.1038/mi.2008.5

Lipinski, S., Till, A., Sina, C., Arlt, A., Grasberger, H., Schreiber, S., & Rosenstiel, P. (2009). DUOX2-derived reactive oxygen species are effectors of NOD2-mediated antibacterial responses. *Journal of Cell Science*, *122*(19), 3522–3530. https://doi.org/10.1242/jcs.050690

Loonen, L. M. P., Stolte, E. H., Jaklofsky, M. T. J., Meijerink, M., Dekker, J., Van Baarlen, P., & Wells, J. M. (2014). REG3γ-deficient mice have altered mucus distribution and increased mucosal inflammatory responses to the microbiota and enteric pathogens in the ileum. *Mucosal Immunology*, *7*(4), 939–947. https://doi.org/10.1038/mi.2013.109

Love, M. I., Huber, W., & Anders, S. (2014). Moderated estimation of fold change and dispersion for RNA-seq data with DESeq2. *Genome Biology*, *15*(12), 550. https://doi.org/10.1186/s13059-014-0550-8

Lu, Y., Su, C., & Liu, H. (2014). *Candida albicans* hyphal initiation and elongation. In *Trends in Microbiology* (Vol. 22, Issue 12, pp. 707–714). Elsevier Ltd. https://doi.org/10.1016/j.tim.2014.09.001

Macfarlane, S., & Macfarlane, G. T. (2003). Regulation of short-chain fatty acid production. *Proceedings of the Nutrition Society*, *62*(1), 67–72. https://doi.org/10.1079/pns2002207

MacFie, T. S., Poulsom, R., Parker, A., Warnes, G., Boitsova, T., Nijhuis, A., Suraweera, N., Poehlmann, A., Szary, J., Feakins, R., Jeffery, R., Harper, R. W., Jubb, A. M., Lindsay, J. O., & Silver, A. (2014). DUOX2 and DUOXA2 form the predominant enzyme system capable of producing the reactive oxygen species H2O2 in active ulcerative colitis and are modulated by 5-aminosalicylic acid. *Inflammatory Bowel Diseases*, *20*(3), 514–524. https://doi.org/10.1097/01.MIB.0000442012.45038.0e

Makki, K., Deehan, E. C., Walter, J., & Bäckhed, F. (2018). The Impact of Dietary Fiber on Gut Microbiota in Host Health and Disease. In *Cell Host and Microbe* (Vol. 23, Issue 6, pp. 705–715). Cell Press. https://doi.org/10.1016/j.chom.2018.05.012

Mar Rodríguez, M., Pérez, D., Javier Chaves, F., Esteve, E., Marin-Garcia, P., Xifra, G., Vendrell, J., Jové, M., Pamplona, R., Ricart, W., Portero-Otin,

M., Chacón, M. R., & Fernández Real, J. M. (2015). Obesity changes the human gut mycobiome. *Scientific Reports*, *5*(1), 14600. https://doi.org/10.1038/srep14600

Martens, E. C., Chiang, H. C., & Gordon, J. I. (2008). Mucosal Glycan Foraging Enhances Fitness and Transmission of a Saccharolytic Human Gut Bacterial Symbiont. *Cell Host and Microbe*, *4*(5), 447–457. https://doi.org/10.1016/j.chom.2008.09.007

Mason, K. L., Downward, J. R. E., Falkowski, N. R., Young, V. B., Kao, J. Y., & Huffnagle, G. B. (2012). Interplay between the gastric bacterial microbiota and *Candida albicans* during postantibiotic recolonization and gastritis. *Infection and Immunity*, *80*(1), 150–158. https://doi.org/10.1128/IAI.05162-11

Meir, J., Hartmann, E., Eckstein, M., Guiducci, E., Kirchner, F., Rosenwald, A., LeibundGut-Landmann, S., & Pérez, J. C. (2018). Identification of *Candida albicans* regulatory genes governing mucosal infection. *Cellular Microbiology*, *20*(8). https://doi.org/10.1111/cmi.12841

Methé, B. A., Nelson, K. E., Pop, M., Creasy, H. H., Giglio, M. G., Huttenhower, C., Gevers, D., Petrosino, J. F., Abubucker, S., Badger, J. H., Chinwalla, A. T., Earl, A. M., Fitzgerald, M. G., Fulton, R. S., Hallsworth-Pepin, K., Lobos, E. A., Madupu, R., Magrini, V., Martin, J. C., … White, O. (2012). A framework for human microbiome research. *Nature*, *486*(7402), 215–221. https://doi.org/10.1038/nature11209

Millsop, J. W., & Fazel, N. (2016). Oral candidiasis. *Clinics in Dermatology*, *34*(4), 487–494. https://doi.org/10.1016/j.clindermatol.2016.02.022

Mitsui, S., Yamaguchi, S., Matsuo, T., Ishida, Y., & Okamura, H. (2001). Antagonistic role of E4BP4 and PAR proteins in the circadian oscillatory mechanism. *Genes and Development*, *15*(8), 995–1006. https://doi.org/10.1101/gad.873501

Mohawk, J. A., Green, C. B., & Takahashi, J. S. (2012). Central and peripheral circadian clocks in mammals. In *Annual Review of Neuroscience* (Vol. 35, pp. 445–462). Annu Rev Neurosci. https://doi.org/10.1146/annurev-neuro-060909-153128

Morris, C. J., Purvis, T. E., Mistretta, J., Hu, K., & Scheer, F. A. J. L. (2017). Circadian Misalignment Increases C-Reactive Protein and Blood Pressure in Chronic Shift Workers. *Journal of Biological Rhythms*, *32*(2), 154–164. https://doi.org/10.1177/0748730417697537

Mukherjee, P. K., Sendid, B., Hoarau, G., Colombel, J. F., Poulain, D., & Ghannoum, M. A. (2015). Mycobiota in gastrointestinal diseases. In *Nature Reviews Gastroenterology and Hepatology* (Vol. 12, Issue 2, pp. 77–87). Nature Publishing Group.

https://doi.org/10.1038/nrgastro.2014.188

Narumi, R., Shimizu, Y., Ukai-Tadenuma, M., Ode, K. L., Kanda, G. N., Shinohara, Y., Sato, A., Matsumoto, K., & Ueda, H. R. (2016). Mass spectrometry-based absolute quantification reveals rhythmic variation of mouse circadian clock proteins. *Proceedings of the National Academy of Sciences*, *113*(24), E3461–E3467. https://doi.org/10.1073/pnas.1603799113

Navabi, N., McGuckin, M. A., & Lindén, S. K. (2013). Gastrointestinal Cell Lines Form Polarized Epithelia with an Adherent Mucus Layer when Cultured in Semi-Wet Interfaces with Mechanical Stimulation. *PLoS ONE*, *8*(7). https://doi.org/10.1371/journal.pone.0068761

Navarro-Garcia, F., Gutierrez-Jimenez, J., Garcia-Tovar, C., Castro, L. A., Salazar-Gonzalez, H., & Cordova, V. (2010). Pic, an autotransporter protein secreted by different pathogens in the Enterobacteriaceae family, is a potent mucus secretagogue. *Infection and Immunity*, *78*(10), 4101–4109. https://doi.org/10.1128/IAI.00523-10

Netea, M. G., Joosten, L. A. B., Van Der Meer, J. W. M., Kullberg, B. J., & Van De Veerdonk, F. L. (2015). Immune defence against Candida fungal infections. In *Nature Reviews Immunology* (Vol. 15, Issue 10, pp. 630–642). Nature Publishing Group. https://doi.org/10.1038/nri3897

Neville, B. A., d'Enfert, C., & Bougnoux, M. E. (2015). *Candida albicans* commensalism in the gastrointestinal tract. In *FEMS yeast research* (Vol. 15, Issue 7). https://doi.org/10.1093/femsyr/fov081

Noble, S. M., Gianetti, B. A., & Witchley, J. N. (2017). *Candida albicans* cell-type switching and functional plasticity in the mammalian host. In *Nature Reviews Microbiology* (Vol. 15, Issue 2, pp. 96–108). Nature Publishing Group. https://doi.org/10.1038/nrmicro.2016.157

Nugent, S. G., Kumar, D., Rampton, D. S., & Evans, D. F. (2001). Intestinal luminal pH in inflammatory bowel disease: Possible determinants and implications for therapy with aminosalicylates and other drugs. In *Gut* (Vol. 48, Issue 4, pp. 571–577). BMJ Publishing Group. https://doi.org/10.1136/gut.48.4.571

Ohkusa, T., Okayasu, I., Ogihara, T., Morita, K., Ogawa, M., & Sato, N. (2003). Induction of experimental ulcerative colitis by Fusobacterium varium isolated from colonic mucosa of patients with ulcerative colitis. *Gut*, *52*(1), 79–83. https://doi.org/10.1136/gut.52.1.79

Panda, S., Antoch, M. P., Miller, B. H., Su, A. I., Schook, A. B., Straume, M., Schultz, P. G., Kay, S. A., Takahashi, J. S., & Hogenesch, J. B. (2002). Coordinated transcription of key pathways in the mouse by the circadian clock. *Cell*, *109*(3), 307–320. https://doi.org/10.1016/S0092-

8674(02)00722-5

Pande, K., Chen, C., & Noble, S. M. (2013). Passage through the mammalian gut triggers a phenotypic switch that promotes *Candida albicans* commensalism. *Nature Genetics*, *45*(9), 1088–1091. https://doi.org/10.1038/ng.2710

Partch, C. L., Green, C. B., & Takahashi, J. S. (2014). Molecular architecture of the mammalian circadian clock. In *Trends in Cell Biology* (Vol. 24, Issue 2, pp. 90–99). Trends Cell Biol. https://doi.org/10.1016/j.tcb.2013.07.002

Pelaseyed, T., Bergström, J. H., Gustafsson, J. K., Ermund, A., Birchenough, G. M. H., Schütte, A., van der Post, S., Svensson, F., Rodríguez-Piñeiro, A. M., Nyström, E. E. L., Wising, C., Johansson, M. E. V., & Hansson, G. C. (2014). The mucus and mucins of the goblet cells and enterocytes provide the first defense line of the gastrointestinal tract and interact with the immune system. In *Immunological Reviews* (Vol. 260, Issue 1, pp. 8–20). Blackwell Publishing Ltd. https://doi.org/10.1111/imr.12182

Peleg, A. Y., Hogan, D. A., & Mylonakis, E. (2010). Medically important bacterialg-fungal interactions. In *Nature Reviews Microbiology* (Vol. 8, Issue 5, pp. 340–349). Nature Publishing Group. https://doi.org/10.1038/nrmicro2313

Pérez, J. C. (2019). *Candida albicans* dwelling in the mammalian gut. In *Current Opinion in Microbiology* (Vol. 52, pp. 41–46). Elsevier Ltd. https://doi.org/10.1016/j.mib.2019.04.007

Pérez, J. C., & Johnson, A. D. (2013). Regulatory Circuits That Enable Proliferation of the Fungus *Candida albicans* in a Mammalian Host. *PLoS Pathogens*, *9*(12), 1–3. https://doi.org/10.1371/journal.ppat.1003780

Phillips, A. W., & Balish, E. (1966). Growth and invasiveness of *Candida albicans* in the germ-free and conventional mouse after oral challenge. *Applied Microbiology*, *14*(5), 737–741. https://doi.org/10.1128/aem.14.5.737-741.1966

Pickard, J. M., Zeng, M. Y., Caruso, R., & Núñez, G. (2017). Gut microbiota: Role in pathogen colonization, immune responses, and inflammatory disease. In *Immunological Reviews* (Vol. 279, Issue 1, pp. 70–89). Blackwell Publishing Ltd. https://doi.org/10.1111/imr.12567

Pihet, M., Carrere, J., Cimon, B., Chabasse, D., Delhaes, L., Symoens, F., & Bouchara, J. P. (2009). Occurrence and relevance of filamentous fungi in respiratory secretions of patients with cystic fibrosis - A review. *Medical Mycology*, *47*(4), 387–397. https://doi.org/10.1080/13693780802609604

Polvi, E. J., Li, X., O'Meara, T. R., Leach, M. D., & Cowen, L. E. (2015). Opportunistic yeast pathogens: Reservoirs, virulence mechanisms, and

therapeutic strategies. *Cellular and Molecular Life Sciences*, *72*(12), 2261–2287. https://doi.org/10.1007/s00018-015-1860-z

Power, S. E., O'Toole, P. W., Stanton, C., Ross, R. P., & Fitzgerald, G. F. (2014). Intestinal microbiota, diet and health. In *British Journal of Nutrition* (Vol. 111, Issue 3, pp. 387–402). Br J Nutr. https://doi.org/10.1017/S0007114513002560

Preitner, N., Damiola, F., Luis-Lopez-Molina, Zakany, J., Duboule, D., Albrecht, U., & Schibler, U. (2002). The orphan nuclear receptor REV-ERBα controls circadian transcription within the positive limb of the mammalian circadian oscillator. *Cell*, *110*(2), 251–260. https://doi.org/10.1016/S0092-8674(02)00825-5

Reid, G. (2004). When microbe meets human. In *Clinical Infectious Diseases* (Vol. 39, Issue 6, pp. 827–830). Oxford Academic. https://doi.org/10.1086/423387

Richard, M. L., Liguori, G., Lamas, B., Brandi, G., da Costa, G., Hoffmann, T. W., Pierluigi Di Simone, M., Calabrese, C., Poggioli, G., Langella, P., Campieri, M., & Sokol, H. (2018). Mucosa-associated microbiota dysbiosis in colitis associated cancer. *Gut Microbes*, *9*(2), 131–142. https://doi.org/10.1080/19490976.2017.1379637

Richardson, J. P., & Moyes, D. L. (2015). Adaptive immune responses to *Candida albicans* infection. *Virulence*, *6*(4), 327–337. https://doi.org/10.1080/21505594.2015.1004977

Ridley, C., & Thornton, D. J. (2018). Mucins: The frontline defence of the lung. In *Biochemical Society Transactions* (Vol. 46, Issue 5, pp. 1099–1106). Portland Press Ltd. https://doi.org/10.1042/BST20170402

Roberton, A. M., & Stanley, R. A. (1982). *In vitro* utilization of mucin by Bacteroides fragilis. *Applied and Environmental Microbiology*, *43*(2), 325–330.

Rogers, T. E., Pudlo, N. A., Koropatkin, N. M., Bell, J. S. K., Moya Balasch, M., Jasker, K., & Martens, E. C. (2013). Dynamic responses of *Bacteroides thetaiotaomicron* during growth on glycan mixtures. *Molecular Microbiology*, *88*(5), 876–890. https://doi.org/10.1111/mmi.12228

Round, J. L., & Mazmanian, S. K. (2009). The gut microbiota shapes intestinal immune responses during health and disease. In *Nature Reviews Immunology* (Vol. 9, Issue 5, pp. 313–323). Nat Rev Immunol. https://doi.org/10.1038/nri2515

Sahar, S., & Sassone-Corsi, P. (2009). Metabolism and cancer: The circadian clock connection. In *Nature Reviews Cancer* (Vol. 9, Issue 12, pp. 886–896). Nat Rev Cancer. https://doi.org/10.1038/nrc2747

Savage, D. C. (1969). Microbial interference between indigenous yeast and lactobacilli in the rodent stomach. *Journal of Bacteriology, 98*(3), 1278–1283. http://www.ncbi.nlm.nih.gov/pubmed/5788704

Saville, S. P., Lazzell, A. L., Monteagudo, C., & Lopez-Ribot, J. L. (2003). Engineered control of cell morphology *in vivo* reveals distinct roles for yeast and filamentous forms of *Candida albicans* during infection. *Eukaryotic Cell, 2*(5), 1053–1060. https://doi.org/10.1128/EC.2.5.1053-1060.2003

SCHAEDLER, R. W., DUBS, R., & COSTELLO, R. (1965). ASSOCIATION OF GERMFREE MICE WITH BACTERIA ISOLATED FROM NORMAL MICE. *The Journal of Experimental Medicine, 122*(1), 77–82. https://doi.org/10.1084/jem.122.1.77

Schaubeck, M., Clavel, T., Calasan, J., Lagkouvardos, I., Haange, S. B., Jehmlich, N., Basic, M., Dupont, A., Hornef, M., Von Bergen, M., Bleich, A., & Haller, D. (2016). Dysbiotic gut microbiota causes transmissible Crohn's disease-like ileitis independent of failure in antimicrobial defence. *Gut, 65*(2), 225–237. https://doi.org/10.1136/gutjnl-2015-309333

Schroeder, B. O. (2019a). Fight them or feed them: how the intestinal mucus layer manages the gut microbiota. *Gastroenterology Report, 7*(1), 3. https://doi.org/10.1093/gastro/goy052

Schroeder, B. O. (2019b). Fight them or feed them: How the intestinal mucus layer manages the gut microbiota. *Gastroenterology Report, 7*(1), 3–12. https://doi.org/10.1093/gastro/goy052

Schulze, J., & Sonnenborn, U. (2009). Übersichtsarbeit: Pilze im Darm - Von kommensalen untermietern zu infektions - erregern. In *Deutsches Arzteblatt* (Vol. 106, Issues 51–52, pp. 837–842). Deutscher Arzte-Verlag GmbH. https://doi.org/10.3238/arztebl.2009.0837

Schwalm, N. D., Townsend, G. E., & Groisman, E. A. (2017). Prioritization of polysaccharide utilization and control of regulator activation in *Bacteroides thetaiotaomicron. Molecular Microbiology, 104*(1), 32–45. https://doi.org/10.1111/mmi.13609

Sedelnikova, O. A., Redon, C. E., Dickey, J. S., Nakamura, A. J., Georgakilas, A. G., & Bonner, W. M. (2010). Role of oxidatively induced DNA lesions in human pathogenesis. In *Mutation Research - Reviews in Mutation Research* (Vol. 704, Issues 1–3, pp. 152–159). Mutat Res. https://doi.org/10.1016/j.mrrev.2009.12.005

Silva, A. J., Pham, K., & Benitez, J. A. (2003). Haemagglutinin/protease expression and mucin gel penetration in El Tor biotype Vibrio cholerae. In *Microbiology* (Vol. 149, Issue 7, pp. 1883–1891). Society for General Microbiology. https://doi.org/10.1099/mic.0.26086-0

Simon, G. L., & Gorbach, S. L. (1986). The human intestinal microflora. *Digestive Diseases and Sciences*, *31*(9), 147–162. https://doi.org/10.1007/BF01295996

Sinkiewicz, G., Cronholm, S., Ljunggren, L., Dahlén, G., & Bratthall, G. (2010). Influence of dietary supplementation with *Lactobacillus reuteri* on the oral flora of healthy subjects. *Swedish Dental Journal*, *34*(4), 197–206. https://pubmed.ncbi.nlm.nih.gov/21306085/

Sokol, H., Leducq, V., Aschard, H., Pham, H. P., Jegou, S., Landman, C., Cohen, D., Liguori, G., Bourrier, A., Nion-Larmurier, I., Cosnes, J., Seksik, P., Langella, P., Skurnik, D., Richard, M. L., & Beaugerie, L. (2017a). Fungal microbiota dysbiosis in IBD. *Gut*, *66*(6), 1039–1048. https://doi.org/10.1136/gutjnl-2015-310746

Sokol, H., Leducq, V., Aschard, H., Pham, H. P., Jegou, S., Landman, C., Cohen, D., Liguori, G., Bourrier, A., Nion-Larmurier, I., Cosnes, J., Seksik, P., Langella, P., Skurnik, D., Richard, M. L., & Beaugerie, L. (2017b). Fungal microbiota dysbiosis in IBD. *Gut*, *66*(6), 1039–1048. https://doi.org/10.1136/gutjnl-2015-310746

Soll, A. H., & Fass, R. (2003). Gastroesophageal reflux disease: Presentation and assessment of a common, challenging disorder. *Clinical Cornerstone*, *5*(4), 2–14. https://doi.org/10.1016/S1098-3597(03)90095-0

Soll, D. R. (2014). The role of phenotypic switching in the basic biology and pathogenesis of *Candida albicans*. In *Journal of Oral Microbiology* (Vol. 6, Issue 1, pp. 1–12). Co-Action Publishing. https://doi.org/10.3402/jom.v6.22993

Sommer, F., & Bäckhed, F. (2015). The gut microbiota engages different signaling pathways to induce Duox2 expression in the ileum and colon epithelium. *Mucosal Immunology*, *8*(2), 372–379. https://doi.org/10.1038/mi.2014.74

Sonnenburg, J. L., Xu, J., Leip, D. D., Chen, C. H., Westover, B. P., Weatherford, J., Buhler, J. D., & Gordon, J. I. (2005a). Glycan foraging *in vivo* by an intestine-adapted bacterial symbiont. *Science, 307*(5717), 1955–1959. https://doi.org/10.1126/science.1109051

Sonnenburg, J. L., Xu, J., Leip, D. D., Chen, C. H., Westover, B. P., Weatherford, J., Buhler, J. D., & Gordon, J. I. (2005b). Glycan foraging *in vivo* by an intestine-adapted bacterial symbiont. *Science*, *307*(5717), 1955–1959. https://doi.org/10.1126/science.1109051

Spinler, J. K., Taweechotipatr, M., Rognerud, C. L., Ou, C. N., Tumwasorn, S., & Versalovic, J. (2008). Human-derived probiotic *Lactobacillus reuteri* demonstrate antimicrobial activities targeting diverse enteric bacterial pathogens. *Anaerobe*, *14*(3), 166–171.

https://doi.org/10.1016/j.anaerobe.2008.02.001

Stecher, B., Hapfelmeier, S., Müller, C., Kremer, M., Stallmach, T., & Hardt, W. D. (2004). Flagella and chemotaxis are required for efficient induction of Salmonella enterica serovar typhimurium colitis in streptomycin-pretreated mice. *Infection and Immunity*, *72*(7), 4138–4150. https://doi.org/10.1128/IAI.72.7.4138-4150.2004

Swidsinski, A., Loening-Baucke, V., Verstraelen, H., Osowska, S., & Doerffel, Y. (2008). Biostructure of Fecal Microbiota in Healthy Subjects and Patients With Chronic Idiopathic Diarrhea. *Gastroenterology*, *135*(2). https://doi.org/10.1053/j.gastro.2008.04.017

Talarico, T. L., & Dobrogosz, W. J. (1989). Chemical characterization of an antimicrobial substance produced by *Lactobacillus reuteri*. *Antimicrobial Agents and Chemotherapy*, *33*(5), 674–679. https://doi.org/10.1128/AAC.33.5.674

Thaiss, C. A., Zeevi, D., Levy, M., Segal, E., & Elinav, E. (2015). A day in the life of the meta-organism: Diurnal rhythms of the intestinal microbiome and its host. *Gut Microbes*, *6*(2), 137–142. https://doi.org/10.1080/19490976.2015.1016690

Thursby, E., & Juge, N. (2017). Introduction to the human gut microbiota. In *Biochemical Journal* (Vol. 474, Issue 11, pp. 1823–1836). Portland Press Ltd. https://doi.org/10.1042/BCJ20160510

Tropini, C., Earle, K. A., Huang, K. C., & Sonnenburg, J. L. (2017). The Gut Microbiome: Connecting Spatial Organization to Function. In *Cell Host and Microbe* (Vol. 21, Issue 4, pp. 433–442). Cell Press. https://doi.org/10.1016/j.chom.2017.03.010

Tu, B. P., Kudlicki, A., Rowicka, M., & McKnight, S. L. (2005). Cell biology: Logic of the yeast metabolic cycle: Temporal compartmentalization of cellular processes. *Science*, *310*(5751), 1152–1158. https://doi.org/10.1126/science.1120499

Tubelius, P., Stan, V., & Zachrisson, A. (2005). Increasing work-place healthiness with the probiotic *Lactobacillus reuteri*: A randomised, double-blind placebo-controlled study. *Environmental Health: A Global Access Science Source*, *4*. https://doi.org/10.1186/1476-069X-4-25

Underhill, D. M., & Iliev, I. D. (2014). The mycobiota: Interactions between commensal fungi and the host immune system. In *Nature Reviews Immunology* (Vol. 14, Issue 6, pp. 405–416). Nature Publishing Group. https://doi.org/10.1038/nri3684

Vaishnava, S., Yamamoto, M., Severson, K. M., Ruhn, K. A., Yu, X., Koren, O., Ley, R., Wakeland, E. K., & Hooper, L. V. (2011). The antibacterial lectin RegIIIγ promotes the spatial segregation of microbiota and host in

the intestine. *Science*, *334*(6053), 255–258.
https://doi.org/10.1126/science.1209791

Valeur, N., Engel, P., Carbajal, N., Connolly, E., & Ladefoged, K. (2004).
Colonization and Immunomodulation by *Lactobacillus reuteri* ATCC
55730 in the Human Gastrointestinal Tract. *Applied and Environmental
Microbiology*, *70*(2), 1176–1181. https://doi.org/10.1128/AEM.70.2.1176-
1181.2004

Van der Sluis, M., De Koning, B. A. E., De Bruijn, A. C. J. M., Velcich, A.,
Meijerink, J. P. P., Van Goudoever, J. B., Büller, H. A., Dekker, J., Van
Seuningen, I., Renes, I. B., & Einerhand, A. W. C. (2006). Muc2-Deficient
Mice Spontaneously Develop Colitis, Indicating That MUC2 Is Critical for
Colonic Protection. *Gastroenterology*, *131*(1), 117–129.
https://doi.org/10.1053/j.gastro.2006.04.020

Vautier, S., Drummond, R. A., Chen, K., Murray, G. I., Kadosh, D., Brown, A.
J. P., Gow, N. A. R., Maccallum, D. M., Kolls, J. K., & Brown, G. D.
(2015). *Candida albicans* colonization and dissemination from the murine
gastrointestinal tract: The influence of morphology and Th17 immunity.
Cellular Microbiology, *17*(4), 445–450. https://doi.org/10.1111/cmi.12388

Velcich, A., Yang, W. C., Heyer, J., Fragale, A., Nicholas, C., Viani, S.,
Kucherlapati, R., Lipkin, M., Yang, K., & Augenlicht, L. (2002). Colorectal
cancer in mice genetically deficient in the mucin Muc2. *Science*,
295(5560), 1726–1729. https://doi.org/10.1126/science.1069094

Velegraki, A., Cafarchia, C., Gaitanis, G., Iatta, R., & Boekhout, T. (2015).
Malassezia Infections in Humans and Animals: Pathophysiology,
Detection, and Treatment. *PLoS Pathogens*, *11*(1), 1–6.
https://doi.org/10.1371/journal.ppat.1004523

Veltkamp, C., Tonkonogy, S. L., De Jong, Y. P., Albright, C., Grenther, W. B.,
Balish, E., Terhorst, C., & Sartor, R. B. (2001). Continuous stimulation by
normal luminal bacteria is essential for the development and perpetuation
of colitis in Tgε26 mice. *Gastroenterology*, *120*(4), 900–913.
https://doi.org/10.1053/gast.2001.22547

Vercellotti, J. R., Salyers, A. A., Bullard, W. S., & Wilkins, T. D. (1977).
Breakdown of mucin and plant polysaccharides in the human colon.
Canadian Journal of Biochemistry, *55*(11), 1190–1196.
https://doi.org/10.1139/o77-178

Vila, T., Sultan, A. S., Montelongo-Jauregui, D., & Jabra-Rizk, M. A. (2020).
Oral candidiasis: A disease of opportunity. In *Journal of Fungi* (Vol. 6,
Issue 1). MDPI AG. https://doi.org/10.3390/jof6010015

Walter, J. (2008). Ecological role of lactobacilli in the gastrointestinal tract:
Implications for fundamental and biomedical research. In *Applied and*

Environmental Microbiology (Vol. 74, Issue 16, pp. 4985–4996). American Society for Microbiology. https://doi.org/10.1128/AEM.00753-08

Wang, Y., Kuang, Z., Yu, X., Ruhn, K. A., Kubo, M., & Hooper, L. V. (2017). The intestinal microbiota regulates body composition through NFIL3 and the circadian clock. *Science*, *357*(6354), 912–916. https://doi.org/10.1126/science.aan0677

Weger, B. D., Gobet, C., Yeung, J., Martin, E., Jimenez, S., Betrisey, B., Foata, F., Berger, B., Balvay, A., Foussier, A., Charpagne, A., Boizet-Bonhoure, B., Chou, C. J., Naef, F., & Gachon, F. (2019). The Mouse Microbiome Is Required for Sex-Specific Diurnal Rhythms of Gene Expression and Metabolism. *Cell Metabolism*, *29*(2), 362-382.e8. https://doi.org/10.1016/j.cmet.2018.09.023

Weiss, G. A., & Hennet, T. (2017). Mechanisms and consequences of intestinal dysbiosis. In *Cellular and Molecular Life Sciences* (Vol. 74, Issue 16, pp. 2959–2977). Birkhauser Verlag AG. https://doi.org/10.1007/s00018-017-2509-x

Weizman, Z., & Alsheikh, A. (2006). Safety and Tolerance of a Probiotic Formula in Early Infancy Comparing Two Probiotic Agents: A Pilot Study. *Journal of the American College of Nutrition*, *25*(5), 415–419. https://doi.org/10.1080/07315724.2006.10719554

Wexler, H. M. (2007). Bacteroides: The good, the bad, and the nitty-gritty. In *Clinical Microbiology Reviews* (Vol. 20, Issue 4, pp. 593–621). https://doi.org/10.1128/CMR.00008-07

Wheeler, M. L., Limon, J. J., Bar, A. S., Leal, C. A., Gargus, M., Tang, J., Brown, J., Funari, V. A., Wang, H. L., Crother, T. R., Arditi, M., Underhill, D. M., & Iliev, I. D. (2016). Immunological Consequences of Intestinal Fungal Dysbiosis. *Cell Host and Microbe*, *19*(6), 865–873. https://doi.org/10.1016/j.chom.2016.05.003

White, S. J., Rosenbach, A., Lephart, P., Nguyen, D., Benjamin, A., Tzipori, S., Whiteway, M., Mecsas, J., & Kumamoto, C. A. (2007). Self-regulation of *Candida albicans* population size during GI colonization. *PLoS Pathogens*, *3*(12), 1866–1878. https://doi.org/10.1371/journal.ppat.0030184

Witchley, J. N., Penumetcha, P., Abon, N. V., Woolford, C. A., Mitchell, A. P., & Noble, S. M. (2019a). *Candida albicans* Morphogenesis Programs Control the Balance between Gut Commensalism and Invasive Infection. *Cell Host and Microbe*, *25*(3), 432-443.e6. https://doi.org/10.1016/j.chom.2019.02.008

Witchley, J. N., Penumetcha, P., Abon, N. V., Woolford, C. A., Mitchell, A. P., & Noble, S. M. (2019b). *Candida albicans* Morphogenesis Programs

Control the Balance between Gut Commensalism and Invasive Infection. *Cell Host and Microbe*, *25*(3), 432-443.e6. https://doi.org/10.1016/j.chom.2019.02.008

Wolf, A. J., & Underhill, D. M. (2018). Peptidoglycan recognition by the innate immune system. In *Nature Reviews Immunology* (Vol. 18, Issue 4, pp. 243–254). Nature Publishing Group. https://doi.org/10.1038/nri.2017.136

Wolf, B. W., Wheeler, K. B., Ataya, D. G., & Garleb, K. A. (1998). Safety and tolerance of *Lactobacillus reuteri* supplementation to a population infected with the human immunodeficiency virus. *Food and Chemical Toxicology*, *36*(12), 1085–1094. https://doi.org/10.1016/S0278-6915(98)00090-8

Wrzosek, L., Miquel, S., Noordine, M. L., Bouet, S., Chevalier-Curt, M. J., Robert, V., Philippe, C., Bridonneau, C., Cherbuy, C., Robbe-Masselot, C., Langella, P., & Thomas, M. (2013). *Bacteroides thetaiotaomicron* and Faecalibacterium prausnitzii influence the production of mucus glycans and the development of goblet cells in the colonic epithelium of a gnotobiotic model rodent. *BMC Biology*, *11*. https://doi.org/10.1186/1741-7007-11-61

Xu, J., Bjursell, M. K., Himrod, J., Deng, S., Carmichael, L. K., Chiang, H. C., Hooper, L. V., & Gordon, J. I. (2003). A genomic view of the human-*Bacteroides thetaiotaomicron* symbiosis. *Science*, *299*(5615), 2074–2076. https://doi.org/10.1126/science.1080029

Xu, J., Chiang, H. C., Bjursell, M. K., & Gordon, J. I. (2004). Message from a human gut symbiont: Sensitivity is a prerequisite for sharing. In *Trends in Microbiology* (Vol. 12, Issue 1, pp. 21–28). Elsevier Ltd. https://doi.org/10.1016/j.tim.2003.11.007

Yadav, M., Verma, M. K., & Chauhan, N. S. (2018). A review of metabolic potential of human gut microbiome in human nutrition. In *Archives of Microbiology* (Vol. 200, Issue 2, pp. 203–217). Springer Verlag. https://doi.org/10.1007/s00203-017-1459-x

Zhang, J.-M., & An, J. (2007). Cytokines, Inflammation, and Pain. *International Anesthesiology Clinics*, *45*(2), 27–37. https://doi.org/10.1097/aia.0b013e318034194e

8. List of Publications

Publications included in this thesis

Marie-Therese Eckstein, Sergio David Moreno-Velásquez, J. Christian Pérez (2020) Gut bacteria shape intestinal microhabitats occupied by the fungus *Candida albicans*. Current Biology, 2020, accepted 09/2020.

Other publications

Lena Böhm, Sanda Torsin, Su Tint, **Marie-Therese Eckstein**, Tobias Ludwig, J. Christian Pérez (2017) The yeast form of the fungus *Candida albicans* promotes persistence in the gut of gnotobiotic mice. PLoS Pathogens, 13(10), e1006699. doi:10.1371/journal.ppat.1006699

Juliane Meir, Elena Hartmann, **Marie-Therese Eckstein**, Eva Guiducci, Florian Kirchner, Andreas Rosenwald, Salomé LeibundGut-Landmann, J. Christian Pérez (2018) Identification of *Candida albicans* regulatory genes governing mucosal infection. Cellular Biology, 2018; 20: e12841 doi.org/10.1111/cmi.12841

Gyu-Sung Cho, Felix Ritzmann, **Marie-Therese Eckstein**, Melanie Huch, Karlis Briviba, Diana Behsnilian, Horst Neve, and Charles M. A. P. Franz (2016) Quantification of Slackia and Eggerthella spp. in Human Feces and Adhesion of Representatives Strains to Caco-2 Cells. Frontiers in Microbiology. 2016; 7: 658. doi: 10.3389/fmicb.2016.00658

9. Curriculum Vitae

Affidavit

Affidavit

I hereby confirm that my thesis entitled „Exploring the biology of the fungus *Candida albicans* in the gut of gnotobiotic mice" is the result of my own work. I did not receive any help or support from commercial consultants. All sources and / or materials applied are listed and specified in the thesis.
Furthermore, I confirm that this thesis has not yet been submitted as part of another examination process neither in identical nor in similar form.

_____   _____
Place, Date   Signature

Eidesstattliche Erklärung

Hiermit erkläre ich an Eides statt, die Dissertation „Untersuchung der Biologie des Hefepilzes *Candida albicans* im Verdauungstrakt gnotobiotischer Mäuse" eigenständig, d.h. insbesondere selbständig und ohne Hilfe eines kommerziellen Promotionsberaters, angefertigt und keine anderen als die von mir angegebenen Quellen und Hilfsmittel verwendet zu haben.
Ich erkläre außerdem, dass die Dissertation weder in gleicher noch in ähnlicher Form bereits in einem anderen Prüfungsvervahren vorgelegen hat.

_____   _____
Ort, Datum   Unterschrift